THE UNIVERSITY
of EDINBURGH

AN INVESTIGATION OF THE ROLE OF *STAPHYLOCOCCUS AUREUS* TOXINS IN A CARTILAGE EXPLANT MODEL OF SEPTIC ARTHRITIS

Innes Donald MacKenzie Smith

Presented for the Degree of Doctor of Philosophy

The University of Edinburgh

2015

DECLARATION

I hereby declare that this thesis was composed by myself and that the work presented within it, unless explicitly stated otherwise, is my own. The work has not been submitted for any other degree or professional qualification.

Innes D. M. Smith

Edinburgh

2015

PREFACE

This thesis consists of experimental work conducted at the Centre for Integrative Physiology (Hugh Robson Building, George Square, Edinburgh) and the Centre for Infectious Diseases (Chancellor's Building, Little France, Edinburgh), The University of Edinburgh, during the period 4th August 2010 to 6th August 2013. Work has been concerned with research into improving our understanding of the role of *Staphylococcus aureus* toxins in the pathogenesis of septic arthritis.

The experimental work was carried out personally under the supervision of Dr Andrew Hall, Professor Hamish Simpson and Professor Sebastian Amyes who helped me familiarise myself with all the experimental techniques.

ACKNOWLEDGEMENTS

I am deeply indebted to Dr Andrew Hall, Professor Hamish Simpson and Professor Sebastian Amyes for their supervision, support, advice and enthusiasm throughout the course of this study. I would especially like to thank Dr Andrew Hall for welcoming me into the Centre for Integrative Physiology and for his unwavering guidance, helpful criticisms, limitless patience and constant encouragement during my time within his research group. Our many lively and stimulating discussions have provided me with numerous 'pearls of scientific wisdom' but have ultimately taught me the methods of science.

I also wish to thank the following individuals: Dr Trudi Gillespie, IMPACT Facility, Centre for Integrative Physiology, The University of Edinburgh, for her expert tuition on the use of the confocal laser scanning microscopes; Dr Cathy Doherty, Department of Medical Microbiology, The University of Edinburgh, for her assistance with all microbiological aspects of the study; Dr Elzbieta Czarniak, Department of Laboratory Medicine, Clinical Microbiology, Royal Infirmary of Edinburgh, for providing *Staphylococcus aureus* clinical isolates; Professor Timothy J. Foster, Trinity College, Dublin, for supplying *S. aureus* strain 8325-4 and its associated isogenic mutants; Margaret Chambers, Blood Transfusion Service, Penicuik, for providing heparinised rabbit blood; and Karol Wòjcik, Aileen Blair, and all the staff at Scotbeef Ltd., Bridge of Allan, for their assistance in the provision of bovine feet.

I would additionally like to extend my thanks to all the staff and students at the Centre for Integrative Physiology, especially those in room 214, for making my time there such an enjoyable and memorable experience. Finally, I would like to thank all my friends and family for helping me maintain my sanity during the preparation of this thesis.

The support of Orthopaedic Research UK (clinical research fellowship) and The Royal College of Surgeons of Edinburgh (small project grant) in the funding of this work is gratefully acknowledged.

DEDICATION

To my parents, for educating me and providing me with endless support and encouragement.

To my wife Julie, for being patient, understanding and always being there for me.

To Breagh and Rannoch, for being welcome distractions.

ABSTRACT

Septic arthritis has the potential to be a highly destructive joint disease. Although numerous bacterial species are capable of inducing septic arthritis, *Staphylococcus aureus* is most commonly implicated, accounting for up to 65% of cases. Whilst this organism is known to produce a diverse array of potential virulence factors, studies investigating a variety of *S. aureus*-related infections have implicated alpha(Hla)-, beta(Hlb)- and gamma(Hlg)-haemolysins as key damaging toxins, with the 'pore-forming' Hla considered to be the most potent. The work presented in this study focused on gaining further insight into the interaction between *S. aureus* toxins and *in situ* chondrocytes during an episode of septic arthritis.

An *in vitro* bovine osteochondral explant model of *S. aureus*-induced septic arthritis was developed in this study. Utilising fluorescence-mode confocal laser scanning microscopy (CLSM), the model, which avoided the complexities of a host immune response, permitted an assessment of the following: (1) the spatial and temporal quantification of *in situ* chondrocyte viability following exposure to both a laboratory 'wild-type' (*S. aureus* 8325-4) and clinical strains of *S. aureus*; (2) the influence of Hla, Hlb and Hlg on *in situ* chondrocyte viability through the use of specific 'haemolysin-knockout' mutant strains; (3) the influence of altered culture medium osmolarity and extracellular Ca^{2+} on Hla-induced *in situ* chondrocyte death; and (4) dynamic changes in intracellular Ca^{2+} within *in situ* chondrocytes following Hla exposure.

S. aureus 8325-4 and *S. aureus* clinical strains rapidly reduced *in situ* chondrocyte viability (>45% chondrocyte death at 40hrs). The increased acidity, observed during bacterial culture, had a minimal effect on chondrocyte viability. Chondrocyte death commenced within the superficial zone (SZ) of cartilage and rapidly progressed to the deep zone (DZ). Simultaneous exposure of SZ and DZ chondrocytes to *S. aureus* 8325-4 toxins (achieved with the use of subchondral bone-free explants) demonstrated that SZ chondrocytes were more susceptible to the toxins than DZ chondrocytes.

When explants were cultured in the presence of a selection of isogenic *S. aureus* mutants, with varying Hla, Hlb and Hlg production capabilities (all originating from *S. aureus* 8325-4), Hla-producing mutants induced significant *in situ* chondrocyte death compared to toxin deficient controls ($Hla^-Hlb^-Hlg^-$). In contrast, mutants producing Hlb and Hlg in the absence of Hla were unable to induce significant chondrocyte death. Hla alone was therefore identified as the key damaging toxin to *in situ* chondrocyte viability.

Raised culture medium osmolarity had no influence on Hla-induced *in situ* chondrocyte death. In the absence of Hla, a high extracellular Ca^{2+} concentration (20mM) had no influence on chondrocyte viability during the experimental period. Hla-induced chondrocyte death increased in the presence of raised extracellular Ca^{2+} concentrations thereby confirming a role of Ca^{2+} in the chondrocyte death pathway. There was no significant difference between *S. aureus* growth in high and low Ca^{2+} culture media.

Finally, when live osteochondral explants stained with the Ca^{2+}-sensitive fluorophore Fluo-4 were cultured with an Hla-containing *S. aureus* supernatant (*S. aureus* 8325-4 ($Hla^{+}Hlb^{+}Hlg^{+}$)) there was a significant rise in intracellular Ca^{2+} in comparison to those explants exposed to a non-Hla-containing supernatant (*S. aureus* DU5938 ($Hla^{-}Hlb^{-}Hlg^{-}$)). The Hla-induced Ca^{2+} transients were always followed by chondrocyte death. Thus, it is likely that Hla-induced chondrocyte death was associated with a rise in intracellular Ca^{2+}.

These findings are of translational relevance. Firstly, toxins released by *S. aureus* have a rapid and fatal action on *in situ* chondrocytes, thereby advocating the prompt and thorough removal of bacteria and their toxins during the treatment of septic arthritis. Secondly, the identification of Hla alone as the key damaging toxin to *in situ* chondrocyte viability, with its destructive action being associated with a rise in intracellular Ca^{2+}, may enable the development of future targeted therapeutic strategies in order to reduce the extent of cartilage destruction during and after an episode of septic arthritis.

TABLE OF CONTENTS

CHAPTER 2: GENERAL MATERIALS & METHODS

CHAPTER 3: A BOVINE CARTILAGE EXPLANT MODEL OF *S. AUREUS*-INDUCED SEPTIC ARTHRITIS

TABLE OF FIGURES

ABBREVIATIONS

ECM	Extracellular matrix
COMP	Cartilage oligomeric matrix protein
SZ	Superficial zone
MZ	Middle zone
DZ	Deep zone
ZC	Zone of calcification
OCJ	Osteochondral junction
WCC	White cell count
CT	Computed tomography
MRI	Magnetic resonance imaging
USPIO	Ultrasmall superparamagnetic iron oxide
MSCRAMMs	Microbial surface components recognising adhesive matrix molecules
IL-1β	Interleukin 1-β
IL-4	Interleukin 4
IL-6	Interleukin 6
IL-8	Interleukin 8
IL-10	Interleukin 10
IL-12	Interleukin 12
TNF-α	Tumour necrosis factor alpha
GMCSF	Granulocyte-macrophage colony-stimulating factor
IFN-γ	Gamma interferon
Th1	T-helper 1
Th2	T-helper 2
MRSA	Methicllin-resistant *S. aureus*
Hib	*Haemophilus influenzae* type b
SCVs	Small-colony variants
PVL	Panton-Valentine leukocidin
TSST-1	Toxic shock syndrome toxin-1
TSS	Toxic shock syndrome
Hla	Alpha-haemolysin

Hlb	Beta-haemolysin
Hlg	Gamma-haemolysin
Hld	Delta-haemolysin
$[Ca^{2+}]_i$	Intracellular Ca^{2+} concentration
$[Ca^{2+}]_o$	Extracellular Ca^{2+} concentration
RYR	Ryanodine receptor
IP_3	Inositol trisphosphate
CLSM	Confocal laser scanning microscopy
3-D	3-Dimensional
TSA	Tryptone soya agar
TSB	Tryptone soya broth
DMEM	Dulbecco's Modified Eagle's Medium
DMSO	Dimethyl sulphoxide
CMFDA	5-chloromethylfluorescein diacetate
PI	Propidium iodide
cfu	Colony forming units
PBS	Phosphate buffered saline
ROI	Region of interest
SD	Standard Deviation
PFGE	Pulsed-field gel electrophoresis
DW	Distilled water
TEN buffer	0.1M Tris Cl, 0.1M EDTA, 0.15M NaCl buffer
EC buffer	*Escherichia coli* buffer
TE buffer	10mM Tris, 5mM EDTA buffer
TBE buffer	40mM Tris Cl, 45mM Boric acid, 1mM EDTA buffer
ADAM10	A-disintegrin and metalloprotease 10
ATP	Adenosine triphosphate
HEPES	4-(2-hydroxyethyl)-1-piperazineethanesulfonic acid
$NaHCO_3$	Sodium bicarbonate
EGTA	Ethylene glycol tetraactetic acid
BAPTA	1,2-bis(o-aminophenoxy)ethane-N,N,N',N'-tetraacetic acid
AM	Acetoxymethyl

%Δ*F*	Percentage change in fluorescence intensity
AU	Arbitrary units
AMPs	Antimicrobial peptides

CHAPTER 1

INTRODUCTION

1.1 Prelude

Articular cartilage is a unique tissue that allows the smooth motion of a joint whilst withstanding considerable forces. Unfortunately, for individuals affected by a variety of joint pathology the loss of cartilage is a common end pathway that results in pain, loss of joint function and subsequent disability. Exciting and challenging aspects of cartilage research may focus on (1) identifying factors that result in cartilage damage and subsequent loss or (2) mechanisms of cartilage regeneration and repair. All basic research in these areas is directed, ultimately, to future clinical benefit. This study focuses on the former by investigating the influence of defined *Staphylococcus aureus* toxins on *in situ* viability of chondrocytes (the sole cell type of articular cartilage). In this thesis, *S. aureus* is exclusively studied, as it is the most commonly implicated organism in septic arthritis, a potentially highly destructive joint disease that arises as a result of bacterial infection. In order to interpret the immediate and long-term effects of *S. aureus* and its toxins on articular cartilage, it is important, firstly, to appreciate the normal structure and physiology of this highly specialised connective tissue.

1.2 Articular Cartilage

Articular cartilage, a form of hyaline cartilage, is the smooth, glistening white material covering the articulating bone ends that serves to provide joint movement with minimal friction i.e. it is the bearing material of synovial joints. It is remarkably resilient to compressive forces, which can exceed 100 atmospheres during standing (Hodge *et al.*, 1986; Afoke *et al.*, 1987; Urban, 1994), yet allows controlled deformation in order to distribute loads. Articular cartilage is alymphatic,

aneural, and avascular (Buckwalter *et al.*, 2005) and its nutrition is entirely reliant on the diffusion of nutrients from the synovial fluid and subchondral bone (Malinin and Ouellette, 2000; Wang *et al.*, 2013).

1.2.1 Composition

Chondrocytes are the only cellular component of articular cartilage. Despite their undistinguished rounded appearance, chondrocytes are highly differentiated and specialised mesenchymal cells that are central to the survival of cartilage (Muir, 1995). In humans, articular cartilage is 65-80% water by wet weight (Pearle *et al.*, 2005; Bhosale and Richardson, 2008) and chondrocytes comprise less than 10% of the structure of cartilage and contribute approximately 1% of its volume (Urban *et al.*, 1993; Buckwalter and Mankin, 1997a). Each cell is therefore embedded within a relatively large volume of extracellular matrix (ECM).

Cartilage can be considered a biphasic structure comprising (1) a fluid phase of water and ions and (2) a solid phase consisting of collagen and proteoglycans (Mow *et al.*, 1984; Athanasiou *et al.*, 1991; Zhu *et al.*, 1993; Pearle *et al.*, 2005). The solid phase has low permeability, primarily as a result of the high frictional resistance established by the dense collagen-proteoglycan matrix (Mow *et al.*, 1984). When a load is applied to cartilage, the interstitial fluid is displaced but due to the low permeability of the solid phase there is resultant high interstitial fluid pressurisation (Soltz and Ateshian, 2000). It has been demonstrated that this fluid pressurisation contributes in excess of 90% of the load support (Park *et al.*, 2003), shielding the collagen-proteoglycan matrix from excessive stresses and reducing friction at the

articular surfaces (Ateshian *et al.*, 1994; Ateshian and Wang, 1995; Soltz and Ateshian, 1998). The low permeability of the solid phase and the subsequent pressurisation of the fluid phase give rise to both the stiffness and resilience properties of articular cartilage (Muir, 1995; Buckwalter *et al.*, 2005).

Water is the most abundant component of articular cartilage, contributing 65 to 80% of its volume (Linn and Sokoloff, 1965). Approximately 30% of this water is associated with the intrafibrillar space (i.e. within the collagen fibers) and a small percentage is within the intracellular space (Loret and Simões, 2004). The remainder is contained in the interfibrillar space (i.e. between the collagen fibers- the pore space of the ECM), where it appears to exist as a gel (Pearle *et al.*, 2005). Dissolved within the water are gases, small proteins, metabolites and inorganic ions such as Na^+, K^+, Ca^{2+} and Cl^- (Linn and Sokoloff, 1965; Buckwalter and Mankin, 1997a). The water concentration varies throughout the depth of cartilage, decreasing from 80% at the articular surface to 65% in the region of the bone-cartilage interface (osteochondral junction) (Venn and Maroudas, 1977; Bhosale and Richardson, 2008). The interaction between water and the structural macromolecules of cartilage substantially influences the mechanical properties of the tissue (Buckwalter *et al.*, 2005). In addition, the flow of water through the cartilage and across the articular surface delivers nutrition to chondrocytes whilst also providing a medium for lubrication (Bhosale and Richardson, 2008).

The solid phase of articular cartilage is comprised of three distinct classes of structural macromolecules: (1) collagens, (2) proteoglycans and (3) non-collagenous

proteins and glycoproteins. Together, these macromolecules contribute 20-40% of the wet weight of cartilage (Buckwalter *et al.*, 2005; Bhosale and Richardson, 2008). However, they differ both in their concentrations within articular cartilage and in their contributions to its properties. Collagens contribute approximately 60% of the dry weight (solid phase) of articular cartilage, proteoglycans contribute 25 to 30%, and non-collagenous proteins and glycoproteins contribute 15 to 20% (Buckwalter *et al.*, 2005). The collagens, which have a half-life in excess of 100 years (Verzijl *et al.*, 2000), form a fibrillar meshwork giving cartilage its form and tensile strength. The proteoglycans, which have a half-life between 3 and 25 years (Maroudas *et al.*, 1998), and non-collagenous proteins either bind to the fibrillar meshwork or become entrapped within it and act to maintain the macromolecular structure of the matrix.

Type II collagen accounts for 90-95% of the total collagen found within the solid phase of cartilage. Like all collagens, Type II collagen is composed of three polypeptide chains (α-chains), which are tightly wound together into a triple helix structure (Buckwalter and Mankin, 1997a). This 'rope-like' structure is stabilised through a combination of hydrogen bonds and cross-links involving lysine residues (Muir, 1995), and provides articular cartilage with important shear and tensile properties (Zhu *et al.*, 1993; LeRoux *et al.*, 2000). The collagen molecules orientate themselves in a staggered end-to-end and side-to-side fashion to form fibrils containing a multitude of holes and overlaps (Pearle *et al.*, 2005), thereby forming a framework that has a 'mesh-like' appearance. Type I, IV, V, VI, IX and XI collagens are also found in cartilage and principally serve to stabilise the type II collagen fibrillar network (Buckwalter *et al.*, 2005; Sophia Fox *et al.*, 2009).

Proteoglycans are the second largest group of macromolecules within the ECM. They are responsible for the turgid nature of cartilage and provide the osmotic properties needed to resist compressive loads (Roughley, 2006). Proteoglycans are heavily glycosolated protein monomers consisting of a protein core with one or more covalently attached glycosaminoglycan chains. Glycosaminoglycans are long unbranched polysaccharide chains consisting of repeating disaccharides that contain an amino sugar (Buckwalter and Mankin, 1997a; Roughley, 2006). Each disaccharide unit contains at least one negatively charged carboxylate or sulphate group. Glycosaminoglycans therefore form strings of negative charges that repel other negative charges i.e. Cl^-, and attract cations i.e. Na^+ and Ca^{2+}. Glycosaminoglycans found in articular cartilage include chondroitin sulfate, keratin sulfate, dermatin sulfate and hyaluronic acid (Poole *et al.*, 1996). The attraction of cations results in an increase in total tissue inorganic ion concentration, which in turn results in an increase in the tissue osmolarity. This creates a so-called 'Donnan effect' (raised extra-osmotic pressure that is attributable to cations attached to negatively charged proteins). However, the resulting influx of water into the ECM is restricted by the surrounding collagen network (Buckwalter *et al.*, 2005).

Articular cartilage contains a variety of proteoglycans that are essential for normal function. These proteoglycans can be divided into two major classes: (1) large aggregating proteoglycan monomers, otherwise known as aggrecans, and (2) small proteoglycans, which include biglycan, fibromodulin and decorin (Buckwalter and Mankin, 1997a). The predominant proteoglycan in articular cartilage, accounting for

approx. 90% of the total ECM proteoglycan mass, is aggrecan (Buschmann *et al.*, 1996; Buckwalter and Mankin, 1997a; Pearle *et al.*, 2005; Sophia Fox *et al.*, 2009). Aggrecan is the largest proteoglycan in cartilage, possessing more than 100 chondroitin sulphate and keratin sulfate chains (Roughley *et al.*, 1995). It fills most of the interfibrillar spaces within the collagen network (Buckwalter and Mankin, 1997a) and is characterised by its ability to associate with hyaluronic acid (hyaluronan) non-covalently to form large proteoglycan aggregates, an association that is stabilised by link proteins (small non-collagenous proteins) (Buckwalter and Mankin, 1997a; Pearle *et al.*, 2005; Sophia Fox *et al.*, 2009). In the constrained environment of the collagen fibrillar network, which itself endows cartilage with its mechanical strength in tension, the electrically charged and 'gel-like' aggrecan provides resistance to compression. The importance of aggrecan to the resistance of compressive loads has been illustrated in animal studies whereby it has been demonstrated that aggrecan concentration is frequently higher in areas of habitually loaded cartilage (Slowman and Brandt, 1986; Kiviranta *et al.*, 1988). Conversely, it is reduced in concentration within experimentally immobilised animal joints (Palmoski *et al.*, 1979; Kiviranta *et al.*, 1987).

In comparison to aggrecan, the small non-aggregating proteoglycans, the most common of which are decorin, biglycan and fibromodulin (Roughley *et al.*, 1995), have shorter protein cores, occupy a small tissue volume and do not contribute to the mechanical behaviour of cartilage (Buckwalter *et al.*, 2005). Despite being the products of distinct genes, the non-aggregating proteoglycans have similar protein structures (Fisher *et al.*, 1989; Oldberg *et al.*, 1989). However, they differ in

glycosaminoglycan composition and function. Although termed 'non-aggregating', these proteoglycans are thought to interact with other matrix components. Decorin and fibromodulin interact with type II collagen fibrils and are believed to play a role in organising and stabilising the type II collagen meshwork (Roughley *et al.*, 1995). Biglycan is primarily found in the pericellular matrix where it is thought to interact with type VI collagen (Wiberg *et al.*, 2001; Wiberg *et al.*, 2002).

A number of non-collagenous proteins and glycoproteins have been identified within articular cartilage, but few have been studied in detail (Roughley, 2001; Buckwalter *et al.*, 2005). Whilst the specific function of the vast majority of these molecules thus remains unknown, it is believed that they have regulatory roles with regard to the structure and function of the cartilage matrix, including matrix assembly, cell-cell and cell-matrix interactions, and matrix metabolism (Chevalier *et al.*, 1994). Anchorin CII, cartilage oligomeric matrix protein (COMP), fibronectins and tenascin have been the most widely studied, yet remain to be characterised fully. Anchorin CII is a collagen binding glycoprotein that is found on the surface of chondrocytes and is thought to aid in the anchorage of chondrocytes to the collagen fibrils of the ECM (Mollenhauer *et al.*, 1984). COMP is a cartilage specific protein that has a preferential localisation to the territorial matrix and also the capacity to bind to chondrocytes (Hedbom *et al.*, 1992; DiCesare *et al.*, 1994). It may have value as a marker of cartilage turnover and has therefore been investigated as a potential indicator of progressive cartilage degeneration in patients with osteoarthritis and rheumatoid arthritis (Saxne and Heinegård, 1992; Lohmander *et al.*, 1994; Sharif *et al.*, 1995). Fibronectins are believed to play an important role in chondrocyte

adhesion, migration and de-differentiation (Chevalier, 1993) while tenascin influences the interaction between chondrocytes and the pericellular matrix by interacting with fibronectin (Chiquet-Ehrismann *et al.*, 1988; Lotz *et al.*, 1989; Chevalier *et al.*, 1994).

1.2.2 Chondrocytes

Chondrocytes are the only cells found within articular cartilage and are embedded within a large volume of ECM (Goldring, 2012). They are surrounded by a specialised microenvironment that effectively insulates the chondrocyte and protects it from the bulk of the load-bearing matrix (Poole *et al.*, 1992). Each chondrocyte is linked at its surface to a proteoglycan and glycoprotein-rich 'pericellular' matrix (sometimes referred to as the glycocalyx), which itself is enclosed by a compacted fibrous pericellular capsule (Poole *et al.*, 1984; Chang and Poole, 1997). There is a close interaction between chondrocytes and their surrounding ECM, with regard to both attachment and communication, and this is primarily achieved through a family of transmembrane receptors known as integrins (Loeser, 2002). Integrins bind to ligands within the ECM to form signalling complexes, which play a key role in chondrocyte survival, proliferation, differentiation, migration and remodelling mechanotransduction, chondrocyte growth, differentiation, migration and proliferation (Adams and Watt, 1993; Salter *et al.*, 1995; Svoboda, 1998; Loeser, 2000; Millward-Sadler and Salter, 2004; Gao *et al.*, 2014).

Collectively, the chondrocyte and its pericellular microenvironment represent the 'chondron' (Poole *et al.*, 1992). These microanatomical units, which can be

visualised under low power light microcopy, either exist as single, double or linear chondron columns (Poole, 1997) **(Figure 1.1)**. Immediately surrounding the chondron is the 'territorial' matrix (Poole *et al.*, 1984). This region is primarily composed of fine collagen fibrils, which form a basket-like network around the cells (Sophia Fox *et al.*, 2009). The matrix that occupies the majority of space between chondrocytes is referred to as the 'interterritorial' matrix and contributes the most to the biomechanical properties of articular cartilage (Guilak *et al.*, 1999; Mow and Guo, 2002). It is characterised by bundles of large collagen fibrils that are arranged parallel to the articular surface within the most superficial zone and perpendicular to the surface within deeper regions.

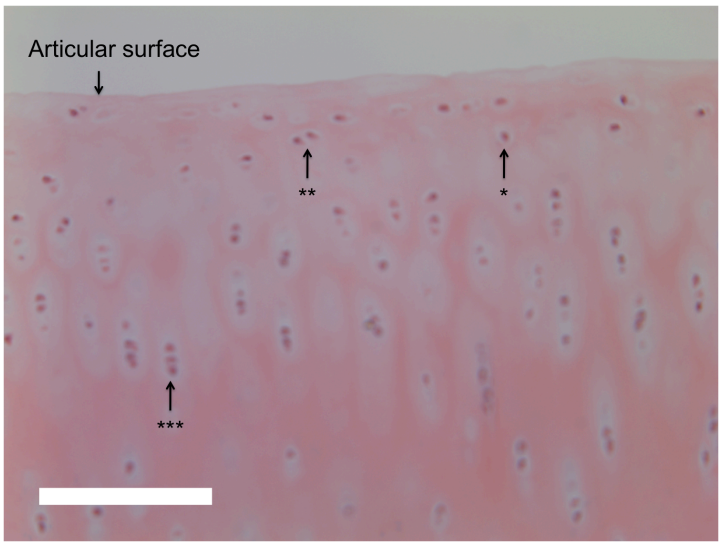

Figure 1.1: Chondron units

A 10μm thick coronal section of haematoxylin and eosin stained bovine articular cartilage, as viewed under a x20 objective, demonstrating the presence of chondrons, which physically separate the chondrocytes from the surrounding ECM. These microanatomical units exist as either single (*), double (**) or linear (***) chondron columns (scale bar = 100μm). Image kindly provided by Dr Asima Karim, Centre for Integrative Physiology, The University of Edinburgh.

Although chondrocytes are the only cells within cartilage they exhibit morphological heterogeneity throughout the depth of cartilage ranging from flattened at the surface to larger and rounder in deeper regions (Goldring, 2012) (**Figure 1.2**). Due to the avascular nature of cartilage, chondrocytes primarily derive their nutrition from nutrient solutes in the synovial fluid. It has been hypothesised that chondrocytes within deeper regions may also rely, to some extent, on the diffusion of nutrients across the osteochondral junction i.e. from the subchondral bone (Malinin and Ouellette, 2000; Wang *et al.*, 2013). Despite the low oxygen tension in articular cartilage, which ranges from 7% O_2 at the articular surface to <1% O_2 within deeper regions (Zhou *et al.*, 2004; Cernanec *et al.*, 2007), individual chondrocytes are actually quite metabolically active, having a glycolytic rate per cell similar to that of cells in well-vascularised tissues (Buckwalter and Mankin, 1997a). However, due to the low cell density the total metabolic activity of the tissue is low.

The primary role of the chondrocyte is to synthesise the macromolecular components that constitute the ECM whilst also regulating matrix metabolism (Muir, 1995; Buckwalter and Mankin, 1997a; Bhosale and Richardson, 2008). Throughout their lifespan, chondrocytes have an intimate relationship with the ECM. Alterations in the macromolecular composition of the ECM are closely monitored by the chondrocytes and, when necessary, controlled matrix synthesis or breakdown is initiated. Matrix breakdown is mediated through the release of a variety of proteolytic enzymes including matrix metalloproteinases and aggrecanases (Buckwalter and Mankin, 1997a; Goldring and Marcu, 2009; Struglics and Hansson,

2012). Chondrocytes can therefore be considered both the architects and cellular building blocks of articular cartilage.

Chondrocytes are regarded as post-mitotic cells, in so much that once skeletal maturity is reached there is no further cell division detectable in healthy adult articular cartilage (Muir, 1995; Goldring and Marcu, 2009). Mature chondrocytes therefore have a long life span and are generally expected to remain viable as long as their host. However, once chondrocytes are lost they are not replaced, and when they are lost in large numbers their importance in the maintenance of cartilage integrity is illustrated: Simon *et al.* (1976) investigating the long-term effect of chondrocyte death induced by localised cryotherapy on rabbit articular cartilage *in vivo*, demonstrated, through histological staining coupled with both normal and polarised light microscopy, that the cartilage was structurally intact at 6 months despite the absence of living chondrocytes. However, by 12 months extensive cartilage fibrillation and softening was evident, changes that were considered to be amongst the first macroscopic appearances associated with degenerative joint disease (Pearle *et al.*, 2005).

Whilst no studies have specifically investigated cartilage degeneration following catastrophic loss of chondrocyte viability in humans, a case report by van Huyssteen and Bracey (1999) possibly highlights the consequences of such an occurrence. Extensive chondrolysis, as evidenced by radiographical loss of joint space, was identified in three consecutive patients 2 to 4 months post anterior cruciate ligament reconstruction. Throughout each of the three procedures, the knee joints were

mistakenly irrigated with 0.2% chlorhexidine instead of the standard 0.02%. In a subsequent study by Campbell *et al.* (2014) osteochondral allografts were exposed to varying concentrations of chlorhexidine and chondrocyte viability assessed. 7 days post-pulse lavage with 0.25% chlorhexidine, which is comparable to the concentration administered to the above patients, chondrocyte viability was 10±19%. In comparison, chondrocyte viability in those allografts pulse lavaged with 0.002% chlorhexidine ranged from 67±4% to 81±22%. It is therefore extremely important to preserve chondrocyte viability during both acute and chronic pathology, and also during surgical instrumentation in order to maintain cartilage integrity.

1.2.3 Articular cartilage structure

The structure of articular cartilage is both complex and heterogeneous. The thickness, cell density, matrix composition and mechanical properties of articular cartilage vary within the same joint, between joints in the same individual and between species (Buckwalter *et al.*, 2005). The full thickness of cartilage extends from the articular surface to the osteochondral junction (bone-cartilage interface) (**Figure 1.2**). Between these two points, articular cartilage is loosely divided into four distinct zones on the basis of depth-associated variation in cell morphology and ECM properties: [1] the superficial (tangential) zone (SZ), [2] the middle zone (MZ), [3] the deep zone (DZ) and [4] the zone of calcification (ZC), otherwise known as the zone of calcified cartilage (**Figure 1.2**) (Buckwalter and Mankin, 1997a; Poole, 1997; Pearle *et al.*, 2005). The demarcation between each zone however can often be difficult to define.

In most species, including humans, the SZ is the smallest zone, accounting for approximately 0-10% depth from the articular surface (Pedersen *et al.*, 2013) and typically consists of two layers (**Figure 1.2**) (Buckwalter *et al.*, 2005). The first of these layers is an acellular sheet of fine fibrils that is known as the lamina splendens (Buckwalter and Mankin, 1997a; Bhosale and Richardson, 2008). Deep to this layer, flattened ellipsoid-shaped chondrocytes lie within a matrix that has a low proteoglycan and high collagen content (Poole *et al.*, 1984). The dense network of collagen fibres, which, along with the chondrocytes, are orientated parallel to the articular surface, provide the tissue with tensile strength, stiffness and durability (Clark, 1990; Wu *et al.*, 2008; Mansfield *et al.*, 2009). This arrangement is also considered to act as a sieve by allowing the passage of nutrients from the synovial fluid into the cartilage whilst, at the same time, preventing the ingress of larger and potentially damaging molecules of the immune system (Buckwalter and Mankin, 1997a).

The MZ provides a functional and anatomical bridge between the SZ and DZ and extends from approx. 10-40% depth from the articular surface (Jadin, 2005; Pedersen *et al.*, 2013) (**Figure 1.2**). The chondrocytes within this zone are at lower density and are more spherical in shape in comparison to the SZ. The collagen fibres have a greater diameter and, in contrast to the SZ, arch obliquely in relation to the articular surface (Poole, 1997). Furthermore, there is a greater concentration of proteoglycans within the matrix of this zone but, conversely, there is a lower water and collagen content (Buckwalter *et al.*, 2005). Functionally, the MZ offers the first line of resistance to compressive forces and thereby acts as a ‘shock absorber’.

Immediately below the MZ lies the DZ, which extends from approx. 40-100% depth from the articular surface (**Figure 1.2**) (Pedersen *et al.*, 2013). It is characterised by spherical chondrocytes that organise themselves into columns as a result of the vertically orientated collagen fibres in this zone (Pearle *et al.*, 2005). These collagen fibres have the widest diameter of all collagen fibres embedded within articular cartilage and extend into the tidemark, the boundary between uncalcified and calcified cartilage (Buckwalter and Mankin, 1997a). The main function of the DZ, which contains the highest concentration of proteoglycans and the lowest water content, is to provide the maximum resistance to compressive forces (Buckwalter and Mankin, 1997a; Pearle *et al.*, 2005).

The deepest layer of cartilage is the ZC and it is this layer that separates articular cartilage from subchondral bone (**Figure 1.2**). The zone is characterised by a sparse population of spherical chondrocytes that are of a lower volume than those from the DZ (Buckwalter and Mankin, 1997a). The chondrocytes are surrounded by uncalcified lacunae and radial collagen fibres that are anchored within a calcified matrix in which there is an absence of proteoglycans (Poole, 1997). The ZC plays a crucial role in tethering cartilage to bone (Keinan-Adamsky *et al.*, 2005; Sophia Fox *et al.*, 2009).

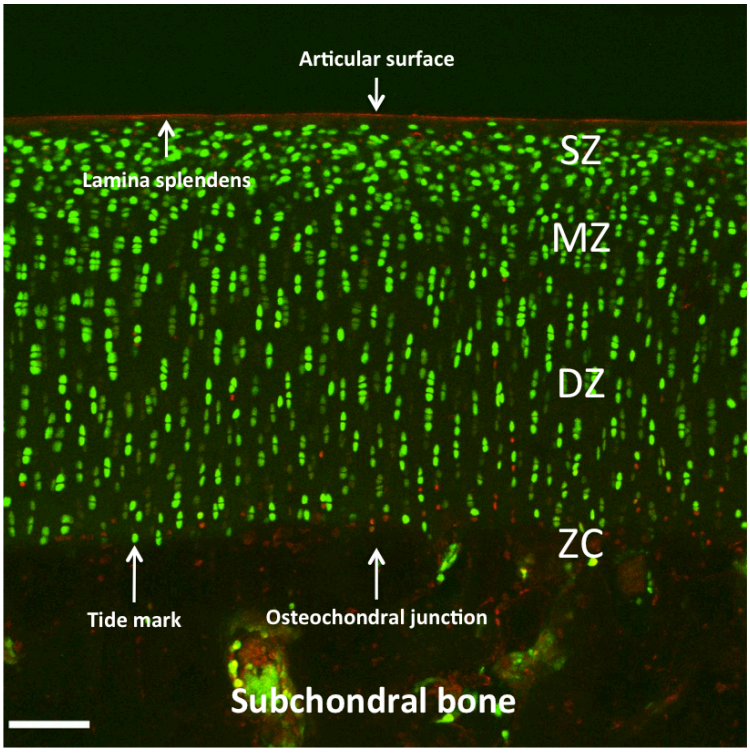

Figure 1.2: Zonal heterogeneity of articular cartilage

Full-thickness coronal section of 5-chloromethylfluorescein diacetate (CMFDA) and propidium iodide (PI) labelled bovine articular cartilage (CMFDA stains the cytoplasm of viable chondrocytes green while PI stains the nuclei of dead or dying cells red; staining was conducted post-cartilage trimming, hence a small number of cells died as a result of the scalpel blade-induced mechanical trauma), acquired using an upright confocal laser scanning microscope coupled with a x10 dry objective, displaying the superficial (SZ), middle (MZ) and deep zones of cartilage along with the zone of calcification (ZC). Note the altered chondrocyte organisation with increasing depth from the articular surface: cells in the SZ are oval, flattened and orientated parallel to the articular surface, whereas those chondrocytes in the MZ and DZ are rounder and arch to orientate more obliquely (MZ) and perpendicular to the articular surface. Important histological/microscopic landmarks are also illustrated (scale bar = 100μm).

1.2.4 Cartilage repair

In 1743 William Hunter stated *'from Hippocrates to the present age it is universally allowed that ulcerated cartilage is a troublesome problem and once destroyed, it*

never repairs'. It has therefore long been established that articular cartilage has a very poor regenerative capacity following injury. There are at least two possible explanations for this phenomenon. Firstly, as mentioned previously, the literature to date suggests that cellular division does not take place in healthy articular cartilage once skeletal maturity has been reached (Muir, 1995; Goldring and Marcu, 2009). Chondrocyte loss, as a consequence of injury or disease, in adulthood is therefore not replaced. Secondly, cartilage is an avascular tissue. In well vasularised tissues such as skin and liver, the healing process follows an established pattern of necrosis, inflammation and repair (Mankin, 1982). An adequate blood supply is essential for the inflammation and repair phases of the response. Necrosis has been shown to be present in partial thickness articular cartilage injuries but no healing process has subsequently been identified (Mankin, 1982). However, if the injury extends beyond the zone of calcification, blood seeps into the wound from the vascularised subchondral bone thereby delivering the necessary inflammatory mediators, growth factors and reparative cells, such as fibroblasts and mesenchymal stem cells, for healing to occur. Unfortunately however, the healing process that ensues is rudimentary and the defect, at best, is filled with mechanically inferior fibrocartilage (Bhosale and Richardson, 2008; Kang *et al.*, 2008). This suboptimal tissue has been shown to degenerate quickly once mechanical load is applied with the eventual formation of an isolated osteoarthritic lesion that may subsequently result in pain and disability (Mankin, 1982; Hunziker, 2002). It is therefore of critical importance that ongoing research should focus on attempts to reduce the extent of cartilage destruction during episodes of pathology and following trauma.

1.2.5 Experimental study of articular cartilage

The assessment of articular cartilage following experimental challenge has largely been conducted on animal models, isolated chondrocytes or cartilage explants. Animal models have the advantage of allowing the analysis of cartilage within a living joint. Thus, the results obtained from such studies reflect a closer correlation and relevance to the clinical setting. Nevertheless, there are disadvantages to the use of live animal models. In some circumstances, the strong and often complex host immune response, inherent in an animal model, can make the assessment of experimental variables difficult. For example, when assessing the impact of a particular bacterial strain on cartilage in an animal model of septic arthritis, it is difficult to distinguish what proportion of the resulting cartilage damage is due to the bacterial toxins and what proportion is due to the host immune response. Albeit, some of these difficulties can be overcome with the use of animals bred with the selective absence of various components of the immune response. In addition, animals are expensive to purchase and maintain, which is a not inconsiderable factor. Animal studies also necessitate the acquisition of animal handling licenses and ethical approval.

In some research circumstances, it is important to remove the host immune response from the experimental environment in order to evaluate the primary effect of particular 'challenges' on articular cartilage more accurately. Accordingly, it is necessary to distance the research model from the living animal. One such model is the use of isolated chondrocytes. In the absence of a host immune response, isolated chondrocytes have the advantage of allowing easier control of experimental

variables. However, in relative comparison to other isolated cell types, chondrocytes are challenging. Despite their apparently stable appearance within healthy living cartilage for many decades, once chondrocytes are isolated within an experimental vessel such as a Petri dish (i.e. taken out of their native environment), they rapidly change their phenotype (i.e. de-differentiate). They develop a 'fibroblast-like' flattened and elongated shape, enter a proliferative cycle and alter the characteristics of the synthesised collagen, producing predominantly type I collagen (Gargiulo *et al.*, 2002). The isolation of 'pure' chondrocytes is thus challenging. However, one experimental method commonly employed to prevent the undesirable change in phenotype is the isolation chondrocytes within agarose constructs (Buschmann *et al.*, 1992).

Articular cartilage explants are simply pieces of cartilage of variable size that are extracted from a synovial joint. When subchondral bone is attached to the cartilage they are referred to as osteochondral explants (**Figure 1.3**). In comparison to isolated chondrocytes, they allow the assessment of cartilage as a tissue, intact with its cellular and matrix components, whilst also permitting tight control of experimental variables in the absence of a host immune response. Cartilage explants, sourced from various animals have frequently been used for research purposes. Some studies have utilised human cartilage explants. However, there are several potential problems associated with their use. Similar to live animal studies, ethical permission is required and, additionally, patient consent is mandatory. Human cartilage is traditionally obtained from the femoral condyles or tibial plateaus of patients undergoing total knee joint replacement (Amin *et al.*, 2011) or the femoral

heads of patients either undergoing total hip replacement or hemiarthroplasty for osteoarthritis and femoral neck fracture, respectively (Démarteau *et al.*, 2006). As these patients are invariably elderly, the common pathology is osteoarthritis and it is often difficult to source healthy non-degenerate cartilage from such surgical discard. In a study by Amin *et al.* (2011), which investigated the chondroprotective effect of raised irrigation solution osmolarity in a human cartilage explant model of sharp mechanical trauma, the femoral condyles of only four patients out of a total of 30 (87% rejection rate) recruited for the study were deemed non-degenerate and suitable for experimental purposes. A further consideration against the use of human cartilage is that studies have demonstrated similar responses by bovine and human cartilage to a variety of experimental challenges (D'Lima *et al.*, 2001).

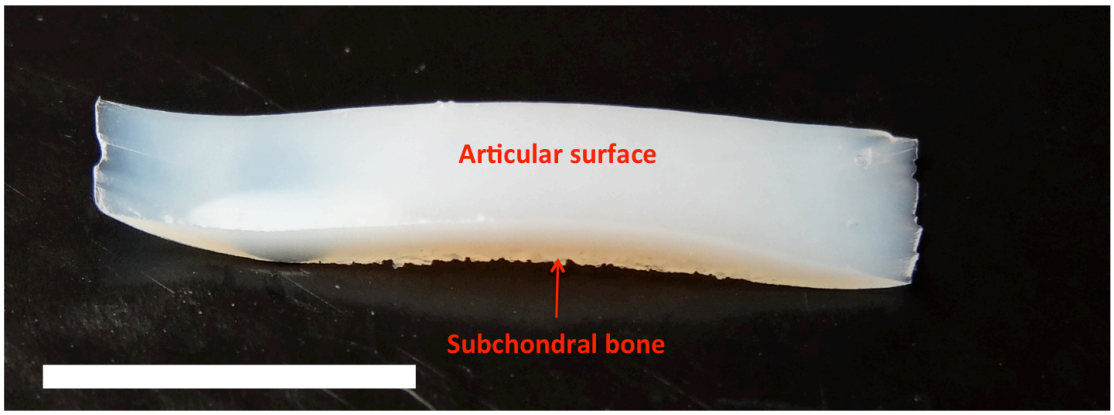

Figure 1.3: Osteochondral explant

Cartilage explants are defined as harvested pieces of articular cartilage, of variable size, for the purpose of *in vitro* experimentation. In comparison to isolated chondrocytes, they permit the study of cartilage as a tissue i.e. with intact cellular and matrix components and thus more accurately mimic the *in vivo* environment (scale bar = 0.5cm).

1.3 Septic Arthritis

One condition that has the potential to cause rapid joint destruction, and thus injury to articular cartilage, is septic arthritis. Septic arthritis, which is considered a rheumatological and orthopaedic emergency, is defined as joint inflammation secondary to bacterial infection (Mathews *et al.*, 2008). The destructive effects of sepsis on articular cartilage were described several centuries ago by William Hunter (1743) who stated: *"when a cartilage is inflamed and soaked in a purulent material, the connecting fibres will be the soonest to give way and the cartilage will become soft and red"*. Patients with septic arthritis typically present with a red, hot and swollen joint that is extremely painful, especially upon movement. Commonly, there are associated features of systemic upset including generalised malaise and a marked pyrexia.

The management of septic arthritis has remained a challenge for centuries. In 1819, Sir Benjamin Brodie wrote of the difficulties in draining a septic joint, advocating *"removal of limb by amputation"* in patients presenting with septic arthritis (Buchanan, 2003; Nade, 2003). Whilst amputation is fortunately very rarely associated with septic arthritis in the present medical era, some patients, despite current therapeutic strategies, still remain inadequately treated (Goldenberg, 1998). Consequently, these patients may be left with devastating lifelong problems such as pain, disfigurement and disability (Weston *et al.*, 1999; Shirtliff and Mader, 2002; Nunn *et al.*, 2007; Mathews *et al.*, 2008). The work presented in this thesis focused on improving our knowledge of the interaction between bacteria and articular cartilage with the hope of developing novel chondroprotective treatments.

1.3.1 Epidemiology

Septic arthritis affects all age groups. However, there are incidence peaks in the very young and the elderly (Shetty and Gedalia, 2004). Although any joint can be affected, there is a propensity for lower limb involvement, with the knee and hip most commonly implicated (Shirtliff and Mader, 2002) followed by the shoulder, wrist, elbow and ankle in varying orders depending on the particular case series assessed (Morgan *et al.*, 1996; Kaandorp *et al.*, 1997a; Weston *et al.*, 1999; Gupta *et al.*, 2001; Abid *et al.*, 2006). Septic arthritis is not exclusively monoarticular with polyarticular involvement being seen in approximately 20% of cases (Dubost *et al.*, 1993; Kaandorp *et al.*, 1997a; Mateo Soria *et al.*, 2009).

In developed countries, the incidence of septic arthritis ranges from 2-10 cases/100,000 persons (Morgan *et al.*, 1996; Weston *et al.*, 1999; Levine and Siegel, 2003; Mathews *et al.*, 2010; Chander and Coakley, 2011) rising to 30-70 cases/100,000 persons in patients who have had prior joint disease i.e. rheumatoid arthritis (Goldenberg, 1998). There is an estimated case fatality rate of 11%, the majority of which are elderly patients with multiple co-morbidities (Gupta *et al.*, 2001; Shirtliff and Mader, 2002; Mathews *et al.*, 2008). Since a significant proportion of cases (approx. 30%) are never confirmed bacteriologically (Nduati and Wamola, 1991; Weston *et al.*, 1999; Mathews *et al.*, 2010), epidemiological studies may underestimate the incidence of septic arthritis and its burden of morbidity and mortality. Risk factors for the development of septic arthritis have been identified from several retrospective and prospective studies and include the following:

rheumatoid arthritis, osteoarthritis, gout, diabetes mellitus, oral corticosteroids, intra-articular steroid injections, cytotoxic therapy, previous joint surgery, recent joint trauma, underlying carcinoma, upper respiratory tract infection, skin ulceration, cellulitis, intravenous drug abuse and alcohol excess (Morgan *et al.*, 1996; Weston *et al.*, 1999; Gupta *et al.*, 2001).

Worldwide, the prevalence of septic arthritis increases in populations from poorer socioeconomic backgrounds. For example, in Northern Australia the incidence of septic arthritis amongst Aboriginal Australians, an impoverished population, was 29 cases/100,000 persons in comparison to 9 cases/100,000 persons in non-Aboriginal Australians (Morgan *et al.*, 1996). Whilst septic arthritis in infants is rare in Western societies, it is more common in sub-Saharan Africa (Nduati and Wamola, 1991; Smith *et al.*, 2002; Akinyoola *et al.*, 2006; Lavy, 2007; Nunn *et al.*, 2007) and can have potentially devastating consequences. Septic arthritis in infants can lead to permanent cartilage damage, osteomyelitis, avascular necrosis of the femoral head (in cases of septic arthritis of the hip) and destruction of the epiphyseal growth plate, leaving the child with permanent joint deformity and thus disability (Lavy, 2007; Nunn *et al.*, 2007).

1.3.2 Diagnosis

Septic arthritis is typically diagnosed on the basis of patient history, clinical examination and laboratory investigations. A positive synovial fluid gram stain or culture confirms the diagnosis and it is therefore imperative that the joint in question is aspirated without delay if septic arthritis is suspected. However, a negative result

cannot exclude a diagnosis of septic arthritis as, disappointingly, synovial fluid gram staining and culture are positive in only 50% and 70% of cases, respectively (Mathews *et al.*, 2010). Blood cultures may aid the diagnosis as a retrospective study by Weston *et al.* (1999) investigating 462 cases demonstrated that 24% of the patients studied had positive blood cultures. Interestingly, in 9% of the patients with confirmed septic arthritis in this particular case series, blood cultures were the only source of a positive microbiological diagnosis.

In addition to gram stain and culture, initial synovial fluid analysis at the bedside may arise suspicion of a diagnosis of septic arthritis. Synovial fluid from a septic joint typically has a turbid and yellow appearance, in some cases appearing as 'frank pus', which is considerably different to the often clear and straw-coloured fluid associated with a reactive effusion secondary to osteoarthritis. Even if subsequent gram stain and culture are negative, the number of white blood cells (leukocytes) in a defined volume (white cell count (WCC)) of synovial fluid is considered helpful (Shirtliff and Mader, 2002). In a retrospective study by Coutlakis *et al.* (2002), the records of 202 consecutive patients with synovial WCCs >2000/mm^3 were reviewed. Septic arthritis was diagnosed in 77% of patients with counts >100,000/mm^3, 47% in the 50,000-100,000/mm^3 range and 5% with counts <50,000/mm^3. Thus, the diagnosis of septic arthritis is unlikely in those patients with a WCC<50,000/mm^3, although it still cannot be excluded.

Further laboratory tests that may guide the clinician to a diagnosis of septic arthritis include an assessment of inflammatory markers. In the blood samples of patients

with septic arthritis, erythrocyte sedimentation rate and C-reactive protein level are usually elevated (Mathews *et al.*, 2010). However, normal values for these parameters have been reported (Li, 2004), especially in malnourished, anaemic and underweight children (Lavy, 2007), and thus an absence of an acute phase response does not exclude a diagnosis of septic arthritis. Nevertheless, once a diagnosis has been established, serial measurements of inflammatory markers, if elevated at presentation, are useful to monitor the response to treatment.

In current clinical practice, imaging studies are neither sensitive nor specific for the diagnosis of septic arthritis (Shirtliff and Mader, 2002; Chander and Coakley, 2011) but are nevertheless useful to either support or dissuade a clinical suspicion of the disease. Plain radiographs frequently appear normal during the first few days of infection. They may also demonstrate the presence of co-existent osteomyelitis or changes consistent with pre-existing joint disease i.e. osteoarthritis. In some cases, fat pad displacement (typically seen in radiographs of the knee and elbow) and joint space widening due to localised oedema and effusion may be evident (Shirtliff and Mader, 2002; Nunn *et al.*, 2007). Plain radiographs however are perhaps most useful as a baseline for future comparison. As the infection progresses, changes such as acute joint space narrowing, indicative of catastrophic articular cartilage destruction, may be become evident. Indeed, the sequelae of an episode of septic arthritis may only become evident months to years post-sepsis. Examples of potential late radiographic changes include secondary osteoarthritis and joint fusion in adults and joint subluxation/dislocation and avascular necrosis of the femoral head in children.

Ultrasonography is a useful investigative tool for identifying intra- and extra-articular abnormalities that may not be evident on plain radiographs. It enables assessment of the intra-articular compartment, joint capsule, and surrounding soft tissues. Its main strength however is the detection of early fluid collections both within and outwith the joint, for which it has both a high specificity and sensitivity (Shirtliff and Mader, 2002). Collections as small as 1-2ml have been shown to be accurately detected (Zieger *et al.*, 1987). It is therefore particularly useful for the detection of effusions and juxta-articular collections in deep joints such as the hip. In addition, it can also be used to guide initial joint aspiration and subsequent drainage procedures in such joints. Given the non-invasive nature of ultrasonography and the lack of ionising radiation, it is a popular investigative technique for the assessment of children with suspected septic arthritis.

When a diagnosis of septic arthritis remains ambiguous or the extent of surrounding bone and soft tissue infection is questioned, computed tomography (CT), magnetic resonance imaging (MRI) or radionuclide scans may be helpful. During the early stages of septic arthritis, CT shares some of the limitations of plain radiographs (Chander and Coakley, 2011). However, CT scans may enable the visualisation of soft tissue swellings, para-articular abscess formation, and the presence of joint effusion that may not be evident on plain radiographs. In addition, a CT scan may be useful for the investigation of joints that are difficult to assess on plain radiographs such as the sacro-iliac and sternoclavicular joints. Like Ultrasonography, CT may also be used to guide the initial aspiration of deep joints.

Although MRI provides a lower resolution of calcified bone structures, it displays considerably greater resolution for soft tissue (Shirtliff and Mader, 2002). Soft tissue abnormalities such as joint effusions, abscesses and tissue oedema are particularly evident on T2 weighted images whereby oedema and fluid are projected 'bright' and fat is 'dark'. However, as with plain radiography, CT and Ultrasonography, MRI is non-specific and is unable to differentiate between infectious and non-infectious arthropathies (Graif *et al.*, 1999). Interestingly, a recent animal study by Lefevre *et al.* (2011) has identified a potential future role for MRI in monitoring the *in vivo* response to antibiotic therapy in patients with septic arthritis. Septic arthritis was induced in rabbits through the intra-articular inoculation of *S. aureus.* Thereafter, the ensuing infection and subsequent response to antibiotic treatment was assessed using MRI coupled with 'ultrasmall superparamagnetic iron oxide' (USPIO) particles. Following injection, USPIO particles are phagocytosed by macrophages, which then become amenable to MR imaging. Macrophages are recruited during the early stages of joint infection and then dissipate with the resolution of infection. Thus, the signal intensity changes according to the extent of USPIO-loaded macrophage infiltration, thereby providing a means of monitoring the response to antibiotic treatment.

Radionuclide scans (otherwise known as bone scans or skeletal scintigraphy), commonly utilising either gallium-67-citrate (^{67}Ga), technetium-99m (^{99m}Tc) or indium-111 (^{111}In)-labelled polyclonal human immunoglobulins or ^{99m}Tc or ^{111}In-labelled autologous leukocytes (Lupetti *et al.*, 2003), are helpful in establishing a diagnosis of infection. Unlike MRI and CT, they permit whole-body imaging and

are therefore extremely useful for the assessment of patients with 'sepsis of unknown origin' i.e. they can be used to localise sepsis. They are also useful for confirming that an abnormality identified on CT or MRI is indeed infectious in origin. In orthopaedic practice, ^{99m}Tc and ^{111}In leukocyte scans are routinely employed during the assessment of patients with painful joint prostheses in order to help distinguish between infection and aseptic loosening (Johnson *et al.*, 1988). Unfortunately however, current radiopharmaceuticals accumulate in both infected and inflamed areas due to non-specific mechanisms of accumulation (Becker and Meller, 2001). Thus, at present, radionuclide scans lack the specificity to differentiate between active infection and inflammation and are therefore not commonly utilised for the diagnosis of septic arthritis.

1.3.3 Management

A joint affected by septic arthritis contains both pus and bacteria and it has long been established that this combination is highly destructive to articular cartilage (Hunter, 1743). Clinical and experimental research to date has demonstrated an undisputed relationship between early and aggressive initiation of joint lavage and a successful outcome (Jackson, 1985; Lane *et al.*, 1990; Jerosch *et al.*, 1995; Stutz *et al.*, 2000; Seara *et al.*, 2002; Ateschrang *et al.*, 2011). Septic arthritis is therefore considered a rheumatological or orthopaedic emergency and current treatment is focused on early institution of appropriate antibiotics and prompt removal of purulent synovial fluid (pus) from the infected joint.

There are a number of ways of removing pus from a septic joint ranging from simple needle aspiration, through tidal irrigation (a technique whereby the joint is aspirated to dryness i.e. no more fluid can be aspirated, followed by the flushing of lavage fluid in and out of the joint through wide bore needles), to invasive surgery, which may take the form of minimally invasive arthroscopy or open arthrotomy. Despite advocates of their own methods making claims for their preferred techniques, there is, at present, no prospective evidence to suggest that any joint irrigation strategy is superior (Manadan and Block, 2004; Ravindran *et al.*, 2009). The preferred method of pus removal therefore tends to be dependent upon local guidelines (Coakley *et al.*, 2006).

Following the initial aspiration of synovial fluid for microbiological analysis, there may be a delay of several hours before the gram stain result is communicated to the clinician and a further 24-48hrs may lapse before the results of the cultures, including antibiotic sensitivities, are available. In addition, for a variety of reasons there may a considerable delay between initial joint aspiration and formal joint lavage i.e. lack of operating theatre availability. It is therefore important that antibiotics are commenced without delay. Which antibiotics, how they are administered and for how long are questions that have not been addressed in any particular studies (Lavy, 2007). A large meta-analysis and systematic review of antibiotic treatment for septic arthritis conducted by Stengel *et al.* (2001) failed to show an advantage of any one antibiotic regime over another. At present, antibiotic regimes are therefore chosen on the basis of the most likely causative organisms and altered accordingly following the acquisition of culture sensitivities. Given the

strong association of *S. aureus* and *Streptococci* with septic arthritis (Chander and Coakley, 2011), antibiotics are usually empirically selected to cover these pathogens (Goldenberg, 1998).

Regardless of antibiotic regime, the general consensus among clinicians is that intravenous antibiotics are advised in the early stages, with a move to oral antibiotics when the patient demonstrates clear signs of clinical improvement coupled with falling inflammatory markers. The majority of clinicians continue with the administration of antibiotics for 4-6 weeks although there is no compelling scientific backing for this duration (Lavy, 2007). Despite previously held historical views that rest after joint infection should be 'uninterrupted and prolonged' (Salter *et al.*, 1981), there is no evidence to suggest that patient immobilisation aids joint recovery following septic arthritis. Indeed, this was confirmed in a lapine study by Salter *et al.* (1981) whereby continuous passive motion gave improved clinical and pathological results following joint infection and injury. Mobilisation is therefore actively encouraged in patients with septic arthritis.

There is evidence from animal studies that the simultaneous administration of systemic antibiotics and intra-articular steroids may have a protective effect in reducing the extent of articular cartilage destruction (Wysenbeek *et al.*, 1998; Lavy, 2007). In a communication by Lane (2000), the successful treatment of a 62 year old man and an 87 year woman, who had ongoing pain and persisting synovitis despite antibiotics and bedside joint lavage, with a single intra-articular steroid administration was described. The return of both patients to a full and independent

life with no sequelae is reported. However, the administration of intra-articular steroids in humans with acute septic arthritis is not common practice, primarily through a fear of provoking overwhelming and unrestrained bacterial sepsis within the joint.

Despite current treatment strategies, some individuals develop an aggressive form of septic arthritis that results in rapid and catastrophic cartilage breakdown. It is all the more devastating for these individuals as subsequent joint replacement in this group is bedeviled by a greater risk of periprosthetic sepsis (Jerry *et al.*, 1988). Worryingly, retrospective studies suggest that some degree of permanent joint damage, involving direct cartilage injury, develops in up to 50% of cases (Kaandorp *et al.*, 1997b; Goldenberg, 1998; Krieg, 1999). This suggests that chondrocyte death may occur during septic arthritis, as these cells are, as previously mentioned, the only living agents capable of cartilage maintenance (Muir, 1995). However, the loss of chondrocytes, which are irreplaceable after skeletal maturity (Goldring and Marcu, 2009), and subsequent loss of cartilage integrity may not be clinically evident for years. Given the lack of long-term prospective studies following-up patients with septic arthritis, it is thus possible that supposedly treated episodes of septic arthritis may have seeded the foundations for future problems such as early onset osteoarthritis.

1.3.4 Pathogenesis

Septic arthritis ensues when bacteria colonise a synovial joint in sufficient numbers to trigger an acute inflammatory reaction. The pathogenesis is multifactorial and depends upon interactions between host joint tissues, the invading bacteria and the

host immune response. There are three defined stages during the development of septic arthritis: (1) bacterial joint colonisation, (2) establishment of infection and (3) induction of the host inflammatory response.

In the majority of cases, bacterial colonisation of a synovial joint arises through the haematogenous spread of bacteria (Goldenberg, 1998; Shirtliff and Mader, 2002; Lavy, 2007). The synovial membrane has no limiting basement plate under the well-vascularised synovium (Shirtliff and Mader, 2002; Lavy, 2007) thereby allowing the easy haematogenous entry of bacteria into the joint. It is unsurprising therefore that septic arthritis is commonly associated with a bacteraemic episode arising from a distant source, typically the chest or urinary tract. In addition, bacteria may also gain access to a joint from an infectious focus within adjacent structures. For example, in infants with metaphyseal osteomyelitis, the presence of small blood vessels crossing the epiphyseal growth plate may permit the extension of infection into the epiphysis and the joint space thereafter (Jackson *et al.*, 1992; De Boeck, 2005).

Rarely, direct joint colonisation may occur following intra-articular injections, surgical instrumentation or penetrating trauma. It has also been suggested that closed injury to a joint may predispose an individual to septic arthritis, the current hypothesis being that capillary blood stasis arising as a result of trauma creates a potential nidus for the development of infection (Lavy, 2007). It has also been postulated that microtrauma at the capillary level may reduce oxygen tension locally, thereby decreasing the efficiency of the host immune response (Shirtliff and Mader, 2002). This may explain why there is a higher incidence of septic arthritis of the

shoulder in children from sub-Saharan Africa (Smith *et al.*, 2002), as children in this part of the world are traditionally 'swung' onto the mother's back by holding the child's arm, thereby causing repeated episodes of minor injury to the shoulder joint. The association between microtrauma and the development of septic arthritis is indeed supported by a lapine study conducted by Olney *et al.* (1987), whereby microtrauma in the presence of bacteraemia was found to render joints susceptible to infection.

Once bacteria gain entry to the closed joint space, low fluid shear conditions within the joint promote bacterial adherence and the establishment of infection (Shirtliff and Mader, 2002). Some bacterial species, such as *S. aureus*, also have a variety of surface receptors for host proteins, termed 'microbial surface components recognising adhesive matrix molecules' (MSCRAMMs), that mediate adherence to host matrix components including fibronectin, laminin, elastin, collagen and hyaluronic acid (Shirtliff and Mader, 2002). Once the joint is colonised, bacteria rapidly proliferate and trigger an acute inflammatory response. During the early stages of infection, the inflammatory cytokines interleukin 1-β (IL-1β) and interleukin 6 (IL-6) are released into the synovial fluid by synovial cells, which subsequently activate the release of acute-phase proteins, for example CRP, from the liver (Lowy, 1998; Osiri *et al.*, 1998). There is also an accompanying influx of host inflammatory cells. The acute-phase proteins bind to the bacteria, promoting opsonisation and activation of the complement system. Phagocytosis of the bacteria is conducted by macrophages, synoviocytes and polymorphonuclear neutrophils and is associated with the further release of inflammatory cytokines including tumour

necrosis factor alpha (TNF-α), granulocyte-macrophage colony-stimulating factor (GMCSF) and interleukin 8 (IL-8) (Shirtliff and Mader, 2002). In addition, there is the further release of IL-1β and IL-6.

At a later stage, cells of the adaptive immune response ($CD4^+$ T cells) enter the joint and may aid bacterial clearance. Adaptive immunity consists of T-cell mediated (T-helper 1 (Th1)) and humoral (T-helper 2 (Th2)) responses but its role in septic arthritis remains to be fully defined. The cytokine gamma interferon (IFN-γ), produced by activated $CD4^+$ Th1 cells, has been shown to reduce mortality and the level of joint destruction in a murine model of Group B *Streptococcus*-induced septic arthritis. This is supported by Puliti *et al.* (2002) who identified that interleukin 12 (IL-12), a heterodimeric cytokine produced mainly by mononuclear phagocytes and B cells, reduced the extent of articular cartilage lesions and that this protective effect was mediated through IL-12 induced release of IFN-γ. In contrast however, a murine study of *S. aureus*-induced septic arthritis conducted by Zhao *et al.* (1998), identified that IFN-γ increased both the frequency and severity of septic arthritis whilst simultaneously, and paradoxically, protecting the mice from overwhelming septicaemia. In a further *S. aureus* murine study by Sasaki *et al.* (2000) investigating interleukin 4 (IL-4) and interleukin 10 (IL-10), cytokines produced by $CD4^+$ Th2 cells, both IL-4 and IL-10 were found to play a role in host resistance to infection through the regulation of IFN-γ. From the experimental studies to date it would therefore appear that particular components of the T-cell mediated immune response are beneficial for some bacterial species while destructive for others.

In the event that the host immune response is unable to contain the infection quickly, a fierce inflammatory response, associated with high levels of cytokines and reactive oxygen species, along with the release of bacterial virulence factors may rapidly cause cartilage destruction (Riegels-Nielsen *et al.*, 1989; Wysenbeek *et al.*, 1998; Shirtliff and Mader, 2002). Elevated cytokine levels stimulate the release of host matrix metalloproteinases, including stromelysin and gelatinase A & B, in addition to other collagen-degrading enzymes (Williams *et al.*, 1990; Williams *et al.*, 1991; García-Arias *et al.*, 2011). Furthermore, inflammatory cells, synovial cells and invading bacteria all release proteolytic enzymes that are capable of degrading the ECM, which may initiate within 8hrs of infection (Smith *et al.*, 1987). Cartilage integrity may be further compromised by the presence of a large joint effusion, which arises as a result of inflammation of the synovium and altered synovial fluid dynamics (Nade, 2003). The joint effusion increases intra-articular pressure, which mechanically impedes the blood and nutrient supply to the joint with subsequent destruction of the synovium and cartilage.

ECM degradation within septic joints is characterised by a rapid reduction in matrix proteoglycans, which typically occurs within 48hrs of infection (Smith and Schurman, 1983). This is followed by a more prolonged period of collagen loss, prior to the emergence of gross morphological changes over the articular surface (Smith *et al.*, 1987). In experimental models, at least 10 days must lapse before loss of collagen is detectable (Smith *et al.*, 1987).

Worryingly, an *in vivo* lapine study of *S. aureus*-induced septic arthritis by Smith *et al.* (1987) identified that some degree of cartilage destruction was still evident regardless of when antibiotics were commenced. Discouragingly, further studies on experimentally-induced *S. aureus* septic arthritis have confirmed the finding that continued cartilage destruction is a common occurrence in spite of joint lavage and the administration of antibiotics (Bobechko and Mandell, 1975; Salter *et al.*, 1981; Smith *et al.*, 1987). These experimental findings are corroborated by more recent retrospective clinical studies, which highlight some degree of joint destruction in up to 50% of patients with septic arthritis despite current treatment strategies (Kaandorp *et al.*, 1997b; Goldenberg, 1998; Krieg, 1999). To conclude, there is scientific evidence to suggest that both bacterial virulence factors and components of the host immune response play an important role in the overall cartilage destruction but it is not yet known what contribution each of these play in the destructive process.

1.3.5 Microbiology

Numerous bacterial species have been implicated in the development of septic arthritis. In adults, the most commonly isolated organism in adults is *S. aureus*, accounting for 40 to 65% of cases (Kaandorp *et al.*, 1997a; Gupta *et al.*, 2001). This increases further to 80% in patients with diabetes or rheumatoid arthritis (Goldenberg, 1998). Over the past decade, there has been concern over the increasing incidence of methicllin-resistant *S. aureus* (MRSA) (Cunningham *et al.*, 1996). Streptococci are also commonly implicated in septic arthritis, with *Streptococcus pyogens*, *Streptococcus pneumoniae* and group A β-haemolytic *Streptococci* being most frequently isolated (Goldenberg, 1998). Group B, C, G and

F *Streptococci* are also not infrequently involved, especially in immunocompromised patients or patients with either diabetes, malignancy or serious genitourinary or gastrointestinal infections (Morgan *et al.*, 1996; Ryan *et al.*, 1997; Schattner and Vosti, 1998). Gram-negative bacilli are identified in up to 20% of cases of septic arthritis and are commonly associated with intravenous drug abuse, the extremes of age, and immunocompromised patients (Morgan *et al.*, 1996; Dubost *et al.*, 2002). Of the gram-negative organisms, *Pseudomonas aeruginosa* and *Escherichia coli* are most frequently isolated (Shirtliff and Mader, 2002).

In neonates under the age of 2 months, the most common organisms associated with community-acquired septic arthritis are group B *Streptococci* followed by *S. aureus* and gram-negative bacilli (Lavy, 2007). Between the ages of 2 months and 4 years, *Haemophilus influenzae* has historically been most frequently implicated (Wilson and Di Paola, 1986; Peltola *et al.*, 1998). However, the overall incidence of *H. influenzae* septic arthritis has reduced considerably following the advent, and subsequent widespread administration, of the *H. influenzae* type b (Hib) vaccine (Peltola *et al.*, 1998). In a study by Bowerman *et al.* (1997), 165 cases of acute haematogenous osteomyelitis or septic arthritis presenting both before and after the introduction of the Hib vaccine were retrospectively analysed. In those patients presenting in the post-Hib vaccine era, *H. influenzae* was virtually non-existent.

In the absence of *H. influenzae*, *S. aureus* and group B *Streptococci* are now the most causative organisms in children of all ages (Dagan, 1993; Luhmann and Luhmann, 1999; De Boeck, 2005). In addition, some studies have reported an increased

incidence of joint infections by *Kingella kingae* (Yagupsky *et al.*, 1992). *K. kingae* is a normal oropharyngeal commensal in young children and its increasing association with septic arthritis is thought to mirror the decline of *H. influenzae* (Shirtliff and Mader, 2002).

Although *S. aureus* and *Streptococci* are the organisms most commonly implicated with septic arthritis in most countries, there are nevertheless some geographical variations. In the USA, the most common cause of septic arthritis in young healthy adults is the diplococcus gram-negative bacterial species *Neisseria gonorrhoeae* (Shirtliff and Mader, 2002). It is an uncommon cause of septic arthritis in Europe however. In sub-Saharan Africa, there is a high prevalence of *Salmonella*-induced septic arthritis in children. In a Malawian case series by Molyneux and French (1982) *Salmonellae* were the causative organisms in 23% of cases. This increased further to 59% in a Zambian case series by Lavy (2007).

1.4 *Staphylococcus aureus*

Given the destructive nature of *S. aureus*-induced septic arthritis and its high prevalence in all age groups, the work presented in this thesis exclusively focuses on this organism. Following a series of clinical observations approximately 140 years ago, Ogston described staphylococcal disease and its role in sepsis and abscess formation (cited by Lowy (1998)). Today, *S. aureus* remains a highly versatile and dangerous pathogen in humans. It is implicated in numerous serious pathologies including pneumonia and toxic shock syndrome. Despite recent advances in antimicrobial treatments, the frequencies of both community- and hospital-acquired

staphylococcal infections have steadily risen, with minimal change in the overall mortality (Kaech *et al.*, 2006; Stahl, 2009). *S. aureus* is therefore a highly adaptive organism, mutating with ease to overcome any obstacles in its path (Prunier *et al.*, 2003; Trong *et al.*, 2005; McAdam *et al.*, 2011).

S. aureus is a gram positive organism that is spherical in shape when viewed under the microscope. It is a facultative anaerobe that can grow by either aerobic respiration or through lactic acid fermentation of glucose (Fuchs *et al.*, 2007). When grown on agar plates, the bacteria cluster into small colonies that are golden in colour, thereby giving rise to the name '*aureus*' (latin for golden), which distinguish *S. aureus* from other staphylococcal species (**Figure 1.4**). A further distinguishing feature is the ability of *S. aureus* to produce 'clumping factor' (Moreillon *et al.*, 1995; Palmqvist *et al.*, 2004). This unique feature forms the basis of the 'latex agglutination test', which is routinely used in clinical practice. In the presence of *S. aureus* clumping factor, previously invisible latex particles clump together to the extent that they become visible to the naked eye (**Figure 1.4**). The test has a sensitivity and specificity of approximately 98% (van Griethuysen *et al.*, 2001) and is therefore an extremely reliable test for the identification of *S. aureus*.

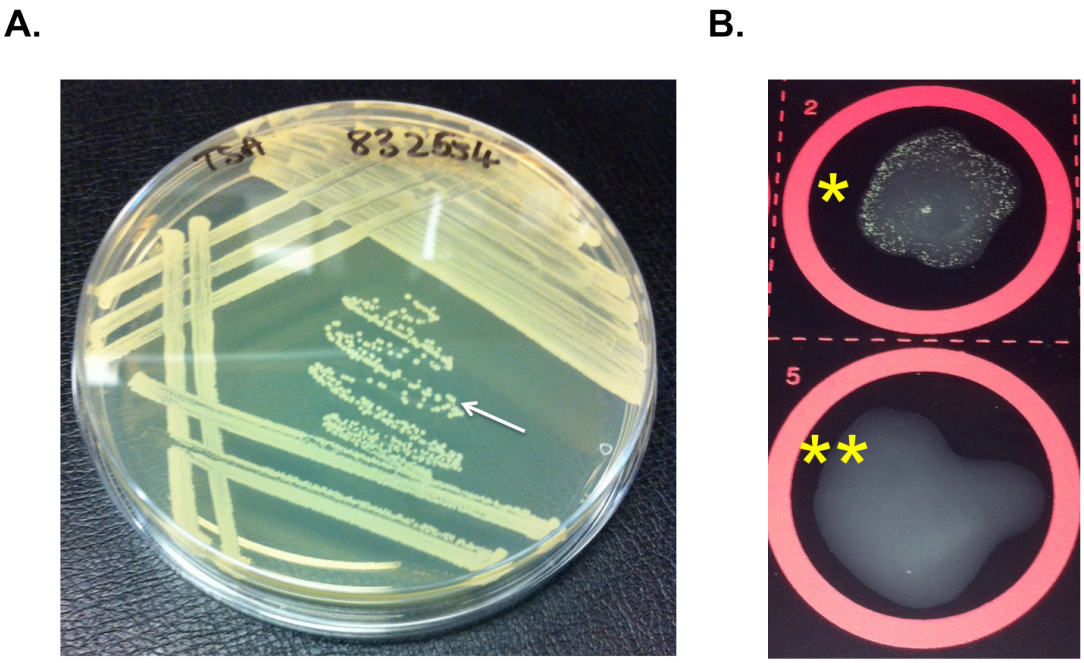

Figure 1.4: *Staphylococcus aureus* – typical appearance and positive identification

(A) When grown on agar plates *S. aureus* forms clusters of small round colonies that appear golden in colour (arrow). (B) The latex agglutination is used to confirm the presence of *S. aureus*. The clumping factor secreted by S. aureus results in the visible agglutination of small latex particles contained within the test solution (*). In comparison, there is no latex agglutination identified in the control sample (**).

S. aureus is known to produce a diverse array of potential virulence factors. Virulence factors are those bacterial components and products that enable the organism to both establish infection and enhance its potential to cause disease (Cunningham *et al.*, 1996). It is a commensal that colonises the axillae, groin, vagina, anterior nares, gastrointestinal tract, pharynx and broken skin surfaces (Noble *et al.*, 1967; Casewell and Hill, 1986). The moist squamous epithelium of the anterior nares is the main ecological reservoir however, with approximately 20% of individuals being persistently nasally colonised with *S. aureus* and a further 60%

being transiently colonised (Foster, 2005; Gordon and Lowy, 2008). Infections are initiated when a breach of the skin or mucosal barrier permits the access of *S. aureus* to adjacent tissues or the blood stream. Whether an infection is contained or spreads depends on a complex interplay between *S. aureus* virulence factors and host defense mechanisms. Individuals with *S. aureus* infections are commonly infected with their colonising strain (Williams *et al.*, 1959). In a multicentre study of *S. aureus* bacteraemia by von Eiff *et al.* (2001), the blood isolates were identical to those from the anterior nares in 82% of patients.

The armamentarium of *S. aureus* virulence factors is extensive, with both structural and secreted products playing a role in the pathogenesis of infection (Lowy, 1998). In order to establish infection, *S. aureus* must firstly adhere to host tissues (Edwards *et al.*, 2010). This is achieved through numerous surface receptors for host proteins, collectively referred to as 'microbial surface components recognising adhesive matrix molecules' (MSCRAMMS) (Gordon and Lowy, 2008). *S. aureus* may simultaneously express MSCRAMMS, otherwise known as adhesins, binding many different ECM proteins including collagen, fibronectin, fibrinogen, vitronectin, thrombospondin, elastin, laminin, bone sialoprotein, hyaluronic acid and osteopontin (Switalski *et al.*, 1993; Shirtliff and Mader, 2002). A number of adhesin genes have been identified and include genes encoding fibronectin binding proteins (*fnbA* and *fnbB*) (Jönsson *et al.*, 1991), fibrinogen binding proteins (*fib*, *cflA*, and *fbpA*) (Bodén and Flock, 1994), a collagen receptor (*cna*) (Patti *et al.*, 1992) and an elastin binding protein (*ebpS*) (Rosenbloom, 1996). A broad specificity adhesin (*map*) mediating low-level binding of several proteins including osteopontin, collagen, bone

sialoprotein, vitronectin, fibronectin and fibrinogen has also been identified (McGavin *et al.*, 1993). Collagen adhesin is considered to be particularly important in the pathogenesis of septic arthritis through its promotion of bacterial adherence to articular cartilage. An *in vitro* study by Switalski *et al.* (1993) identified that collagen receptor-positive strains adhered to both isolated type II collagen and cartilage explants in a time-dependent process. However, in the presence of blocking collagen receptor-specific antibodies bacterial adherence was inhibited.

Once *S. aureus* adheres to host tissues it is able to grow and persist through the use of a variety of evasive strategies. Firstly, *S. aureus* can form biofilms on both host and prosthetic tissue surfaces, which essentially shield the bacteria from the host immune response and antimicrobials (Donlan and Costerton, 2002). It is for this reason that infected joint prostheses are particularly difficult to treat. Secondly, *in vitro* studies have demonstrated that *S. aureus* can invade and subsequently survive within the immune privileged intracellular compartment of a variety of mammalian cells (Hudson *et al.*, 1995; Lammers *et al.*, 1999). Menzies and Kourteva (1998) and Kahl *et al.* (2000) have further demonstrated that whilst within this compartment they may also induce apoptosis of the host cell, thus enhancing the overall tissue destruction through the process of host cell internalisation (Menzies and Kourteva, 1998; Kahl *et al.*, 2000). Thirdly, *S. aureus* is able to form small-colony variants (SCVs), which are believed to play a key role in persistent and recurrent infections. *S. aureus* can produce a variant population that may be phenotypically very different to the parent strain, thereby conferring great survival flexibility (Proctor and Peters, 1998).

SCVs represent naturally occurring subpopulations of *S. aureus* that typically grow slowly and produce small non-pigmented and non-haemolytic colonies that demonstrate a number of other atypical characteristics including reduced coagulase production and increased resistance to both aminoglycosides and cell wall active antibiotics (Proctor *et al.*, 1995; Proctor and Peters, 1998). *In vitro* studies have demonstrated that SCVs can hide within host cells, where they are relatively protected form the host immune response and antibiotics (Kahl *et al.*, 1998; Gordon and Lowy, 2008). Once the host immune response has abated and antibiotic therapy has been completed, SCVs may revert to the highly virulent and rapidly growing parent form, lyse the host cell and re-establish infection (Proctor and Peters, 1998). The presence of quiescent intracellular SCVs may explain why *S. aureus* has the ability to lie dormant following an episode of infection, sometimes for many decades, prior to re-emergence as clinical disease in exactly the same location.

S. aureus displays many other characteristics that help it evade the host immune response during an infection. Firstly, neutrophil chemotaxis (the migration of neutrophils from the blood stream to the site of infection) is inhibited through the secretion of 'chemotaxis inhibitory protein of staphylococci' (CHIPS), which is produced by approximately 60% of *S. aureus* strains (de Haas *et al.*, 2004). Secondly, *S. aureus* demonstrates resistance to phagocytosis through the avoidance of opsonins (molecules that mark a cell for phagocytosis) present in normal serum, which include antibodies recognising cell surface components such as peptidoglycan and teichoic acid (Foster, 2005). This is achieved through the expression of surface-

associated anti-opsonic proteins and a polysaccharide capsule, both of which interfere with the deposition of antibodies and complement formation or their access to neutrophil complement receptor and Fc receptor. *S. aureus* phagocytosis by neutrophils is therefore compromised as it requires the recognition of bound complement and antibody. For example, protein A, a MSCRAMM, is a wall-anchored protein that binds the Fc region of the immunoglobulin IgG in an orientation that prevents its recognition by the corresponding neutrophil Fc receptor (Uhlén *et al.*, 1984; Foster, 2005; Gordon and Lowy, 2008). In addition, the majority of *S. aureus* clinical isolates express a thin microcapsular layer that is composed of serotype 5, 8 or 336 capsular polysaccharide (O'Riordan and Lee, 2004; Roghmann *et al.*, 2005). Animal infection models have identified that expression of type 5 and 8 capsular polysaccharide is associated with increased virulence (Luong and Lee, 2002). Studies conducting *in vitro* phagocytosis assays have identified that, in the presence of normal serum opsonins, the presence of the capsule reduced the uptake of *S. aureus* by neutrophils, indicating that the capsule is anti-opsonic (Nilsson *et al.*, 1997; Thakker *et al.*, 1998).

1.4.1 *S. aureus* toxins

In addition to immune evasion strategies, *S. aureus* may also indirectly attack the cells of the innate immune response through the release of toxins that specifically target and lyse leukocytes. These toxins are collectively referred to as leukotoxins and contribute to abscess formation through the widespread killing of neutrophils attempting to engulf and kill bacteria (Foster, 2005). Indeed, abscess formation is a typical feature of *S. aureus* infection (Cheng *et al.*, 2009). Four key leukotoxins

have been identified: Panton-Valentine leukocidin (PVL), gamma-haemolysin, leukocidin E/D and leukocidin M/F-PV-like (Menestrina *et al.*, 2003). Arguably the most widely studied leukotoxin is PVL, which is a two-component pore-forming toxin (i.e. it destroys host cells through the formation of cell membrane pores) that has a high affinity for neutrophils and macrophages (Lina *et al.*, 1999; Lipinska *et al.*, 2011). It is implicated in a rapidly growing number of serious skin infections (Diep *et al.*, 2004), severe necrotising pneumonia (Gillet *et al.*, 2002) and necrotising fasciitis (Miller *et al.*, 2005).

Another toxin that is frequently associated with *S. aureus* is toxic shock syndrome toxin-1 (TSST-1). This toxin first came to light as a result of a well-defined clinical syndrome in menstruating females associated with the use of high-absorbency tampons. Toxic shock syndrome (TSS) comprises fever, an erythematous rash, skin desquamation and hypotension, frequently associated with multi-organ failure (Cunningham *et al.*, 1996). Most cases have no associated bacteraemia, thereby implicating that TSS results from the systemic intoxication with a product or products elaborated by *S. aureus* (Dinges *et al.*, 2000). The gene for TSST-1 is found in 20% of *S. aureus* isolates (Lowy, 1998). In contrast, TSST-1 is detected in all *S. aureus* isolates from patients with TSS (Cunningham *et al.*, 1996). TSST-1 is a 22kDa protein and is regarded as a superantigen, stimulating non-specific T-cell proliferation by interacting directly with major histocompatibility complex class II molecules (Cunningham *et al.*, 1996). This leads to the massive systemic release of inflammatory cytokines and, ultimately, circulatory collapse.

1.4.2 *S. aureus* haemolysins

One of the cardinal features of *S. aureus* is its ability to secrete toxins that damage the membranes of host cells and not just cells of the innate immune response. It has been hypothesised that the purpose of destructive *S. aureus* toxins is to convert local host tissues into nutrients required for bacterial growth (Dinges *et al.*, 2000). Whilst *S. aureus* produces a diverse array of toxins that may contribute to host tissue destruction including, in addition to those already mentioned, proteolytic enzymes, enterotoxins A-E, and exfoliative toxins (ETA and ETB) (Tomita and Kamio, 1997; Dinges *et al.*, 2000), it is a group of exotoxins known as 'haemolysins' that are believed to be key virulence factors. This knowledge has been obtained from studies investigating a variety of *S. aureus*-related infections (O'Callaghan *et al.*, 1997; Schmitz *et al.*, 1997; Dajcs *et al.*, 2002; Hayashida *et al.*, 2009).

The haemolysins, so-called because of their ability to lyse erythrocytes, consist of four toxins: alpha(Hla)-, beta(Hlb)-, gamma(Hlg)- and delta(Hld)-haemolysin (otherwise known as alpha(α)-, beta(β)-, gamma(γ)- and delta(δ)-toxin).

1.4.2.1 Alpha-haemolysin

Hla is a 33kDa pore-forming toxin that is secreted by the majority of *S. aureus* clinical isolates and is believed to play a major role in the pathogenesis of *S. aureus* infections including pneumonia (Bubeck-Wardenburg *et al.*, 2007), sepsis (Patel *et al.*, 1987), brain abscess (Kielian *et al.*, 2001) and corneal infections (Callegan *et al.*, 1994; Hume *et al.*, 2000). Hla is encoded by the gene *hla*, which was sequenced by Gray and Kehoe (1984), and is released by the bacteria in a monomer form before

integrating into the host cell membrane and organising with other membrane-bound Hla monomers into cylindrical heptamers (**Figure 1.5**) (Gouaux, 1998). It is in this oligomeric form that Hla is capable of inducing eukaryotic cell death. Once the cylindrical heptamer has formed on the cell membrane, a 1- to 2-nm transmembrane pore is established (**Figure 1.5**) that permits both the influx and efflux of ions and small molecules that ultimately results in the disruption of the ionic equilibrium, osmotic swelling and cellular demise (Dinges *et al.*, 2000). Hla is active against a wide variety of mammalian cells but has extraordinarily marked activity against rabbit (lapine) erythrocytes, a feature that permits its laboratory identification on rabbit blood agar plates. In addition to its pore-forming abilities, Hla has also been shown to induce the release of pro-inflammatory cytokines and chemokines including IL-6, IL-1β, IL-1α, IL-8, TNF-α, KC and MIP-2 (Bhakdi *et al.*, 1989; Dragneva *et al.*, 2001; Onogawa, 2002; Bartlett *et al.*, 2008; Hruz *et al.*, 2009), thereby potentially further enhancing tissue destruction.

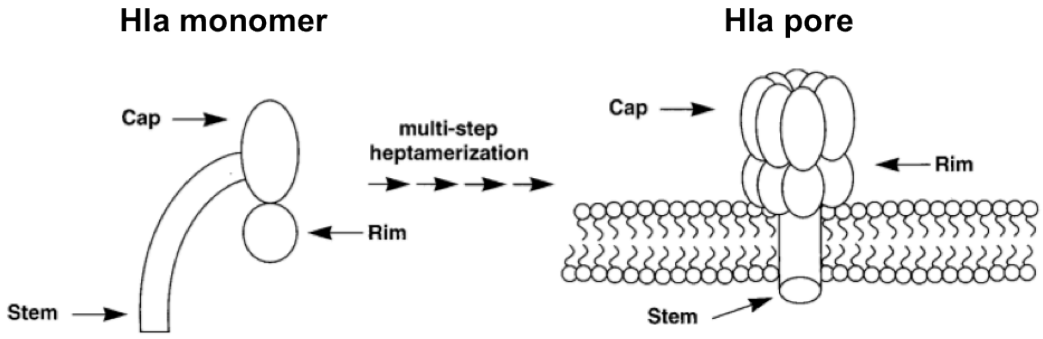

Figure 1.5: Formation of the Hla heptameric pore in a eukaryotic cell membrane

Hla is released from *S. aureus* in a monomer form. The rim domain of the toxin adheres to the plasma membrane and subsequent intertwining of the stem regions results in the formation of a transmembrane pore. Diagram taken from Dinges *et al.* (2000).

1.4.2.2 Beta-haemolysin

Hlb is a 35kDa toxin that was first identified in 1935 (cited by Dinges *et al.* (2000)). It is encoded by the *hlb* gene, a gene that was cloned and sequenced by Projan *et al.* (1989) and Coleman *et al.* (1986) and, in contrast to Hla, is highly haemolytic for sheep but not rabbit erythrocytes (Huseby *et al.*, 2007; Burnside *et al.*, 2010). Hlb is a Mg^{2+} dependent sphingomyelinase C that degrades sphingomyelin in the outer phospholipid layer of the erythrocyte membrane (Coleman *et al.*, 1986). The varied interspecies sensitivity to erythrocyte lysis by this toxin correlates with the sphingomyelin content in the erythrocyte outer membrane (Dinges *et al.*, 2000). The extremely high content of sphingomyelin in sheep erythrocytes thus renders them highly susceptible to lysis in the presence of Hlb. The haemolytic activity of Hlb is enhanced when erythrocytes incubated (37°C) in the presence of this toxin are chilled for a short period bellow 10°C (Wiseman, 1975; Coleman *et al.*, 1986; Huseby *et al.*, 2007). It is therefore frequently referred to as the 'hot-cold' haemolysin.

Hlb has been shown to play an important role in *S. aureus*-induced mastitis (Bramley *et al.*, 1989), pneumonia (Hayashida *et al.*, 2009) and corneal infections (bacterial keratitis) (O'Callaghan *et al.*, 1997). In addition, experimental studies have suggested that Hlb may play a role in the establishment of *S. aureus*-induced sinusitis through the impairment of nasal epithelial cell ciliary function (Kim *et al.*, 2000). Furthermore, a study by Katayama *et al.* (2013) investigating *S. aureus* murine ear colonisation demonstrated that the colonisation efficiency of a Hlb-producing mutant

was 50-fold greater than that of a Hlb-deficient mutant, thereby concluding that Hlb plays a major role in skin colonisation. This finding was further strengthened through the subsequent observation that Hlb had elevated cytotoxicity for human primary keratinocytes.

1.4.2.3 Gamma-haemolysin

Hlg is similar in both structure and function to PVL in that it is a bicomponent pore-forming toxin that has a high affinity for leukocytes (Dinges *et al.*, 2000; Yamashita *et al.*, 2011) i.e. it is a leukocidin. Together, they belong to a group of toxins known as the syrengohymenotropic toxins (Prévost *et al.*, 1995). Whilst PVL is only made by 2 to 3% of *S. aureus* strains, Hlg is secreted by virtually every strain (Siqueira *et al.*, 1997). Unlike PVL however, Hlg is able to lyse other mammalian cells, in particular erythrocytes. Hlg can be difficult to identify on laboratory blood agar plates due to the inhibitory effect of impurities in the agar on toxin activity. Hlg was first described in 1938 and is encoded by the *hlg* gene (cited by Dinges *et al.* (2000)). Together with TSST-1 it is believed to play an important role in the pathogenesis of toxic shock syndrome (Clyne *et al.*, 1988).

1.4.2.4 Delta-haemolysin

The final haemolysin is Hld, a 26 amino acid peptide encoded by the *hld* gene and produced by 97% of *S. aureus* isolates (Wiseman, 1975; Janzon and Arvidson, 1990; Burnside *et al.*, 2010). Hld, which was first reported in 1947 (cited by Verdon *et al.* (2009)), is able to lyse erythrocytes and a variety of mammalian cells as well as membrane bound organelles (Dinges *et al.*, 2000). It is also capable of lysing

bacterial protoplasts, spheroplasts, lysosomes and lipid spherules (Kreger *et al.*, 1971). Hld is believed to form an α-helix with hydrophobic and hydrophilic domains on either side and it has been proposed that it acts as a surfactant (Dinges *et al.*, 2000). At high concentrations it induces a detergent-like solubilisation of the plasma membrane, resulting in the formation of disc-shaped structures known as micelles and, ultimately, cell lysis (Verdon *et al.*, 2009). At present however, the exact contribution of Hld to *S. aureus* virulence *in vivo* remains unknown (Dinges *et al.*, 2000).

In summary, *S. aureus* is known to produce 4 haemolysins, all of which have the potential to induce target cell membrane damage: Hla, Hlb, Hlg and Hld (listed in chronological order of discovery). Hla acts by creating heptameric pores in a target membrane, Hlb presents sphingomyelinase C activity, Hlg is a bicomponent toxin that also acts by creating membrane pores and Hld permeabilises the target membrane.

1.4.3 Haemolysins and septic arthritis

Despite the numerous toxins produced by *S. aureus* it is not yet known which of these are directly damaging to chondrocyte viability. Mutant *S. aureus* strains with altered toxin profiles, established through genetic deletion or mutation, have helped to elucidate the roles of different virulence factors in an *in vivo* murine model of septic arthritis. These studies suggest that Hla may act alone or in conjunction with either protein A or Hlg to promote erosive joint damage in septic arthritis (Gemmell *et al.*, 1997; Nilsson *et al.*, 1999).

1.5 Hla-induced cell death and a potential role of calcium

A common finding of several studies investigating a variety of *S. aureus*-related pathology, including septic arthritis, is a likely central destructive role of Hla (Patel *et al.*, 1987; Callegan *et al.*, 1994; Gemmell *et al.*, 1997; Hume *et al.*, 2000; Kielian *et al.*, 2001; Ragle and Bubeck-Wardenburg, 2009; Wilke and Bubeck-Wardenburg, 2010). Whilst studies conducted by Walev *et al.* (1993) and Valeva *et al.* (2000) suggested that the important primary trigger of Hla-induced cellular demise was the influx of Na^+ coupled with the efflux of K^+ (Walev *et al.*, 1993; Valeva *et al.*, 2000), there is growing experimental evidence supporting a key role of Ca^{2+} in the eukaryotic cell death pathway (Seeger *et al.*, 1984; Suttorp *et al.*, 1985; Bhakdi and Tranum-Jensen, 1991; Jonas *et al.*, 1994; Kwak *et al.*, 2012; Berube and Bubeck-Wardenburg, 2013).

In health, Ca^{2+} is regarded as a ubiquitous intracellular messenger responsible for the control of numerous physiological cellular functions including exocytosis, gene transcription, cell differentiation and muscle contraction (Clapham, 1995; Berridge *et al.*, 1998). Indeed, it may be argued that mammalian life would not exist without Ca^{2+} as successful fertilisation of the egg relies upon a prolonged Ca^{2+} oscillation that ultimately triggers the cell division cycle (Berridge *et al.*, 2000). Thereafter, Ca^{2+} continues to play an important and essential role in the development and maintenance of cellular life. In chondrocytes, Ca^{2+} signalling has been shown to play an important role in ECM synthesis, cytoskeletal remodelling, and cell hyperpolarisation (Clark *et al.*, 1994; Valhmu and Raia, 2002; Erickson *et al.*, 2003;

Millward-Sadler and Salter, 2004; Madden *et al.*, 2014). Paradoxically however, a prolonged high intracellular Ca^{2+} concentration ($[Ca^{2+}]_i$) may lead to cell death (Clapham, 1995; Berridge *et al.*, 1998; Huser and Davies, 2007). In the majority of eukaryotic cells, Ca^{2+} exerts its major signalling function when it is transiently elevated within the cytosolic compartment (Huser and Davies, 2007). These Ca^{2+} transients have been shown to take various forms including waves, global or localised spikes, oscillations, micro-gradients and nano-gradients (Petersen *et al.*, 1994). Ca^{2+} transients may also spread from the cytoplasm into organelles such as the nucleus and mitochondria.

The $[Ca^{2+}]_i$ of most resting cells, including chondrocytes (Wilkins *et al.*, 2000), is approx.100nM, which is 20 000-fold lower than the 2mM found extracellulary in most tissues (Clapham, 1995). This rises to approx. 1000nM however during episodes of stimulation e.g. hormone stimulation, mechanical deformation or depolarisation (Petersen *et al.*, 1994). $[Ca^{2+}]_i$ is regulated by the simultaneous interplay of several counteracting processes (**Figure 1.6**). These can be divided into Ca^{2+} 'on' and 'off' mechanisms depending on whether they serve to increase or decrease $[Ca^{2+}]_i$ (Berridge *et al.*, 2000). The 'on' mechanisms include various plasma membrane channels, which regulate the inexhaustible supply of extracellular Ca^{2+} and include mechanically-activated Ca^{2+} channels, receptor-operated Ca^{2+} channels, store-operated Ca^{2+} channels and the well characterised voltage-dependent Ca^{2+} channels (prevalent in excitable cells) (Petersen *et al.*, 1994). There are also channels on the endoplasmic reticulum, the organelle that harbours the major intracellular Ca^{2+} pool (Clapham, 1995), that release Ca^{2+} from this finite

intracellular store (Berridge, 1993). Two important types of Ca^{2+} release channels have been identified within the endoplasmic reticulum, namely the ryanodine (RYR) and the inositol trisphosphate (IP_3) receptors (Petersen *et al.*, 1994). Both function to release Ca^{2+} from intracellular stores into the cytoplasm. Interestingly, the main activator of these channels is Ca^{2+} itself and this phenomenon is referred to as 'Ca^{2+}-induced Ca^{2+} release', a process that is believed to be central to Ca^{2+} signalling (Berridge *et al.*, 2000).

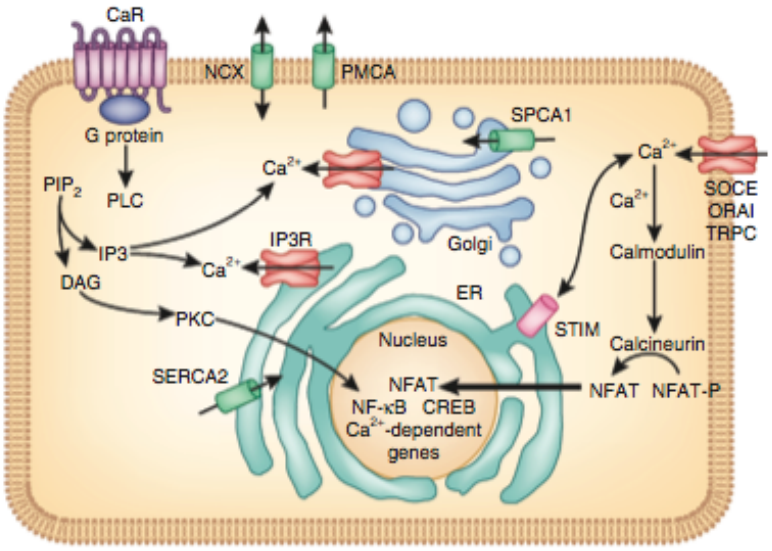

Figure 1.6: The major regulators of intracellular Ca^{2+} homeostasis

Plasma membrane pumps and channels (plasma membrane Ca^{2+} ATPase (PMCA), Na^{+}/Ca^{2+} exchanger (NCX) and store-operated Ca^{2+} channels (SOCE)) regulate the influx and efflux of Ca^{2+} from the cytoplasm. G-protein-coupled receptors such as Ca^{2+}-sensing receptor (CaR) initiate signals (e.g. inositol trisphosphate (IP3)) that modify compartmentalised Ca^{2+} stores. Ca^{2+} ATPases on organelles (e.g. sarco (endo)plasmic reticulum Ca^{2+} ATPase (SERCA) and secretory pathway Ca^{2+} ATPase isoform 1 (SPCA1)) monitor and restore intracellular Ca^{2+} storage sites. ER, endoplasmic reticulum; DAG, diacylglycerol; NFAT, nuclear factor of activated T cells; IP3R, inositol trisphosphate receptor; PKC, protein kinase C; PLC, phospholipase C; PIP_2, phosphatidylinositol 4,5-bisphosphate; STIM, stromal interaction molecule; TRPC, transient receptor potential C. Diagram taken from Mascia *et al.* (2012).

The 'off' mechanisms are more diverse and are employed by cells to remove Ca^{2+} from the cytosolic compartment. They include Ca^{2+} ATPases, located on the plasma membrane and endoplasmic reticulum (Carafoli, 1991; Petersen *et al.*, 1993; Berridge *et al.*, 2000), in addition to exchangers that utilise concentration gradients of other ions to provide the 'driving force' to transport Ca^{2+} out of the cell i.e. the Na^{+}/Ca^{2+} exchange (Petersen *et al.*, 1994). Furthermore, the cytosol contains slowly diffusible Ca^{2+}-binding proteins that are capable of rapidly buffering Ca^{2+} (Neher and Augustine, 1992). It is believed that these buffers act in the immediate vicinity of the Ca^{2+} release channels and the subsequent saturation of these buffers may be essential for both Ca^{2+} spike initiation and Ca^{2+} wave propagation (Petersen *et al.*, 1993). Finally, organelles other than the endoplasmic reticulum are believed to play an important role in Ca^{2+} homeostasis by sequestering or releasing Ca^{2+}. For example, mitochondria sequester Ca^{2+} rapidly during the development of the Ca^{2+} signal prior to releasing it slowly during the recovery phase (Duchen, 1999). The uptake of Ca^{2+} by the mitochondria is believed to be important in determining both the amplitude and spatio-temporal patterns of Ca^{2+} signals (Jouaville *et al.*, 1995; Budd and Nicholls, 1996; Duchen, 1999).

When the Ca^{2+} equilibrium is disturbed through injury, the fate of the cell relies on its ability to restore normal $[Ca^{2+}]_i$ through the previously described 'off' mechanisms. If this is not achieved then the cell will ultimately die. Persistently high $[Ca^{2+}]_i$ can lead to the rapid disintegration of cells (necrotic cell death) through the activity of Ca^{2+}-sensitive proteases (Trump and Berezesky, 1995; Berridge *et al.*,

1998). In addition, elevated $[Ca^{2+}]_i$ has also been implicated in apoptotic cell death (Berridge *et al.*, 1998; Duchen, 1999), a process that can be both physiological and pathological, and is thought to be mediated through Ca^{2+}-induced changes in gene transcription (Trump and Berezesky, 1995). Many cellular insults have the potential to affect $[Ca^{2+}]_i$ rapidly through their influence on one or more of the following: energy metabolism, ion translocation systems, trans-membrane signalling and plasma membrane integrity (Berridge *et al.*, 1998; Kristian and Siesjo, 1998; Huser and Davies, 2007). In the case of Hla, it is hypothesised that, in the presence of a marked concentration gradient between the intra- and extracellular compartments, the transmembrane Hla pores established on the plasma membrane permit a rapid influx of Ca^{2+} and subsequent overwhelming rise in $[Ca^{2+}]_i$ that is ultimately fatal to the cell (Berube and Bubeck-Wardenburg, 2013).

1.6 Confocal laser scanning microscopy (CLSM)

The maintenance of healthy articular cartilage is highly sophisticated and relies upon complex interactions between chondrocytes and the ECM (Muir, 1995). Such interactions are absent when chondrocytes are removed from their native environment i.e. during the experimental assessment of isolated *in vitro* chondrocytes, thereby potentially altering the susceptibility of these chondrocytes to experimental challenge. Thus, in order to acquire a more accurate representation of the *in vivo* situation, it would be advantageous to assess both the temporal and spatial responses of *in situ* chondrocytes following *S. aureus* toxin exposure.

Recent advances in microscopic techniques have permitted the assessment of undisturbed *in situ* cells without the need for physical sectioning. One such advanced high-resolution technique is confocal laser scanning microscopy (CLSM), which enables the generation of 3-Dimensional (3-D) images of fluorescently labelled *in situ* tissue architecture and microstructure following laser excitation (Dailey *et al.*, 1999; Klaus *et al.*, 2003; Sorensen *et al.*, 2003; Lin *et al.*, 2005). CLSM has even enabled *in vivo* imaging both in animals (Unal Cevik and Dalkara, 2003; Cockburn *et al.*, 2013; Pérez-Alvarez *et al.*, 2013; Williams *et al.*, 2013; Vacaru *et al.*, 2014) and in humans (Rajadhyaksha *et al.*, 1995; Jalbert *et al.*, 2003). CLSM is central to the hypotheses investigated in this thesis and an overview of its principles is detailed.

1.6.1 Overview

The concept of confocal microscopy was originally developed by Marvin Minsky in 1955 while he was a post-doctoral student at Harvard University (Jones *et al.*, 2005). He wished to image neural networks in unstained preparations of brain tissue and was driven by a desire to image biological events *in situ* with a clarity that exceeded conventional microscopes (Dailey *et al.*, 1999). However, due to a lack of the necessary intense light sources for imaging and a sufficiently powerful computer processor to handle large amounts of data, the idea was short lived. It was only 30 years later, following the development of powerful lasers and advanced computer processors, that confocal microscopy became an established technique within the scientific community. Nevertheless, despite significant technological advances Minsky's key concepts remain unchanged.

Unlike a conventional wide-field microscope, a confocal microscope creates a sharp high-resolution image of a tissue specimen by rejecting out-of-focus light from above and below the focal plane of interest (**Figure 1.7**). The image obtained represents a thin cross-section section of the specimen, which is acquired without the need for physical sectioning. Such a section is referred to as an 'optical section' and a series of consecutive optical sections along the vertical axis can be combined using imaging software to create a three-dimensional (3-D) reconstruction of the imaged volume of the specimen (**Figure 1.8**).

1.6.2 Principles

Standard wide-field fluorescent microscopy involves the simultaneous illumination of an entire specimen by a light source i.e. the entire specimen is flooded evenly with light (Combs, 2010). Consequently, the entire specimen is excited at the same time and the resulting fluorescence is captured by the microscope's photodetector or camera. However, a significant proportion of the captured fluorescence is out-of-focus (Claxton *et al.*, 2006) i.e. it originates from above and below the focal plane of interest, which ultimately compromises image quality. In contrast, CLSM permits the point-by-point illumination of a specimen (Semwogerere and Weeks, 2008). Coherent light, of known wavelength, is released from a gas or solid-state laser (excitation source) and passes through a spatial filter and beam expander before being reflected by a dichroic mirror (otherwise known as a beam splitter) and focused by an objective lens onto a single point (focal volume) on the specimen (**Figure 1.7**). Thereafter, emitted light travels back along a similar path to the

excitation light but on this occasion, as it is of longer wavelength than the excitation light, it passes through the dichroic mirror and is focused onto a 'pinhole aperture' (Jones *et al.*, 2005).

The pinhole aperture is unique to confocal microscopy (Combs, 2010) and is the source of the term 'confocal'. In-focus light i.e. light from the focal plane converges on the pinhole and passes through it. Conversely, out-of-focus light is unable to converge on the pinhole and is therefore rejected (**Figure 1.7**). Upon passing through the pinhole, only in-focus light proceeds to the photodetector where it is converted to an electrical signal and ultimately a computer-generated image (Claxton *et al.*, 2006). Like conventional microscopes, the objective lens can be changed according to the detail of study required.

The detected light originating from an illuminated volume element (single point) within the specimen represents one pixel in the resulting image. As the laser scans over the specimen, a whole image is obtained pixel-by-pixel and line-by-line. The laser beam is scanned across the sample in the horizontal plane with the use of motorised oscillating mirrors. Information can be gathered from different focal planes by either raising or lowering the microscope stage or objective lens. Using computer software, a 3-D image of the specimen can be generated by assembling a stack of 2-D images (optical sections) from successive focal planes. This is collectively referred to as a '*z-stack*' (North, 2006) (**Figure 1.8**).

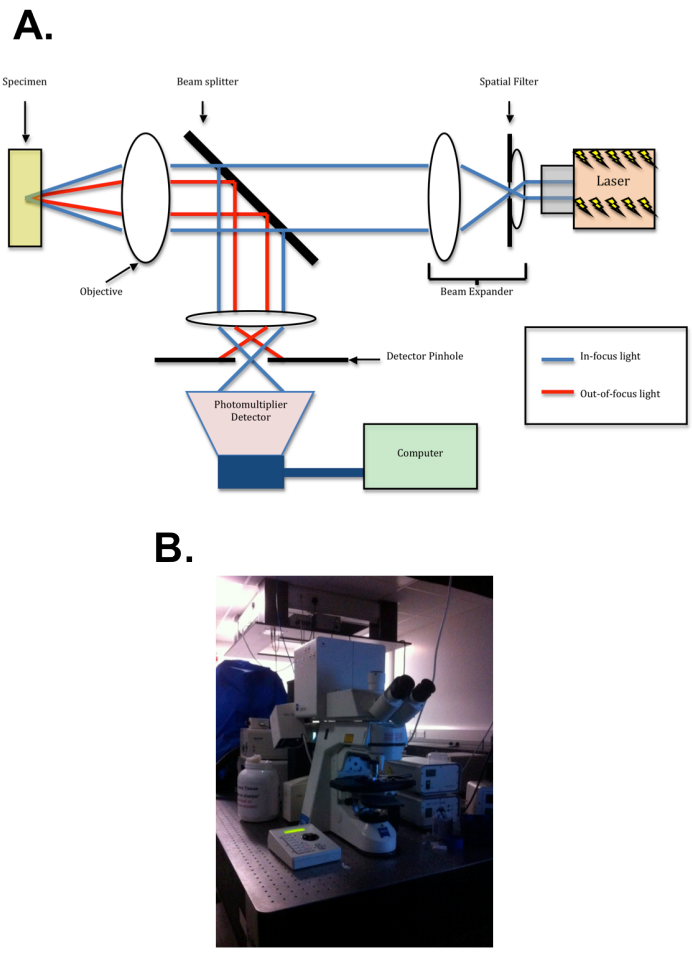

Figure 1.7: Confocal laser scanning microscopy

(A) Simplified diagram of the system setup of a confocal laser scanning microscope illustrating the principles of point-by-point illumination and the rejection of out-of-focus light (adapted from Jones *et al.* (2005)). Light from the laser reflects off the beam splitter (dichroic mirror) and excites one point on the fluorescently labelled specimen. The dye in the specimen is excited by the laser light and subsequently emits light of a different wavelength i.e. it fluoresces. The emitted light passes through the beam splitter and is focused onto the detector pinhole. Out-of-focus light is prevented from reaching the photomultiplier detector by the pinhole. The entire specimen is progressively illuminated through the use of a set of rotating mirrors (not shown). **(B)** One of the confocal microscope systems utilised during this study.

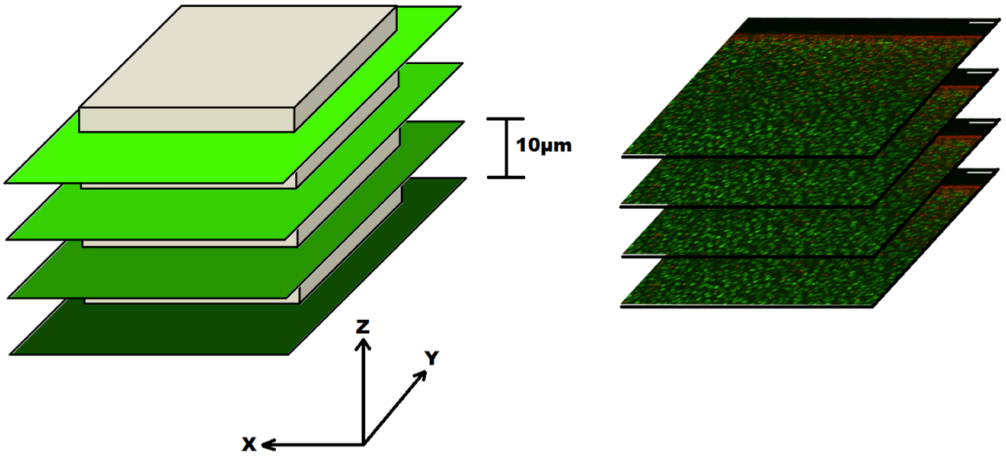

Figure 1.8: CLSM optical sectioning

Using computer software, a series of 2-D images from successive focal planes along the *z-axis* can be combined to form a 3-D image of the specimen. This is collectively referred to as a '*z-stack*'. Image kindly provided by Mr Joseph Winstanley, Centre for Integrative Physiology, The University of Edinburgh.

In the scientific world, most confocal microscopes acquire optical sections by stimulating fluorescence from fluorophores embedded within various components of the specimen (Jones *et al.*, 2005; Waters, 2009). A fluorophore is defined as a chemical compound that emits light upon light excitation (Semwogerere and Weeks, 2008). There are a vast number of highly specific fluorophores available and those chosen will depend on the particular study. For example, fluorophores are available to distinguish between living and dead/dying cells while others permit the dynamic assessment of alterations within the intracellular environment i.e. pH and Ca^{2+} concentration. It is possible to label the same specimen with multiple fluorophores, thereby enabling several parameters to be investigated at the one time (Nwaneshiudu

et al., 2012). Current advances in CLSM have primarily focused on the generation of novel fluorophores (Jones *et al.*, 2005).

The combination of fluorophores and CLSM is frequently referred to as 'fluorescence-mode' CLSM. The fluorophores are the only visible component with this particular form of confocal microscopy i.e. unstained microstructure is not visible. All fluorophores have unique excitation and emitted light spectra (Tsien and Waggoner, 2006). The laser light source is used to excite the fluorescently labelled tissue with a wavelength that is close to the peak excitation wavelength of the chosen fluorophore and filters are set to capture the wavelength of the emitted light, which is of a longer wavelength than the excitation wavelength. With point-by-point illumination of the fluorophore labelled specimen a 3-D image of the emitted fluorescence is generated.

1.6.3 CLSM and articular cartilage

Fluorescence-mode CLSM has become a popular experimental tool in the field of cartilage research over the past 20 years as a result of its diversity and unprecedented high-resolution non-invasive imaging (Jones *et al.*, 2005). It has previously been used to characterise both healthy and non-degenerate articular cartilage (Bush and Hall, 2003), assess the morphology and deformation behavior of chondrocytes (Guilak *et al.*, 1999), image components of the ECM (Poole *et al.*, 1992), study the response of articular cartilage to mechanical trauma (Amin *et al.*, 2008), and investigate cartilage repair techniques (Huntley *et al.*, 2005).

1.7 Rationale and aims of the thesis

The rationale of this work is based on gaining further insight into the interaction between *S. aureus* haemolysins and *in situ* chondrocytes during an episode of septic arthritis. It is envisaged that the knowledge acquired during this study may be of translational relevance with regard to both current clinical practice and the future development of novel chondroprotective therapeutic strategies. The objectives of this thesis may be summarised as follows:

1. To develop an *in vitro* model of *S. aureus*-induced septic arthritis that, in conjunction with fluorescence-mode CLSM, allows the spatial and temporal quantification of *in situ* chondrocyte viability following *S. aureus* culture with bovine articular cartilage.

2. Utilise this model, which avoids the complexities of a host immune response, to assess the influence of *S. aureus* haemolysins on *in situ* chondrocyte viability through the use of specific 'haemolysin-knockout' isogenic mutant strains of *S. aureus* (see Chapter 4).

3. Assess the influence of altered culture medium osmolarity and extracellular Ca^{2+} on *S. aureus* haemolysin-induced *in situ* chondrocyte death. The rationale for assessing these parameters is detailed in Chapter 5.

4. To attempt to measure dynamic changes in intracellular Ca^{2+} concentrations within *in situ* chondrocytes using a live-cell CLSM imaging system and

thereafter assess alterations in intracellular Ca^{2+} during *S. aureus* haemolysin exposure.

1.8 Hypothesis

This thesis tested the hypothesis that Hla is the key damaging *S. aureus* toxin to *in situ* chondrocyte viability and that its destructive action is associated with a rise in intracellular Ca^{2+}.

1.9 Overview of the chapters

In Chapter 2, general methodologies relevant to all 'results chapters' (Chapters 3-6) are provided including a description of an *in vitro* model of *S. aureus*-induced septic arthritis. The technique of CLSM to assess 3-D *in situ* chondrocyte viability following *S. aureus* haemolysin exposure and the subsequent methods for quantitative analyses are described.

Chapters 3-6 comprise the main results section and encompass all of the objectives of the thesis. Each results chapter contains a methodology section detailing additional methodology specific to that particular chapter. In Chapter 3, temporal and spatial *in situ* bovine chondrocyte viability following exposure to an established laboratory strain and clinical strains of *S. aureus* is assessed. In Chapter 4, the chondrocyte damaging potential of *S. aureus* Hla, Hlb and Hlg is investigated. In Chapter 5, the influence of both altered culture medium osmolarity and extracellular Ca^{2+} concentrations on *S. aureus* haemolysin-induced *in situ* chondrocyte death is

studied. In Chapter 6, alterations in intracellular Ca^{2+} levels within *in situ* chondrocytes during exposure to *S. aureus* haemolysins are examined.

In Chapter 7, the merits and limitations of this work are discussed. The translational relevance of the findings, with regards to both current and future clinical practice, are also considered.

Finally, the appendix includes a copy of a peer-reviewed published paper, which is based on the findings presented in Chapter 3 of this thesis. In addition, a list of published abstracts and presentations relating to this work is provided.

CHAPTER 2

GENERAL MATERIALS & METHODS

The materials and methods presented within this chapter represent general methodology relevant to all 'results' chapters (Chapters 3-6). Where appropriate, additional materials and methods specific to the individual experiments presented within a particular results chapter are addressed within that chapter.

2.1 BIOCHEMICALS AND SOLUTIONS

Biochemicals were obtained from Invitrogen Ltd (Paisley, UK) unless otherwise stated. Formaldehyde solution (4% v/v in normal saline) was obtained from Fisher Scientific (Loughborough, UK) and normal saline (0.9% w/v) was obtained from Baxter's Healthcare (Thetford, UK).

2.1.1 Bacterial and tissue culture media

The standard bacterial culture media were tryptone soya agar (TSA) and tryptone soya broth (TSB, Oxoid Ltd, Basingstoke, UK). The standard tissue culture medium was serum-free Dulbecco's Modified Eagle's Medium (DMEM). However, several distinct variants of DMEM were utilised for the experimental work presented in this thesis and the particular variants used for each study are detailed within the materials and methods section of each results chapter. Penicillin (50 U/ml) and streptomycin (50μg/ml) were added to DMEM for all experiments not involving bacterial culture.

2.1.2 Fluorescent probes

A two-fluorophore cell viability assay was utilised to identify live and dead cells:

1. LIVE CELLS: 5-chloromethylfluorescein diacetate (CMFDA) passes freely through the plasma membrane and is subsequently cleaved by cytosolic

esterases in metabolically active cells only i.e. in living cells; a process that removes the acetate groups (Jones *et al.*, 2005). The resultant molecule (5-chloromethylfluorescein), which fluoresces green following laser excitation (see section 2.6 for details), is impermeable to cell membranes and is therefore retained within the cell where it produces a uniform cytoplasmic staining (Stoddart *et al.*, 2006). CMFDA cell tracker Green™ was prepared as a 1mM stock solution in the solvent dimethyl sulphoxide (DMSO).

2. DEAD CELLS: Propidium iodide (PI) is impermeable to the plasma membrane of living cells (Krishan, 1975; Fried *et al.*, 1976; Jones and Senft, 1985). Once membrane integrity is compromised however, PI passes freely into the cell where it binds irreversibly to nuclear DNA (Unal Cevik and Dalkara, 2003). The DNA-PI complex fluoresces red following laser excitation (see section 2.6 for details) and therefore identifies the nuclei of dead or dying cells (membrane-compromised cells) only (Krishan, 1975; Jones and Senft, 1985; Huntley *et al.*, 2005). PI was used as an aqueous 1mM stock solution that was obtained directly from the manufacturer.

The use of CMFDA and PI is an accepted method utilised by many studies to label living and dead cells fluorescently, respectively (Jones and Senft, 1985; Bush and Hall, 2003; Lewis *et al.*, 2003; Unal Cevik and Dalkara, 2003; Huntley *et al.*, 2005; Jones *et al.*, 2005; Amin *et al.*, 2008; Bubeck-Wardenburg and Schneewind, 2008).

2.2 BACTERIA

2.2.1 Bacterial storage

For long-term storage purposes, all acquired *S. aureus* strains and clinical isolates were streaked onto TSA plates (with antibiotics where appropriate) with a sterile loop. Following 24hrs incubation (37°C), 'neat' bacteria were harvested with a sterile harvesting stick and transferred to vials containing 10% v/w skimmed milk (Oxoid Ltd., Basingstoke, UK). Thereafter, the vials were placed into -80°C storage.

2.2.2 Preparation of defined bacterial aspirates

When required, bacteria were thawed from -80°C storage and streaked onto TSA plates (with antibiotics where appropriate - see Chapter 4 for details regarding antibiotic resistance profiles of defined *S. aureus* isogenic mutant strains). Following 24hrs incubation (37°C), TSB (10ml), with antibiotics where appropriate, was inoculated with several individual bacterial colonies from the 24hr TSA plate of a given bacterial strain and cultured in a shaking incubator (37°C; 24hrs). Serial dilutions in normal saline, to a maximum of 10^{-6}, were performed on the 24hr TSB culture in order to calculate the number of colony forming units (cfu; a single cfu is defined as a bacterium that is capable of reproducing to form a group or 'colony' of the same bacterial sepcies; the number of cfu is therefore a measure of the number of active bacteria) in 1ml of 24hr TSB. Thereafter, 100µl of 10^{-4}, 10^{-5}, and 10^{-6} dilutions were spread evenly onto TSA plates and incubated (37°C; 24hrs) (**Figure 2.1**). Colonies, which appeared as isolated 'islands' of bacterial growth were then counted using a colony counter (Stuart®, Bibby Scientific Ltd, Stone, UK). Bacterial counts were performed on a number of cultures for each bacterial

strain/clinical isolate studied and a count of approx. $1.0x10^9$ cfu/ml (counts ranged from 1.0 to $1.25x10^9$ cfu/ml) was consistently obtained. Based on these results, a 24hr culture of each strain grown in 10ml TSB was diluted in DMEM to produce a final bacterial concentration of approx. $1.0x10^5$ cfu/ml DMEM (**Figure 2.1)**.

2.2.3 Preparation of defined bacterial supernatants

The 40hr cultures of a defined *S. aureus* strain were pooled and centrifuged (3400g; 10mins) to separate bacteria from toxins. The supernatant, containing the toxins, was harvested and filter-sterilised (0.22μm filter, Sigma-Aldrich, Gillingham, UK).

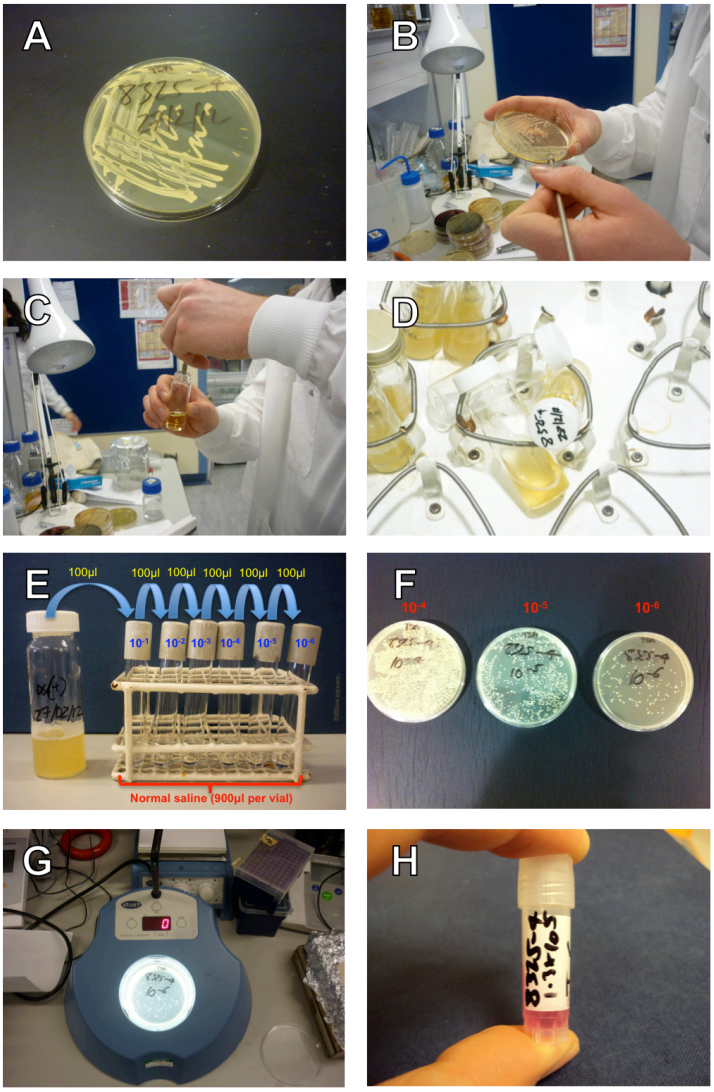

Figure 2.1: Preparation of a defined bacterial aspirate

A TSA plate was inoculated with the designated *S. aureus* strain and incubated (37°C; 24hrs) (**A**). Several individual colonies were then harvested from the TSA plate (**B**) and used to inoculate 10ml TSB (**C**). Following 24hrs incubation (37°C) in a shaker incubator (**D**), serial dilutions in normal saline, to a maximum of 10^{-6}, were performed on the 24hr TSB culture (**E**). Thereafter, 100µl of 10^{-4}, 10^{-5}, and 10^{-6} dilutions were spread evenly onto TSA plates and incubated (37°C; 24hrs) (**F**). Colonies were then counted using a colony counter (**G**). Based on these counts, and the assumption that the designated *S. aureus* strain would have a consistent growth curve in a standardised volume of TSB, a second overnight TSB culture was diluted in DMEM to give a final bacterial concentration of approx. $1.0x10^5$ cfu/ml (**H**).

2.3 BOVINE ARTICULAR CARTILAGE EXPLANTS

Bovine articular cartilage explants were harvested as oval osteochondral (articular cartilage with subchondral bone attached) blocks unless otherwise stated. The technique of harvesting these explants is detailed below.

2.3.1 Source of bovine tissue

Metacarpophalangeal joints of 3-year-old cows were washed, skinned, de-hoofed and opened within 12hrs of slaughter (**Figure 2.2**). Joints were opened within an extraction hood that was thoroughly cleansed with 70% ethanol spray prior to the commencement of each dissection i.e. an aseptic environment. All instruments were sterilised in 70% ethanol. Care was taken throughout the metacarpophalangeal joint exposure to prevent both contamination and iatrogenic injury (i.e. mechanical injury) of the articular surface. Only healthy joints, with no evidence of cartilage damage/degeneration, were used.

2.3.2 Cartilage explant harvesting

Prior to release of the collateral and intra-articular ligaments, the proximal limb was elevated to approx. 45° with the left hand, thereby permitting posterior reflection of the distal limb and the drainage of synovial fluid upon their release (**Figure 2.2** and **Figure 2.3**). Osteochondral explants were harvested from the convex weight-bearing articular surface between the intercondylar ridges (**Figure 2.2**). As the thickness, cell density, physical and biochemical characteristics of articular cartilage have been shown to vary according to mechanical load (Roberts *et al.*, 1986a; Roberts *et al.*, 1986b; Castano Oreja *et al.*, 1995; Adams, 2006; Rogers *et al.*, 2006), explants were

harvested from weight-bearing surfaces only in order to permit standardisation. Initial attempts to harvest osteochondral explants with a number-11 scalpel were unsuccessful, yielding small chondral 'flakes' lacking subchondral bone. The absence of subchondral bone also resulted in marked 'curling' of the explants, which is well characterised (Gibson and Davis, 1958; Fry and Robertson, 1967), rendering subsequent imaging and cell viability quantification difficult. Internal 'interlocked stresses' exist within the matrix (Fry and Robertson, 1967), with the outer layer of the tissue i.e. articular surface being maintained in tension (Chappuis *et al.*, 1983; Verteramo and Seedhom, 2004), and when these forces are unopposed i.e. when the subchondral bone anchor is removed the cartilage curls in the direction of the articular surface. The problems encountered with the number-11 scalpel were deemed to be due to the narrow and straight nature of the blade and subsequent use of the broader and convex shaped number-24 scalpel blade enabled the consistent harvesting of osteochondral explants with approx. 0.5mm subchondral bone attached (**Figure 2.3**).

Upon harvesting, each osteochondral explant was quickly transferred to a sterile Falcon tube containing DMEM with the harvesting scalpel blade. Once the harvesting procedure was complete, the explants were thoroughly irrigated in DMEM in order to remove the synovial fluid and reduce the chance of unwanted bacterial and fungal contamination. Thereafter, the explants were transferred to a sterile tissue culture flask using a 'no-touch' technique and re-suspended in a defined volume of fresh DMEM (5ml). This was achieved by firstly draining the DMEM carefully from the Falcon tube in order to retain the explants within the vessel and

thereafter inverting the Falcon tube so that the opening of the tube aligned with the opening of a vertically positioned tissue culture flask. The subsequent 'tapping' of the opening of the Flacon tube against the opening of the tissue culture flask resulted in the explants 'falling' into the tissue culture flask.

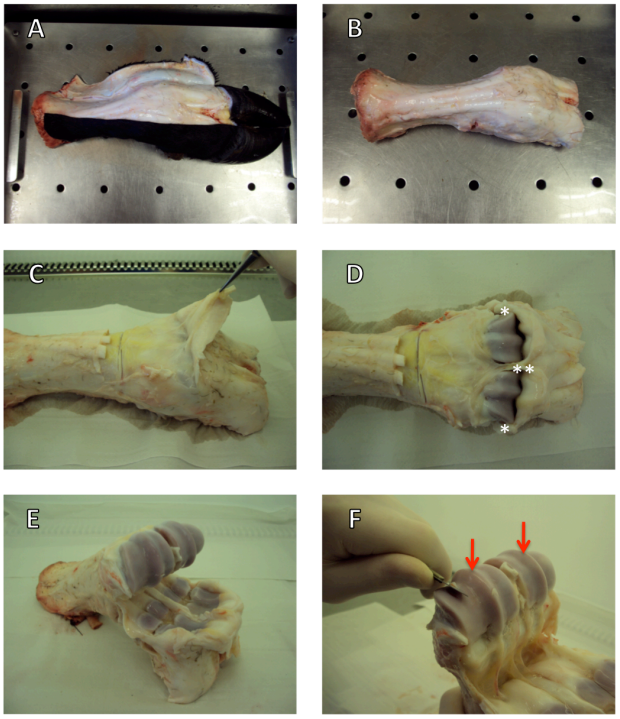

Figure 2.2: The exposure of the bovine metacarpophalangeal (anterior approach)

(**A**) Each bovine foot was washed in running water to remove excess dirt and skinned using a number-24 scalpel. (**B**) The hoof was removed and the skinned specimen generously sprayed with 70% ethanol to reduce the risk of cartilage contamination upon subsequent exposure of the joint. (**C**) The extensor tendons were divided, revealing the underlying joint capsule. (**D**) The joint capsule was dissected at its proximal margin and reflected distally to expose the joint. The collateral (*) and intra-articular (**) ligaments were divided and the distal limb reflected posteriorly in order to permit adequate joint exposure. (**E**) The articular surface was carefully inspected for evidence of degenerative disease/cartilage injury/contamination and if present the joint was discarded. (**F**) If the articular surface appeared healthy, osteochondral explants were harvested from the weight-bearing regions between the intercondylar ridges (arrows) with a fresh number-24 scalpel.

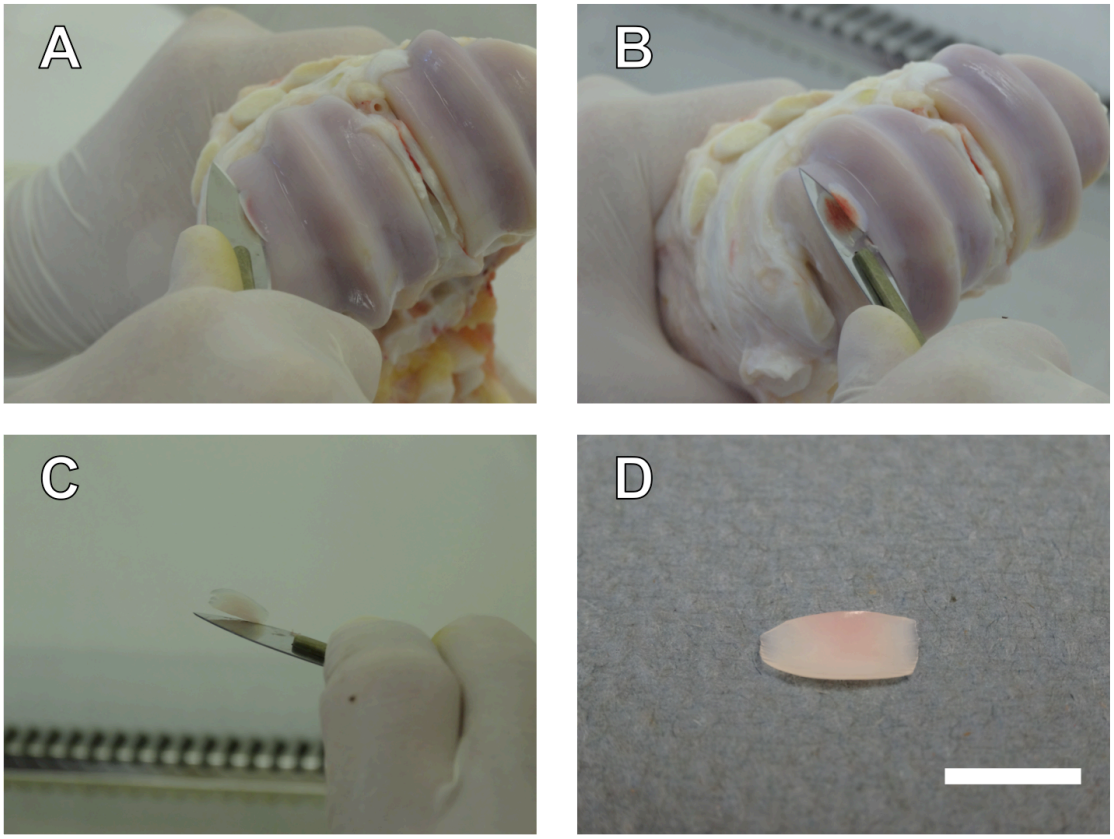

Figure 2.3: Osteochondral explant acquisition from the bovine metacarpophalangeal joint

(**A**) A sterile number-24 scalpel blade was engaged with the articular surface of the proximal limb at an angle that permitted the capture of an osteochondral explant i.e. not too steep or shallow. (**B**) Due to the convex nature of the number-24 scalpel blade, a steady forward and backward 'rocking' motion of the blade steadily yielded an osteochondral explant with approx. 0.5mm subchondral bone attached. The proximal limb of the joint was stabilised with the left hand throughout the harvesting procedure (note- these images were taken for illustration purposes only and a sterile chainmail glove should be worn on the stabilising hand at all times in order to prevent scalpel injury). (**C**) The explant was immediately transferred to a vessel containing DMEM using the harvesting blade i.e. a 'no touch' technique. (**D**) An example of a typical oval osteochondral explant (scale bar = 1cm).

2.4 INCUBATION

2.4.1 Bacterial culture studies

For each experiment, osteochondral explants from each foot were placed into separate tissue culture flasks containing DMEM (5ml). Thereafter, 25μl (approx. $2.5x10^3$ cfu) of a given *S. aureus* aspirate was injected into each flask. This concentration was chosen as it was in the range used by previous direct joint-inoculation *in vivo* studies of septic arthritis (Riegels-Nielson *et al.*, 1987; Lefevre *et al.*, 2011). In addition, preliminary experiments identified that it produced a measurable degree of chondrocyte death within a reasonable time period that was neither overwhelming nor weak. All flasks were incubated (37°C; 5% CO_2) for 40hrs unless otherwise stated.

2.4.2 Bacterial culture-supernatant studies

Bacterial culture-supernatants were prepared as previously described (see section 2.2.3). Thereafter, explants were incubated (37°C; 5% CO_2) with defined supernatants over 6hrs.

2.5 CELL VIABILITY STAINING AND FIXATION

At 0, 18, 24 and 40hrs (bacterial culture studies) or 0, 2, 4 and 6hrs (bacterial supernatant studies), explants were aseptically removed and trimmed so as to create two straight edges (**Figure 2.4**). Explants were then incubated (1hr; 21°C) in penicillin- and streptomycin-containing DMEM with CMFDA (10μM) and PI (10μM), which labelled living and dead chondrocytes green and red, respectively (Huntley *et al.*, 2005; Amin *et al.*, 2008). Explants were subsequently fixed (4%

formaldehyde) prior to storage (4°C) in phosphate buffered saline (PBS). For CLSM, explants were secured to the base of a Petri dish with Blu-Tack (Bostik, Leicester, UK) and re-submerged in PBS.

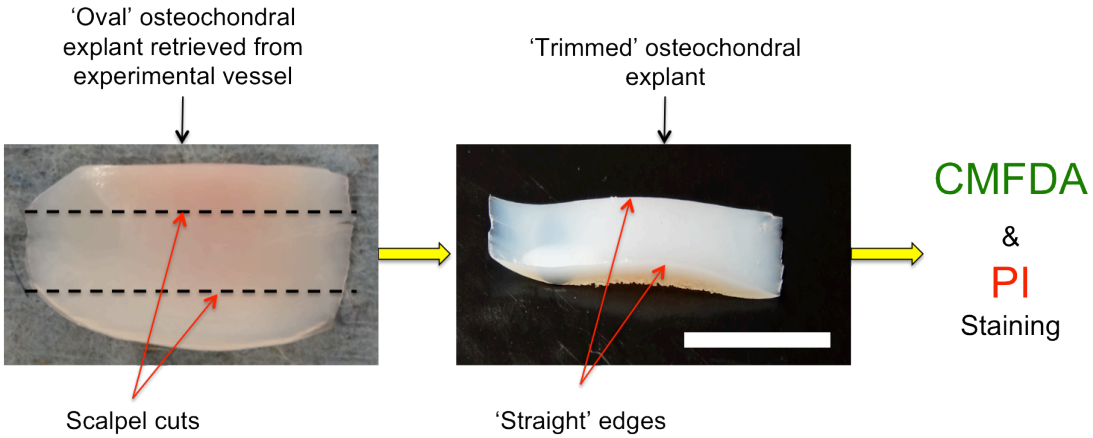

Figure 2.4: The preparation of osteochondral explants for cell viability staining

Upon retrieval from the experimental vessel, the oval osteochondral explant was trimmed, as depicted, with the single 'push-through' motion of a number-24 scalpel, establishing two straight edges (scale bar = 0.5cm). Thereafter, the explant was stained with CMFDA and PI.

2.6 CLSM

An upright Zeiss LSM510 Axioskop (Carl Zeiss Ltd., Welwyn Garden City, UK) CLSM, fitted with a x10/0.3 dry objective, was used to acquire optical sections of CMFDA- and PI-labelled *in situ* chondrocytes using established methods (Huntley *et al.*, 2005; Amin *et al.*, 2008). A 'multi-track protocol', utilising argon and helium-neon lasers, bandpass filters (500 to 550nm) and long pass filters (>560nm), permitted capture and visualisation of the fluorescence emitted from CMFDA (excitation wavelength (λex)=488nm, emission wavelength (λem)=517nm) and PI (λex=543nm, λem=650nm), respectively. Detector gain, detector sensitivity and laser power were adjusted to obtain optimal image quality without excessive dye bleaching or pixel saturation. The pinhole diameter was set to one Airy unit in order to achieve the optimal balance between image resolution and signal strength (Jones *et al.*, 2005).

For the purpose of image analysis in the present study, articular cartilage was loosely characterised into three distinct zones on the basis of depth-associated variation in cell and ECM properties: the superficial (SZ; up to 10% depth from the articular surface), middle (MZ; 10-40%) and deep zones (DZ; 40-100%) (Buckwalter and Mankin, 1997a; Jadin, 2005) (**Figure 2.5B**). Bovine cartilage is thinner than human cartilage (Athanasiou *et al.*, 1991) and depending on the joint assessed, varies in thickness from approx. 0.8 to 2.5mm (Schinagl *et al.*, 1997; Moo *et al.*, 2011; Pedersen *et al.*, 2013). However, cartilage zones within bovine cartilage have been shown to be comparable to those in human cartilage (Pedersen *et al.*, 2013). Depending on the experiment, images were obtained in either the axial or coronal

plane. For axial images (**Figure 2.5A**), the focal plane was moved through the tissue at 10μm increments (i.e. in the z-direction) from the articular surface to a depth of 100μm, thereby enabling detailed visualisation of chondrocytes within the entirety of the SZ and a small portion of the MZ. Axial images were always acquired with the cut-edge at the margin of the field-of-view for standardisation purposes (**Figure 2.5A**). Preliminary experiments that attempted image acquisition at 5μm intervals resulted in the creation of large file sizes that frequently could not be handled by the Volocity 4 software (Improvision, Coventry, UK) used throughout this study. In addition, imaging times were considerably prolonged with no apparent gain in cellular detail. Furthermore, previous studies using similar experimental techniques utilised 10μm increments successfully for the assessment of chondrocyte viability in human and bovine cartilage (Huntley *et al.*, 2005; Amin *et al.*, 2008; Amin *et al.*, 2009a; Amin *et al.*, 2009b; Amin *et al.*, 2010; Amin *et al.*, 2011).

For coronal images (**Figure 2.5B**), the focal plane was moved in a similar manner but from the 'cut-edge', which was created immediately prior to explant staining, into the tissue (i.e. in the y-direction) to a depth of 100μm, thereby enabling visualisation of the full thickness of cartilage. In both the axial and coronal plane, fluorescence was poor at depths greater than 100μm and therefore 100μm was set as the depth limit for image acquisition. Each optical section measured 921x921μm and had an image resolution of 1024x1024 pixels.

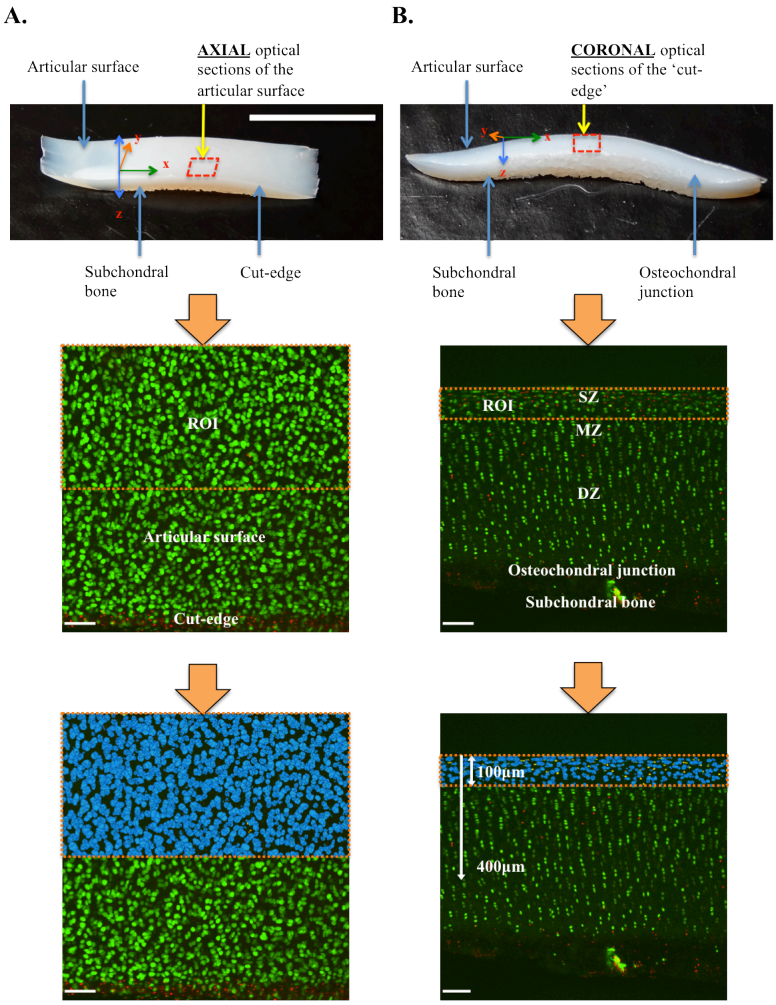

Figure 2.5: Axial and coronal imaging of CMFDA- and PI-labelled osteochondral explants and the subsequent quantification of *in situ* chondrocyte death

The x-, y- and z-axes of the trimmed osteochondral explants are illustrated (scale bar=0.5cm). Axial imaging (**A**) involved the acquisition of serial optical sections at 10µm intervals from the articular surface into the tissue to a depth of approx. 100µm i.e. focused imaging of SZ chondrocytes. For subsequent axial projections, live/dead cell counts were performed within a region of interest (ROI) that did not include the cut-edge shown. Coronal imaging involved the acquisition of serial optical sections at 10µm intervals from the cut-edge i.e cut surface into the tissue to a depth of approx. 100µm, thereby enabling the imaging of the the full thickness of cartilage. For coronal projections, chondrocyte viability was quantified within ROIs at 100µm intervals from the articular surface to a depth of 400µm. Living and dead cells were marked blue and yellow, respectively, following automated identification (scale bar = 100µm).

2.7 QUANTITATIVE ANALYSES

2.7.1 Percentage chondrocyte death

For reconstructed 3-D CLSM projections, the percentage chondrocyte death ((number of dead cells/total number of living and dead cells) x 100) was calculated within a defined region of interest (ROI) by using Volocity 4 imaging software to perform automated live/dead cell counts. The technique for automated cell counting within a particular ROI was based on a validated and reproducible protocol (Jomha *et al.*, 2003; Lin *et al.*, 2005; Amin *et al.*, 2008). Individual objects (cells) in both the green (living) and red (dead) channels were identified by establishing upper and lower limit percentage voxel (volumetric pixel) intensity thresholds (Lin *et al.*, 2005). These limits were set using a histogram of measured values for all objects identified in each channel and enabled the exclusion of background fluorescence. The upper limit was set at 100% for all images. However, the lower limits for each channel required minor adjustments (minimum 3% for green channel and 8% for red channel) in order to accommodate for variations in fluorescent dye loading and detector sensitivity between images. All cells touching the margin of the ROI were included in the counts. In addition, combined objects (two cells in close proximity incorrectly identified as single objects) within the ROI were separated using a dedicated feature embedded within the Volocity 4 software.

The above protocol returned a list of measured objects of variable size in the green and red channels. However, in order to discriminate between background noise and actual cells, objects were further excluded on the basis of volume. The volume of healthy, living chondrocytes typically ranges from 500-1200μm^3 (Bush *et al.*, 2005).

Therefore, when ordered by volume, objects in the green channel <500μm^3 and in the red channel <200μm^3 were attributable to background noise and thus excluded from the cell counts. The remaining objects were presented as the final automated live and dead cell count by the Volocity 4 software. In order to confirm visually the automated capture of living and dead cells within each ROI, living and dead cells were marked blue and yellow, respectively (**Figure 2.5**). Whilst good correlation between automated and manual counts has been identified, the reproducibility of the counts generated by the automated algorithm has been shown to be significantly better in comparison to human evaluation (Jomha *et al.*, 2003).

2.7.2 Axial and coronal regions of interest

The positioning and dimension of each ROI on axial and coronal CLSM reconstructions was standardised as follows:

1. Axial CLSM reconstructions

For axial projections, the percentage chondrocyte death was calculated within a 50% field-of-view region of interest (ROI) measuring 921x461x100μm (x-y-z axes, respectively). This ROI was created in order to avoid the cell death artefact induced by the scalpel blade at the cut-edge (Amin *et al.*, 2008) (**Figure 2.5A**).

2. Coronal CLSM reconstructions

For coronal projections, percentage chondrocyte death was quantified at 100μm intervals, within a ROI measuring 921x100x100μm (x-y-z axis, respectively), to a depth of 400μm from the cartilage surface (**Figure 2.5B**). Throughout this study, it

was observed that the thickness of bovine cartilage was usually between 600 and 700μm. However, in some explants the osteochondral junction was located between 400 and 500μm and therefore to avoid potential overlap of the osteochondral junction, the maximum depth limit for chondrocyte viability analysis was set at 400μm.

2.8 STATISTICAL ANALYSES

Statistical analyses were performed using SigmaPlot version 12 (Systat Software Inc., Chicago, USA). *N* refers to the number of feet from separate animals (independent experiments) and *n* refers to the number of individual explants (i.e. replicates) analysed per foot for each experimental group at each experimental time point. Values of all replicates were averaged to obtain a single observation for that animal.

All the assumptions underlying the statistical analyses were fulfilled. Normality and homogeneity of variance of all data were assessed using the 'Shapiro-Wilk' and 'Levene's equality of variance' tests, respectively. If the experimental data sets passed these tests, then appropriate parametric statistical analyses were conducted and if not, then suitable non-parametric statistical analyses were performed. It is appreciated that there are several numerical tests available to assess for normality. However, recent literature suggests that the Shapiro-Wilk test is the most powerful numerical normality test (Ghasemi and Zahediasl, 2012).

The specific parametric and non-parametric statistical tests used to analyse each experiment are detailed within each results chapter. Data are presented as means ± Standard Deviation (SD) with the level of significance set at $p<0.05$.

CHAPTER 3

A BOVINE CARTILAGE EXPLANT MODEL OF *S. AUREUS*-INDUCED SEPTIC ARTHRITIS

3.1 INTRODUCTION

This study primarily focuses on the laboratory 'wild-type' strain *S. aureus* 8325-4, a well-characterised prophage-cured derivative of strain NCTC8325 (Novick, 1967; Gemmell *et al.*, 1997). It is known to produce large amounts of Hla, Hlb, Hlg, Hld, protein A, lipase hyalonurate, staphylokinase, metalloproteinase, serine proteinase, coagulase, nuclease and acid phosphatase but does not produce any enterotoxins, PVL or TSST-1 (O'Reilly *et al.*, 1986; Nilsson *et al.*, 1999; Dajcs *et al.*, 2002; Monecke *et al.*, 2013). NCTC8325 was originally isolated from a sepsis patient in 1960 and its lineage remains a valuable resource for basic *S. aureus* research (Herbert *et al.*, 2010).

In addition to *S. aureus* 8325-4, this study also investigates clinical 'isolates' of *S. aureus*, isolated from the joint aspirates of patients presenting with *S. aureus*-induced septic arthritis. Tenover *et al.* (1995) define an **isolate** as "*a general term for a pure culture of bacteria obtained by subculture of a single colony from a primary isolation plate, presumed to be derived from a single organism, for which no information is available aside from its genus and species*". They further define a **strain** as "*an isolate or group of isolates that can be distinguished from other isolates of the same genus and species by phenotypic characteristics or genotypic characteristics or both. A strain is a descriptive subdivision of a species*". Some clinical infections are the result of a defined bacterial 'strain', which enables focused treatment strategies and future directed research. For example, outbreaks of haemorrhagic colitis with associated haemolytic uraemic syndrome following the consumption of contaminated cold meat products are typically associated with the

bacterium *Escherichia coli* 0157, a specific verotoxin-producing strain of *E. coli* (Sharp *et al.*, 1994; Waters *et al.*, 1994; Pennington, 2010).

At present, no studies have investigated whether *S. aureus*-induced septic arthritis is associated with a particular strain of *S. aureus*. Thus, in order to assess whether the acquired *S. aureus* clinical isolates were indeed the same *S. aureus* strain, clonally related or independent strains, pulsed-field gel electrophoresis (PFGE) was conducted. PFGE was first described by Schwartz and Cantor (1984) and is now considered the gold standard technique for *S. aureus* genotyping as it is one of the most reliable, discriminatory and reproducible typing procedures to enable the detection of a high degree of DNA polymorphism (Murchan *et al.*, 2003; Stranden *et al.*, 2003). It is based on the digestion of bacterial genomic DNA, which is achieved through the use of a restriction endonuclease (Liu *et al.*, 1996). The restriction endonuclease recognises few digestion sites in the chromosome, thereby generating large DNA fragments that can be effectively separated by periodically shifting the orientation of the electrical field (Levene and Zimm, 1987; Benson and Ferrieri, 2001).

Previous work investigating bacteria and associated toxins has primarily focused on isolated chondrocytes, cartilage explants or animal models (Smith and Schurman, 1983; Lee *et al.*, 2001). Isolated chondrocytes have the advantage of allowing easier control of experimental conditions but have the disadvantage of not allowing the study of chondrocytes in their 'native' extracellular environment. In contrast, chondrocytes within cartilage remain within their 'native' environment but studies to

date have utilised assays for either the release of ECM components (Jasin, 1983; Smith and Schurman, 1983) or degradative enzymes (Williams *et al.*, 1991) as experimental end-points. Although these may provide an important indication of ECM destruction, they give no information on chondrocyte viability following bacterial exposure. An *in vitro* model of septic arthritis whereby *in situ* chondrocyte death can be both directly visualised and quantified, whilst at the same time allowing better control of experimental variables in the absence of the complexities of a host immune response, would be highly desirable.

It is likely that there are two major mechanisms to the cartilage destruction that occurs in septic arthritis: (1) bacteria and associated toxins, and (2) components of the host immune response. However, the contribution from each of these is currently unknown. This study focuses on the former and aims to provide fundamental information about the effect of *S. aureus* and its toxins on *in situ* chondrocyte viability separate from the potentially confounding effect of the host immune response present in *in vivo* animal models. CLSM has been used to spatially define and quantify *in situ* chondrocyte death in a bovine cartilage model of septic arthritis (see Chapter 2), which is a novel approach in the field of septic arthritis research. Cartilage hydration following bacterial exposure has also been measured in order to assess cartilage integrity, as increased cartilage water content is a sensitive indicator of early cartilage matrix disruption (Buckwalter and Mankin, 1997b; Berberat *et al.*, 2009).

This study was conducted to improve the understanding of the interaction between bacteria and *in situ* chondrocytes with a view, ultimately, to improving the treatment

of septic arthritis.

3.2 HYPOTHESES

The first hypothesis was that both a laboratory strain and clinical isolates of *S. aureus* have a rapid and potent effect on *in situ* chondrocyte viability and cartilage integrity. The second hypothesis was that *S. aureus*-induced chondrocyte death commences within the superficial zone (SZ) of cartilage and progresses to deeper layers. The third hypothesis was that all investigated clinical isolates were independent strains of *S. aureus*.

3.3 MATERIALS & METHODS

3.3.1 Biochemicals and solutions

The standard tissue culture medium for this study was serum-free DMEM (Catalogue no. 41966; 340mOsm/Kg H_2O; pH7.4) with L-glutamine (4mM), D-glucose (25mM), sodium pyruvate (1mM) and sodium bicarbonate (44mM). DMEM of three pH values was used: pH7.4, pH6.4 and pH5.4 (adjusted using HCl; measured using a pH meter (FiveEasy™ pH, Mettler-Toledo Ltd., Leicester, UK)).

3.3.2 *S. aureus* strains and isolates

S. aureus strain 8325-4 was kindly provided by Professor T.J. Foster, Dept. Microbiology, Trinity College, Dublin, Ireland. A total of 5 *S. aureus* clinical isolates (**Table 3.1**), isolated from joint aspirates of patients presenting with *S. aureus*-induced septic arthritis, were obtained. Isolates 36V, 28G and 12R were randomly selected by an impartial observer for an *in situ* chondrocyte viability study.

Isolate	Gender	Age	Source
36V*	Male	46	Right Hip
28G*	Male	74	Right Wrist
12R*	Male	69	Left Knee
49L	Male	79	Right Hip
78B	Male	73	Right knee

Table 3.1: Source and details of *S. aureus* clinical isolates utilised in this study. (*) Denotes isolates randomly selected by an impartial observer for *in situ* chondrocyte viability study.

3.3.3 Pulsed-field gel electrophoresis

The main procedural steps for PGFE subtyping of *S. aureus* isolates are outlined in **Figure 3.1**. PFGE was conducted on *S. aureus* 8325-4 and all *S. aureus* clinical isolates (**Table 1**).

The following buffers were obtained from Severn Biotech Ltd, Kidderminster, UK for PFGE: TEN buffer (0.1M **T**ris Cl, 0.1M **E**DTA, 0.15M **N**aCl), EC (*E. coli*) buffer (6mM Tris Cl, 1M NaCl, 0.1M EDTA, 0.5% Brij 58, 0.2% deoxycholate, 0.5% Sarkosyl), TE buffer (10mM **T**ris, 5mM **E**DTA, pH 7.5) and 0.5X TBE buffer (40mM **T**ris Cl, 45mM **B**oric acid, 1mM **E**DTA, pH 8.3). Several individual colonies of a particular test isolate were harvested from a TSA plate using a sterile harvesting stick and transferred to an Eppendorf tube (microcentrifuge tube) containing TEN buffer (1ml), thereby establishing a test isolate suspension. The Eppendorf tube was then centrifuged (13 000rpm) for 2mins. Following

centrifugation, the pellet was re-suspended in EC buffer (500µl). Thereafter, lysostaphin (2µl of 1mg/ml solution (dissolved in 20mM sodium acetate)) and 1.2% low melt agarose (500µl) were added. The entire volume of the suspension within the Eppendorf tube was then pipetted into a plug mould and left at room temperature for 15mins. After 15mins, the plug was placed into a bijoux containing EC buffer (3ml), which was subsequently placed into a water bath (37°C) for 1hr. Thereafter, the EC buffer was removed and replaced with TE buffer (3ml) prior to a further 1hr incubation (55°C) period. Upon completion of this incubation period, the TE buffer was replaced with fresh TE buffer and the plug was refrigerated (4°C) until required.

Following removal from refrigerated storage, a portion of the plug (approx. 2mm x 2mm) was cut with a sterile number-11 scalpel blade and transferred to a fresh Eppendorf tube, to which distilled water (DW) (90µl) and reaction buffer (10µl) were added. The Eppendorf tube was then placed into a refrigerator (4°C) for 30mins. Thereafter, the buffer was carefully removed using a fine pastette and replaced with DW (90µl), reaction buffer (10µl), bovine serum albumin (2µl; 1mg/ml), dithiothreitol (2µl; 1.5mg/100µl DW) and restriction enzyme (2µl; *Xba*I). Finally, the Eppendorf tube was immersed in a water bath (25°C) for 5hrs. The above procedure was simultaneously conducted for each *S. aureus* isolate investigated.

A pulsed field agarose gel was prepared by adding pulsed field agarose (1g) to 0.5X TBE buffer (100ml). The liquid agarose was poured into a gel mould and allowed to set. Upon setting, plugs within the Eppendorf tube (one plug per isolate investigated) were placed into the wells in the gel. Thereafter, the gel was

transferred to the centre of a PFGE tank containing approx. 2L 0.5X TBE buffer (buffer continuously circulated by circulator pump). PGFE was performed using a contour-clamped homogenous electric field apparatus (CHEF DRII System, BIO-RAD Laboratories Ltd, CA, USA). Running parameters were as follows: 14°C; 200V (6V/cm); initial pulse time, 5secs; final pulse time, 40secs; and total time, 20hrs. *Saccharomyces cerevisiae* chromosomal DNA (Mortimer and Schild, 1985) in 1.0% low-melt agar (BIO-RAD Laboratories Ltd, CA, USA) was used as a molecular size standard (MSS) (DNA size marker).

After the electrophoresis run was completed, the gel was stained with Gel Red (7.5µl in 250ml 0.1M NaCl) for 20mins in a covered container. Thereafter, the gel was photographed using a gel doc system (Molecular Imager® Gel Doc™ XR System, BIO-RAD Laboratories Ltd, CA, USA) and visually analysed. Strains were defined as either (1) representing the same strain if they possessed 100% similarity to the restriction fragment patterns of DNA (PFGE profile) or (2) having a clonal relationship if they possessed 85% similarity between PFGE profiles. The 85% cut-off for clonal relationship was chosen as it was considered that similarities above this level could be accounted for by changes consistent with a single genetic event i.e. point mutation or an insertion or deletion of DNA (Tenover *et al.*, 1995; Ejrnaes *et al.*, 2006).

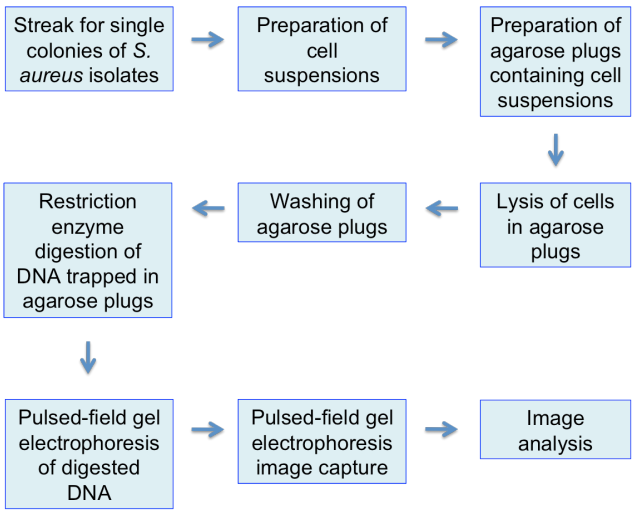

Figure 3.1: Main procedural steps for pulsed-field gel electrophoresis of *S. aureus* isolates

3.3.4 Bovine chondral explants

For the experiment investigating the sensitivity of SZ chondrocytes to bacterial toxins, chondral (subchondral bone-free) explants were obtained. This was achieved by flattening the angle of the number-24 scalpel blade upon engaging the articular surface. Instead of a forward and backward rocking motion (as per the harvesting of osteochondral explants), the blade was simply pushed through the cartilage in a plane that was parallel to the bone-cartilage interface. For all other experiments, osteochondral explants were harvested as previously described (see Chapter 2)

3.3.5 Bacterial culture and pH studies

For each experiment, osteochondral explants from each joint were placed into separate tissue culture flasks containing DMEM (5ml). Thereafter, 25µl ($2.5x10^3$ cfu) of a given bacterial aspirate was added to each flask. A similar experiment was conducted whereby cartilage explants were cultured in non-infected DMEM at pH

values of 7.4, 6.4 or 5.4. For a post-infection long-term chondrocyte viability study, explants were initially cultured with *S. aureus* 8325-4 for 40hrs. The infected culture medium was then aspirated and the cartilage rinsed with normal saline in order to remove residual bacteria and their toxins. Fresh DMEM containing penicillin (50 U/ml) and streptomycin (50µg/ml) was then added, and the culture resumed for a further 14 days. The 8325-4 strain was known to be sensitive to penicillin (**Figure 3.2**) and therefore would not grow in culture medium containing this antibiotic.

3.3.6 Bacterial supernatant study

The 40hr cultures of *S. aureus* 8325-4 were pooled and centrifuged (3400g; 10mins) to separate bacteria from toxins. The supernatant, containing the toxins, was harvested and filter-sterilised (0.22µm filter). Subchondral bone-free explants were then exposed to the supernatant (37°C; 5% CO_2) over a 6hr time-course.

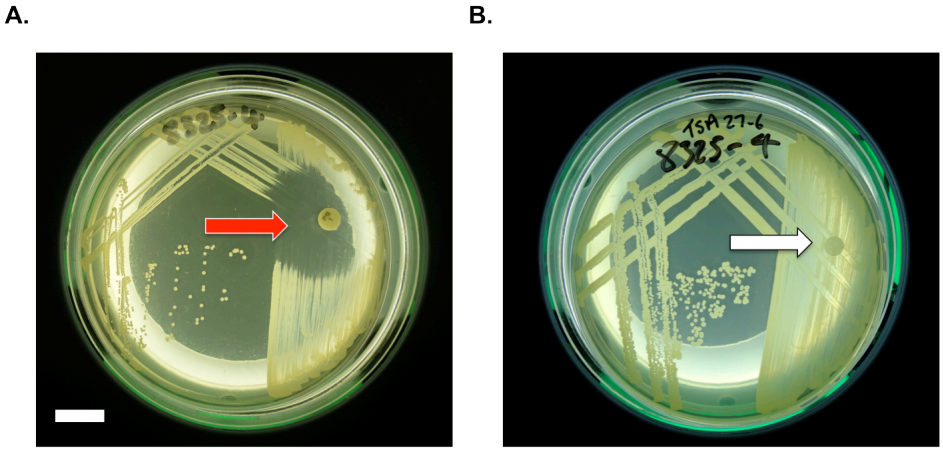

Figure 3.2: Confirmation of *S. aureus* 8325-4 sensitivity to penicillin

(**A**) The presence of a penicillin-impregnated disc resulted in no bacterial growth in the immediate vicinity of the disc (red arrow), thereby confirming *S. aureus* 8325-4 sensitivity to penicillin. (**B**) In comparison there was bacterial growth around a non-antibiotic loaded disc (white arrow) (scale bar=1cm).

3.3.7 Cartilage water content

Cartilage explants were cultured with *S. aureus* 8325-4 or non-infected DMEM of pH7.4 or 5.4. At 0, 24 and 40hrs, explants were aseptically retrieved from the flasks and excess moisture removed by placing the explants briefly between folded filter paper. The explants were then placed in pre-weighed glass vials, weighed (total wet weight (a)) and dried at 60°C until constant weight (total dry weight (b)) (Huntley *et al.*, 2005). Water content was calculated as: ((a – b)/a) x 100%.

3.3.8 Statistical analysis

Parametric data were analysed using either one-way between-groups ANOVA (clinical isolate, cartilage water content and DMEM coronal studies), with *post hoc* Dunnett's or Bonferroni tests, or paired and unpaired Student's two-tailed t-tests (8325-4 versus DMEM axial study, post-infection viability study and SZ study). One-way between-groups Kruskal-Wallis ANOVA (pH study), with *post hoc* Dunn's test, or Mann-Whitney U tests (8325-4 versus DMEM coronal study) were used to analyse non-parametric data.

3.4 RESULTS

3.4.1 *S. aureus* 8325-4 rapidly reduced *in situ* chondrocyte viability

To test this bovine cartilage explant model of septic arthritis, *in situ* chondrocyte death was quantified in the axial plane using osteochondral explants cultured in the presence or absence (DMEM control) of *S. aureus* 8325-4. In explants cultured with *S. aureus* 8325-4, chondrocyte death increased relatively slowly between 18 and

24hrs (**Figure 3.3A**). However, between 24 and 40hrs there was a rapid reduction in chondrocyte viability with 88.3±21.3% chondrocyte death at 40hrs. In comparison, there was negligible chondrocyte death at 40hrs in the control group (0.1±0.2%) with the difference in chondrocyte viability between the two groups at 40hrs being significant ($p<0.001$; **Figure 3.3A and B**).

3.4.2 Reduced culture medium pH had a minimal effect on *in situ* chondrocyte viability

During the above experiments, the culture medium became progressively acidic (**Figure 3.4A**), with pH values of approx. 6.4 and 5.4 being measured at 24 and 40hrs, respectively. There was the possibility that chondrocyte death might be due, in part, to acidic medium pH, induced by bacterial growth and metabolism (Smith, 1991) rather than an action of bacterial toxins. To assess the contribution of acidity on chondrocyte viability, explants were incubated in media of pH7.4, 6.4 and 5.4 in the absence of bacteria. Although there was no difference in chondrocyte viability between the groups at 18hrs ($p=0.18$) and 24hrs ($p=0.14$), at 40hrs there was a small but significant increase in chondrocyte death in the explants exposed to pH5.4 (4.7±7%; $p<0.01$) compared to pH6.4 (0.05±0.06%; **Figure 3.4B**). The extent of chondrocyte death at pH5.4 (40hrs) was however considerably lower than that inflicted by *S. aureus* 8325-4 (**Figure 3.3A**) and therefore contributed no more than approx. 5% of the overall 40hr chondrocyte death induced by *S. aureus* 8325-4.

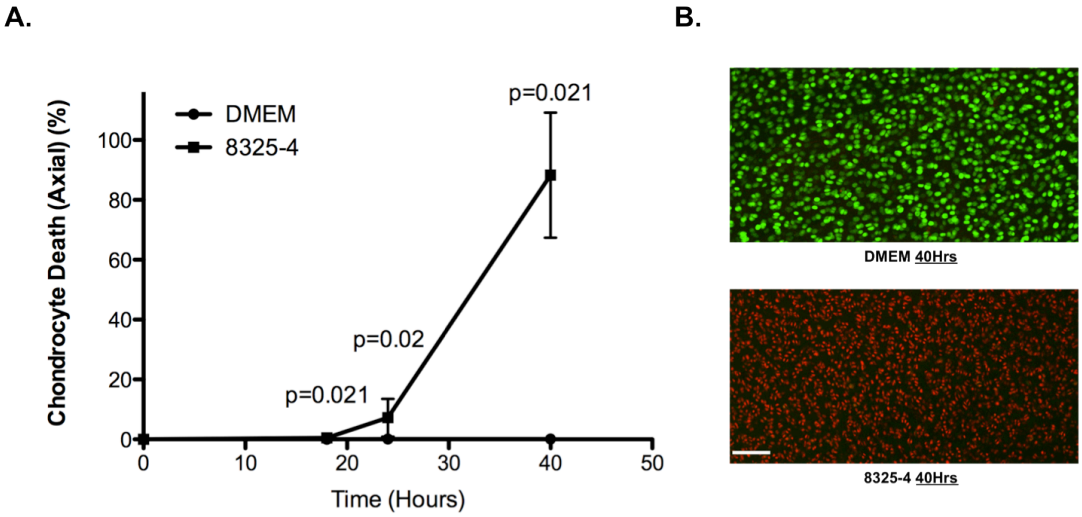

Figure 3.3: Increased *in situ* chondrocyte death by *S. aureus* 8325-4

Line graph (**A**) shows chondrocyte death in the presence or absence (DMEM control group) of *S. aureus* 8325-4 (*N*=4[*n*=2]; p values represent 8325-4 versus DMEM control group by unpaired Student's two-tailed t-test). The CLSM images (**B**) display the marked difference between the *S. aureus* 8325-4 and DMEM control groups at 40hrs (scale bar=100μm).

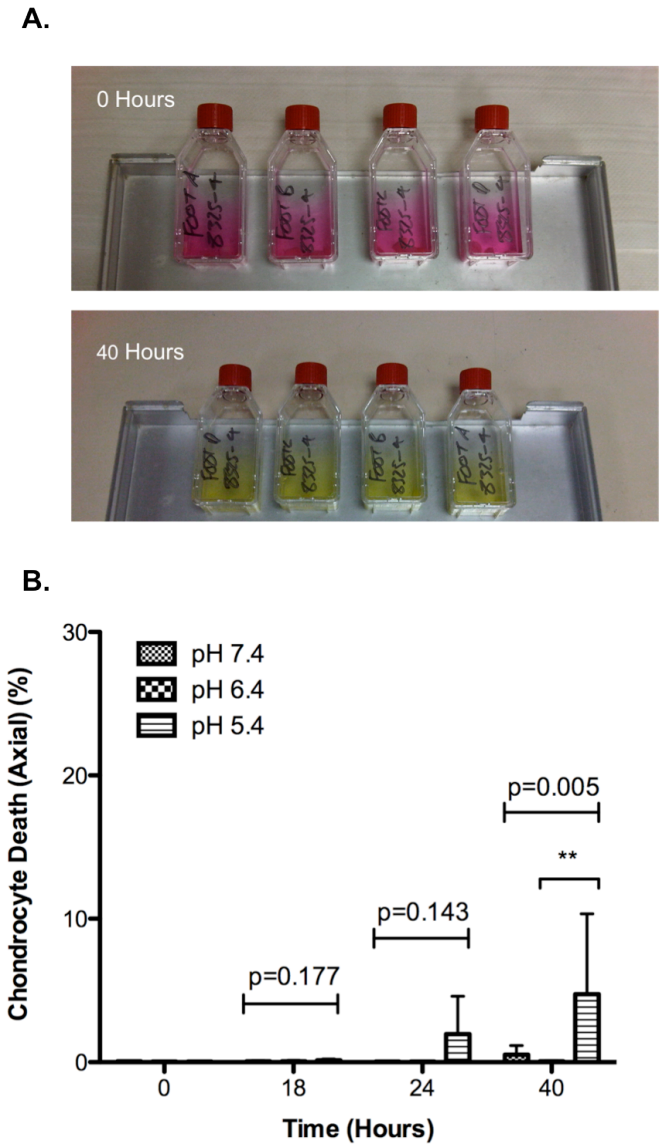

Figure 3.4: Acidic culture medium induced a small decrease in *in situ* chondrocyte viability

Reduced culture medium pH was noted during 40hr *S. aureus* 8325-4 culture, as depicted by a change in culture medium colour (DMEM contains phenol red which is pH sensitive and progresses through orange to yellow as the medium becomes more acidic) (**A**). The bar graph (**B**) demonstrates *in situ* chondrocyte viability, in the absence of bacteria, in pH 7.4 (control), 6.4 and 5.4 culture medium (N=6[n=1]; numerical p values represent one-way between-groups Kruskal-Wallis ANOVA; ** $p<0.01$ pH5.4 versus pH6.4 by *post hoc* Dunn's test).

3.4.3 PFGE typing demonstrated all *S. aureus* clinical isolates to be independent *S. aureus* strains

In order to assess whether the *S. aureus* clinical isolates were the same *S. aureus* strain, clonally related or independent strains, PFGE was conducted. Thereafter, the DNA restriction patterns (i.e. the 'bands' on the PFGE gel) of the clinical isolates and *S. aureus* 8325-4 were compared in order to determine their relatedness. Although there were some similarities between isolates, each isolate was sufficiently different (less than 85% similarity - see section 3.3.3) to be considered an independent strain (**Figure 3.5**). In addition, each clinical strain was considerably different to *S. aureus* 8325-4. Thus, the *S. aureus* clinical isolates will now be referred to as 'strains'.

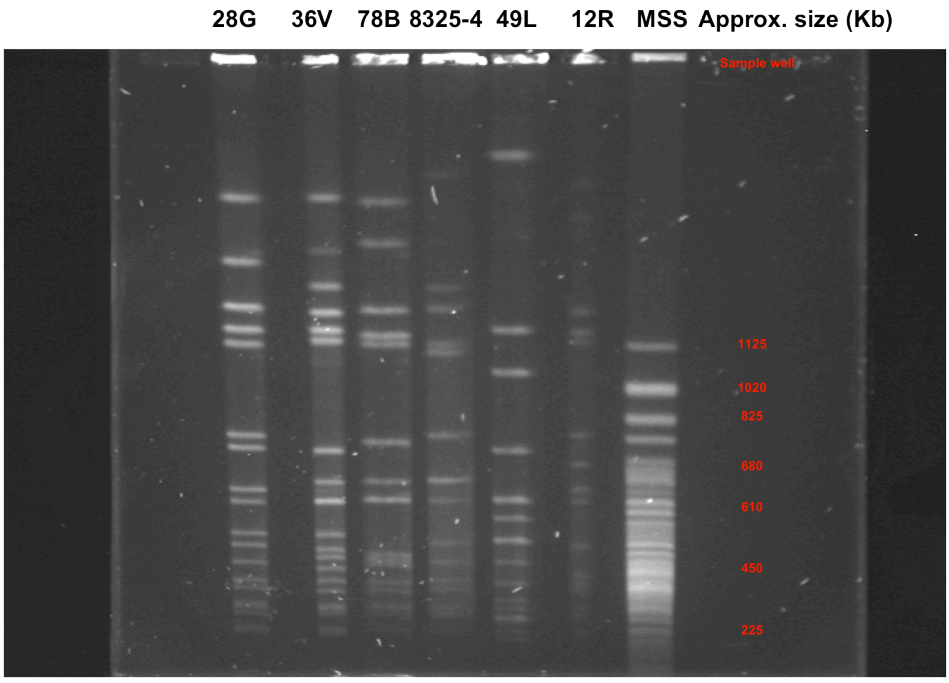

Figure 3.5: PFGE of *S. aureus* clinical isolates and *S. aureus* 8325-4

The PFGE patterns of each clinical isolate were sufficiently different (see section 3.3.3) to render each isolate an independent *S. aureus* strain. MSS, molecular size standard.

3.4.4 Comparison between *S. aureus* clinical strains and *S. aureus* 8325-4

In order to validate the use of *S. aureus* 8325-4 in the experimental model, its potency was compared with clinically relevant strains of *S. aureus*. Although none of the clinical strains (**Table 3.1**) were as potent as *S. aureus* 8325-4, each clinical strain produced >45% chondrocyte death at 40hrs (**Figure 3.6A**). In contrast, all the clinical strains had a more potent effect than *S. aureus* 8325-4 at 18 and 24hrs. There was, however, variation between the potencies of the clinical strains at 18 and 24hrs (**Figure 3.6A and B**). Statistical tests comparing the clinical strains with the DMEM control group demonstrated the 36V strain alone to be significantly different at 18hrs (31.3±10%; $p<0.001$), the 28G (58.4±22.2%; $p<0.001$) and 36V (47.5±12%; $p<0.001$) strains at 24hrs, and all strains at 40hrs (**Figure 3.6A**).

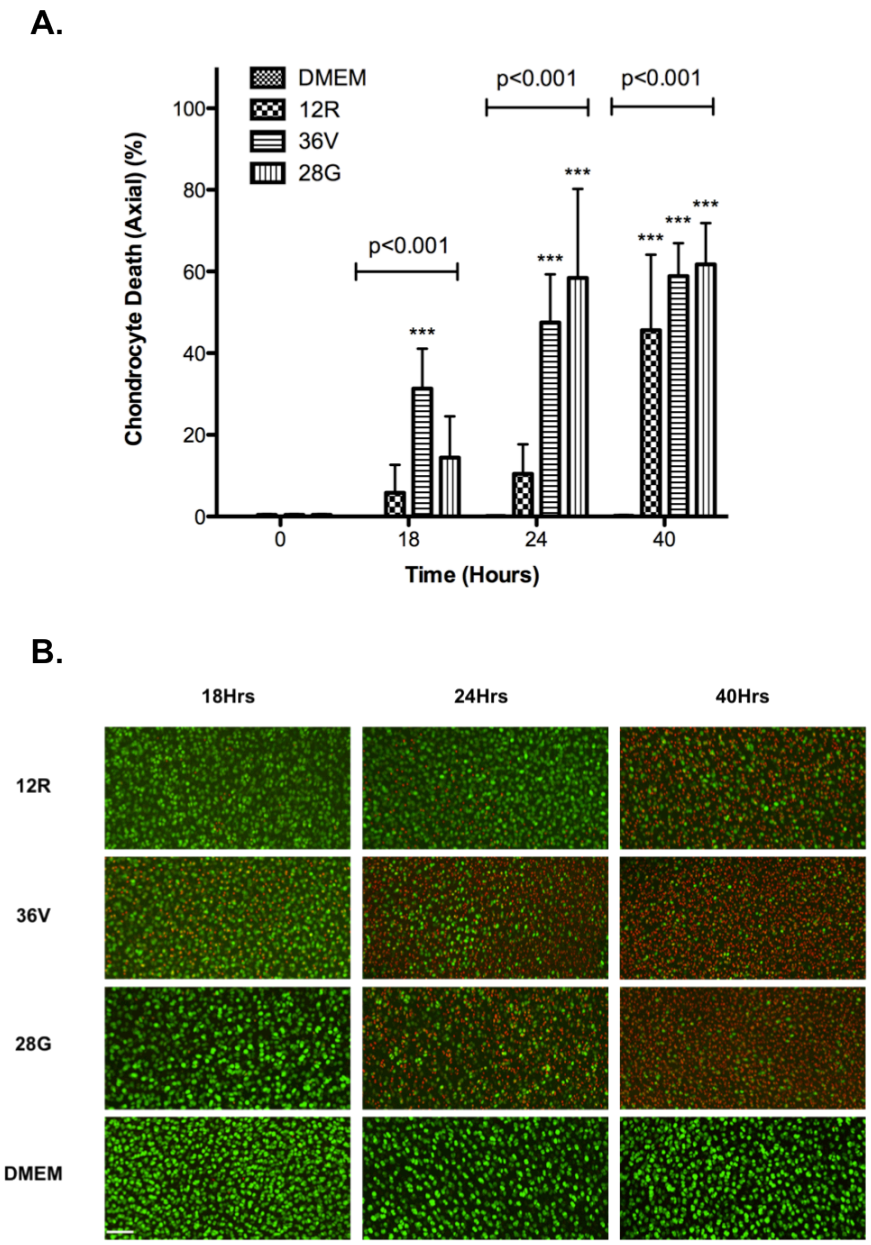

Figure 3.6: *S. aureus* clinical strains had a damaging effect on *in situ* chondrocyte viability

The bar graph (**A**) displays a significant difference between the DMEM control group and the clinical strains from 18hrs onwards (N=4[n=2]; numerical p values represent one-way between-groups ANOVA; *** p<0.001 versus DMEM control group by *post hoc* Dunnett's test). The panels (**B**) show CLSM images of explants exposed to the clinical strains with marked chondrocyte death induced by all strains at 40hrs in comparison to the DMEM control group. However, the potencies of the strains vary at 18 and 24hrs (scale bar=100μm).

3.4.5 Chondrocyte death induced by *S. aureus* 8325-4 commenced within the SZ of osteochondral explants and progressed to deeper zones

In order to assess chondrocyte viability throughout articular cartilage following bacterial exposure, a separate population of explants was cultured in either the presence or absence of *S. aureus* 8325-4, but here they were imaged and quantified in the coronal plane (**Figure 2.5B**). In the absence of bacteria, there was no change in chondrocyte viability over time (**Figure 3.7A**). The chondrocyte death, which was present throughout, was due to the scalpel cut as previously reported (Amin *et al.*, 2008). Chondrocytes within the most superficial 100μm were more susceptible to cutting trauma than those within deeper layers. With the exception of 18hrs, there was significantly more chondrocyte death within the superficial 100μm, compared to deeper intervals, at each time point (**Figure 3.7A**). However, chondrocyte death did not exceed 13% within any of the intervals studied. In comparison, there was progressive chondrocyte death in explants exposed to *S. aureus* 8325-4 (**Figure 3.7B**) which commenced within the SZ and rapidly progressed to deeper layers (**Figure 3.7B and C**).

It was hypothesised that the extensive chondrocyte death induced by *S. aureus* 8325-4 at 40hrs (**Figure 3.7B and C**) might compromise cartilage integrity. An early feature of cartilage degeneration is increased cartilage water content (Bollet and Nance, 1966; Buckwalter and Mankin, 1997b). Accordingly, this was measured in explants cultured in the presence or absence of *S. aureus* 8325-4 at 24 and 40hrs. In addition, explants incubated at pH5.4, previously shown to induce a small but significant decline in chondrocyte viability (**Figure 3.4B**), were also investigated.

There was no difference in the water content of the explants between the groups at 24 (p=0.995) or 40hrs (p=0.46) (**Figure 3.8**), thereby indicating no immediate loss of cartilage integrity.

3.4.6 Post-infection *in situ* chondrocyte viability study

In order to assess the longer-term effects on chondrocyte viability following infection, cartilage explants were cultured with *S. aureus* 8325-4 for 40hrs prior to rinsing with normal saline. Explants were then incubated in penicillin- and streptomycin-containing DMEM for a further 14 days. Chondrocyte viability was determined in the coronal plane at 40hrs and 16 days as previously described. The mean cell death throughout the analysed depth intervals at 40hrs was 87.1±21.3%, and this was not significantly different at 16 days (91.4±17.3%; p=0.16 by paired Student's two-tailed t-test; N=4[n=2]) (**Figures 3.9 and 3.10**). This demonstrated that the PI-stained chondrocytes at 40hrs were dead and incapable of labelling green with CMFDA to indicate that they had recovered viability.

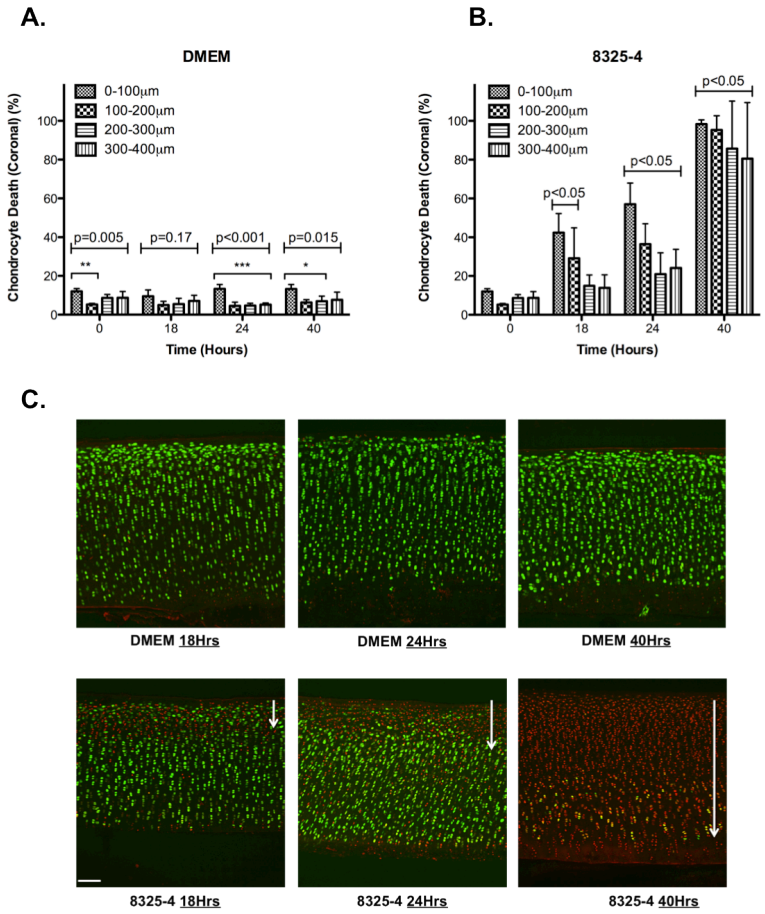

Figure 3.7: The zonal pattern of chondrocyte death with osteochondral explants following exposure to *S. aureus* 8325-4

In the absence of bacteria (**A**), chondrocyte death at each time point was minimal and consistent within each depth interval. Apart from 18hrs, there was significantly increased chondrocyte death within the first 100µm in comparison to deeper zones (N=4[n=2]; numerical p values represent one-way between-groups ANOVA; * $p<0.05$; ** $p<0.01$; *** $p<0.001$ versus 0-100µm depth interval by *post hoc* Bonferroni test). In those explants exposed to *S. aureus* 8325-4 (**B**), chondrocyte death commenced within the SZ and extended to deeper layers (N=4[n=2]; $p<0.05$ versus comparable depth interval in DMEM control group by Mann-Whitney U test). The panels (**C**) display CLSM images of explants cultured in either the presence or absence of *S. aureus* 8325-4 and provide a visual representation of chondrocyte death commencing within the SZ and progressing (white arrows) to deeper layers (scale bar=100µm).

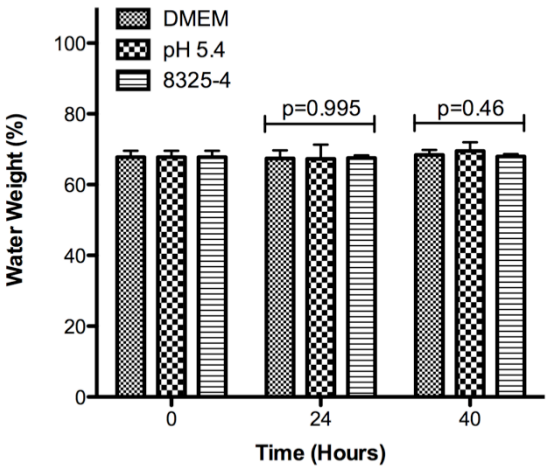

Figure 3.8: Cartilage dry weight study

There was no change in cartilage water content following 40hrs culture in the presence of *S. aureus* 8325-4 and pH5.4 culture medium (*N*=4[*n*=2]; p values represent one-way between-groups ANOVA).

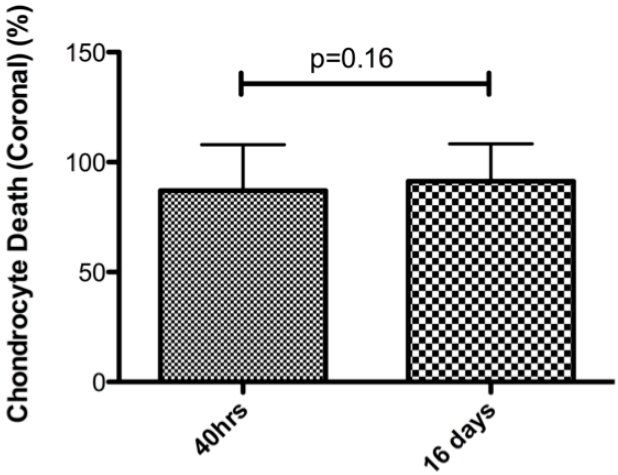

Figure 3.9: Post-infection long-term *in situ* chondrocyte viability

Following 40hrs culture with *S. aureus* 8325-4, explants were irrigated with normal saline and transferred to fresh culture medium containing penicillin and streptomycin (see section 3.3.5 for details). There was no significant change in chondrocyte viability between 40hrs and 16 days (14 days post-irrigation) (*N*=4[*n*=2]).

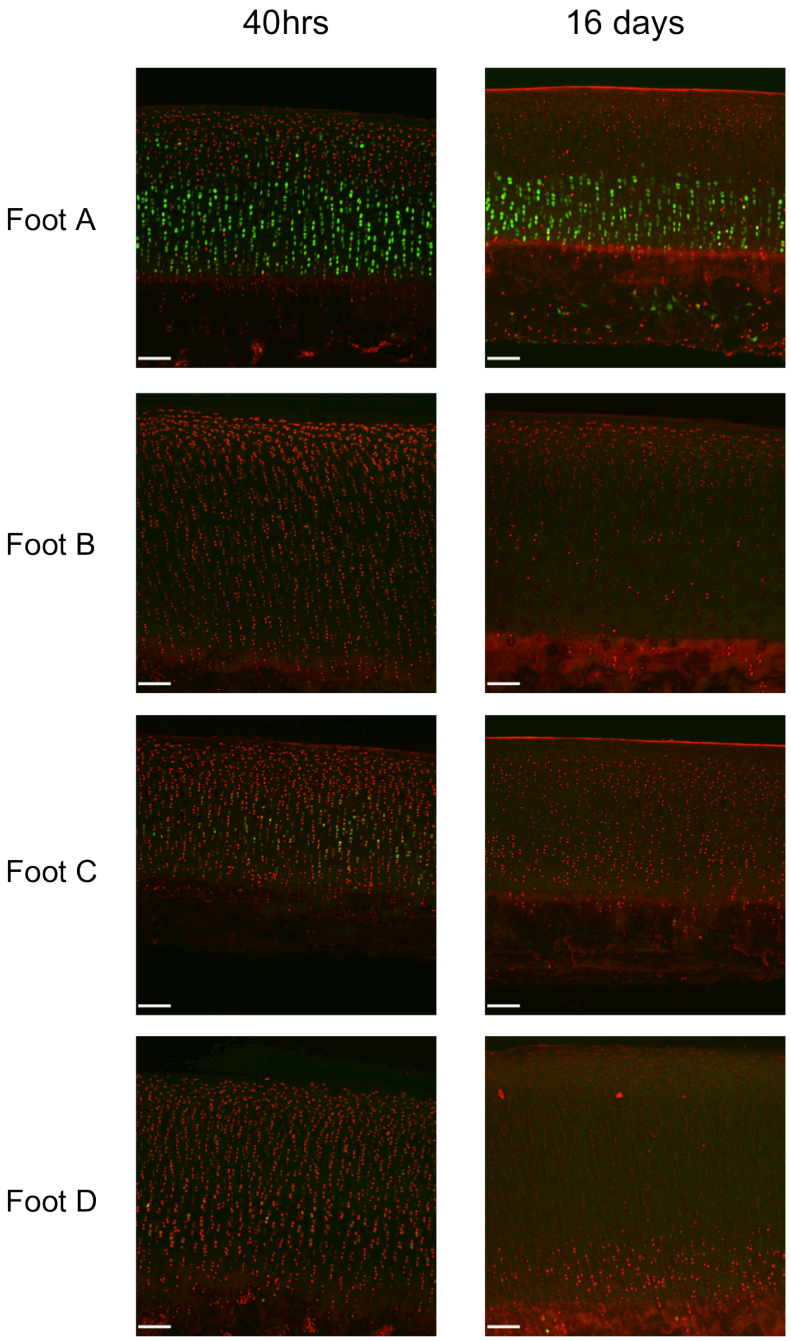

Figure 3.10: CLSM images from the long-term post-infection chondrocyte viability study

CMFDA- and PI-labelled explants from each foot at 40hrs and 16 days (14 days post-irrigation) are displayed. There was no evidence of increased CMFDA staining at 16 days in any of the feet (scale bar=100μm).

3.4.7 SZ chondrocytes were more susceptible to *S. aureus* 8325-4 toxins than cells within deeper zones

Chondrocyte death, following exposure to *S. aureus* 8325-4, commenced within the SZ (**Figure 3.7B and C**). However, as osteochondral explants were utilised it could not be concluded that SZ chondrocytes were more susceptible to *S. aureus* 8325-4 toxins as the subchondral bone may have acted as a diffusion barrier to bacterial toxins, thereby protecting DZ chondrocytes (**Figure 3.11A**). In order to assess the susceptibility of SZ and DZ chondrocytes to *S. aureus* 8325-4 toxins, subchondral bone-free cartilage explants were exposed to *S. aureus* 8325-4 toxins for 6hrs and chondrocyte death analysed within the SZ and DZ (**Figure 3.11A**). In the absence of subchondral bone, it would be expected that toxin exposure to chondrocytes within the SZ and DZ was equal (**Figure 3.11A**). At 0hrs, chondrocyte death was comparable in the SZ and DZ ($p=0.36$) (**Figure 3.11B and C**). However, after 6hrs incubation with *S. aureus* 8325-4 toxins, 49.1±2.5% of the SZ cells were dead compared to only 18.7±8.7% in the DZ ($p<0.001$). There was significantly more chondrocyte death in the SZ at 6hrs compared to 0hrs ($p<0.001$). In contrast, there was minimal difference in chondrocyte viability between 0 and 6hrs in the DZ ($p=0.57$). These results therefore suggest that SZ chondrocytes were considerably more susceptible to *S. aureus* 8325-4 toxins than DZ chondrocytes.

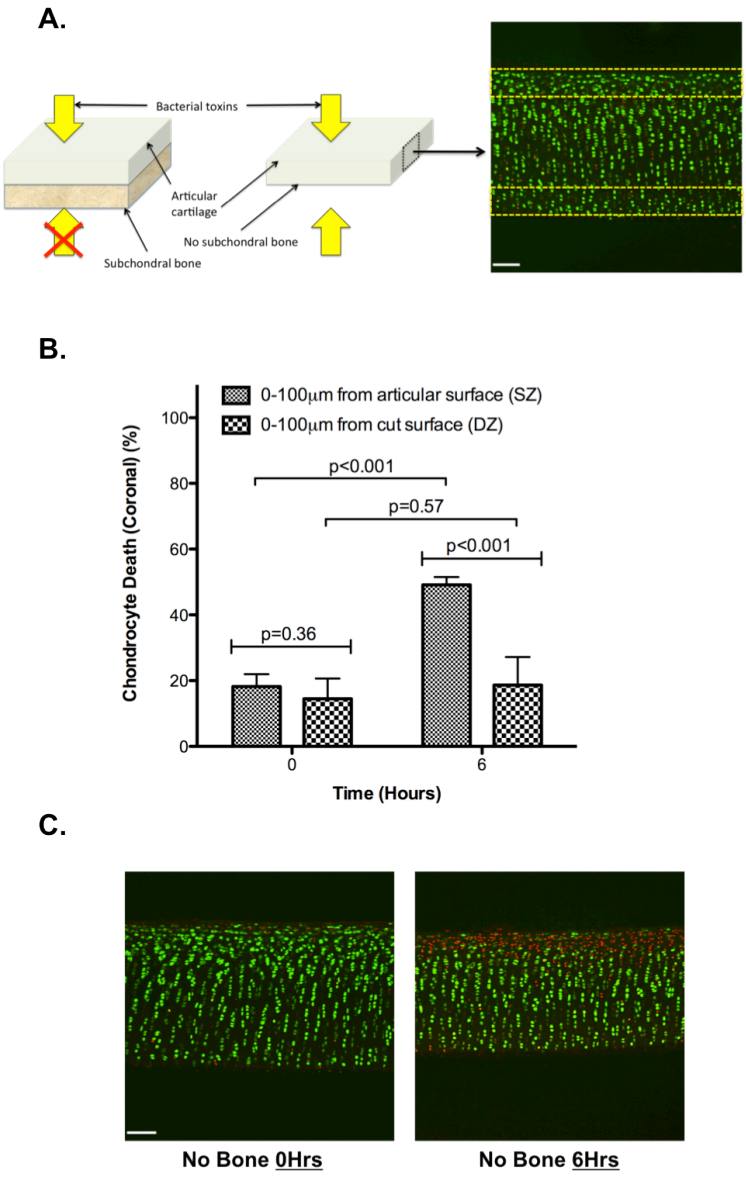

Figure 3.11: Increased susceptibility of SZ chondrocytes to *S. aureus* 8325-4 toxins

Subchondral bone-free explants (**A**), which permitted exposure of both SZ and DZ chondrocytes to experimental challenge, were cultured with *S. aureus* 8325-4 toxins for 6hrs and chondrocyte viability was assessed within defined regions of interest (dashed yellow boxes). The bar chart (**B**) demonstrates no difference in chondrocyte viability between the SZ and DZ at 0hrs (N=4[n=2]; p=0.36 by unpaired Student's two-tailed t-test). However, at 6hrs there was significantly more chondrocyte death within the SZ in comparison to the DZ (p<0.001). The CLSM reconstructions (**C**) provide a clear visual representation of the increased susceptibility of SZ chondrocytes to *S. aureus* 8325-4 toxins (scale bar = 100μm).

3.5 DISCUSSION

This study utilised CLSM to determine changes to *in situ* chondrocyte viability during exposure to a laboratory strain and clinical isolates of *S. aureus*. The results demonstrated that toxins released by *S. aureus* had a potent damaging effect on chondrocytes whereas the increased acidity occurring during bacterial culture had a minimal effect. Chondrocyte death commenced in the SZ of cartilage, suggesting that these cells were more susceptible to the toxins compared to DZ chondrocytes. Furthermore, despite extensive chondrocyte death induced by *S. aureus* 8325-4 toxins, cartilage water content was not significantly altered compared to non-infected controls.

This study utilised *S. aureus* 8325-4 as it can induce severe septic arthritis in animal models (Gemmell *et al.*, 1997; Nilsson *et al.*, 1999). To the author's knowledge, no studies have measured the bacterial concentrations within the infected synovial fluid of humans presenting with *S. aureus*-induced septic arthritis. Hence, it was difficult to match levels in the current experiments with those in a septic joint. A low aspirate concentration and volume comparable to previous *in vivo* direct joint-inoculation studies (Riegels-Nielson *et al.*, 1987) was therefore used. The increase in chondrocyte death was dramatic, with approx. 90% cells dead at 40hrs (**Figure 3.3A**). However, the culture medium became more acidic (**Figure 3.4A**) raising the possibility that cell death may, in part, be due to elevated medium acidity. Nevertheless, control experiments established that there was a minimal effect on chondrocyte viability at reduced pH (**Figure 3.4B**). This may reflect the membrane

transport adaptations present in articular chondrocytes required for survival in the relatively acidic environment of the ECM (Simpkin *et al.*, 2007).

Given that the experimental end-point of this study was chondrocyte death, one may question the importance of determining the mechanism of cell death i.e. necrosis versus apoptotosis. The primary goal of the experimental work presented in this chapter was to assess the chondrocyte death-inducing potential of *S. aureus* toxins using an *in vitro* model of *S. aureus*-induced septic arthritis. Chondrocyte death arising as a result of apoptosis or necrosis was therefore not the major focus, as the final outcome, irrespective of the cell death pathway, was chondrocyte death. Nevertheless, given the rate of cell death observed in the current study it is likely that it was necrotic in nature. This is supported by the findings of Lee *et al.* (2001) who identified that isolated chondrocytes exposed to a high inocula of *S. aureus* underwent necrosis while chondrocytes exposed to a low inocula of *S. aureus* or its ultrafiltrate underwent apoptosis.

One potential criticism of the use of *S. aureus* 8325-4 is that it may have become considerably distant, in terms of cartilage damaging potential, compared to strains of *S. aureus* currently isolated from patients presenting with septic arthritis. However, it was demonstrated that although *S. aureus* 8325-4 was more potent than clinical strains at 40hrs, the latter still exerted a strong effect (>45% chondrocyte death) (**Figure 3.6A**). Indeed, there were differences between all the clinical strains at each time point (**Figure 3.6A and B**) but this was expected, as different strains will have different growth curves and toxin production capabilities.

The *S. aureus* 8325-4 coronal study demonstrated that chondrocyte death commenced within the SZ and spread to deeper layers (**Figure 3.7B and C**). This observation could potentially be explained by the diffusion of bacterial toxins from the articular surface through cartilage. However, when chondrocytes within the SZ and DZ were exposed simultaneously to *S. aureus* 8325-4 toxins (**Figure 3.11A**) there was significantly more cell death in the surface compared to the deeper zones (**Figure 3.11B and C**), suggesting that SZ chondrocytes were inherently more sensitive to *S. aureus* toxins. At present, there is no explanation for this observation but it could arise from differences in the permeability of the ECM to toxin diffusion, and/or properties of the resident chondrocytes in the various zones. In any event, due to the proximity between the sensitive SZ chondrocytes and the cartilage/synovial fluid interface, rapid and thorough removal of bacteria and their toxins during surgical washout would be particularly important.

At the end of the 40hr time-course experiments with *S. aureus* 8325-4, although there was almost complete chondrocyte death throughout the cartilage (**Figure 3.7B and C**), the tissue appeared macroscopically normal. Furthermore, there was no significant change to cartilage water content after bacterial toxin exposure (**Figure 3.8**) and no recovery in chondrocyte viability following rinsing with saline and antibiotic treatment (**Figure 3.9 and 3.10**). Chondrocytes in cartilage do not normally divide once skeletal maturity is reached (Archer, 1994; Muir, 1995) and thus cartilage devoid of chondrocytes will likely become degenerate, as the maintenance of the ECM will be lost. There is a risk therefore that following a

supposedly-treated episode of septic arthritis, radiographs without any joint space abnormality may be misinterpreted as showing normal, biomechanically competent cartilage whereas in fact the progressive degeneration and loss of this cartilage would be inevitable. There are no published human studies investigating the time-course of cartilage loss in tissue devoid of chondrocytes. However, Simon *et al.*(1976) investigating the long-term effect of localised cryotherapy-induced chondrocyte death in lapine articular cartilage *in vivo*, demonstrated histologically that the cartilage was structurally intact at 6 months despite the absence of living chondrocytes. Nevertheless, by 12 months extensive cartilage fibrillation and softening were evident, which were considered to be amongst the first macroscopic changes associated with degenerative joint disease (Pearle *et al.*, 2005).

The interpretation of the current experiments had the benefit that the host immune response was not involved in chondrocyte death. Following bacterial joint colonisation *in vivo*, inflammatory cytokines are released into the joint by synovial cells and there is an accompanying influx of host inflammatory cells (Shirtliff and Mader, 2002). Through opsonisation and phagocytosis, the immune response ultimately acts to remove bacteria. However, evidence from animal studies suggests that the immune response may paradoxically contribute further to cartilage destruction (Shirtliff and Mader, 2002; Tissi *et al.*, 2004). At present, it remains unknown as to what extent *in vivo* chondrocyte death and subsequent cartilage damage is due to bacteria and their products, and what is due to the immune response. The findings from an *in vivo* lapine study of septic arthritis by Smith *et al.* (1987) support a significant role of bacteria and their soluble toxins by demonstrating

that the overall cartilage destruction, as measured by proteoglycan and collagen loss, declined the earlier antibiotics were administered. From the current experiments, it was concluded that it was probable that bacterial toxins had a significant and rapid effect on chondrocyte viability *in vivo*.

The finding that all acquired *S. aureus* clinical isolates, obtained from the joint aspirates of patients presenting with clinically and microbiologically confirmed septic arthritis, were independent *S. aureus* strains (**Figure 3.5**) was of further interest. Although only 5 clinical isolates were investigated, the observation in the current study nevertheless provides convincing evidence that *S. aureus*-induced septic arthritis is not attributable to any one particular *S. aureus* strain. Due to the likely interspecies polymorphism, in particular with regard to growth profiles, toxin production capabilities and antibiotic resistance, the finding also confirms that the treatment of *S. aureus*-induced septic arthritis will remain a challenge. The emergence of multi-drug resistance strains further highlights this (Lowy, 2003; Kaatz *et al.*, 2005; Appelbaum, 2007; Howden *et al.*, 2011).

This study has provided new insights into chondrocyte death following cartilage exposure to *S. aureus* and builds upon previous work highlighting damage to the ECM. By identifying the factors that cause chondrocytes within some cartilage zones to be more susceptible to toxins than others and characterising the toxin-induced cell death pathway, treatment strategies may be developed in order to protect these vulnerable cells with the ultimate goal of reducing the extent of cartilage destruction during and after an episode of septic arthritis.

CHAPTER 4

THE INFLUENCE OF *S. AUREUS* ALPHA-, BETA- AND GAMMA-HAEMOLYSIN ON *IN SITU* CHONDROCYTE VIABILITY

4.1 INTRODUCTION

Studies investigating a variety of *S. aureus*-related infections have implicated the exotoxins Hla, Hlb and Hlg as major virulence factors (Cunningham *et al.*, 1996; O'Callaghan *et al.*, 1997; Dajcs *et al.*, 2002; Hayashida *et al.*, 2009). Interestingly, these studies suggest that Hla, Hlb and Hlg have varying destructive roles with regard to different *S. aureus*-related infections (Dajcs *et al.*, 2002; Hayashida *et al.*, 2009; Katayama *et al.*, 2013). For example, Katayama *et al.* (2013) found that Hlb played an important role in *S. aureus* skin colonisation by specifically damaging keratinocytes while Bubeck-Wardenburg and Schneewind (2008) identified that Hla was key to *S. aureus* virulence in a murine model of pneumonia. Whilst Hld also belongs to the same family of toxins, it is not currently believed to be a major *S. aureus* virulence factor (Dinges *et al.*, 2000).

Murine models of septic arthritis have implied that Hla and Hlg are key contributory factors to the cartilage destruction following joint infection, with little apparent role for Hlb (Gemmell *et al.*, 1997; Nilsson *et al.*, 1999). However, there remains some uncertainty as to the exact role and contributions of each of these toxins to the overall pathological effect on cartilage. Using similar murine models, Gemmell *et al.* (1997) concluded that Hla, in the presence of protein A, was the main damaging agent while Nilsson *et al.* (1999) found that Hla and Hlg in combination were required to exert a potent effect, with Hla alone being of minor importance.

Although it is appreciated that animal models provide essential information, the influence of a complex host immune response can potentially produce results that

may be ambiguous and difficult to interpret. The current study describes the influence of Hla, Hlb and Hlg on *in situ* chondrocyte viability using the *in vitro* bovine cartilage explant model of *S. aureus*-induced septic arthritis described in Chapter 3. In order to determine the efficacy of Hla, Hlb and Hlg, a selection of isogenic *S. aureus* mutants, with respect to Hla, Hlb and Hlg expression (**Table 4.1**), originating from the laboratory 'wild-type' strain 8325-4 studied in Chapter 3 were utilised. *In situ* chondrocyte viability was visualised and quantified by CLSM as previously described (see Chapter 2).

4.2 HYPOTHESIS

This study tested the hypothesis that Hla alone was the key damaging *S. aureus* toxin to *in situ* chondrocyte viability.

4.3 MATERIALS & METHODS

4.3.1 Biochemicals and solutions

The standard tissue culture medium used in this study was serum-free DMEM (Catalogue no. 41966; 340mOsm/Kg H_2O; pH7.4) with L-glutamine (4mM), D-glucose (25mM), sodium pyruvate (1mM) and sodium bicarbonate (44mM). Tetracycline (2μg/ml) and erythromycin (10μg/ml) were obtained from Sigma-Aldrich (Gillingham, UK) and added to TSA and TSB depending on the antibiotic resistance profile of the isogenic mutant strain investigated (**Table 4.1**).

4.3.2 Bacterial strains

S. aureus 8325-4 and its associated isogenic mutants (**Table 4.1**) were kindly provided by Professor Timothy J. Foster, Dept. Microbiology, Trinity College, Dublin, Ireland. The bacterial mutants contained combined mutations affecting Hla (*hla*::Em^r), Hlb (*hlb*::ϕ42E) and Hlg (Δ*hlg*::Tc^r) synthesis. The erythromycin and tetracycline resistance associated with the Hla and Hlg mutations respectively, enabled the selective growth of specific mutants in antibiotic-loaded culture media. Prior to experimentation, the toxin profile of the isogenic mutants was confirmed by plating each strain onto 5% v/v rabbit and sheep blood TSA plates, with or without tetracycline (2μg/ml) and erythromycin (10μg/ml) as appropriate, and assessing for haemolytic activity (Haque and Baldwin, 1964; Burnside *et al.*, 2010; Herbert *et al.*, 2010). Erythrocyte lysis in the immediate vicinity of the bacterial colonies, which manifested as clear regions in the blood agar, was indicative of haemolysis (**Figure 4.1**). Heparinised sheep blood was obtained from E&O Laboratories Ltd, Bonnybridge, UK, and heparinised rabbit blood was obtained from the Scottish National Blood Transfusion Service, Penicuik, UK.

4.3.3 Statistical analysis

Parametric data were analysed using one-way between-groups ANOVA with *post hoc* Dunnett's test (40hr $Hla^-Hlb^-Hlg^-$ vs $Hla^-Hlb^+Hlg^+$ vs $Hla^-Hlb^-Hlg^+$ study, 40hr 8325-4 ($Hla^+Hlb^+Hlg^+$) vs $Hla^-Hlb^-Hlg^-$ v $Hla^+Hlb^-Hlg^-$ study and 6hr 8325-4 vs $Hla^-Hlb^-Hlg^-$ vs $Hla^+Hlb^-Hlg^-$ vs $Hla^-Hlb^+Hlg^+$ supernatant coronal study), and unpaired Student's two-tailed t-tests (6hr 8325-4 ($Hla^+Hlb^+Hlg^+$) vs $Hla^-Hlb^+Hlg^+$ supernatant study). A Mann-Whitney U test (unpaired data; 40hr 8325-4 ($Hla^+Hlb^+Hlg^+$) vs Hla^-

$Hlb^{-}Hlg^{-}$ study and 6hr 8325-4 ($Hla^{+}Hlb^{+}Hlg^{+}$) vs $Hla^{-}Hlb^{-}Hlg^{-}$ supernatant study) was used to analyse non-parametric data.

***S. aureus* strain**	**Genotype**	**Phenotype**	**Toxins Produced**	**Given Name**
8325-4	Wild Type	Hla^{+} Hlb^{+} Hlg^{+}	Hla, Hlb & Hlg	8325-4
DU5938	*hlb*::ϕ42E *hla*::Em^{r} Δ*hlg*::Tc^{r}	Hla^{-} Hlb^{-} Hlg^{-}	None	Hla^{-} Hlb^{-} Hlg^{-}
DU5946	*hlb*::ϕ42E Δ*hlg*::Tc^{r}	Hla^{+} Hlb^{-} Hlg^{-}	Hla	Hla^{+} Hlb^{-} Hlg^{-}
DU1090	*hla*::Em^{r}	Hla^{-} Hlb^{+} Hlg^{+}	Hlb & Hlg	Hla^{-} Hlb^{+} Hlg^{+}
DU5720	*hla*::Em^{r} *hlb*::ϕ42E	Hla^{-} Hlb^{-} Hlg^{+}	Hlg	Hla^{-} Hlb^{-} Hlg^{+}

Table 4.1: The isogenic *S. aureus* mutant strains, originating from *S. aureus* 8325-4, used in this study. The genotype, phenotype and toxins produced by each strain are shown (Tc^{r}= tetracycline resistance; Em^{r}= erythromycin resistance).

4.4 RESULTS

4.4.1 Identification of toxin profiles of *S. aureus* isogenic mutant strains

To test whether the isogenic mutant strains produced the designated toxin profiles (**Table 4.1**), strains were plated onto 5% rabbit and sheep blood TSA. Hla is haemolytic to rabbit and sheep erythrocytes, Hlb is haemolytic to sheep erythrocytes only, whereas Hlg is haemolytic to rabbit erythrocytes only (Traber *et al.*, 2008; Burnside *et al.*, 2010). Positive blood agar plate haemolysis was observed by the presence of distinct clear regions around the bacterial colonies (**Figure 4.1A and B**), which indicated erythrocyte lysis. The 8325-4 ($Hla^{+}Hlb^{+}Hlg^{+}$) and $Hla^{+}Hlb^{-}Hlg^{-}$

strains induced potent rabbit erythrocyte haemolysis (**Figure 4.1A**). However, minimal, but detectable, haemolysis was observed with the $Hla^{-}Hlb^{+}Hlg^{+}$ and $Hla^{-}Hlb^{-}Hlg^{+}$ strains (**Figure 4.1A**). There was no evidence of rabbit erythrocyte haemolysis with the $Hla^{-}Hlb^{-}Hlg^{-}$ strain (**Figure 4.1A**). The 8325-4 ($Hla^{+}Hlb^{+}Hlg^{+}$), $Hla^{+}Hlb^{-}Hlg^{-}$ and $Hla^{-}Hlb^{+}Hlg^{+}$ strains were positive for sheep erythrocyte haemolysis whereas the $Hla^{-}Hlb^{-}Hlg^{+}$ and $Hla^{-}Hlb^{-}$ Hlg^{-} strains were negative (**Figure 4.1B**). All mutants therefore produced the appropriate toxin profiles.

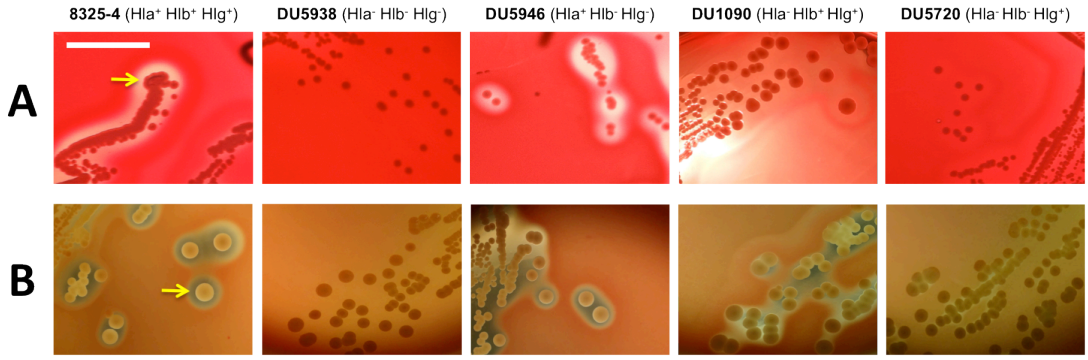

Figure 4.1: Confirmation of the haemolytic properties of the isogenic mutant strains used in this study

Each strain was plated onto 5% rabbit (**A**) and sheep (**B**) blood TSA and incubated for 24hrs. Haemolysis is shown by the presence of clear regions around the bacterial colonies (yellow arrows provide examples of haemolysis) (scale bar=1cm).

4.4.2 *S. aureus* haemolysins induced *in situ* chondrocyte death

In order to confirm that haemolysins contributed to *in situ* chondrocyte death, osteochondral explants were cultured in the presence of either the 8325-4 ($Hla^{+}Hlb^{+}Hlg^{+}$) or $Hla^{-}Hlb^{-}Hlg^{-}$ strains. Chondrocyte death over 40hrs was then quantified in axial CLSM images of fluorescently-labelled chondrocytes as

previously described (see Chapter 2). Thus, a strain producing Hla, Hlb and Hlg was compared with a strain that was unable to produce these toxins. In the explants cultured with *S. aureus* 8325-4 ($Hla^{+}Hlb^{+}Hlg^{+}$) there was significant chondrocyte death at each time point (**Figure 4.2A**). Between 24 and 40hrs there was a rapid reduction in chondrocyte viability with 66.2±20.1% (p=0.029) of the chondrocyte population dying at 40hrs. In comparison, there was only 6.7±8.9% chondrocyte death at 40hrs in those explants exposed to the $Hla^{-}Hlb^{-}Hlg^{-}$ strain (**Figure 4.2A and B**). This was not significant however in comparison to the baseline level of chondrocyte death at 0hrs (*N*=4[*n*=2]; p=0.11 by Wilcoxon signed-rank test (paired data)).

In order to assess the damaging potential of the 40hrs 8325-4 ($Hla^{+}Hlb^{+}Hlg^{+}$) culture toxins independent of bacteria (i.e. to assess whether unspecified bacterial cell wall co-factors were required for haemolysins to exert their virulence), the bacteria were removed by both centrifugation and filter sterilisation leaving a toxin-rich supernatant in which toxin levels remained relatively unchanged. Fresh osteochondral explants were subsequently exposed to either the 8325-4 ($Hla^{+}Hlb^{+}Hlg^{+}$) or $Hla^{-}Hlb^{-}Hlg^{-}$ supernatants. In comparison to explants exposed to the $Hla^{-}Hlb^{-}Hlg^{-}$ supernatant, explants exposed to the 8325-4 ($Hla^{+}Hlb^{+}Hlg^{+}$) supernatant demonstrated significant chondrocyte death at each time point (**Figure 4.2C and D**). Indeed, there was no measurable chondrocyte death at any time point in those explants exposed to the $Hla^{-}Hlb^{-}Hlg^{-}$ supernatant (**Figure 4.2C**).

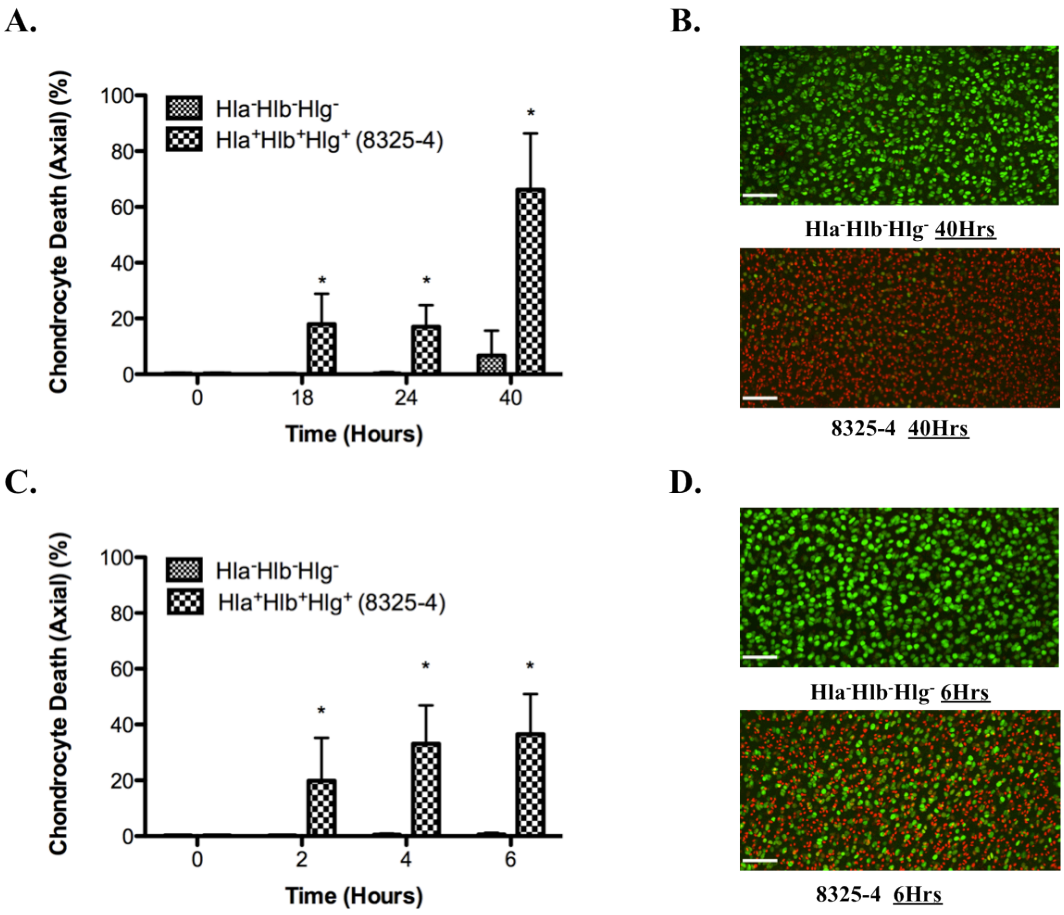

Figure 4.2: Haemolysins played a key role in inducing *in situ* chondrocyte death

Osteochondral explants cultured in the presence of the 8325-4 ($Hla^+Hlb^+Hlg^+$) strain demonstrated significant chondrocyte death at each time point (**A**). In comparison, chondrocyte death in the presence of the $Hla^-Hlb^-Hlg^-$ strain was minimal (*N*=4[*n*=2]; * $p<0.05$ 8325-4 ($Hla^+Hlb^+Hlg^+$) versus $Hla^-Hlb^-Hlg^-$ strain by Mann-Whitney U test). The CLSM images display the marked difference between the two strains at 40hrs (**B**). Osteochondral explants exposed to the 40hr 8325-4 ($Hla^+Hlb^+Hlg^+$) strain culture supernatant demonstrated rapid and significant chondrocyte death over a 6hr time period in comparison to explants exposed to the $Hla^-Hlb^-Hlg^-$ strain supernatant (**C**) (*N*=4[*n*=2]; * $p<0.05$ 8325-4 ($Hla^+Hlb^+Hlg^+$) versus $Hla^-Hlb^-Hlg^-$ supernatant by Mann-Whitney U test). The CLSM images (**D**) demonstrate the marked difference between the two supernatants at 6hrs (scale bar=100μm).

4.4.3 Hlb and Hlg induced minimal *in situ* chondrocyte death

In order to assess the contributions of Hlb and Hlg, osteochondral explants were cultured with the $Hla^{-}Hlb^{+}$ Hlg^{+} and $Hla^{-}Hlb^{-}$ Hlg^{+} strains. The $Hla^{-}Hlb^{-}Hlg^{-}$ strain was used as a control as it had previously been shown to induce minimal chondrocyte death (**Figure 4.2A**) whilst producing similar changes to the culture medium as the 8325-4 ($Hla^{+}Hlb^{+}Hlg^{+}$) strain. Although there was significantly more chondrocyte death observed in those explants exposed to the $Hla^{-}Hlb^{-}Hlg^{+}$ strain in comparison to the $Hla^{-}Hlb^{-}Hlg^{-}$ strain at 24hrs ($p=0.027$ by *post hoc* Dunnett's test), the level of chondrocyte death was still extremely low (1.3±0.5%). By 40hrs however there was no significant difference between the strains ($p=0.12$) (**Figure 4.3A and B**). The maximum chondrocyte death achieved was 4.1±3.4% by the $Hla^{-}Hlb^{+}Hlg^{+}$ strain (**Figure 4.3A**), which was not significant in comparison to the baseline level of chondrocyte death observed at 0hrs ($p=0.14$ by paired Student's t-test). Additionally, this level of chondrocyte death was considerably less than that observed at the same time point with the 8325-4 ($Hla^{+}Hlb^{+}Hlg^{+}$) strain (**Figures 4.2A and 4.3A**) and also less than the chondrocyte death induced by the $Hla^{-}Hlb^{-}Hlg^{-}$ strain during the initial 40hr 8325-4 ($Hla^{+}Hlb^{+}Hlg^{+}$) vs $Hla^{-}Hlb^{-}Hlg^{-}$ strain experiment (**Figure 4.2A**). Hla therefore appeared to be the key damaging toxin to *in situ* chondrocyte viability as the only difference between the 8325-4 ($Hla^{+}Hlb^{+}Hlg^{+}$) and $Hla^{-}Hlb^{+}Hlg^{+}$ strains was the ability to produce Hla. Hlb and Hlg thus had no significant role in inducing *in situ* chondrocyte death.

A.

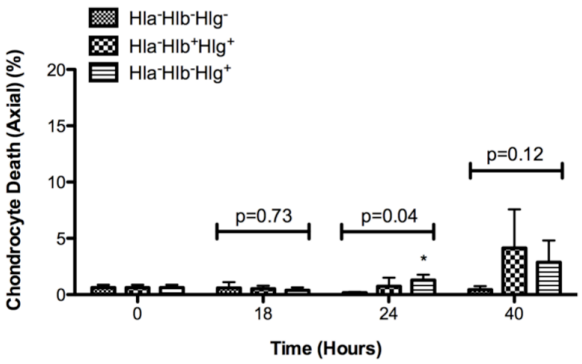

B.

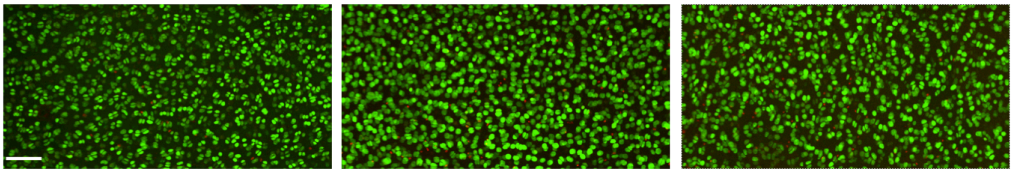

Hla-Hlb-Hlg- 40Hrs | Hla-Hlb+Hlg+ 40Hrs | Hla-Hlb-Hlg+ 40Hrs

Figure 4.3: Hlb and Hlg had a minimal impact on *in situ* chondrocyte viability

Osteochondral explants cultured in the presence of the Hla$^-$Hlb$^-$Hlg$^-$, Hla$^-$Hlb$^+$Hlg$^+$ and Hla$^-$Hlb$^-$Hlg$^+$ strains exhibited minimal chondrocyte death at each time point (**A**) (*N*=4[*n*=2]; numerical p values represent probability from one-way ANOVA; * p<0.05 versus Hla$^-$Hlb$^-$Hlg$^-$ strain by *post hoc* Dunnett's test). The CLSM images (**B**) represent the chondrocyte death induced by each strain at 40hrs (scale bar=100μm).

4.4.4 Hla induced significant and rapid *in situ* chondrocyte death

In order to confirm that Hla alone was the key damaging toxin to *in situ* chondrocyte viability, explants were cultured in the presence of the following strains: 8325-4 ($Hla^+Hlb^+Hlg^+$), $Hla^+Hlb^-Hlg^-$ and $Hla^-Hlb^-Hlg^-$ (control). Compared to the control group, explants exposed to the 8325-4 ($Hla^+Hlb^+Hlg^+$) and $Hla^+Hlb^-Hlg^-$ strains exhibited significant chondrocyte death at each time point (**Figure 4.4A and B**). Although there was a significant difference between the 8325-4 ($Hla^+Hlb^+Hlg^+$) and $Hla^+Hlb^-Hlg^-$ strains at 24hrs ($p=0.01$) there was no significant difference at 40hrs ($p=0.2$ by unpaired Student's t-test).

To confirm further that Hla was the main cause of chondrocyte death, explants were exposed to the 40hr culture supernatants of the 8325-4 ($Hla^+Hlb^+Hlg^+$) and $Hla^-Hlb^+Hlg^+$ strains, where the only difference between the supernatants was the presence or absence of Hla, respectively. There was negligible chondrocyte death in the explants exposed to the $Hla^-Hlb^+Hlg^+$ supernatant while there was significant chondrocyte death at each time point in those explants exposed to the 8325-4 ($Hla^+Hlb^+Hlg^+$) supernatant (**Figure 4.5A and B**). These results therefore confirmed that *S. aureus* Hla was the key damaging toxin to *in situ* chondrocyte viability.

A.

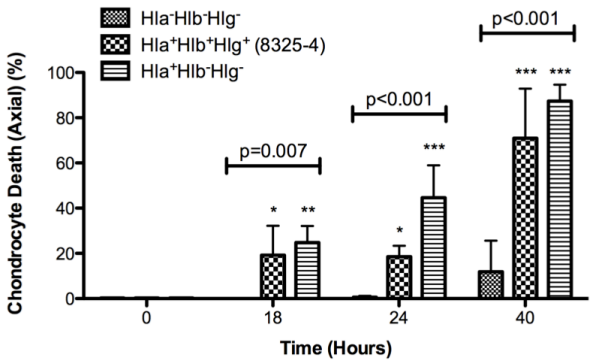

B.

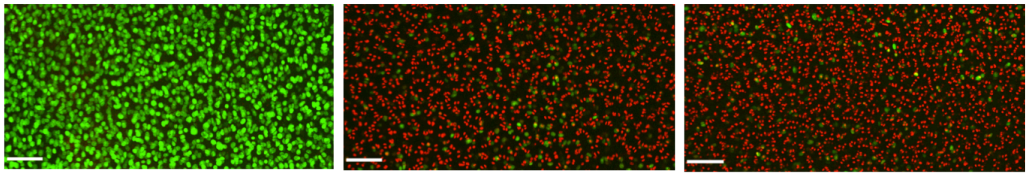

Hla-Hlb-Hlg- 40Hrs **8325-4 40Hrs** **Hla+Hlb-Hlg- 40Hrs**

Figure 4.4: The 8325-4 ($Hla^{+}Hlb^{+}Hlg^{+}$) and $Hla^{+}Hlb^{-}Hlg^{-}$ strains had comparable potencies

In comparison to the $Hla^{-}Hlb^{-}Hlg^{-}$ strain control group, the 8325-4 ($Hla^{+}Hlb^{+}Hlg^{+}$) and $Hla^{+}Hlb^{-}Hlg^{-}$ strains induced similar chondrocyte death over the experimental period (**A**) (*N*=4[*n*=2]; numerical p values represent probability from one-way ANOVA; * p<0.05; ** p<0.01; *** p<0.001 versus $Hla^{-}Hlb^{-}Hlg^{-}$ strain by *post hoc* Dunnett's test). The CLSM images (**B**) represent the chondrocyte death induced by each strain at 40hrs (scale bar=100μm).

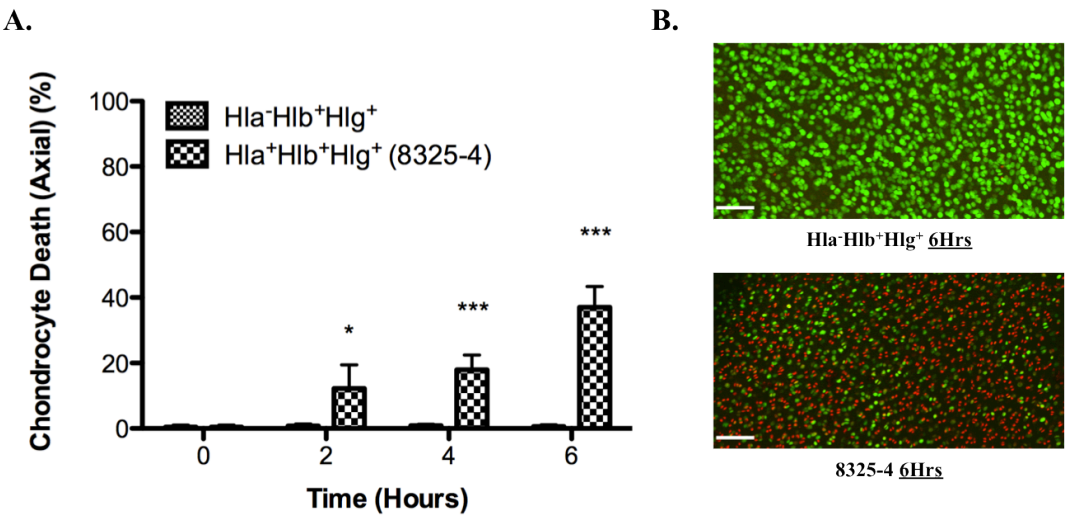

Figure 4.5: Hla alone was the key damaging agent to the viability of *in situ* chondrocytes within bovine cartilage

Osteochondral explants cultured with $Hla^{-}Hlb^{+}Hlg^{+}$ supernatant were compared with explants cultured with 8325-4 ($Hla^{+}Hlb^{+}Hlg^{+}$) supernatant. The only difference between the two culture supernatants was the presence or absence of alpha-toxin. There was significant chondrocyte death at each experimental time point in those explants exposed to the 8325-4 supernatant in comparison to those explants exposed to the $Hla^{-}Hlb^{+}Hlg^{+}$ supernatant (**A**) (N=4[n=2]; * $p<0.05$; *** $p<0.001$ by unpaired Student's two-tailed t-test). The CLSM images (**B**) display the influence of Hla on *in situ* chondrocyte viability (scale bar=100μm).

4.4.5 Hla-induced chondrocyte death commenced within the SZ of cartilage

All axial studies (see above) involved the imaging of osteochondral explants to a depth of approx. 100μm, thereby permitting quantification of chondrocyte death within the entirety of the SZ and a portion of the MZ (**Figure 2.5**). In order to confirm (1) that Hla-induced chondrocyte death commenced within the SZ and (2) to ensure that Hlb and Hlg did not induce chondrocyte death within deeper layers of cartilage i.e. chondrocyte death that would not be detected upon axial imaging,

osteochondral explants were exposed to the $Hla^{-}Hlb^{-}Hlg^{-}$, 8325-4 ($Hla^{+}Hlb^{+}Hlg^{+}$), $Hla^{+}Hlb^{-}Hlg^{-}$ and $Hla^{-}Hlb^{+}Hlg^{+}$ strain supernatants and imaged by CLSM in the coronal plane (**Figure 2.5**). As observed previously (**Figure 3.7**), there was a dead cell artefact induced by the scalpel cut at 0hrs (**Figure 4.6**). However, on this occasion there was no significant change in chondrocyte viability between depth intervals at 0hrs ($p=0.17$ by one-way ANOVA).

Explants exposed to the $Hla^{-}Hlb^{-}Hlg^{-}$ strain (control) exhibited no significant chondrocyte death above 0hr values for each depth interval at 6hrs ($p=0.07$ by one-way ANOVA) (**Figure 4.6A**). Compared to the control group, explants exposed to the 8325-4 ($Hla^{+}Hlb^{+}Hlg^{+}$) and $Hla^{+}Hlb^{-}Hlg^{-}$ supernatants demonstrated significant chondrocyte death ($p<0.001$) within the first depth interval (0-100μm) (**Figure 4.6A, B and C**). In those explants exposed to the $Hla^{-}Hlb^{+}Hlg^{+}$ supernatant, there was no change in chondrocyte viability within the first depth interval ($p=0.28$) or indeed throughout the analysed depth of cartilage (**Figure 4.6D**). This further confirmed that Hlb and Hlg had no significant role in the induction of *in situ* chondrocyte death within the SZ but also that Hlb and Hlg did not specifically induce chondrocyte death within deeper layers, which would not have been detected upon axial imaging.

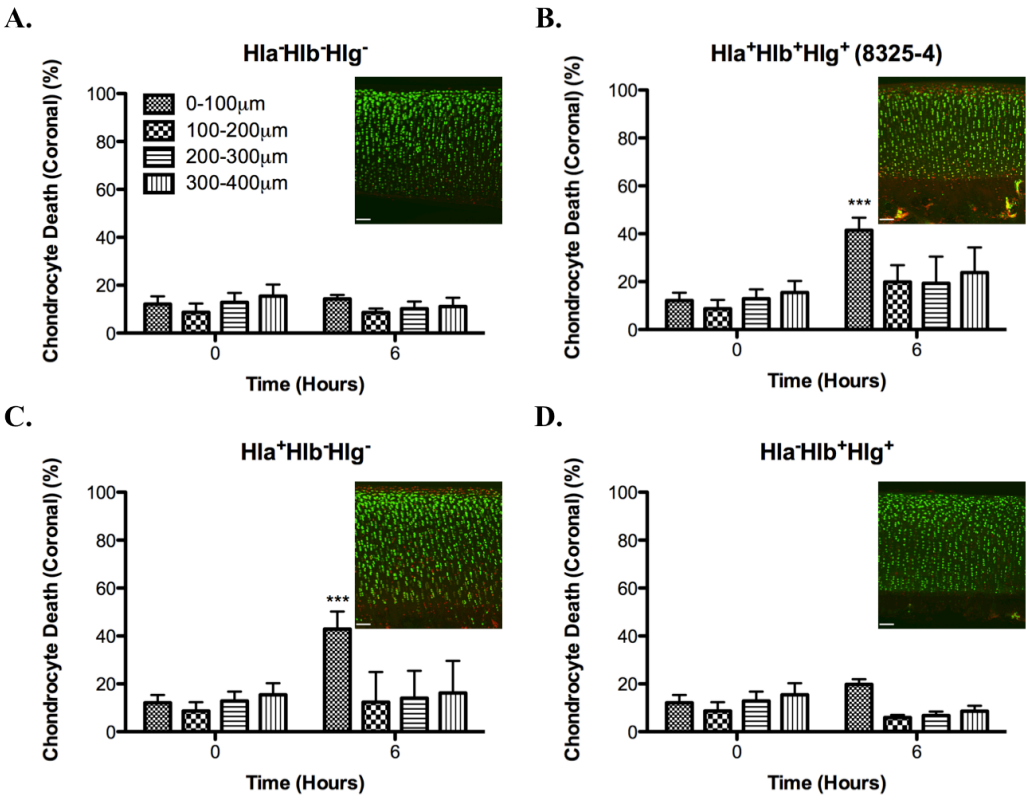

Figure 4.6: Hla-induced chondrocyte death commenced within the SZ of cartilage

The depth-related pattern of chondrocyte death in osteochondral explants exposed to the 40hr $Hla^{-}Hlb^{-}Hlg^{-}$, 8325-4 ($Hla^{+}Hlb^{+}Hlg^{+}$), $Hla^{+}Hlb^{-}Hlg^{-}$, and $Hla^{-}Hlb^{+}Hlg^{+}$ strain supernatants was assessed. Compared to the $Hla^{-}Hlb^{-}Hlg^{-}$ control group (**A**), there was significantly more chondrocyte death within the first 100μm of those explants exposed to the Hla-containing 8325-4 ($Hla^{+}Hlb^{+}Hlg^{+}$) (**B**) and $Hla^{+}Hlb^{-}Hlg^{-}$ (**C**) supernatants. There was no change in chondrocyte viability in those explants exposed to the $Hla^{-}Hlb^{+}Hlg^{+}$ strain supernatant (**D**) (*N*=4[*n*=2]; numerical p values represent one-way ANOVA; * $p<0.05$; ** $p<0.01$; *** $p<0.001$ versus $Hla^{-}Hlb^{-}Hlg^{-}$ strain supernatant by *post hoc* Dunnett's test). The CLSM inserts (**A-D**) provide a visual representation of the zonal pattern of chondrocyte death following explant exposure to that particular strain's 40hr culture supernatant (scale bar=100μm).

4.5 DISCUSSION

This study has utilised CLSM to determine changes to the viability of *in situ* bovine chondrocytes following exposure to a variety of *S. aureus* isogenic mutants with differing haemolysin production capabilities (**Table 4.1**). Compared to previous *in vivo* animal studies that used similar isogenic mutant strains to induce septic arthritis (Gemmell *et al.*, 1997; Nilsson *et al.*, 1999), the direct impact of Hla, Hlb and Hlg on *in situ* chondrocyte viability has been assessed in a bovine cartilage model, which did not have the complexities of a host immune response. Two major findings emerge from this study. Firstly, *S. aureus* Hla was unequivocally the key damaging toxin to *in situ* chondrocyte viability in this experimental model, with Hlb and Hlg having no significant role. Secondly, Hla-induced chondrocyte death commenced within the SZ of cartilage.

All the isogenic mutants investigated (**Table 4.1**) were created from the same mother strain (8325-4) by the controlled mutations of genes conferring production of particular haemolysins (O'Reilly *et al.*, 1986; Nilsson *et al.*, 1999). By combining these mutations with defined antibiotic resistance cassettes i.e. tetracycline or erythromycin, it was possible to ensure that the correct mutant had grown in the presence of specific culture conditions i.e. TSA with tetracycline. However, in order to confirm the toxin production profiles of the isogenic mutants (**Table 4.1**) prior to investigation, and to exclude the presence of spontaneous mutations, all mutants were tested for their ability to haemolyse rabbit and sheep blood agar (**Figure 4.1**).

The Hla and Hlb-producing mutants displayed the expected haemolytic activity on rabbit (Hla) and sheep (Hla & Hlb) blood agar plates (Traber *et al.*, 2008; Burnside *et al.*, 2010) (**Figure 4.1A and B**). Hlg production however was more difficult to assess, as impurities in agar are known to have an inhibitory effect on its activity (Dinges *et al.*, 2000; Burnside *et al.*, 2010). Indeed, previous studies using similar isogenic mutants only assessed for alpha- and beta-haemolytic activity (ability to haemolyse rabbit and sheep erythrocytes, respectively) (O'Callaghan *et al.*, 1997; Nilsson *et al.*, 1999). However, in the presence of appropriate antibiotics, the inhibition of gamma haemolysis was used as a positive selection feature for the $Hla^{-}Hlb^{-}Hlg^{+}$ and $Hla^{-}Hlb^{+}Hlg^{+}$ strains when cultured on rabbit blood agar. As expected, the $Hla^{-}Hlb^{-}Hlg^{-}$ strain induced neither sheep nor rabbit erythrocyte haemolysis (**Figure 4.1A and B**). All the mutant strains utilised in this study therefore exhibited the expected haemolysin production profiles thereby offering a useful and specific experimental model to test the potency of the various toxins.

In order to establish whether haemolysins played a role in inducing *in situ* chondrocyte death, cell viability was assessed in explants exposed to either the 8325-4 or $Hla^{-}Hlb^{-}Hlg^{-}$ strains, as strain 8325-4 produced Hla, Hlb and Hlg. In contrast, the $Hla^{-}Hlb^{-}Hlg^{-}$ strain was unable to produce these toxins yet still produced all the other unspecified 8325-4 toxins i.e. they were both identical apart from the ability to produce Hla, Hlb and Hlg. There was a significant difference between the chondrocyte-damaging potential of the two strains (**Figures 4.2A and B**) with the 8325-4 ($Hla^{+}Hlb^{+}Hlg^{+}$) and $Hla^{-}Hlb^{-}Hlg^{-}$ strains inducing approximately 66% and 7% chondrocyte death at 40hrs, respectively. This demonstrated that one, all, or a

combination of Hla, Hlb and Hlg was necessary to induce potent *in situ* chondrocyte death. Although the 7% chondrocyte death induced by the $Hla^{-}Hlb^{-}Hlg^{-}$ strain was found not be significant, it likely represented chondrocyte death induced by the acidic culture medium conditions (see Chapter 3) and/or other non-specified *S. aureus* toxins. In addition to Hla, Hlb and Hlg, *S. aureus* 8325-4 is known to produce a diverse array of potential virulence factors including exoenzymes, capsular polysaccharides, protein A and Hld (Cunningham *et al.*, 1996). As $Hla^{-}Hlb^{-}Hlg^{-}$ was derived directly from *S. aureus* 8325-4, the toxin profiles of both strains were identical apart from the ability to produce Hla, Hlb and Hlg i.e. whatever unspecified toxins were produced by *S .aureus* 8325-4 were also produced by the $Hla^{-}Hlb^{-}Hlg^{-}$ strain. In addition, the $Hla^{-}Hlb^{-}Hlg^{-}$ strain established comparable culture conditions i.e. reduced culture medium pH with bacterial growth. The $Hla^{-}Hlb^{-}Hlg^{-}$ strain was therefore considered a valid control for subsequent experiments.

At present, *S. aureus*-induced septic arthritis is treated with a combination of intravenous antibiotics and joint lavage, which takes the form of either surgical washout or serial bedside aspirations. Whilst antibiotics may adequately destroy the bacteria, there remains a concern with serial bedside aspirations that *S. aureus* toxins may remain within the joint. Nevertheless, some animal models of *S. aureus* infection have suggested that the presence of bacterial cell-wall-anchored proteins, such as protein A, are required for certain haemolysins to exert their virulence (Gemmell *et al.*, 1997). Thus, with the knowledge that haemolysins play a key role in the induction of *in vivo* joint destruction (Gemmell *et al.*, 1997; Nilsson *et al.*, 1999), the influence of isolated haemolysins on *in situ* chondrocyte viability was

assessed. This was achieved by exposing cartilage explants to the 40hr culture supernatants of the 8325-4 ($Hla^+Hlb^+Hlg^+$) and $Hla^-Hlb^-Hlg^-$ strains, whereby, in the absence of bacteria, relatively constant toxin concentrations were present throughout the experimental period. In comparison to the $Hla^-Hlb^-Hlg^-$ supernatant, there was significant chondrocyte death in those explants exposed to the 8325-4 ($Hla^+Hlb^+Hlg^+$) supernatant at each experimental time point (**Figures 4.2C and D**). In contrast to the 40hr culture experiment, there was negligible chondrocyte death induced by the $Hla^-Hlb^-Hlg^-$ strain supernatant over 6hrs (**Figures 4.2A and C**). A possible explanation for this finding may be that the acidity and/or non-specified toxins possibly accounting for the small degree of chondrocyte death over 40hrs was not apparent with the 6hr assay. Taken together, the findings from this supernatant study demonstrated a destructive influence of haemolysins on chondrocyte viability in the absence of bacteria. This advocates the prompt and thorough washout of all septic joints.

In order to establish the individual roles of Hla, Hlb and Hlg, a series of experiments followed whereby *in situ* chondrocyte death induced by specific isogenic mutant strains over 40hrs were compared. Hlb and Hlg had no significant role in inducing *in situ* chondrocyte death (**Figures 4.3A and B**). However, Hla alone appeared to be the key damaging toxin as the $Hla^+Hlb^-Hlg^-$ strain was of a comparable potency to the 8325-4 ($Hla^+Hlb^+Hlg^+$) strain (**Figures 4.4A and B**). To confirm the destructive role of Hla further, a comparison was made between the 40hr 8325-4 ($Hla^+Hlb^+Hlg^+$) and $Hla^-Hlb^+Hlg^+$ supernatants, as the only difference between the two supernatants was the presence or absence of Hla, respectively. In comparison to those explants

exposed to the 8325-4 ($Hla^+Hlb^+Hlg^+$) supernatant, explants exposed to the $Hla^-Hlb^+Hlg^+$ supernatant exhibited negligible chondrocyte death throughout the experimental period (**Figures 4.5A and B**), thereby confirming the highly virulent nature of Hla.

All the experiments that ultimately culminated in the identification of Hla as the key damaging *S. aureus* toxin to *in situ* chondrocyte viability involved the assessment of explants in the axial plane, whereby image acquisition was performed to a depth of approx. 100μm from the articular surface. As the SZ of cartilage was considered to be up to 10% of the overall depth of cartilage from the articular surface (Jadin, 2005; Pearle *et al.*, 2005) (bovine and human cartilage (Pedersen *et al.*, 2013)), this permitted the estimation of chondrocyte viability within the entirety of the SZ and a portion of the MZ. Given that chondrocytes within the SZ were closest to the synovial fluid harbouring the bacterial toxins *in vivo*, assessment of the sensitivity of these cells to Hla, Hlb and Hlg in the first instance was considered appropriate. In addition, axial imaging allowed the quantification of chondrocytes within a region of cartilage that did not have any 'cut-edge' dead cell artifact (**Figure 2.5A**).

In order to assess whether Hla-induced chondrocyte death commenced within the SZ of cartilage and to ensure that Hlb and Hlg did not induce chondrocyte death within deeper layers of cartilage, the coronal assessment of osteochondral explants exposed to the $Hla^-Hlb^-Hlg^-$ (control), 8325-4 ($Hla^+Hlb^+Hlg^+$), $Hla^+Hlb^-Hlg^-$ and $Hla^-Hlb^+Hlg^+$ supernatants was conducted. Explant trimming was only performed at the time of fluorescent staining i.e. upon removal from the culture vessel containing the

bacterial supernatant, as the mechanical injury induced by the scalpel cut may have rendered some chondrocytes more susceptible to the toxins. Thus, the imaged cut-edge was never exposed to toxins directly. The chondrocyte death observed within each depth interval at 0hrs (**Figure 4.6**) represented the previously observed (**Figure 3.7**) background level of chondrocyte death induced by the 'cut-edge'. There was no significant difference in chondrocyte viability within any of the analysed depth intervals between 0 and 6hrs in those explants exposed to the $Hla^{-}Hlb^{-}Hlg^{-}$ supernatant (**Figure 4.6A**). At 6hrs, explants cultured in the presence of the Hla-containing 8325-4 and $Hla^{+}Hlb^{-}Hlg^{-}$ supernatants exhibited significant chondrocyte death within the first depth interval with no change in chondrocyte viability observed within deeper layers (**Figures 4.6B and C**). In comparison, there was no significant change in chondrocyte viability throughout the analysed depth of cartilage in those explants exposed to the Hlb and Hlg-containing $Hla^{-}Hlb^{+}Hlg^{+}$ supernatant (**Figure 4.6D**). This therefore confirmed that Hlb and Hlg had no significant role in inducing *in situ* chondrocyte death in our *ex vivo* model and that Hla-induced chondrocyte death commenced within the SZ of the osteochondral explants.

There were several possible explanations for the observation of Hla-induced chondrocyte death commencing within the SZ. Firstly, it may be that the subchondral bone (**Figure 2.5B**) acted as a barrier to Hla penetration, thereby protecting DZ chondrocytes, and thus the observed chondrocyte death within the SZ was simply due to the proximity of SZ chondrocytes to the culture medium containing Hla i.e. chondrocyte death was due to Hla diffusion through the ECM from the articular surface. Secondly, it may be that SZ chondrocytes were inherently

more susceptible to Hla than chondrocytes within deeper layers. Indeed, it has already been established that SZ chondrocytes have different properties in comparison to chondrocytes from deeper zones with regard to both metabolic activity and vulnerability to damage. For example, Simpkin *et al.* (2007) (Simpkin *et al.*, 2007) demonstrated that bovine SZ chondrocytes regulated pH through a bicarbonate-dependent mechanism that was not present in chondrocytes within deeper zones. In a further study by Hauselmann *et al.* (1996), human SZ chondrocytes were found to be more susceptible to IL-1-induced damage than chondrocytes from deeper layers, with SZ chondrocytes being shown to have twice the number of high-affinity binding sites for IL-1 than DZ chondrocytes. The receptor for Hla on eukaryotic cells has recently been identified as 'A-disintegrin and metalloprotease 10' (ADAM10) (Wilke and Bubeck-Wardenburg, 2010; Inoshima *et al.*, 2011; Powers *et al.*, 2012). Another possibility therefore was that there are higher levels of ADAM10 expression in SZ chondrocytes in comparison to chondrocytes from deeper zones, thereby making them more susceptible to Hla.

The increased susceptibility of SZ chondrocytes to Hla was of major concern. It has previously been identified that SZ chondrocytes have unique characteristics with regard to ECM metabolism, which are essential for producing and maintaining the smooth surface of healthy articular cartilage (Siczkowski and Watt, 1990), a prerequisite to withstanding the mechanical stresses associated with normal joint activity (Buckwalter and Mankin, 1997a). Damage to the SZ sets in motion a cascade of events that ultimately culminates in full thickness destruction of cartilage (Hollander *et al.*, 1995). It is therefore of critical importance that research should

focus on protecting these vulnerable yet key cellular building blocks of articular cartilage.

The *ex vivo* findings presented in this chapter differed substantially from previous *in vivo* studies and it is important to consider possible explanations. In a study by Gemmell *et al.* (1997), septic arthritis was established in mice using a variety of *S. aureus* mutants with varying deficiencies for protein A, Hla, Hlb, coagulase, clumping factor and accessory gene regulator. The study concluded that Hla, in combination with protein A, was of major importance to the pathogenicity of *S. aureus*-induced septic arthritis. In a further study by Nilsson *et al.* (1999), murine septic arthritis was induced utilising the same mutant strains as those used in the present study, in addition to others. They concluded that the simultaneous presence of Hla and Hlg were crucial for the development and progression of *S. aureus*-induced septic arthritis, with Hla alone being of minor importance. A common finding between the present study and previous *in vivo* studies was the importance of Hla in the pathogenesis of *S. aureus*-induced septic arthritis. In contrast, we have demonstrated that Hla, in the absence of both Hlb and Hlg, can exert a rapid and fatal action on *in situ* chondrocytes (**Figure 4.4**). Protein A is a cell wall surface protein that aids *S. aureus* survival in the presence of a host immune response by binding the Fc portion of IgG and the Fc receptors of polymorphonuclear leukocytes, thereby preventing bacterial opsonisation and phagocytosis (Cunningham *et al.*, 1996; Widaa *et al.*, 2012). However, the current experimental model had no immune response present. Furthermore, it was unlikely that there was significant protein A production in the culture vessels as protein A synthesis is known to be very low in most complex

culture media (Nilsson *et al.*, 1999). In addition, protein A would not have been present in the supernatant studies, as bacteria were not present, yet there was still significant Hla-induced chondrocyte death. Thus, it seems probable that the Hla-induced chondrocyte death observed in the present study was independent of both Hlg and protein A.

As previously discussed in Chapter 3, a potential limitation of the current study was that the *S. aureus* aspirate concentration used to inoculate the culture vessels, and subsequent bacterial and Hla levels during the incubation period thereafter, may not be in the physiological range in comparison to those found *in vivo*. To the author's knowledge, no studies have analysed bacterial toxin concentrations within infected synovial fluid in humans presenting with *S. aureus*-induced septic arthritis. Hence, it was difficult to match levels in the current experiments with those in a septic joint. Thus, a further potential criticism of this study was that the time course in these experiments may differ considerably to those *in vivo*. However, patients with 'fight-bite' septic arthritis typically present between 18 and 24hrs post injury (i.e. they become symptomatic at this stage) (Kelly *et al.*, 1996), which are time points in the current experimental model when chondrocyte death was detectable. Fight-bite septic arthritis classically occurs when the metacarpophalangeal joint of a clenched fist is punctured by the tooth of another individual and is subsequently inoculated with contaminated saliva, most frequently with *S. aureus* (Perron *et al.*, 2002; Talan *et al.*, 2003). In a small case series by Kelly *et al.* (1996), those patients presenting within 24hrs and adequately treated had a good functional outcome but those presenting beyond 24hrs had a poor outcome with longterm joint morbidity, likely

reflecting considerable chondrocyte death at the time of presentation. Thus, the rate of Hla-induced chondrocyte death in the current *in vitro* model may be comparable to those *in vivo* albeit in the absence of a host immune response. Regardless, the aim of this study was to investigate the impact of *S. aureus* Hla, Hlb and Hlg on *in situ* chondrocyte viability in the absence of the complexities of a host immune response and the aspirate concentration utilised during this study made this achievable.

With *S. aureus* accounting for 40 to 65% of cases of septic arthritis (Kaandorp *et al.*, 1997a; Gupta *et al.*, 2001), the data presented in this study may have clinical relevance for the treatment of septic arthritis. The rapid and fatal action of Hla on *in situ* chondrocyte viability highlights the importance of rapid and thorough joint lavage in all patients presenting with septic arthritis, with surgical washout likely to offer the most comprehensive form of irrigation. Although antibiotics may kill or inhibit the growth of bacteria within the infected joint, they do not have the ability actively to remove bacterial toxins i.e. Hla. The findings of the current experiments have demonstrated that in the absence of viable bacteria, Hla caused significant chondrocyte death (**Figure 4.5**). However, some studies have also suggested that Hla at sublethal levels may stimulate cells to produce pro-inflammatory cytokines (Bhakdi *et al.*, 1989; Suttorp *et al.*, 1993; Onogawa, 2002), thereby potentially worsening the immune mediated destruction of articular cartilage. Therefore, antibiotic therapy alone should never be considered appropriate.

The identification of a specific damaging toxin offered a potential future therapeutic target. Firstly, by attempting to block the activity of Hla, for example by Hla-

neutralising antibodies or selective blockade of ADAM10, it is possible that chondrocyte death may be significantly reduced during and after an episode of *S. aureus*-induced septic arthritis, thereby reducing the extent of subsequent cartilage loss. Encouragingly, a murine study of *S. aureus*-induced pneumonia conducted by Bubeck-Wardenburg and Schneewind (2008) has demonstrated protection in those animals immunised with a mutant form of Hla (Hla_{H35L}) that was unable to form pores i.e. it was unable to lyse cells. In addition, the subsequent administration of Hla-specific antibodies to non-vaccinated animals also conferred protection. A further potential therapeutic target is the Hla-induced cell death pathway following formation of the Hla pore on the plasma membrane. However, a further understanding of this pathway is required before this avenue can be explored.

CHAPTER 5

THE INFLUENCE OF RAISED CULTURE MEDIUM CALCIUM CONCENTRATION ON *S. AUREUS* ALPHA-HAEMOLYSIN-INDUCED *IN SITU* CHONDROCYTE DEATH

5.1 INTRODUCTION

In Chapter 4, it was identified that *S. aureus* Hla, a 'pore-forming' exotoxin secreted by almost all strains of *S. aureus* (Bhakdi and Tranum-Jensen, 1991; Powers *et al.*, 2012; Thay *et al.*, 2013), was the most potent agent affecting *in situ* chondrocyte viability. It has been proposed that Hla-mediated destruction of sensitive cells, which includes bovine chondrocytes (see Chapter 4), relies on the formation of a 1- to 3-nm pore spanning the plasma membrane (Gray and Kehoe, 1984; Dinges *et al.*, 2000). Hla is a chromosomally encoded toxin (Ragle and Bubeck-Wardenburg, 2009) and is secreted as a water soluble 293-residue monomer (Bubeck-Wardenburg and Schneewind, 2008) with a molecular weight of 33kDa (Dinges *et al.*, 2000). Following binding to the host cell membrane, monomers undergo a series of conformational changes and ultimately aggregate to form a heptameric β-barrel structure that penetrates the lipid bilayer of the plasma membrane (**Figure 1.5**) (Gray and Kehoe, 1984; Bhakdi and Tranum-Jensen, 1991; Dinges *et al.*, 2000). Interaction of Hla monomers with the recently identified cell membrane receptor ADAM10 is thought to be a prerequisite to the initiation of the sequence of events that results in cytolytic pore formation (Wilke and Bubeck-Wardenburg, 2010; Inoshima *et al.*, 2011). It is currently believed that pore formation triggers alterations in ion gradients, the rapid egression of vital molecules such as adenosine triphosphate (ATP), activation of stress-signalling pathways, and loss of membrane integrity, culminating in eventual cell death (Suttorp *et al.*, 1985; Bhakdi and Tranum-Jensen, 1991; Walev *et al.*, 1993; Dinges *et al.*, 2000).

It has been hypothesised that enhanced Ca^{2+} entry may play a key role in the Hla-induced eukaryotic cell death pathway (Suttorp *et al.*, 1985; Bhakdi and Tranum-Jensen, 1991). Whilst Ca^{2+} is essential for the maintenance of cellular life, it also, paradoxically, plays an important role in cell death (Berridge *et al.*, 1998; Zhivotovsky and Orrenius, 2011). This occurs when Ca^{2+} levels are irretrievably increased. The intracellular Ca^{2+} concentration ($[Ca^{2+}]_i$) within chondrocytes is normally tightly controlled in the range of 80-100nM (Hall *et al.*, 1996a; Yellowley *et al.*, 1997; Wilkins *et al.*, 2000; Sánchez *et al.*, 2003). In contrast, the extracellular Ca^{2+} concentration ($[Ca^{2+}]_o$) within the interstitial fluid of the ECM is estimated to be approximately 6-15mM (Urban, 1994). A considerable concentration gradient therefore exists between the extracellular and intracellular spaces. Hence, the presence of unregulated Ca^{2+}-permeable pores spanning the plasma membrane may permit a markedly increased rate of diffusion of Ca^{2+} across the cell membrane. It is possible therefore that the influx of Ca^{2+} through the Hla pore is the key upstream signal for the establishment of downstream death mechanisms that ultimately result in chondrocyte death.

No studies have yet investigated the role of Ca^{2+} in *S. aureus* Hla-induced *in situ* chondrocyte death. A further understanding of the mechanism through which this toxin causes chondrocyte death may provide an opportunity either to optimise current treatments or to develop novel therapeutic strategies with the aim of reducing the extent of chondrocyte death, and thus cartilage destruction, during and after an episode of septic arthritis. As a first step towards clarifying the role of Ca^{2+} in the Hla-induced chondrocyte death pathway, the objective of this study was therefore to

determine the influence of $[Ca^{2+}]_o$ on *S. aureus* Hla-induced *in situ* chondrocyte death using the previously described bovine cartilage explant model of septic arthritis (see Chapters 2 and 3). The *S. aureus* laboratory 'wild-type' strain 8325-4 along with a selection of isogenic mutants, with regard to Hla, Hlb and Hlg expression were utilised. At designated time points, *in situ* chondrocyte viability was imaged and quantified within defined regions-of-interest in the axial plane of cartilage (i.e. within SZ of cartilage) as previously described (see Chapter 2).

In order to assess the influence of raised $[Ca^{2+}]_o$ on Hla-induced chondrocyte death, it was necessary to add $CaCl_2$ to the culture media. However, this also resulted in a simultaneous rise in culture medium osmolarity. *In situ* chondrocytes are osmotically sensitive, responding to changes in extracellular osmolarity with reciprocal changes in cell volume (Bush and Hall, 2001a; Bush *et al.*, 2005). These changes are primarily the result of water movement across the plasma membrane, arising as a consequence of the differential osmotic pressure gradient (Hoffmann *et al.*, 2009). In almost all eukaryotic cells, including chondrocytes, water movement is extremely rapid with a corresponding change in cell volume occurring within seconds (McGann *et al.*, 1988; Bush and Hall, 2001a). However, it is important for chondrocytes to maintain constant cell volume in order optimise cellular function (Urban *et al.*, 1993; Urban, 1994). This is achieved through the activation of specific active membrane transporters that release or accumulate solutes in response to cell swelling or shrinkage, respectively (Hall *et al.*, 1996a; Hall *et al.*, 1996b; Bush *et al.*, 2010). Nevertheless, such mechanisms typically take considerably longer (minutes to hours) than the initial response following osmotic challenge (Bush and Hall,

2001b; Hoffmann *et al.*, 2009). It was therefore deemed necessary to firstly assess the influence of raised culture medium osmolarity (through both sucrose and NaCl addition) *per se* on Hla-induced chondrocyte death. To maintain experimental consistency in the $[Ca^{2+}]_o$ studies thereafter, it was considered important to ensure that all solutions were osmotically balanced.

Two commonly utilised osmolytes are NaCl and Sucrose (Urban *et al.*, 1993; Amin *et al.*, 2008; Amin *et al.*, 2009a). Following a series of experiments detailed within this chapter, sucrose was chosen to osmotically balance all culture media following the addition of $CaCl_2$. Although the metabolic effects on chondrocytes are similar for both osmolytes (Urban *et al.*, 1993), sucrose was chosen for two reasons. Firstly, it is known to maintain an extracellular osmotic pressure gradient without being metabolised by chondrocytes (Dingle *et al.*, 1969). Secondly, although raised osmolarity decreases cellular volume with both sucrose and NaCl, resulting in the subsequent concentration of intracellular contents, the use of NaCl may result in further perturbations to the intracellular ionic environment (Dingle *et al.*, 1969). For example, it has been suggested that raised extracellular Na^+ concentrations may have an influence on intracellular Ca^{2+} concentrations through the presence of a Na^+/Ca^{2+} exchange system on the plasma membrane of chondrocytes (Wilkins *et al.*, 2000; Sánchez *et al.*, 2006).

5.2 HYPOTHESES

The first hypothesis was that raised culture medium osmolarity had no influence on Hla-induced chondrocyte death. The second hypothesis was that increased $[Ca^{2+}]_{o,}$

to the levels investigated in this study, did not influence *S. aureus* growth. The third hypothesis was that increasing the $[Ca^{2+}]_o$ increased the rate of Hla-induced chondrocyte death.

5.3 MATERIALS & METHODS

5.3.1 Biochemicals and solutions

Two distinct variants of DMEM were utilised during this study:

1. DMEM (powder; Catalogue no. 12800-058) with L-glutamine (4mM), D-glucose (25mM), sodium pyruvate (1mM), $CaCl_2$ (1.8mM) was prepared in 1litre of sterile de-ionized water. 4-(2-hydroxyethyl)-1-piperazineethanesulfonic acid (HEPES, 25mM) was added and the pH adjusted to 7.4 using HCl. The osmolarity of the final prepared medium was 300mOsm (measured).
2. 'Ca^{2+}-free' DMEM (aqueous medium, pH 7.4; Catalogue no. 21068-028) with D-glucose (25mM) and sodium bicarbonate ($NaHCO_3$; 44mM), to which L-glutamine (4mM) and sodium pyruvate (1mM) were added. The osmolarity of the final prepared medium was 300mOsm. As this proprietary medium did not contain any added $CaCl_2$ and was free of Ca^{2+}-containing inorganic salts it has been referred to as Ca^{2+}-free (0mM) DMEM in this chapter. It is accepted however that a nominal amount of free Ca^{2+}may still be present due to a potential 'carry over' from the water used to formulate the media.

5.3.2 Measuring and adjusting medium osmolarity

The osmolarity of all solutions was measured using a freezing point osmometer (Advanced Micro Osmometer, Model 3300, Vitech Scientific Ltd, West Sussex, UK). Three osmolarity measurements were taken for each prepared solution and the mean rounded to the nearest multiple of five. For example, the osmolarity of DMEM (1) was measured using three different samples as 297 mOsm, 301 mOsm and 298 mOsm. The mean osmolarity of DMEM (1) was therefore 298.7 mOsm and is reported as 300 mOsm. Medium osmolarity was increased by adding measured amounts of either sucrose or NaCl (sucrose and NaCl obtained from Sigma-Aldrich, Gillingham, UK).

5.3.3 Varying medium Ca^{2+} concentration

Medium Ca^{2+} concentration was varied between 0 and 20mM by adding $CaCl_2$ (1M stock solution, VWR International Ltd., Lutterworth, UK). The addition of $CaCl_2$ increased the osmolarity of the culture medium and, thus, to standardise osmolarity each solution was osmotically balanced to approx. 360mOsm with sucrose, as previously discussed (see section 5.1). For the majority of experiments, DMEM with HEPES buffering was used in preference to $NaHCO_3$-CO_2 as the presence of HCO_3^- in the culture medium may have had the potential to reduce ionised Ca^{2+} concentrations through the precipitation of $CaCO_3$. However, Ca^{2+}-free DMEM was only available with a $NaHCO_3$-CO_2 buffering system and therefore a separate study utilising this medium was conducted in order to investigate the influence of a Ca^{2+}-free medium on Hla-induced chondrocyte death.

5.3.4 Bacterial Strains

S. aureus 8325-4 along with the following isogenic mutant strains were utilised for this study: DU5938 ($Hla^-Hlb^-Hlg^-$), DU5946 ($Hla^+Hlb^-Hlg^-$), DU1090 ($Hla^-Hlb^+Hlg^+$) (**Table 4.1**). Aspirates were established as previously described (see Chapter 2)

5.3.5 Bacterial counts and preparation of defined bacterial aspirates

For the study investigating TSB bacterial growth in the presence of (1) elevated osmolarity (through sucrose addition) and (2) high Ca^{2+} (20mM), 10ml TSB was inoculated with approx. $5.0x10^3$ cfu and incubated (37°C; 24hrs). Thereafter, bacterial counts were conducted as previously described (see Chapter 2). Bacterial growth in normal TSB acted as the control.

5.3.6 High and low $[Ca^{2+}]_o$ *S. aureus* 8325-4 supernatant study

The 40hr cultures of *S. aureus* 8325-4 were pooled and centrifuged (3400g; 10mins) to separate bacteria from toxins. The supernatant, containing the toxins, was harvested and filter-sterilised (0.22μm filter). The supernatant was then equally divided in two. $CaCl_2$ was added to one half in order to raise the $[Ca^{2+}]_o$ to 20mM while sucrose was added to the other half in order to osmotically balance the two groups. The osmolarity of the high and low $[Ca^{2+}]_o$ supernatants was 360mOsm.

5.3.7 Statistical analysis

Parametric data were analysed using either one-way between-groups ANOVA (bacterial growth, *S. aureus* isogenic mutant study and 0mM Ca^{2+} study), with *post*

hoc Bonferroni tests, or unpaired Student's two-tailed t-tests (sucrose and NaCl osmolarity and *S. aureus* 8325-4 supernatant study). A one-way between-groups Kruskal-Wallis ANOVA (extracellular Ca^{2+} sensitivity study), with *post hoc* Dunn's test, was used to analyse non-parametric data. For the study investigating *S. aureus* 8325-4 growth in altered TSB culture medium conditions, *N* refers to the number of independent cultures per experimental group.

5.4 RESULTS

5.4.1 Raised culture medium osmolarity had no influence on *S. aureus* Hla-induced *in situ* chondrocyte death

Prior to assessing the influence of $[Ca^{2+}]_o$, preliminary experiments were conducted in order to assess the impact of raised culture medium osmolarity on Hla-induced *in situ* chondrocyte death i.e. to exclude the possibility that any observed changes in chondrocyte viability with raised $[Ca^{2+}]_o$ were not simply due to the influence of elevated osmolarity. Explants were cultured with *S. aureus* 8325-4 for 40hrs in the presence of low (300mOsm) or high (480mOsm; sucrose addition) osmolarity culture media. There was no significant difference in chondrocyte death between the high and low osmolarity groups at each experimental time point (**Figure 5.1A**), with both groups reaching approx. 100% chondrocyte death at 40hrs. To confirm further that osmolarity *per se* had no influence on Hla-induced chondrocyte death, the experiment was repeated but on this occasion NaCl was added to the culture medium in order to increase the osmolarity by the same amount. Again, there was no significant difference between the high and low osmolarity groups at each time point (**Figure 5.1B**). Additionally, there was no significant difference between the

480mOsm Sucrose and NaCl groups at 18 (p=0.052; unpaired Student's two-tailed t-test), 24 (p=0.2) and 40hrs (p=0.58).

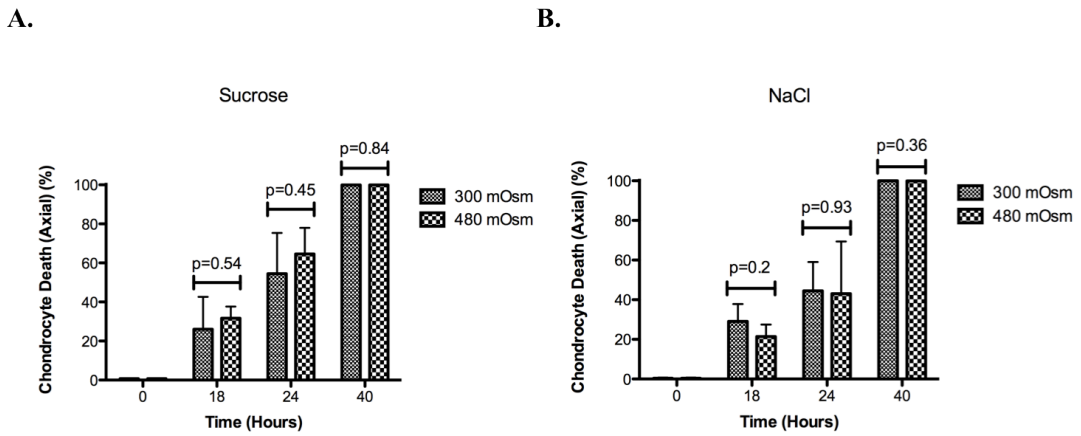

Figure 5.1: Raised culture medium osmolarity had no influence on *S. aureus* Hla-induced *in situ* chondrocyte death

The cell death in explants cultured with *S. aureus* 8325-4 at an osmolarity of 300mOsm were compared with those cultured at an osmolarity of 480mOsm. There was no significant difference in chondrocyte death between the high and low osmolarity groups at any time point for both the sucrose **(A)** and NaCl **(B)** experiments (*N*=4[*n*=2] for both experiments; p values represent low versus high osmolarity by unpaired Student's two-tailed t-test).

5.4.2 A high culture medium Ca^{2+} concentration had no influence on *S. aureus* 8325-4 growth

Before assessing the influence of $[Ca^{2+}]_o$ on Hla-induced chondrocyte death, it was important first of all to test whether increasing culture medium Ca^{2+} concentrations increased *S. aureus* growth. TSB ($[Ca^{2+}]_o$=20mM; 380mOsm) was inoculated with *S. aureus* 8325-4 and incubated for 24hrs (*N*=3). TSB osmotically-balanced with sucrose ($[Ca^{2+}]_o$<1mM; 380mOsm) was utilised to assess the influence of osmolarity on bacterial growth. Standard TSB ($[Ca^{2+}]_o$<1mM; 320mOsm) acted as the control

(*N*=3). At 24hrs, the number of CFUs in the culture media were measured (**Table 5.1**). A one-way between-groups ANOVA demonstrated no significant difference (p=0.12) in the bacterial counts between the groups, thereby indicating that, in comparison to standard TSB (<1mM Ca^{2+}), both raised $[Ca^{2+}]_o$ and osmolarity, to the levels investigated in this study, had no significant effect on *S. aureus* 8325-4 growth.

TSB culture medium conditions (mOsm)	24hr bacterial counts (CFU)
Standard (320)	$1.92x10^9 \pm 0.28x10^9$
+ 20mM Calcium (380)	$1.35x10^9 \pm 0.26x10^9$
+ Sucrose (380)	$1.93x10^9 \pm 0.42x10^9$

Table 5.1: *S. aureus* 8325-4 growth in altered TSB culture medium conditions.

The number of CFU in 10ml defined TSB following 24hrs incubation is displayed (*N*=3). Values are means ± SD.

5.4.3 An elevated $[Ca^{2+}]_o$ had no influence on *in situ* chondrocyte viability in the absence of Hla

In order to determine whether an elevated $[Ca^{2+}]_o$, to the level investigated in this study, had an impact on *in situ* chondrocyte viability, explants were cultured in high Ca^{2+} (20mM) culture medium with the following *S. aureus* isogenic mutants: $Hla^+Hlb^-Hlg^-$, $Hla^-Hlb^+Hlg^+$ and $Hla^-Hlb^-Hlg^-$ (control) (**Table 4.1**). There was a significant difference between the strains at 24hrs (p<0.001), with subsequent *post-hoc* testing demonstrating significantly increased chondrocyte death induced by the $Hla^+Hlb^-Hlg^-$ strain in comparison to the $Hla^-Hlb^+Hlg^+$ (p<0.001) and $Hla^-Hlb^-Hlg^-$ (p<0.001) strains (**Figure 5.2A and B**). There was no significant difference (p=1.0)

between the chondrocyte death induced by the Hla$^-$Hlb$^+$Hlg$^+$ and the Hla$^-$Hlb$^-$Hlg$^-$ strains. The minimal chondrocyte death observed in the explants exposed to the Hla$^-$Hlb$^+$Hlg$^+$ and Hla$^-$Hlb$^-$Hlg$^-$ isogenic mutants over the study period demonstrated, firstly, that a $[Ca^{2+}]_o$ of 20mM had no significant impact on chondrocyte viability during the study period. Secondly, Hlb and Hlg played no significant role in *S. aureus*-induced *in situ* chondrocyte death, thereby further confirming the findings presented in Chapter 4 (**Figure 4.3**).

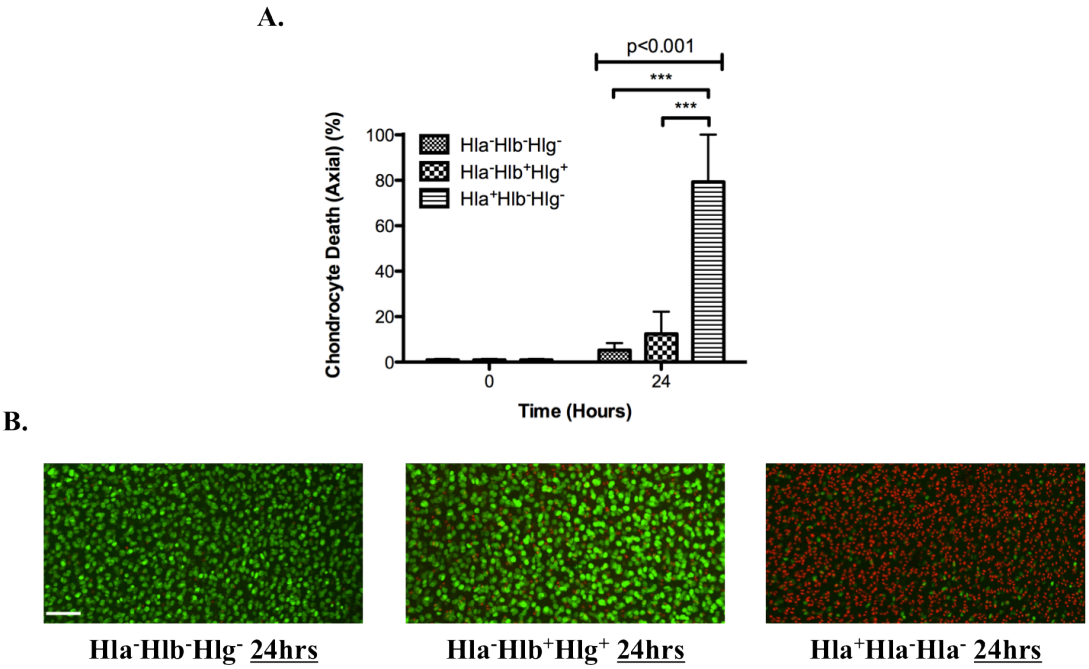

Figure 5.2: Minimal *in situ* chondrocyte death in the absence of Hla in high Ca^{2+} culture medium

Chondrocyte death in osteochondral explants cultured for 24hrs with the Hla$^+$Hlb$^-$Hlg$^-$, Hla$^-$Hlb$^+$Hlg$^+$ and Hla$^-$Hlb$^-$Hlg$^-$ isogenic mutants in the presence of 20mM Ca^{2+} were compared (**A**). There was significantly more chondrocyte death induced by the Hla$^+$Hlb$^-$Hlg$^-$ strain compared to the Hla$^-$Hlb$^+$Hlg$^+$ and Hla$^-$Hlb$^-$Hlg$^-$ strains (*N*=4[*n*=2]; numerical p value represents one-way between-groups ANOVA; *** p<0.001 Hla$^+$Hlb$^-$Hlg$^-$ versus Hla$^-$Hlb$^+$Hlg$^+$ and Hla$^-$Hlb$^-$Hlg$^-$ strains by *post hoc* Bonferroni test). The CLSM images **(B)** represent the chondrocyte death induced by each isogenic mutant at 24hrs (scale bar=100μm).

5.4.4 The rate of Hla-induced *in situ* chondrocyte death increased with raised culture medium $[Ca^{2+}]_o$

In order to assess the influence of $[Ca^{2+}]_o$ on Hla-induced *in situ* chondrocyte death, osteochondral explants were cultured with *S. aureus* 8325-4 for 40hrs in culture media with varying Ca^{2+} concentrations (**Figure 5.3A**). The osmolarity of all media were maintained at 360mOsm (sucrose addition), which had previously been shown to have no influence on Hla-induced *in situ* chondrocyte death (**Figure 5.1A**). There was a significant difference in chondrocyte viability between the experimental groups at 18 (p=0.01) and 24hrs (p=0.02) (**Figure 5.3A and B**). Subsequent *post-hoc* Dunn's tests revealed that there was significantly more chondrocyte death in the 10 and 20mM Ca^{2+} groups in comparison to the 1.8mM group at 18hrs and the 20mM group alone to be significant at 24hrs. There was no significant difference between the 10 and 20mM groups at 18hrs (p=1.0) or 24hrs (p=0.7). By 40hrs there was no significant difference between the groups (p=0.45), with all groups reaching approx. 100% chondrocyte death (**Figure 5.3A and B**). This experiment therefore demonstrated that in the presence of a raised culture medium Ca^{2+} concentration, the rate of Hla-induced *in situ* chondrocyte death increased. However, given that there was no significant difference between the 10 and 20mM groups at each time point, there was the suggestion of a maximal Ca^{2+} level above which there was no significantly increased rate of chondrocyte death.

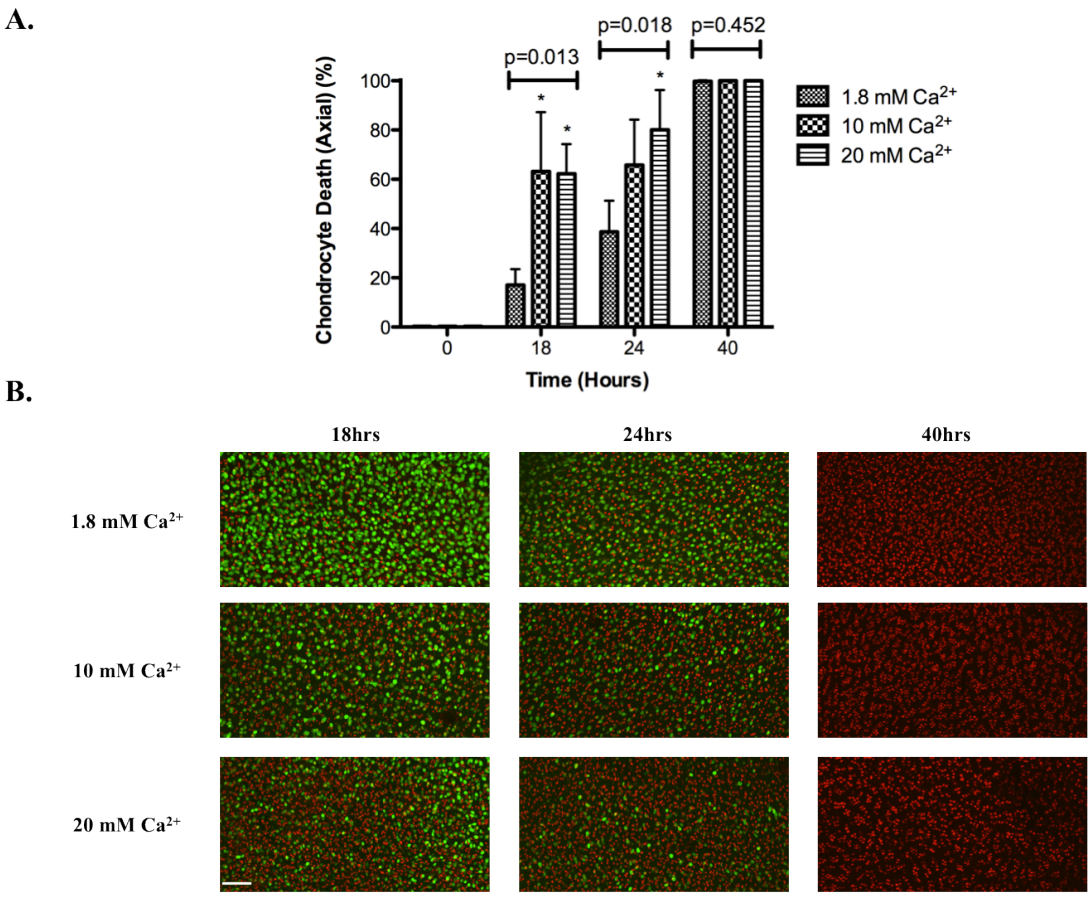

Figure 5.3: The influence of elevated $[Ca^{2+}]_o$ on *S. aureus* Hla-induced *in situ* chondrocyte death

Osteochondral explants were cultured with *S. aureus* 8325-4 in media over the range 1.8 to 20mM Ca^{2+} (**A**) with the osmolarity of media corrected to 360mOsm. There was a significant difference in chondrocyte death between the groups at 18 and 24hrs (*N*=4[*n*=2]; numerical p values represent one-way between-groups Kruskal-Wallis ANOVA; * $p<0.05$ 10 and 20mM versus 1.8mM Ca^{2+} by *post hoc* Dunn's test). By 40hrs, chondrocyte death was comparable between the groups. The CLSM images **(B)** represent the chondrocyte death at each time point in the presence of varying $[Ca^{2+}]_o$ concentrations (scale bar=100μm).

5.4.5 Hla-induced chondrocyte death was still evident in the presence of 0mM Ca^{2+} culture medium

In order to assess the influence of Ca^{2+}-free culture medium on Hla-induced chondrocyte death, explants were cultured with *S. aureus* 8325-4 for 24hrs in culture media containing the following $[Ca^{2+}]_o$: 0, 1.8 and 10mM. The osmolarity of each group was adjusted to 360mOsm (sucrose addition). At 24hrs, there was significantly more chondrocyte death in those explants cultured in DMEM containing 10mM Ca^{2+} in comparison to those explants cultured in media containing 0 and 1.8mM (**Figure 5.4**). There was detectable chondrocyte death in both the 0 and 1.8mM groups. However, there was no significant difference between the 0 and 1.8mM groups at 24hrs (p=1.0). This experiment therefore further demonstrated increased chondrocyte death in the presence of an elevated $[Ca^{2+}]_o$. It also demonstrated that some degree of chondrocyte death still occurred in the presence of Ca^{2+}-free culture medium.

5.4.6 Ca^{2+} played an important role in the Hla-induced chondrocyte death pathway

In order to obtain further evidence to test the hypothesis that increasing the $[Ca^{2+}]_o$ increased the rate of Hla-induced chondrocyte death, explants were cultured for 6hrs in high (20mM) or low (1.8mM) Ca^{2+} *S. aureus* 8325-4 supernatants. The supernatants had identical Hla concentrations and this was achieved by equally dividing a 40hr *S. aureus* 8325-4 supernatant. The osmolarity of each group was maintained at 360mOsm (sucrose addition). At 6hrs there was significantly more chondrocyte death (p=0.015) in the explants exposed to the supernatant supplemented with Ca^{2+} ($[Ca^{2+}]_o$=20mM) in comparison to the low Ca^{2+}-containing

supernatant ($[Ca^{2+}]_o$=1.8mM) (**Figure 5.5A and B**). There was approx. twice as much death in the explants exposed to the high Ca^{2+} supernatant. Taken together, these results suggest that Ca^{2+} played an important role in the cell death pathway mediated by Hla.

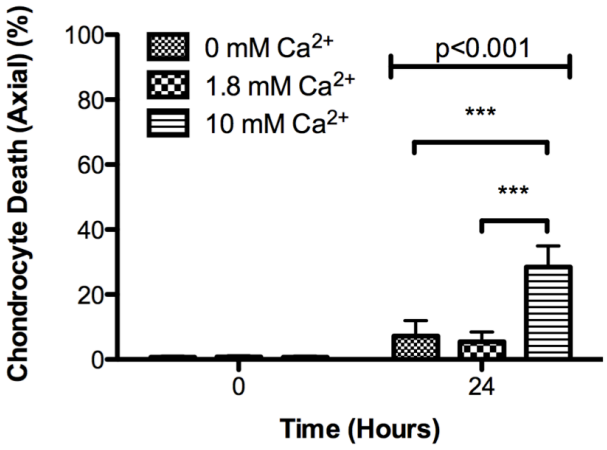

Figure 5.4: The influence of 0mM Ca^{2+} culture medium on Hla-induced chondrocyte death

Osteochondral explants were cultured with *S. aureus* 8325-4 in media over the range 0 to 10mM Ca^{2+} with the osmolarity of media corrected to 360mOsm. There was a significant difference between the groups at 24hrs (*N*=4[*n*=2]; numerical p value represents one-way between-groups ANOVA; *** p<0.001 0mM and 1.8mM versus 10mM Ca^{2+} by *post hoc* Bonferroni test). Chondrocyte death in those explants cultured in the presence of 0mM was comparable to those explants cultured in 1.8mM.

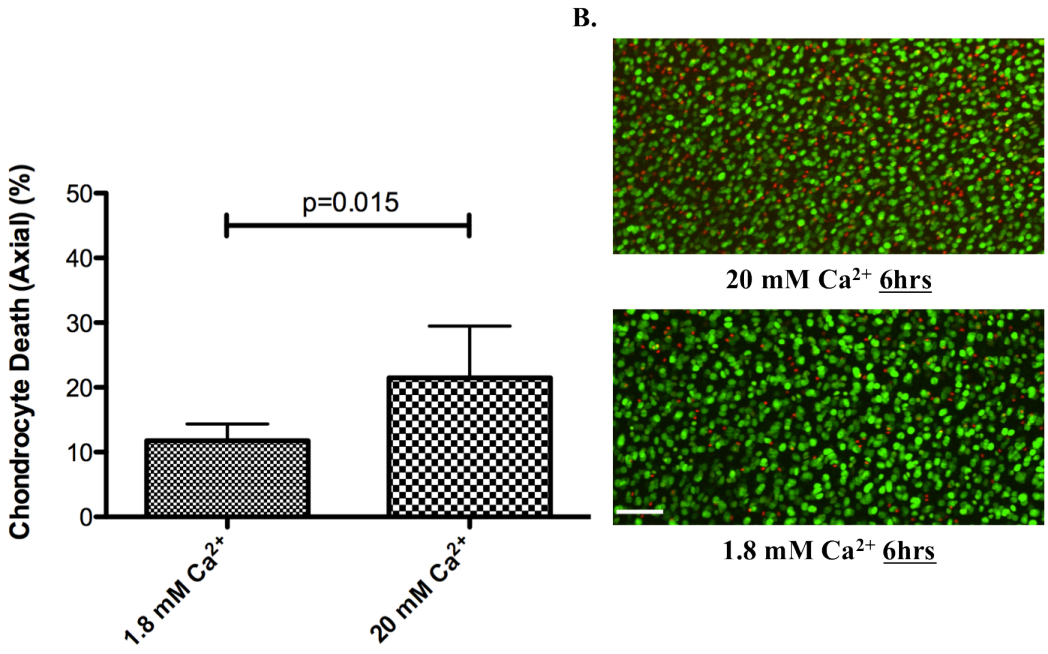

Figure 5.5: A *S. aureus* 8325-4 supernatant supplemented with Ca^{2+} increased *in situ* chondrocyte death

Osteochondral explants were exposed to either a high (20mM) or low (1.8mM) Ca^{2+} *S. aureus* 8325-4 supernatant for 6hrs. The supernatants were osmotically balanced and had comparable Hla concentrations. There was significantly more chondrocyte death in the explants exposed to the high Ca^{2+} supernatant in comparison to those explants exposed to the low Ca^{2+} supernatant (**A)** (*N*=6[*n*=2]; p value represents the results from an unpaired Student's two-tailed t-test). The CLSM images **(B)** show an example of the chondrocyte death induced by each supernatant at 6hrs (scale bar=100μm).

5.5 DISCUSSION

In this study, CLSM was used to determine changes to the viability of *in situ* bovine chondrocytes during exposure to *S. aureus* 8325-4 and associated isogenic mutants in the presence of altered culture medium conditions. Several key findings emerge from this study. Firstly, increased culture medium osmolarity had no significant effect on Hla-induced *in situ* chondrocyte death. Secondly, a raised culture medium Ca^{2+} concentration, to the maximum level investigated in this study, had no significant effect on *S. aureus* 8325-4 growth. Thirdly, in the absence of Hla, a high extracellular Ca^{2+} concentration had no influence on chondrocyte viability during the experimental period. Finally, Hla-induced chondrocyte death increased in the presence of raised extracellular Ca^{2+} concentrations.

The main objective of this study was to assess the influence of elevated $[Ca^{2+}]_o$ on Hla-induced *in situ* chondrocyte death. In order to achieve this goal, the addition of $CaCl_2$ to culture media was required. However, with the addition of $CaCl_2$ the osmolarity of the medium rose (i.e. for every 1mM of added $CaCl_2$, the osmolarity of the culture medium rose by 3mOsm). Thus, assessing the influence of, for example, 1.8 versus 20mM Ca^{2+} culture medium on Hla-induced *in situ* chondrocyte death would actually inadvertently assess two independent variables: (1) elevated Ca^{2+} and (2) elevated osmolarity. It would therefore be impossible to determine whether any observed effects were due to elevated Ca^{2+}, raised osmolarity or both. It was thus necessary to first of all assess the influence of raised culture medium osmolarity on Hla-induced chondrocyte death prior to commencing any experiments investigating the influence of elevated Ca^{2+}.

Using two separate osmolytes, sucrose and NaCl, no significant difference was identified in Hla-induced *in situ* chondrocyte death between high (480mOsm) and low (300mOsm) osmolarity culture media (**Figure 5.1**). This finding enabled the confident osmotic adjustment of Ca^{2+} solutions for subsequent experiments. Sucrose was chosen to increase the osmolarity of solutions, as previously discussed (see section 5.1). Others may consider that $MgCl_2$ would have been a more appropriate osmolyte, as it would have enabled the maintenance of a consistent divalent cation concentration between Ca^{2+} solutions. However, studies have suggested increased *S. aureus* growth and toxin production in the presence of elevated culture medium Mg^{2+} concentrations (Ochiai, 2001) and, accordingly, it was not utilised in the current study.

Before assessing the influence of elevated $[Ca^{2+}]_o$ on Hla-induced chondrocyte death, it was considered important to assess the influence of raised Ca^{2+} concentrations on bacterial growth, as previous studies have highlighted an important role of Ca^{2+} for the growth of several bacterial species/strains (Onoda *et al.*, 2000; Patrauchan, 2005; Cruz *et al.*, 2012). No other studies have specifically investigated the effect of Ca^{2+} on the growth of *S. aureus* 8325-4. It was therefore possible that raised culture medium Ca^{2+} concentrations in this *in vitro* model may have stimulated *S. aureus* 8325-4 growth, with an associated increase in Hla levels. This would have provided a possible explanation for any observed differences in chondrocyte viability between the Ca^{2+} concentrations studied. Nevertheless, there was no significant difference between the bacterial counts in high and low Ca^{2+} culture media (osmolarity of each

solution equal) at 24hrs (**Table 5.1**), indicating no influence of elevated Ca^{2+}, to the maximum level studied, on *S. aureus* 8325-4 growth. In addition, raised osmolarity *per se* also had no influence on bacterial growth (**Table 5.1**). Given the various defined phases of bacterial growth (Harris *et al.*, 2002), it is appreciated that this was a crude experimental strategy to assess *S. aureus* 8325-5 growth and future studies will therefore establish and compare growth curves during similar culture conditions. Furthermore, although 24hr bacterial counts were comparable in the current study, it was not possible to exclude the possibility that high Ca^{2+}stimulated bacteria to produce more Hla. A potential future experiment to address this question would be to compare Hla activity between high and low Ca^{2+} 24hr *S. aureus* 8325-4 cultures by conducting a rabbit red cell haemolytic titre (Nilsson *et al.*, 1999).

It has been hypothesised that the membrane-spanning pores established by Hla disturb the ionic equilibrium between the intra and extracellular compartments (Bhakdi and Tranum-Jensen, 1991). Some studies have suggested that the influx of Na^{+} coupled with the efflux of K^{+} (Walev *et al.*, 1993; Essmann *et al.*, 2003) is a key event in the Hla-induced death pathway while other studies have suggested that an influx of Ca^{2+} is an important primary trigger (Suttorp *et al.*, 1985; Bhakdi and Tranum-Jensen, 1991). Prior to assessing the influence of Ca^{2+} on Hla-induced chondrocyte death, a preliminary experiment was conducted to assess whether a Ca^{2+} concentration of 20mM, which exceeds published ECM (6-15mM) (Urban, 1994) and synovial fluid (approx. 4mM) (Wan *et al.*, 2008) levels, would influence *in situ* chondrocyte viability during the experimental period. Hla-deficient isogenic mutants exhibited minimal, but detectable, chondrocyte death in comparison to an Hla-

producing mutant, which induced significant chondrocyte death (**Figure 5.2**). This suggested that chondrocytes were capable of maintaining intracellular Ca^{2+} homeostasis, even in the presence of elevated extracellular levels. Intracellular Ca^{2+} within chondrocytes is controlled tightly in the range of 80-100nM (Hall *et al.*, 1996a; Yellowley *et al.*, 1997; Wilkins *et al.*, 2000; Sánchez *et al.*, 2003). Transport systems in the endoplasmic reticulum, mitochondria and plasma membrane are believed to play a key role in maintaining the ionic $[Ca^{2+}]_i$ equilibrium within eukaryotic cells (Berridge *et al.*, 1998). Given the large concentration gradient between the intra and extra-cellular compartments, it would thus appear that chondrocytes are uniquely adapted to regulating intracellular Ca^{2+} levels in the face of high extracellular levels. The small, but detectable chondrocyte death observed in those explants exposed to the $Hla^{-}Hlb^{-}Hlg^{-}$ and $Hla^{-}Hlb^{+}Hlg^{+}$ mutants may reflect Ca^{2+}-induced enhanced potency of Hlb and Hlg and other *S. aureus* toxins. Regardless, this experiment further confirmed the destructive influence of Hla.

With culture medium Ca^{2+} concentrations initially ranging from 1.8 to 20mM, elevated Hla-induced *in situ* chondrocyte death was identified with higher Ca^{2+} concentrations (**Figure 5.3**). This experiment was conducted using culture medium containing a HEPES buffering system rather than a bicarbonate system, as there was concern that the presence of bicarbonate would precipitate calcium carbonate, thereby reducing the availability of free Ca^{2+}. Whilst the rate of Hla-induced chondrocyte death increased between 1.8 and 10mM, there was no significant difference between 10 and 20mM at each time point (**Figure 5.3**). This finding suggested that there was a maximal Ca^{2+} level between 1.8 and 10mM above which

there was no significantly increased rate of chondrocyte death. By 40hrs however there was almost complete chondrocyte death in each experimental group, thereby demonstrating potent Hla-induced chondrocyte death even at low medium Ca^{2+} concentrations. Ultimately, this experiment demonstrated higher rates of Hla-induced chondrocyte death in the presence of elevated Ca^{2+} concentrations.

Given that elevated Ca^{2+} concentrations resulted in an increased rate of chondrocyte death, it was considered important to assess the influence of 0mM Ca^{2+} culture medium on Hla-induced chondrocyte death. Unfortunately, 0mM Ca^{2+} culture media was only available with a bicarbonate buffer and therefore a further extracellular Ca^{2+} sensitivity experiment was conducted. Whilst there was significantly more chondrocyte death in those explants exposed to 10mM at 24hrs there was still a detectable level of chondrocyte death in those explants cultured in 0mM Ca^{2+} medium, which was comparable to that of the 1.8mM Ca^{2+} group. It was perhaps unsurprising that Hla-induced chondrocyte death still occurred in the presence of 0mM culture medium as the negatively charged proteoglycans within the cartilage matrix have a strong affinity for cations such as Ca^{2+} and thus a reasonable Ca^{2+} concentration was likely to have been maintained within the ECM. It is also possible that trace amounts of Ca^{2+} remained in the medium i.e. the medium wasn't truly Ca^{2+}-free. The reduced chondrocyte death observed in the 1.8 and 10mM Ca^{2+} groups (during the study to assess the influence of 0mM Ca^{2+} culture medium on Hla-induced chondrocyte death) in comparison to the same experimental time point in the initial extracellular Ca^{2+} sensitivity experiment (**Figures 5.3 and 5.4**) possibly

reflected the presence of bicarbonate in the culture medium i.e. reduced Ca^{2+} availability.

One potential criticism of the extracellular Ca^{2+} sensitivity experiment was that the increased rate of Hla-induced chondrocyte death observed in the presence of elevated Ca^{2+} concentrations may have been due to Ca^{2+}-induced stimulation of Hla production by *S. aureus* 8325-4. To date, no studies have investigated the influence of raised extracellular Ca^{2+} concentrations on *S. aureus* Hla-production. Interestingly, in *Pseudomonas aeruginosa* Ca^{2+} has been identified to be an important regulatory ion that influences the production of extracellular enzymes and toxins (Patrauchan, 2005; Sarkisova *et al.*, 2005). However, when explants exposed to a high-Ca^{2+} *S. aureus* 8325-4 supernatant (bicarbonate-free) were compared with explants exposed to an osmotically balanced low-Ca^{2+} supernatant of identical Hla concentration, there was approx. twice as much chondrocyte death in those explants exposed to the high-Ca^{2+} supernatant (**Figure 5.5**). In the absence of viable bacteria, this experiment therefore provided convincing experimental evidence that Ca^{2+} was involved in the Hla-induced chondrocyte death pathway.

A further potential criticism of the findings presented in this chapter is that they provide no indication as to which stage of the Hla-induced chondrocyte death pathway Ca^{2+} is involved. For example, Ca^{2+} may enter the chondrocyte through the membrane-spanning pores established by Hla with the resultant rise in intracellular Ca^{2+} concentrations triggering death pathways or, alternatively, Ca^{2+} may enter the cell as a result of loss of membrane integrity (i.e. at a later stage) and thereafter

accelerating established death pathways. However, the goal of the current study was to identify if Ca^{2+} was indeed involved in the Hla-induced chondrocyte death pathway and this was achieved.

To conclude, this study builds upon the knowledge obtained in Chapter 4 that Hla is critical to *S. aureus*-induced *in situ* chondrocyte death in a bovine cartilage explant model of septic arthritis by demonstrating an important role of extracellular Ca^{2+} in the Hla death pathway. A further understanding of the role of Ca^{2+} in this pathway may enable future targeted therapeutic strategies to reduce the extent of chondrocyte death during and after an episode of septic arthritis.

CHAPTER 6

A DYNAMIC ASSESSMENT OF INTRACELLULAR CALCIUM FOLLOWING THE EXPOSURE OF *IN SITU* CHONDROCYTES TO *S. AUREUS* ALPHA-HAEMOLYSIN

6.1 INTRODUCTION

Alterations in intracellular Ca^{2+}, Na^{+} and K^{+} concentrations have been hypothesised to be key events in the Hla-induced cell death pathway (Berube and Bubeck-Wardenburg, 2013). However, there remains some uncertainty as to the exact roles of these ions. Some studies have suggested that the influx of Ca^{2+} through the membrane-spanning Hla pore is the main trigger of cellular death mechanisms (Suttorp *et al.*, 1985) while other studies have suggested that Hla pores do not permit the passage of divalent cations and that the important primary trigger is the influx of Na^{+} coupled with the efflux of K^{+} (Walev *et al.*, 1993; Valeva *et al.*, 2000). In Chapter 5, the rate of Hla-induced *in situ* chondrocyte death was found to have increased with elevated $[Ca^{2+}]_o$, thereby adding strength to the argument that Ca^{2+} plays a key role in the Hla-mediated chondrocyte death pathway. In this chapter, the role of Ca^{2+} in the Hla-induced cell-death pathway has been further explored.

The emergence of cytosolically-trapped fluorescent probes that change their emission/absorption spectra upon Ca^{2+}-binding, coupled with advanced multi-track CLSM live-cell imaging systems, has enabled the characterisation and quantification of dynamic changes in $[Ca^{2+}]_i$ within a variety of eukaryotic cells in response to external perturbations (Smith *et al.*, 1991; Smith *et al.*, 1992; Papadimitriou *et al.*, 1994; Trump and Berezesky, 1995). Indeed, recent studies by Han *et al.* (2012) and Madden *et al.* (2014) utilised such methods to investigate chondrocyte Ca^{2+} signalling within osteochondral explants during dynamic loading conditions. Both studies assessed changes in $[Ca^{2+}]_i$ through a 'ratiometric' technique whereby chondrocytes were stained simultaneously with two Ca^{2+}-sensitive fluorophores:

Fluo-4 and Fura Red. As $[Ca^{2+}]_i$ increases, the intensity of Fluo-4 fluorescence increases (Gee *et al.*, 2000; Walczysko *et al.*, 2000) whilst, paradoxically, the intensity of Fura Red fluorescence decreases. Thus, a ratio can be established between the intensity of fluorescence of the two stains. This ratio remains unchanged in the event of a shift in the focal plane or photobleaching and will only rise in the event of an increase in $[Ca^{2+}]_i$.

Most fluorescent Ca^{2+} indicators are based on the Ca^{2+} chelators ethylene glycol tetraactetic acid (EGTA) or 1,2-bis(o-aminophenoxy)ethane-N,N,N',N'-tetraacetic acid (BAPTA) modified to incorporate fluorescent reporter groups (Thomas *et al.*, 2000). In this study, indicators with acetoxymethyl(AM)-ester linkage (Fluo-4 AM and Fura Red AM) have been used to introduce the indicators into living *in situ* chondrocytes, the AM-ester groups being cleaved by endogenous cytosolic esterases releasing the Ca^{2+}-sensitive form of the indicator intracellularly. Thereafter, alterations in $[Ca^{2+}]_i$ within *in situ* chondrocytes were assessed following experimental challenge.

This study aims to build on the knowledge obtained from the extracellular Ca^{2+} study detailed in the Chapter 5 by attempting to assess dynamic changes in $[Ca^{2+}]_i$ within viable *in situ* chondrocytes following Hla exposure. Live-cell CLSM coupled with Ca^{2+}-sensitive fluorophores has been used to assess changes in $[Ca^{2+}]_i$, represented by changes in fluorophore fluorescence, following ionomycin and, thereafter, Hla exposure. Exposure of *in situ* chondrocytes to ionomycin permitted validation of the dynamic experimental CLSM system prior to experimentation with Hla. Ionomycin

is an effective and widely studied Ca^{2+} ionophore (a chemical that induces a rise in $[Ca^{2+}]_i$) that is produced by the bacterium *Streptomyces conglobatus* (Liu and Hermann, 1978). It functions by both facilitating the transport of Ca^{2+} across the plasma membrane, through the creation of plasma membrane pores that are preferentially permeable to Ca^{2+}, and also by stimulating the release of Ca^{2+} from intracellular stores (Himmel *et al.*, 1990; Morgan and Jacob, 1994). When administered in sufficiently high doses, ionomycin will induce cell death (Gwag *et al.*, 1999).

6.2 HYPOTHESES

The first hypothesis was that Hla-induced chondrocyte death is associated with an overwhelming rise in $[Ca^{2+}]_i$. The second hypothesis was that SZ chondrocytes more rapidly succumb to alterations in $[Ca^{2+}]_i$ in comparison to chondrocytes from deeper zones.

6.3 MATERIALS AND METHODS

6.3.1 Biochemicals and Solutions

Ionomycin was prepared as a 10mM stock solution in DMSO. The following DMEM variants were used during this study:

3. 'Phenol red-free' DMEM (aqueous medium, pH 7.4, 340mOsm; Catalogue no. 21063-029) with HEPES (25mM), L-glutamine (4mM), D-glucose (25mM) and $CaCl_2$ (1.8mM). A phenol red-free medium has been shown to improve sensitivity and 'signal to noise' ratio during CLSM imaging (Frigault *et al.*, 2009)

4. ‘Bicarbonate-free’ DMEM (powder; Catalogue no. 12800-058) with L-glutamine (4mM), D-glucose (25mM), sodium pyruvate (1mM), $CaCl_2$ (1.8mM) was prepared in 1litre of sterile de-ionized water. HEPES (25mM) was added and the pH adjusted to 7.4 using HCl. The osmolarity of the final prepared medium was 340mOsm (adjusted with sucrose).

6.3.2 Fluorescent probes

The following fluorescent probes were utilised for the experimental work presented in this chapter:

1. LIVE CELLS: **CMFDA** was used to stain living cells as previously described in Chapter 2.
2. DEAD CELLS: **PI** was used to stain dead or dying cells as previously described in Chapter 2.
3. INTRACELLULAR Ca^{2+}: the following two stains were used to assess dynamic changes in $[Ca^{2+}]_i$:
    1. **Fluo-4 AM**: passes freely through the plasma membrane of viable cells in a non-fluorescent form (Fluo-4 AM) and is cleaved by cytosolic esterases into the fluorescent ‘Fluo-4’. Fluo-4 binds to intracellular free Ca^{2+} and fluoresces green following laser excitation (Paredes *et al.*, 2008). The level of fluorescence increases with Ca^{2+} binding (Gee *et al.*, 2000) and thus as $[Ca^{2+}]_i$ increases the intensity of Fluo-4 fluorescence also increases. Fluo-4 AM (50μg) was prepared as a 1mM stock solution in DMSO.

2. **Fura Red AM**- passes freely through the plasma membrane of viable cells in a non-fluorescent form (Fura Red AM) and is cleaved by cytosolic esterases into the fluorescent 'Fura Red'. Fura-Red binds to free Ca^{2+} and fluoresces red following laser excitation (Kurebayashi *et al.*, 1993). In contrast to Fluo-4 however, the level of fluorescence decreases with Ca^{2+} binding (Walczysko *et al.*, 2000) and therefore as $[Ca^{2+}]_i$ increases the intensity of Fura Red fluorescence decreases. Fura Red AM (50μg) was prepared as a 1mM stock in 20% pluronic acid (v/w in DMSO; pluronic acid is believed to facilitate dye entry into cells (Pecze *et al.*, 2013)).

6.3.3 Bacterial supernatants

S. aureus 8325-4 ($Hla^+Hlb^+Hlg^+$) and DU5938 ($Hla^-Hlb^-Hlg^-$) were cultured with osteochondral explants in bicarbonate-free DMEM and the 40hr culture supernatants harvested as previously described in Chapter 2.

6.3.4 Tissue culture

Osteochondral explants were harvested as previously described in Chapter 2. For all studies, explants were harvested into DMEM (phenol red-free) and incubated (37°C; 5% CO_2) for 24hrs prior to experimentation. At the time of experimentation, explants were removed from the tissue culture flasks, trimmed as previously described (see Chapter 2) and stained with specified fluorescent stains. For the cut-edge study (see section 6.4.5 for study rationale), explants were transferred to culture vessels containing either fresh 340mOsm ('normal' osmolarity) or 600mOsm

(sucrose addition; 'high' osmolarity) phenol red-free DMEM and incubated for 2hrs (37°C) prior to trimming and staining. This enabled the *in situ* chondrocytes to respond to the altered osmotic environment prior to scalpel wounding.

6.3.5 Fluorescent stain combinations

The following fluorescent stain combinations were utilised during this study:

1. **CMFDA** and **PI**: explants were incubated (1hr; 21°C) in phenol red-free DMEM with CMFDA (10μM) and PI (10μM).
2. **Fluo-4** and **PI**: explants were incubated (30mins at 37°C followed by 30mins at 21°C) in phenol red-free DMEM with Fluo-4 (15μM) and PI (10μM). For the cut-edge study, explants were stained in either high or normal osmolarity phenol red-free DMEM (see above).
3. **Fluo-4** and **Fura Red**: explants were incubated (30mins at 37°C followed by 30mins at 21°C) in phenol red-free DMEM with Fluo-4 (15μM) and Fura Red (60μM).

The staining of all explants was conducted in a Falcon tube (15ml). For the staining of explants with Fluo-4, Fura Red or both, the stains were protected from excessive light exposure by wrapping the Falcon tube with tinfoil.

6.3.6 Coverslip preparation and cartilage explant mounting

Unless stated otherwise, all experiments presented in this chapter were conducted using an inverted microscope system and therefore, unlike in the previous chapters, all cartilage explants were mounted onto glass cover slips 'articular-surface-down'

(**Figure 6.1A**). However, prior to the commencement of each experiment, three 'rows' of clear nail varnish, measuring approx. 3 x 10mm with an approx. 5mm gap between each row, were established. Upon drying, the viscous nature of the nail lacquer generated an approx. 1mm elevated platform. The subsequent placement of each explant across the three elevated rows created a gap that enabled adequate exposure of the articular surface, and thus *in situ* chondrocytes, to the experimental fluid (**Figure 6.1B**). Each explant was secured with Blu-Tack prior to submersion in a defined medium. Upon cartilage mounting, the coverslip was placed into a POCmini-2 open tissue culture microscope chamber system (HemoGenix®, Inc., Colorado, USA) and, thereafter, the explant submerged in specified culture medium (**Figure 6.1C**).

The pilot study to assess the rate of Hla-induced *in situ* chondrocyte death in a live-cell system was conducted using the Zeiss LSM510 upright microscope and therefore the explants were mounted as previously described (see Chapter 2).

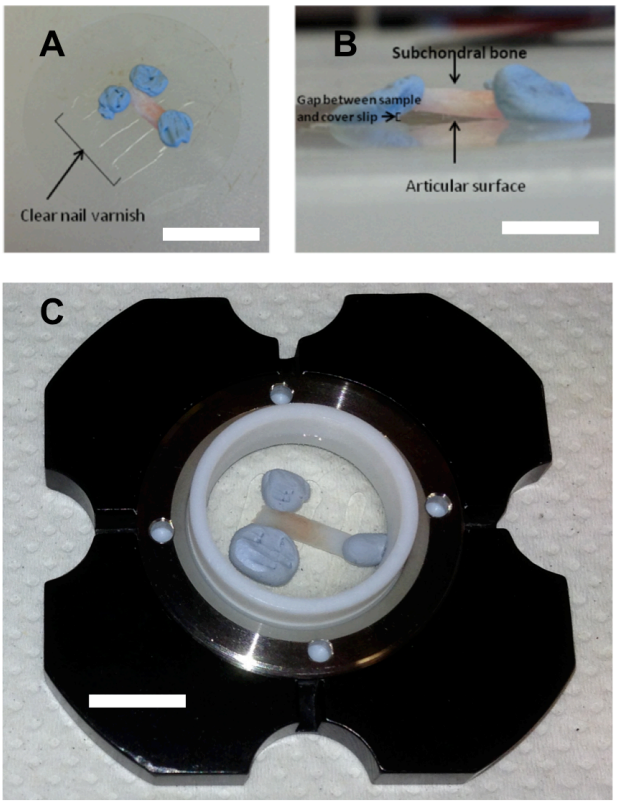

Figure 6.1: Coverslip preparation for imaging on Nikon A1 inverted CLSM system

Osteochondral explants were placed 'articular-surface-down' between 3 rows of dried nail varnish and secured with 3 Blu-Tack balls (A). The nail varnish rows, coupled with the Blu-Tack balls, permitted adequate exposure of the articular surface to the experimental culture medium whilst remaining sufficiently close to the glass cover slip for CLSM imaging (B). Each coverslip was secured into a watertight POCmini-2 open tissue culture microscope chamber system and thereafter the explant was submerged in the designated experimental culture medium prior to CLSM imaging (C) (scale bar=1cm). Images A and B kindly provided by Frances Greaney, Centre for Integrative Physiology, The University of Edinburgh.

6.3.7 Live-cell studies

The following dynamic live-cell studies were conducted:

1. **Ionomycin study:** Explants stained with (1) Fluo-4 and PI and (2) Fluo-4 and Fura Red were submerged in pre-warmed phenol red-free DMEM (600μl; 37°C) containing PI (15μM) and transferred to a pre-heated (37°C) and humidified microscope cage incubator (Okolab, Ottaviano, Italy). For the Fluo-4 and PI study, images were acquired every 2mins over an initial 22min period. At 22mins, 300μl DMEM was carefully removed from the experimental chamber and replaced with pre-warmed (37°C) DMEM containing ionomycin (100μM). Thereafter, images were acquired every 2mins for a further 46mins. For the Fluo-4 and Fura Red ratiometric study, once the microscope settings had been optimised, 300μl DMEM was carefully removed from the experimental chamber and replaced with pre-warmed (37°C) DMEM containing ionomycin (100μM) as per above. Thereafter, images were acquired every 10secs over a 5min period. The final concentration of ionomycin within the tissue culture microscope chamber for both studies was 50μM.
2. **Preliminary assessment of live-cell time course in the presence of Hla:** Explants stained with CMFDA and PI were submerged in pre-warmed phenol red-free DMEM (5ml; 37°C) and transferred to a heated (37°C) microscope stage (Zeiss warm stage, Linkam Scientific Instruments, Surrey, UK). Thereafter, the DMEM was carefully removed and replaced with pre-warmed (37°C) *S. aureus* 8325-4 supernatant, to which was added PI (15μM). Images of the same region of cartilage were acquired in the axial plane at 0, 2, 4 and 6hrs with an upright Zeiss LSM510 microscope as previously described (see Chapter 2).

3. **Hla study:** Explants were stained with Fluo-4 and PI prior to submersion in either pre-warmed *S. aureus* 8325-4 ($Hla^{+}Hlb^{+}Hlg^{+}$) or $Hla^{-}Hlb^{-}Hlg^{-}$ supernatant (1ml; 37°C) containing PI (10μM). Thereafter, they were immediately transferred to the microscope cage incubator and images were acquired every 5mins for 6hrs.
4. **Cut-edge study (see section 6.4.5 for study rationale):** Explants were trimmed as previously described and incubated (37°C) in high (600mOsm) and normal (340mOsm) osmolarity phenol red-free DMEM for 2hrs. Thereafter, they were stained with Fluo-4 and PI in phenol red-free DMEM of identical osmolarity. Microscope settings were optimised and a single image was acquired.

6.3.8 CLSM

For the pilot study investigating the rate of Hla-induced *in situ* chondrocyte death in a live tissue model, axial images of CMFDA- and PI-labelled chondrocytes were acquired at 0, 2, 4 and 6hrs using an upright Zeiss LSM510 CLSM system as previously described in Chapter 2.

For all remaining experiments, axial images were acquired with an inverted Nikon A1R CLSM system (Nikon UK, Kingston Upon Thames, Surrey, UK) using a x10/0.3 CFI Plan Fluor air objective lens (**Figure 6.2**). Each optical section measured 921 x 921μm and had an image resolution of 512x512 pixels. With the exception of the Fluo-4 and Fura Red ratiometric study, whereby a single z-slice was acquired every 10secs over a 5min time-course, the focal plane was moved through

the tissue in 10μm increments from the articular surface normally to a depth of 100μm at defined time intervals over a designated time period (see above). Only a single axial image was obtained for each explant in the cut-edge study.

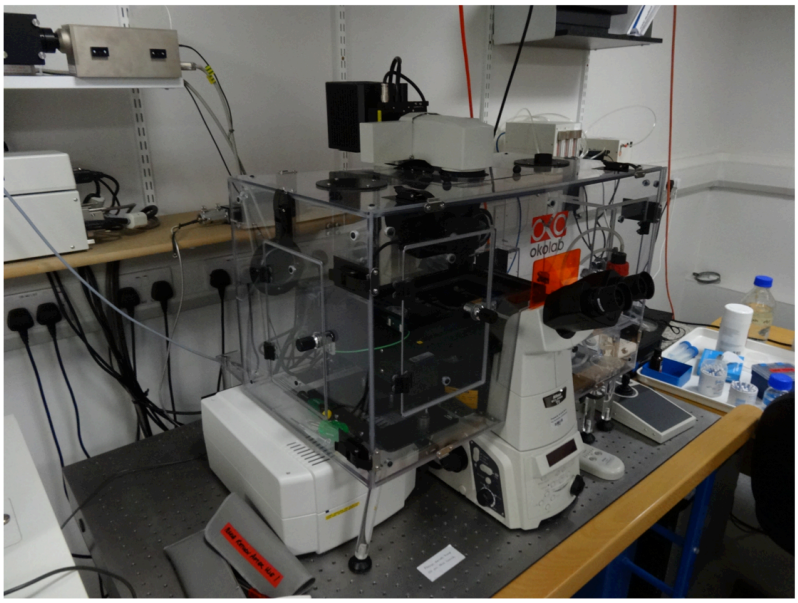

Figure 6.2: The Nikon A1R CLSM imaging system, with attached Perspex incubator chamber, that was utilised during this study for assessing alterations in $[Ca^{2+}]_i$ within living *in situ* chondrocytes following experimental challenge

For the experiments utilising a combination of Fluo-4 and PI, a channel series protocol for multicolour images was used in order to minimise 'bleed-through' (fluorescence emission overlap between two fluorophores), with the same high voltage gain and digital offset settings being applied to both control and treated samples. Fluo-4 was excited at 488nm and signal (emitted light) collected from 500-550nm while PI was excited at 561nm and signal collected from 570-620nm (band-pass filters permitted the separation and capture of the fluorescence emitted from Fluo-4 and PI). For the experiment utilising a combination of Fluo-4 and Fura Red,

a spectral scan of Fluo-4 emission from a Fluo-4 only loaded cartilage explant revealed a 'red shift' in the emission profile (i.e. a shift towards the Fura Red emission spectrum) compared to the published emission spectrum (www.lifetechnologies.com) (**Figure 6.3**). In order to remove this red shifted Fluo-4 signal from the Fura Red detection channel, a virtual filter (adjustable spectral grating) protocol was used. Fluo-4 and Fura Red were excited at 488nm and detected between 504nm to 558nm and 642 to 696nm, respectively (Han et al, 2011); an optical configuration set-up was employed on the Nikon A1R in order to use the virtual filter sequentially. This protocol minimised any 'bleed-through' of the Fluo-4 signal into the Fura Red acquisition channel.

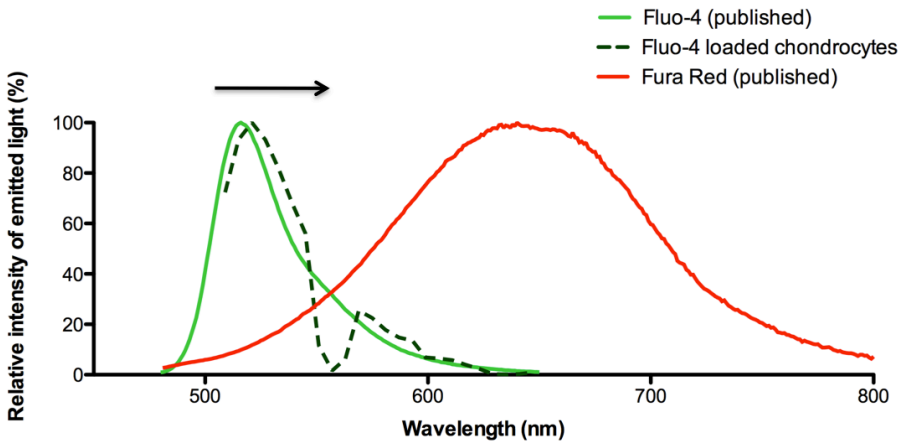

Figure 6.3: Emitted fluorescence from Fluo-4- and Fura Red-loaded cells

A spectral scan of Fluo-4 emission (excitation at 488nm) from Fluo-4-only loaded *in situ* chondrocytes revealed a 'red-shift' (indicated by black arrow) in the emission profile (i.e. a shift towards the Fura Red emission spectrum). This necessitated the establishment of a 'virtual filter' protocol in order to minimise 'bleed-through' of the Fluo-4 signal into the Fura Red acquisition channel. *In situ* chondrocyte Fluo-4 emission data kindly provided by Dr Trudi Gillespie, IMPACT facility, The University of Edinburgh.

6.3.9 Quantitative analysis

The following quantitative analysis methodology was used for each experiment:

1. **Pilot study assessing the rate of Hla-induced *in situ* chondrocyte death in a live cartilage explant model**: chondrocyte death was assessed within a 50% 'field-of-view' ROI using Volocity 4 software as previously described in Chapter 2. However, in order to ensure that the same region of cartilage was assessed at each designated time point, an explant corner i.e. a defined landmark was imaged and thus a small region of cut-edge was incorporated in the analysis.
2. **Fluo-4 and PI ionomycin study**: for the initial Fluo-4 and PI ionomycin study, a 50% field-of-view ROI, identical in both placement and dimensions to those utilised in the previous chapters (**Figure 6.4A**), was established using Nikon NIS Elements version 4.0 software (Nikon UK, Kingston Upon Thames, Surrey, UK). Thereafter, the percentage change in fluorescence intensity (%ΔF) of the Fluo-4 (%Δ$F_{\text{Fluo-4}}$) and PI (%ΔF_{PI}) stains within this ROI (i.e. the global response of all cells within this ROI) from 0hrs (T_0) over the experimental period was calculated as follows: (($F\ T_x - F\ T_0$)/$F\ T_0$ x 100) ($F\ T_0$ = arbitrary units (AU) of fluorescence at 0hrs; $F\ T_x$ = arbitrary units of fluorescence at designated time point). Given the potential differences in both Fluo-4 stain uptake and subsequent response between explants, calculation of %ΔF enabled the standardised assessment of ΔF between explants.
3. **Fluo-4 and Fura Red ratiometric ionomycin study:** the 50% field-of-view ROI utilised for the above Fluo-4 and PI ionomycin study was further

subdivided into quadrants (**Figure 6.4B**). Thereafter, 3 cells within each quadrant were chosen by an impartial observer (12 cells in total per explant) and the $\%\Delta F_{\text{Fluo-4}}$ and $\%\Delta F_{\text{Fura Red}}$ from T_0 within each cell was assessed. This was achieved by creating a 'Bezier' ROI (a combination of linked curves around an object) around each chosen chondrocyte using the Nikon NIS Elements version 4.0 software (**Figure 6.4C**).

4. **Hla study**: the $\%\Delta F_{\text{Fluo-4}}$ and $\%\Delta F_{\text{PI}}$ from T_0 within individual cells following exposure to either an Hla-containing 8325-4 or $Hla^{-}Hlb^{-}Hlg^{-}$ supernatant was conducted using the same methodology as the above Fluo-4 and Fura Red ionomycin study.
5. **Cut-edge study (see section 6.4.5 for study rationale)**: ROIs measuring 921x100x100μm (x-y-z axes, respectively), which were further subdivided into quadrants, were positioned at both the cut-edge and the distal margin of the field-of-view (i.e. as far away from the cut-edge as possible) (**Figure 6.4D**). Bezier ROIs were established around 3 cells per quadrant (12 cells per ROI; chosen by an impartial observer) and the mean Fluo-4 fluorescence (AU) within each cell was assessed.

6.3.10 Statistical analysis

Data were analysed using either paired or unpaired Student's t-tests. For all experiments, *N* refers to the number of feet from separate animals (independent experiments). For the Fluo-4 and PI ionomycin and preliminary Hla live-cell studies, *n* refers to the number of cartilage explants analysed per foot for each experimental group. For all other experiments, *n* refers to the number of cells analysed per

cartilage explant (one cartilage explant per foot was investigated during these experiments).

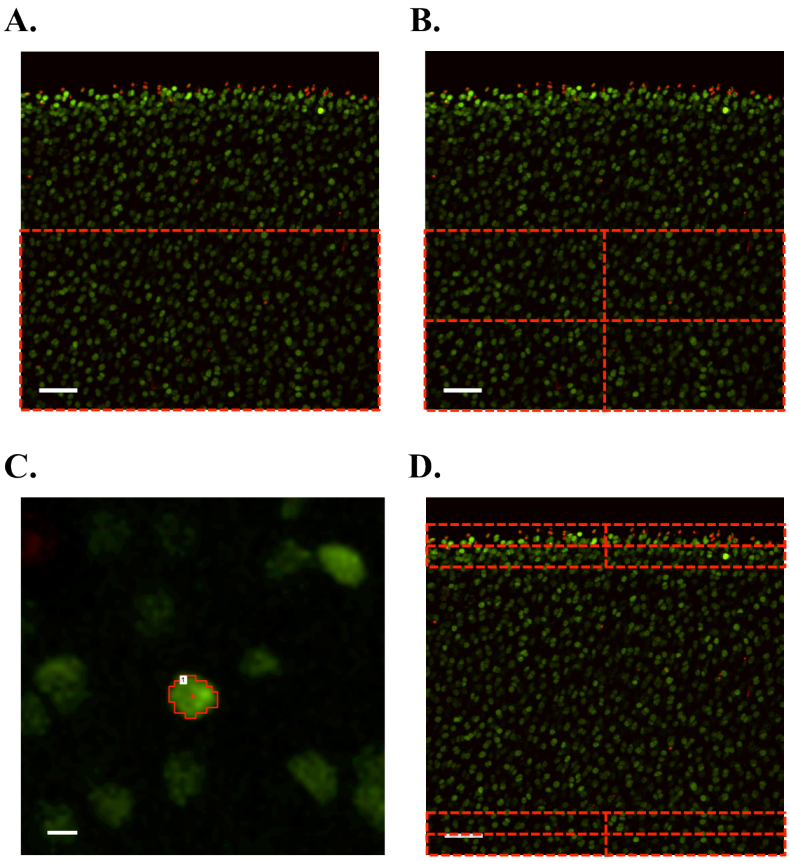

Figure 6.4: ROIs utilised for the intracellular Ca^{2+} imaging experiments

A 50% ROI (demarcated by broken red line) (**A**), as previously described (see chapter 2), was initially utilised to assess alterations in $[Ca^{2+}]_i$ within all cells contained within the ROI following exposure to ionomycin. For the Fluo-4/Fura Red ionomycin ratiometric and 8325-4 ($Hla^+Hlb^+Hlg^+$) vs $Hla^-Hlb^-Hlg^-$ supernatant studies, the 50% ROI was further subdivided in quadrants (**B**) and 3 cells were analysed within each quadrant (12 cells in total per explant). Single cell analysis was achieved by creating a 'Bezier' ROI (demarcated by solid red line) around each chosen chondrocyte (**C**). For the cut-edge study, ROIs measuring 921x100x100 (x-y-z axes, respectively), which were further subdivided into quadrants, were positioned at both the cut-edge and the distal margin of the field-of-view (**D**) and 3 cells within each quadrant were analysed (scale bar A, B & D=100μm; scale bar C=10μm).

6.4 RESULTS

6.4.1 Fluo-4 and PI ionomycin study

In order to assess whether *in situ* chondrocytes could be loaded with Fluo-4, and a response i.e. a change in fluorescence visualised thereafter, preliminary experiments were conducted using the Ca^{2+} ionophore ionomycin. These experiments confirmed the successful Fluo-4 loading of *in situ* chondrocytes (**Figure 6.5**). When explants were sequentially imaged over a 22min control period (prior to the addition of ionomycin), the mean $\%\Delta F_{\text{Fluo-4}}$ and $\%\Delta F_{\text{PI}}$ was -3.7±6.2% and 0.75±1.2%, respectively, thereby indicating no adverse effects of sequential laser excitation on both the Fluo-4 stain and chondrocyte viability. However, when ionomycin was administered there was a rapid and significant (p=0.02) rise in Fluo-4 fluorescence indicating a sharp rise in $[Ca^{2+}]_i$ (**Figure 6.5**). This was followed by a significant (p=0.02) rise in PI fluorescence indicating that the rise in $[Ca^{2+}]_i$ was ultimately fatal to the chondrocytes (**Figure 6.5**). This correlates with previously published findings that ionomycin, when administered in sufficiently high doses, will induce eukaryotic cell death (Gwag *et al.*, 1999; Francis *et al.*, 2013; Morotomi-Yano *et al.*, 2014).

6.4.2 Fluo-4 and Fura Red ratiometric study

In order to confirm that the observed rise in Fluo-4 fluorescence in the above study did indeed represent a rise in $[Ca^{2+}]_i$, a further ionomycin experiment was conducted using a combination of Fluo-4 and Fura Red stains. As previously discussed (see section 6.1), these two stains act in a paradoxical manner when $[Ca^{2+}]_i$ rises (**Figure 6.6A and B**) and thus a ratio of Fluo-4 and Fura Red fluorescence ($R_{\text{Fluo-4/Fura Red}}$) can be established. In the absence of a rise in $[Ca^{2+}]_i$, a shift in the focal plane or

photobleaching stains, which could be visually represented by an apparent change in fluorescence, would result in a $R_{Fluo\text{-}4/Fura\ Red}$ that remained unchanged. However, if there was a rise in $R_{Fluo\text{-}4/Fura\ Red}$ then one could be confident that the observed change in fluorescence was due to a rise in $[Ca^{2+}]_i$ (Han *et al.*, 2012; Madden *et al.*, 2014). Prior to the administration of ionomycin, the mean $R_{Fluo\text{-}4/Fura\ Red}$ was 0.54±0.07, which was comparable with previously published data in chondrocytes (Han *et al.*, 2012; Madden *et al.*, 2014). Following the administration of ionomycin, there was a rapid and significant (p=0.002) rise in the mean $R_{Fluo\text{-}4/Fura\ Red}$ ratio to 2.02±0.56 (**Figure 6.6C and D**), thereby confirming that the previously observed rise in Fluo-4 fluorescence did indeed represent a rise in $[Ca^{2+}]_i$. Thus, subsequent experiments utilising Fluo-4 could be performed with the confidence that any observed increase in Fluo-4 fluorescence represented an increase in $[Ca^{2+}]_i$.

A.

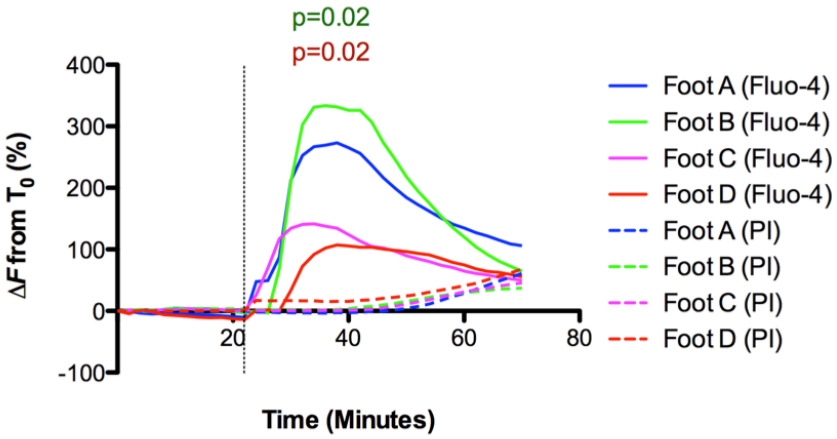

B.

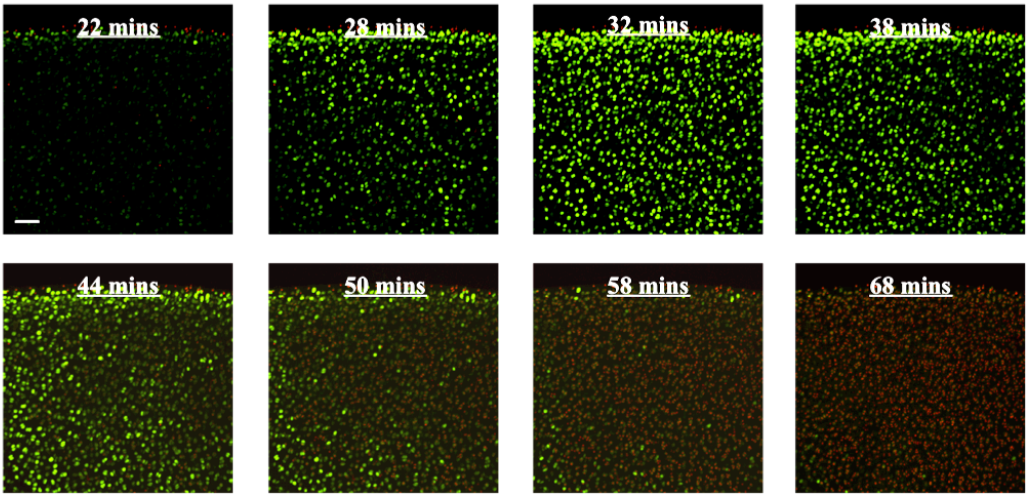

Figure 6.5: Alterations in chondrocyte $[Ca^{2+}]_i$ following the administration of ionomycin

(**A**) Following ionomycin administration (represented by broken vertical black line), there was a significant rise in Fluo-4 fluorescence (green numeric p value) and thus $[Ca^{2+}]_i$ in all explants. This was followed by a significant rise in PI fluorescence (red numeric p value) suggesting cellular demise which appeared to follow the $[Ca^{2+}]_i$ rise (N=4[n=1]; numerical p values represent mean %ΔF pre- versus post-ionomycin administration by paired Student's two-tailed t-test). The CLSM images **(B)** represent changes in Fluo-4 and PI fluorescence following ionomycin administration (scale bar=100μm).

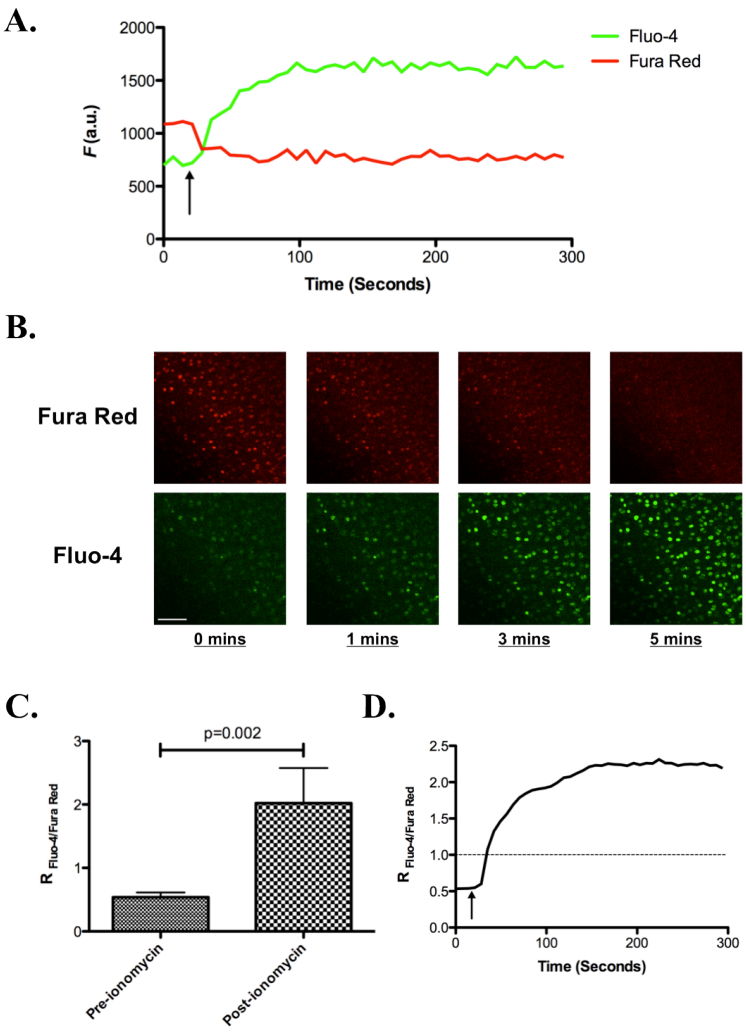

Figure 6.6: Ratiometric assessment of $[Ca^{2+}]_i$ alterations in Fluo-4- and Fura Red-loaded *in situ* chondrocytes

Line graph (**A**) represents the typical response of a Fluo-4- and Fura Red-loaded *in situ* chondrocyte following ionomycin exposure (indicated by black arrow). The CLSM images (**B**) demonstrate the paradoxical changes in the observed Fluo-4 and Fura Red fluorescence within the same sample population of cells following ionomycin administration (scale bar=100μm). There was a significant rise in $R_{Fluo\text{-}4/Fura\ Red}$ following ionomycin administration (**C**) (*N*=6[*n*=12]; numerical p values represent $R_{Fluo\text{-}4/Fura\ Red}$ pre- versus post-ionomycin administration by paired Student's two-tailed t-test). Line graph (**D**) provides an example of the $R_{Fluo\text{-}4/Fura\ Red}$ change in an *in situ* chondrocyte following ionomycin exposure with the horizontal dashed line representing the 'crossover point' when Fluo-4 fluorescence intensity exceeded that of Fura Red.

6.4.3 Preliminary Hla live-cell study

Prior to investigating the influence of Hla on *in situ* chondrocyte $[Ca^{2+}]_i$, a study was conducted in order to determine an appropriate experimental time period for the Hla Ca^{2+} imaging study. Living *in situ* chondrocytes stained with CMFDA and PI were exposed to Hla-containing 8325-4 supernatant for 6hrs. Chondrocyte death became apparent between 2 and 4hrs with 26.44±8.29% chondrocyte death observed at 6hrs (**Figure 6.7**). Nevertheless, it was possible that alterations in $[Ca^{2+}]_i$ may have considerably preceded the emergence of chondrocyte death (PI stained cells) and therefore a 6hr experimental time course, imaging at 5 minute intervals from 0hrs, was considered appropriate for the Hla Ca^{2+} imaging study.

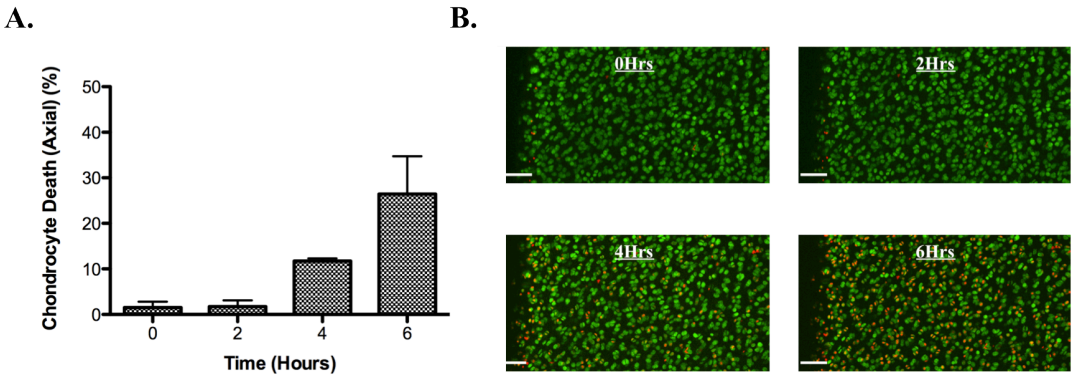

Figure 6.7: Preliminary live-cell viability assessment following Hla exposure

In order to determine a suitable experimental time period for live-cell $[Ca^{2+}]_i$ analysis following Hla exposure, CMFDA and PI loaded chondrocytes were exposed to an Hla-containing *S. aureus* 8325-4 supernatant for 6hrs. Chondrocyte death became apparent between 2 and 6hrs (**A**), thereby indicating that a 6hr experimental time period would be suitable for $[Ca^{2+}]_i$ imaging (N=2[n=1]). CLSM images (**B**) display progressive chondrocyte death following Hla exposure in a dynamic live-cell study (scale bar=100μm).

6.4.4 The influence of Hla on *in situ* chondrocyte $[Ca^{2+}]_i$

When Fluo-4 and PI labelled chondrocytes were incubated in the presence of Hla-containing 8325-4 supernatant , the maximum $\%\Delta F_{Fluo\text{-}4}$ and $\%\Delta F_{PI}$ encountered over the experimental time period was significantly elevated in comparison to those explants incubated in the presence of the $Hla^{-}Hlb^{-}Hlg^{-}$ supernatant (116.5±9.67% vs 30.69±13.44% (Fluo-4) and 156.74±40.15% vs 25.57±7.92% (PI), respectively) (**Figure 6.8A**). Thus, there was a significant rise in chondrocyte $[Ca^{2+}]_i$ following Hla exposure that was associated with cellular demise given the significantly elevated PI fluorescence (**Figure 6.8B and C**).

Further assessment of the change in Fluo-4 and PI fluorescence in Hla-exposed chondrocytes demonstrated a significantly elevated $\%\Delta F_{PI}$ at the point of maximum $\%\Delta F_{Fluo\text{-}4}$ (**Figure 6.8B and 6.9A**). In addition, at the time point considered to represent the first detectable rise in Fluo-4 fluorescence, defined as an increase in $\%\Delta F_{Fluo\text{-}4}$ two standard deviations above the mean of the preceding values (baseline), there was also a detectable and significant rise in PI fluorescence (**Figure 6.8B and 6.9B**). Thus, there appeared to be a simultaneous rise in both Fluo-4 and PI fluorescence in Hla exposed *in situ* chondrocytes. The mean time for the Ca^{2+} transient, defined as the time interval from the point of $\%\Delta F_{Fluo\text{-}4}$ rising two standard deviations above the baseline to falling two standard deviations below the baseline, was 22.71±9.51mins. Finally, the mean $\%\Delta F_{PI}$ within chondrocytes exposed to the $Hla^{-}Hlb^{-}Hlg^{-}$ supernatant over the 6hr experimental period was 5.4±11.89% thereby further confirming no adverse effects of sequential laser excitation on cell viability, which has been reported previously (Knight *et al.*, 2003).

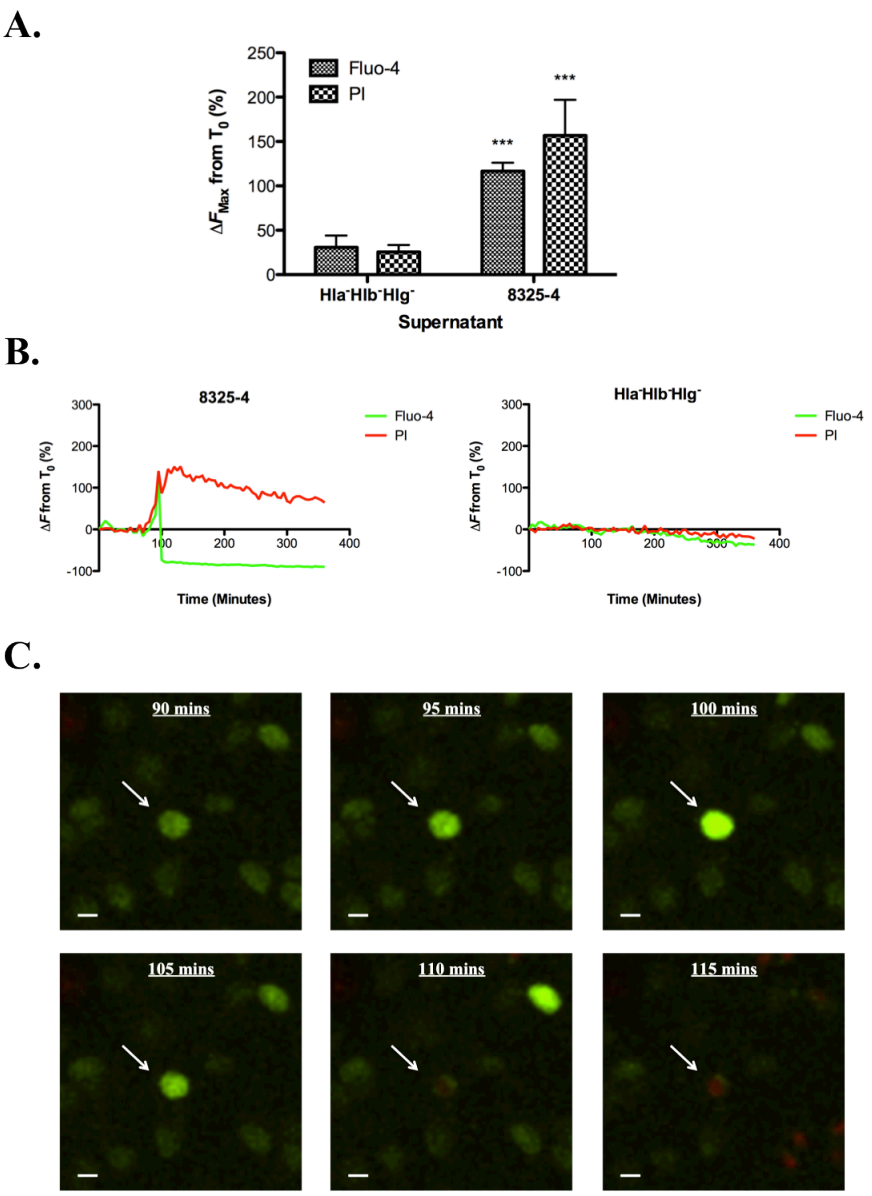

Figure 6.8: Hla induced a rise in $[Ca^{2+}]_i$ that was associated with chondrocyte death

There was a significant rise in both Fluo-4 and PI fluorescence in those chondrocytes exposed to an Hla-containing *S. aureus* 8325-4 supernatant (**A**), indicating that a rise in $[Ca^{2+}]_i$ is associated with Hla-induced chondrocyte death (N=4[n=12]; *** p<0.001 8325-4 ($Hla^+Hlb^+Hlg^+$) versus $Hla^-Hlb^-Hlg^-$ by unpaired Student's two-tailed t-test) The line graphs (**B**) provide examples of the change in Fluo-4 and PI fluorescence in chondrocytes exposed to the 8325-4 ($Hla^+Hlb^+Hlg^+$) and $Hla^-Hlb^-Hlg^-$ strain supernatants, respectively. The CLSM images (**C**) provide a visual representation of the progressive increase in Fluo-4 fluorescence, and thus $[Ca^{2+}]_i$, that precedes chondrocyte demise (scale bar=10μm).

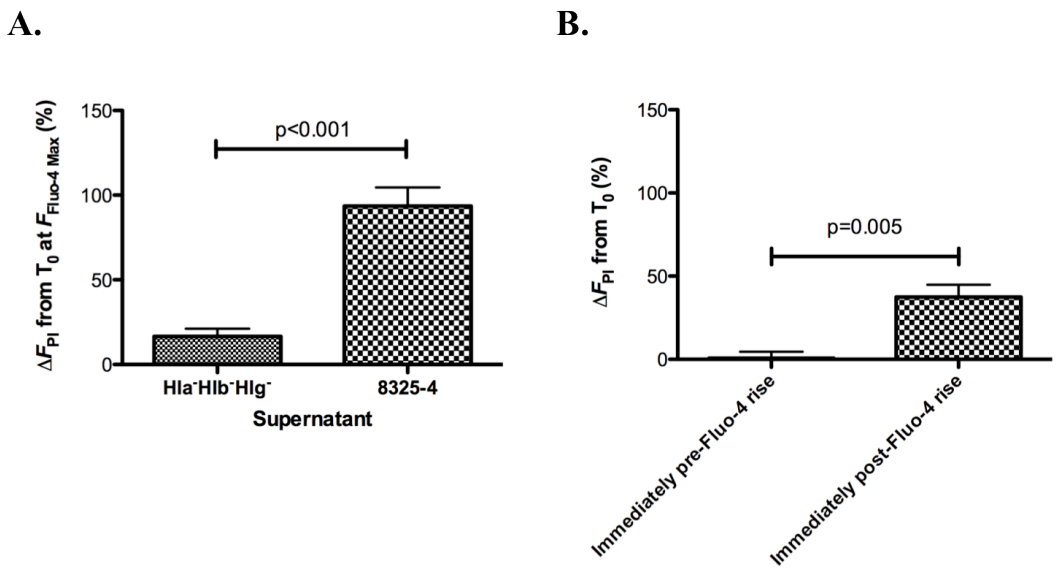

Figure 6.9: The rise in Fluo-4 fluorescence within *in situ* chondrocytes exposed to Hla was associated with a simultaneous rise in PI fluorescence

PI fluorescence was significantly elevated at the point of peak Fluo-4 fluorescence in those chondrocytes exposed to Hla (*N*=4[*n*=12]; p values represent 8325-4 ($Hla^+Hlb^+Hlg^+$) versus $Hla^-Hlb^-Hlg^-$ by unpaired Student's two-tailed t-test). In all chondrocytes assessed, at the point of earliest detectable rise in Fluo-4 fluorescence there was also a significant rise in PI fluorescence, indicating a simultaneous rise in both Fluo-4 and PI fluorescence following Hla exposure (*N*=4[*n*=12]; p values represent change in PI fluorescence immediately pre- and post-Fluo-4 rise by paired Student's two-tailed t-test).

6.4.5 An assessment of chondrocyte $[Ca^{2+}]_i$ at the cut-edge

The above study investigating alterations in chondrocyte $[Ca^{2+}]_i$ following Hla exposure was conducted in the axial plane and therefore primarily assessed the response of *in situ* chondrocytes within the SZ of cartilage i.e. imaging was to a depth of approx. 100μm from the articular surface. In order to embark upon the assessment of $[Ca^{2+}]_i$ alterations within different cartilage zones following Hla exposure, coronal imaging would be required. This presented a challenge as it

necessitated live-cell imaging through a scalpel-wounded cut-edge. Indeed, a serendipitous observation during the ionomycin and 8325-4 vs $Hla^{-}Hlb^{-}Hlg^{-}$ supernatant axial studies was the apparent increased $[Ca^{2+}]_i$ of chondrocytes located within the immediate vicinity of the cut-edge (**Figure 6.10**). When the level of Fluo-4 fluorescence within chondrocytes in the region of the cut-edge was compared with chondrocytes distant to the cut-edge in explants cultured in phenol red-free DMEM (340mOsm), there was approx. 4 times higher Fluo-4 fluorescence levels within chondrocytes in the region of the cut-edge (**Figure 6.11A**).

Amin *et al.* (2008) previously demonstrated that exposure of a scalpel-induced cut-edge to a hyperosmolar medium significantly reduced chondrocyte death and in a later study (Amin *et al.*, 2009a) suggested that Ca^{2+} may play a role in early chondrocyte death arising as a result of mechanical trauma. Therefore, in order to attempt to reduce the Ca^{2+} signal and thus the level of Fluo-4 fluorescence, osteochondral explants were exposed to a hyperosmolar medium (600mOsm) pre- and post-trimming. However, the level of chondrocyte Fluo-4 fluorescence remained significantly elevated at the cut-edge despite exposure to the hyperosmolar medium (**Figure 6.11B**). In addition, there was no significant difference in the level of Fluo-4 fluorescence between chondrocytes exposed to 340 and 600mOsm media ($p=0.69$ by unpaired Student's t-test). Therefore, given the ongoing significantly elevated Fluo-4 fluorescence within chondrocytes at the cut-edge despite attempted reduction strategies, it was considered unreasonable to pursue any further response of chondrocytes to Hla within different cartilage zones, given that the $[Ca^{2+}]_i$ within these cells would already be elevated prior to the commencement of experimentation.

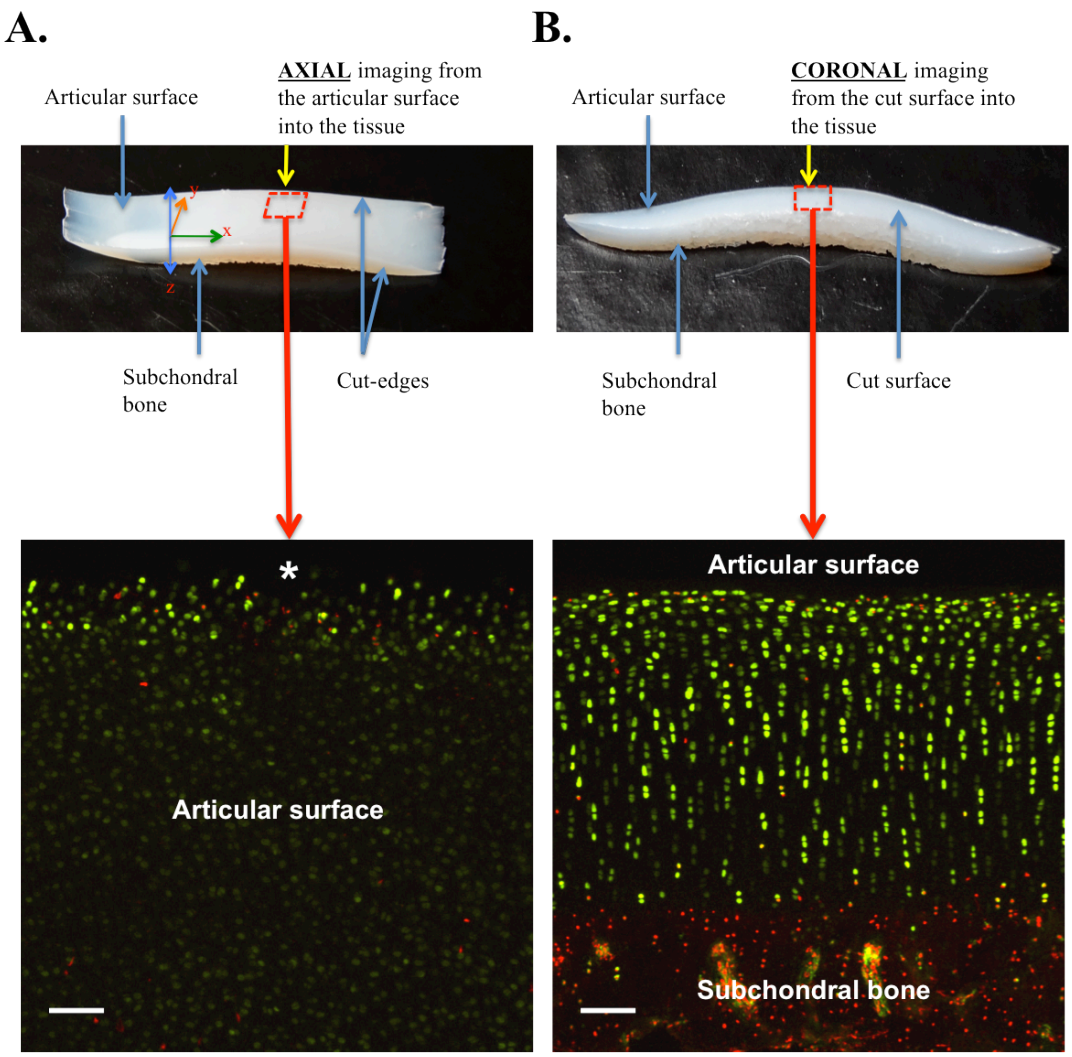

Figure 6.10: Increased Fluo-4 fluorescence within chondrocytes in the vicinity of the cut-edge

It was noted during the axial studies presented in this chapter that there was an increased level of Fluo-4 fluorescence within chondrocytes in the region of the cut-edge (**A**). The axial CLSM image represents an explant from the ionomycin study (see section 6.4.1) prior to the addition of ionomycin. Note the increased Fluo-4 fluorescence, and thus $[Ca^{2+}]_i$, at the cut-edge (*). When the cut-edge of the same explant was imaged in the coronal plane (**B**), this confirmed increased chondrocyte Fluo-4 fluorescence throughout the cut surface i.e. throughout the depth of cartilage (scale bar=100μm).

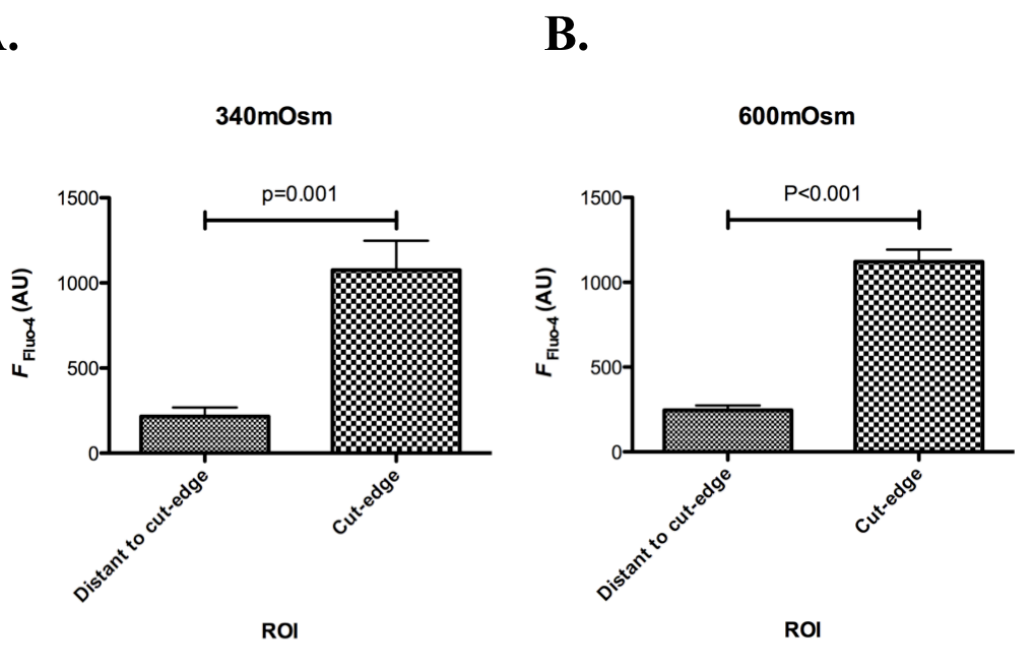

Figure 6.11: The influence of raised osmolarity on resting chondrocyte $[Ca^{2+}]_i$ within the immediate vicinity of the cut-edge

In explants cultured in phenol red-free DMEM (340mOsm) pre- and post-trimming, there was significantly elevated fluo-4 fluorescence in chondrocytes within the immediate vicinity of the cut edge (**A**). Chondrocyte fluorescence within the cut-edge ROI remained significantly elevated when explants were cultured in hyperosmolar (600mOsm) DMEM (**B**) (*N*=3[*n*=12]; p values represent chondrocyte fluo-4 fluorescence within the cut-edge ROI vs chondrocyte fluorescence within the ROI distant to the cut-edge by unpaired Student's two-tailed t-test).

6.5 DISCUSSION

In this study, Ca^{2+}-sensitive fluorophores coupled with live-cell CLSM were used to assess alterations in $[Ca^{2+}]_i$ within *in situ* chondrocytes following ionomycin and, thereafter, Hla exposure. Whilst numerous studies investigating changes in $[Ca^{2+}]_i$ within a variety of eukaryotic cells have used a similar experimental strategy, to the author's knowledge it has not been used to investigate the pathology of *S. aureus*-induced septic arthritis. This study firstly demonstrated that alterations in Fluo-4 and Fura Red fluorescence within *in situ* chondrocytes could be successfully visualised and assessed following ionomycin administration. Subsequent experimentation with Hla demonstrated a significant rise in chondrocyte $[Ca^{2+}]_i$ that was associated with chondrocyte death. A further incidental and serendipitous finding was the elevated $[Ca^{2+}]_i$ within chondrocytes in the region of the scalpel-induced cut-edge.

One of the major benefits of live- over fixed-tissue imaging was that *in situ* cells could be dynamically assessed within their native environment. For straightforward experimental endpoints such as *in situ* cell viability assays, the assessment of fixed tissue was adequate but it would not be possible, for example, to assess alterations in $[Ca^{2+}]_i$ within such specimens i.e. all the cells would be dead. One disadvantage of the use of live-tissue imaging however was the potential for cellular phototoxicity arising as a result of prolonged periods of focused high intensity laser excitation of the tissue. Indeed, a study by Knight *et al.* (2003) demonstrated that serial laser excitation of Fluo-4-loaded isolated chondrocytes imaged over a 1hr period (image acquisition every 10secs) induced Ca^{2+} oscillations, transients and a reduction in cell viability. In contrast, no such adverse effects were encountered with regards to

$[Ca^{2+}]_i$ homeostasis or chondrocyte viability in the control samples of the current study, some of which were imaged for 6hrs (**Figures 6.8 and 6.9**). Possible explanations may be the use of a refined and less intense laser in this study, more prolonged periods between image acquisition and a protective effect of the surrounding ECM.

The primary objective of this study was to assess alterations in $[Ca^{2+}]_i$, depicted by changes in Ca^{2+}-sensitive fluorophore fluorescence, following Hla exposure. Preliminary experiments utilising a Ca^{2+} ionophore were necessary in order to confirm that Fluo-4-loaded *in situ* chondrocytes could respond to a rise in $[Ca^{2+}]_i$. Ionomycin was chosen on the basis that it has previously been shown to reliably induce a rise in $[Ca^{2+}]_i$ in many eukaryotic cell types (Liu and Hermann, 1978; Erdahl *et al.*, 1994; Morgan and Jacob, 1994; Foerster *et al.*, 2010). This was indeed the case with *in situ* chondrocytes, with a rapid increase in Fluo-4 fluorescence being observed following ionomycin exposure, ultimately culminating in chondrocyte demise (**Figure 6.5**). To obtain further confidence that the observed rise in Fluo-4 fluorescence represented a true rise in $[Ca^{2+}]_i$ and not just a shift in the focal plane or photobleaching, Fluo-4- and Fura Red-loaded chondrocytes were also challenged with ionomycin. This resulted in a rapid and significant rise in $R_{Fluo\text{-}4/Fura\ Red}$ (**Figure 6.6**) thereby confirming a rise in $[Ca^{2+}]_i$. One may argue that a Fluo-4 and Fura Red ratiometric analysis should have been used for the subsequent Hla studies. However, Fura Red and PI have similar emission spectra (www.lifetechnologies.com) and therefore the two stains could not be used simultaneously. One possible option for future studies would be to utilise the Ca^{2+}-sensitive ratiometric fluorophore Fura-2 in

combination with PI. Fura-2 has dual emission spectra following excitation at 340nm and 380nm, repectively (www.lifetechnologies.com). When excited at 340nm, emitted fluorescence intensity increases as $[Ca^{2+}]_i$ increases whilst when excited at 380nm, emitted fluorescence intensity decreases as $[Ca^{2+}]_i$ increases (Malgaroli *et al.*, 1987). The use of Fura-2 was not explored in the current study, as the laser excitation sources available were unable to excite down to 340nm. Ultimately, the goal of this study was to assess whether Hla-induced chondrocyte death was associated with a rise in $[Ca^{2+}]_i$ and this was achieved with a combination of Fluo-4 and PI.

When *in situ* chondrocytes were exposed to the Hla-containing 8325-4 supernatant there was a significant rise in Fluo-4 fluorescence, and thus $[Ca^{2+}]_i$, in comparison to those explants exposed to the $Hla^-Hlb^-Hlg^-$ supernatant (**Figure 6.8**). The small change in Fluo-4 and PI fluorescence in those explants exposed to the $Hla^-Hlb^-Hlg^-$ supernatant may possibly be explained by either a slight shift in the focal plane during the initial experimental period or the influence of unspecified *S. aureus* toxins. The Hla-induced Ca^{2+}transient lasted between 20 and 25mins in the majority of cells analysed with cell death being witnessed in all cells thereafter. Cellular demise following the Ca^{2+} transient was identified through the inability of the cells to contain plasma membrane-insoluble cytosolic Fluo-4 and persistently elevated nuclear PI fluorescence, both of which indicated catastrophic loss of plasma membrane integrity. Given that images were acquired every 5mins, this was a fairly crude estimation of the Hla-induced intracellular Ca^{2+} transient dynamic and it was possible that it may have lasted longer or shorter in some of the cells analysed.

However, the primary goal of this study was to identify whether or not there was a rise in $[Ca^{2+}]_i$ following Hla exposure and this was achieved. Future experiments may refine the imaging interval in order to obtain a more detailed appreciation of the Hla-induced intracellular Ca^{2+} transient.

Further assessment of the relationship between Fluo-4 and PI fluorescence in the presence of Hla demonstrated a significant rise in PI fluorescence that coincided with the first detectable rise in Fluo-4 fluorescence (**Figure 6.9**), thereby suggesting a simultaneous rise in Fluo-4 and PI fluorescence. There were two possible explanations for this finding. Firstly, membrane integrity had already been compromised prior to the start of the Ca^{2+} transient and that the observed transient simply represented the end-stage influx of Ca^{2+} down the considerable concentration gradient between the extra- and intracellular compartments i.e. Hla induced chondrocyte death was not triggered by the influx of Ca^{2+} through membrane-bound Hla pores. Indeed, Walev *et al.* (1993) and Valeva *et al.* (2000) raised the possibility that divalent cations such as Ca^{2+} could not pass through Hla pores and that it was the influx of Na^+ coupled with the efflux of K^+ that initiated cell death.

An alternative explanation may be that Hla pores permitted the passage of both Ca^{2+} and PI into the chondrocyte. Interestingly, Jonas *et al.* (1994) identified that when isolated peripheral blood human T lymphocytes were exposed to a high concentration of Hla, the plasma membrane became permeabilised to both Ca^{2+} and PI. However, when the cells were exposed to a low concentration of Hla, the plasma membrane was found to be impermeable to Ca^{2+} and PI, thereby suggesting that the

Hla pore size may be dependent on Hla concentration. Additionally, studies conducted by Kennedy *et al.* (2009) and Knapp *et al.* (2010) investigating alpha-toxin of *Clostridium septicum*, which was similar in both size and structure to *S. aureus* Hla, identified that the toxin permeabilised cell membranes to Ca^{2+} and PI, respectively. In a further study by Koschinski *et al.* (2006) investigating alpha-haemolysin of *Escherichia coli*, which was a similar pore-forming toxin to *S. aureus* Hla, identified that it also permeabilised cell membranes to Ca^{2+} and PI. Moreover, following toxin washout the cells subsequently became impermeable to Ca^{2+} and PI.

If the observed Ca^{2+} influx in the current study was simply due to diffusion down a concentration gradient established through the loss of membrane integrity then one would have expected the transient to be extremely rapid given the substantial difference between $[Ca^{2+}]_i$ and $[Ca^{2+}]_o$ in articular cartilage (Urban, 1994; Hall *et al.*, 1996a; Yellowley *et al.*, 1997). As the transient exceeded 20mins in the majority of cells and given the published literature to date on similar pore-forming toxins, it was likely that membrane-bound Hla pores permitted the passage of Ca^{2+}, along with PI, into the chondrocyte and that this influx of Ca^{2+} was the primary trigger of cell death. In order to confirm that this was indeed the case, an experimental strategy whereby the assessment of $[Ca^{2+}]_i$ and chondrocyte viability following Hla pore blockade would be required. If Hla pore blockade inhibited both a rise in $[Ca^{2+}]_i$ and chondrocyte death then this would provide convincing evidence that the passage of Ca^{2+} into the cell was predominantly via the Hla pore and that the rise in $[Ca^{2+}]_i$ triggered cell death thereafter. Whilst Hla-specific monoclonal antibodies have been shown to inhibit the activity of Hla in animal models (Bubeck-Wardenburg and

Schneewind, 2008; Ragle and Bubeck-Wardenburg, 2009), their mode of action has been identified as the inhibition of Hla heptamer formation (Tkaczyk *et al.*, 2012) i.e. at a pre-pore conformational stage and thus would be unsuitable for the inhibition of mature membrane-spanning Hla pores. However, the recent identification of β-cyclodextrin derivatives as Hla pore-blocking agents may enable such a confirmatory experiment in the future (Karginov *et al.*, 2007; McCormick *et al.*, 2009; Ragle *et al.*, 2010; Inoshima *et al.*, 2011; Yannakopoulou *et al.*, 2011). Encouragingly, Ragle *et al.* (2010) demonstrated that administration of a β-cyclodextrin compound in a murine model of *S. aureus* pneumonia both prevented and treated disease while a study by McCormick *et al.* (2009) demonstrated that the administration of methyl-β-cyclodextrin-cholesterol in a murine model of *S. aureus* keratitis was effective in arresting corneal damage. It was thus tempting to speculate that the administration of β-cyclodextrin compounds in a murine model of *S. aureus*-induced septic arthritis may be similarly advantageous.

The study assessing chondrocyte $[Ca^{2+}]_i$ alterations in response to Hla was conducted in the axial plane and predominantly assessed SZ chondrocytes to a depth of approx. 100μm from the articular surface. In order to assess whether alterations in $[Ca^{2+}]_i$ varied between chondrocytes from different cartilage zones, and thus attempt to explain why SZ chondrocytes were previously shown to be more susceptible to Hla than chondrocytes from deeper cartilage zones (see Chapters 3 and 4), the coronal imaging of Fluo-4 loaded *in situ* chondrocytes would be necessary. It was hypothesised that Hla-induced intracellular Ca^{2+} transients were more prolonged within chondrocytes from deeper zones in comparison to SZ chondrocytes.

However, a consistent observation during the experiments detailed within this chapter was increased Fluo-4 fluorescence within chondrocytes in the region of the cut-edge (**Figure 6.10**). In some cells, the increased fluorescence was observed to be present for several hours prior to eventual cellular demise while in other cells it remained elevated for the duration of the experiment. Whilst this was an interesting observation, the assessment of $[Ca^{2+}]_i$ following mechanical trauma was not the goal of this study and it presented a challenge for the intended coronal imaging experiments as it would result in the assessment of cells in which $[Ca^{2+}]_i$ was already considerably disturbed prior to Hla exposure.

Amin *et al.* (2009a) previously identified that Ca^{2+} may play a role in early chondrocyte death following mechanical cutting trauma and also that exposure of a scalpel-induced cut-edge to a hyperosmolar medium significantly reduced chondrocyte death (Amin *et al.*, 2008; Amin *et al.*, 2010). It was therefore hypothesised that exposure of the cut-edge to a hyperosmolar solution would reduce or prevent alterations in $[Ca^{2+}]_i$ within cells in this region, thereby enabling the Hla coronal study to proceed. However, despite being exposed to a hyperosmolar medium, $[Ca^{2+}]_i$ remained significantly elevated within these cells and the experiment was thus abandoned. A possible explanation for the raised $[Ca^{2+}]_i$ within chondrocytes at the cut-edge may be that the cells were 'sublethally' damaged and the raised $[Ca^{2+}]_i$ reflected intracellular reparative mechanisms. Nevertheless, a potential future strategy to overcome the elevated $[Ca^{2+}]_i$ at the cut-edge might involve the culture of trimmed explants in a hyperosmolar medium for several days prior to experimentation. This may enable the disappearance of stain uptake in dying

cells and the recovery of damaged cells. Alternatively, future studies could focus on alterations in $[Ca^{2+}]_i$ within chondrocytes isolated from different cartilage zones i.e. isolated cells.

To conclude, this *in vitro* live-cell imaging study has demonstrated that Hla-induced *in situ* chondrocyte death is associated with a rise in $[Ca^{2+}]_i$. Future studies may attempt to confirm whether Ca^{2+} entry is via the membrane-spanning Hla pores.

CHAPTER 7

GENERAL DISCUSSION

In this chapter, the experimental model utilised during this study to improve the current understanding of the articular cartilage destruction associated with *S. aureus*-induced septic arthritis is discussed and novel aspects of the methodology highlighted. The key study conclusions are presented and their translational relevance to current clinical practice and future scientific research are considered.

7.1 A cartilage explant model of *S. aureus*-induced septic arthritis

A key aim of this study was an attempt to model septic arthritis in a cartilage explant model. In the clinical setting, establishment of infection involves a complex and dynamic interaction between pathogen and host. The author is conscious of the fact that the current model used has inherent limitations in this regard and there is therefore no claim to mirror infection *in vivo*.

One potential and important issue was the level of infection established, which may have been overly aggressive in the absence of the contributory influence *in vivo* of the host immune response or, in contrast, too weak as a consequence of the inoculum concentration used to establish infection. Nevertheless, the concentration chosen produced a measurable degree of chondrocyte death within a reasonable time period that was neither overwhelming nor weak. To date, the author is not aware of any studies that have measured the bacterial concentrations within the infected synovial fluid of humans presenting with *S. aureus*-induced septic arthritis. Hence, it was exceedingly difficult to exactly match levels in the experimental model with those in a septic joint. Ultimately, the goal of the current study was to assess the influence of

key *S. aureus* toxins on chondrocyte viability and the level of infection established within the experimental model enabled this to be achieved.

One of the strengths of the *in vitro* cartilage explant model of septic arthritis presented in this study may paradoxically also be considered a limitation. The absence of the complexities of a host immune response enabled the formulation of more accurate conclusions in regard to the chondrocyte-damaging potential of specific *S. aureus* toxins. On the one hand, it could be considered that the destructive influence of such toxins would be significantly dampened *in vivo* by the host immune response. Nevertheless, evidence from animal studies suggests that the immune response may paradoxically contribute further to the overall cartilage destruction (Shirtliff and Mader, 2002; Tissi *et al.*, 2004). It is currently entirely speculative as to what extent *in vivo* chondrocyte death and subsequent cartilage destruction is due to the bacterial toxin component and that due to the immune response engaged to 'retaliate' as a response, but it is likely that both contribute significantly.

Bovine osteochondral explants (**Figure 2.3**) were utilised for all experiments unless stated otherwise as preliminary studies with cartilage explants devoid of subchondral bone had highlighted a major problem: the lack of a subchondral bone anchor resulted in marked 'curling' of the explants (author observation), rendering subsequent axial-plane CLSM image acquisition extremely difficult. Furthermore, to achieve a more accurate representation of the *in vivo* environment, the assessment of articular cartilage bound to subchondral bone was considered important. Indeed, the

observation by Amin *et al.* (2009b) that the presence of subchondral bone influenced chondrocyte survival in articular cartilage during explant culture further emphasised the importance of the use of osteochondral explants. All oval (harvested form) osteochondral explants were trimmed to form rectangular explants immediately prior to fluorescent staining (**Figure 2.4**) in order to permit (1) a standardised method of CLSM imaging and quantification in the axial plane and (2) the capture of 'flush' coronal images. In addition, it ensured that no coronal images were obtained of mechanically damaged chondrocytes that had been exposed to *S. aureus* toxins for the experimental period, as the cutting trauma may have rendered them more susceptible to *S. aureus* toxins.

A further potential limitation of the use of the current bovine model is that a great degree of caution should be exercised before extrapolating conclusions to the clinical setting. The sensitivity of *in situ* chondrocytes to *S. aureus* toxins may be considerably different in human articular cartilage. However, there are significant practical problems with the use of human cartilage, namely it is extremely difficult to source a consistent and regular supply of non-degenerate human cartilage. Nevertheless, studies have demonstrated similar responses by bovine and human cartilage to a variety of experimental challenges (D'Lima *et al.*, 2001; Démarteau *et al.*, 2006), thereby supporting the use of bovine cartilage for experimental assessments. Regardless, and despite the inherent challenges, ultimately it will be necessary to conduct experimental research with human osteochondral explants in order to assess the sensitivity of human chondrocytes to *S. aureus* haemolysins.

The role of cartilage explants to investigate the destructive roles of *S. aureus* on articular cartilage has been previously reported (Jasin, 1983; Williams *et al.*, 1991) and their use in the current study was therefore not a novel experimental strategy. However, there were two major benefits to the use of cartilage explants in comparison to *in vivo* animal models and isolated chondrocytes: (1) as mentioned previously, there was the avoidance of the complexities of a host immune response and (2) cell-matrix interactions remained intact, thereby making any observed cellular responses more representative of those *in vivo*.

Previous studies have primarily focused on *S. aureus*-induced damage to the ECM, assessing the release of matrix components and matrix-digesting enzymes as experimental endpoints, but gave no indication of chondrocyte viability following bacterial toxin exposure (Jasin, 1983; Smith and Schurman, 1983; Williams *et al.*, 1991). Chondrocytes, the only cellular component of articular cartilage (Muir, 1995), govern matrix turnover and thus a damaged matrix with large numbers of viable chondrocytes may have the capacity for repair. As chondrocytes do not normally divide once skeletal maturity has been reached (Archer, 1994; Muir, 1995), a damaged matrix with a paucity of viable chondrocytes will ultimately degrade and the cartilage will inevitably become degenerate (Simon *et al.*, 1976). It was therefore considered important to analyse *in situ* chondrocyte viability following exposure to key *S. aureus* toxins and this was achieved through the modality of fluorescence-mode CLSM. Whilst CLSM is a well-established research tool, the author is not aware of its use for the assessment and subsequent characterisation of *in situ*

chondrocyte death following *S. aureus* toxin exposure and it therefore presented a novel and exciting investigative strategy within the field of septic arthritis research.

7.2 Fluorescence-mode CLSM

For the majority of experiments, low-power (x10) CLSM images of fluorescently labelled osteochondral explants (fixed and living specimens) were obtained in one of two orthogonal planes: axial or coronal. A series of optical sections acquired in these planes were combined using imaging software (Volocity 4 and Nikon NIS Elements version 4.0) to produce 3-D reconstructions of the imaged volume of cartilage and defined analyses were conducted thereafter. For the majority of experiments, images were acquired in the axial plane as it provided a more comprehensive evaluation of cells in the SZ (i.e. the articular surface) in comparison to that possible from thin coronal sections of cartilage. The SZ was of particular interest as firstly, it harbours, in the majority of species (Pedersen *et al.*, 2013), the highest cell density in cartilage and plays a key role in resisting both tensile and shearing forces (Buckwalter and Mankin, 1997a; Hunziker, 2002; Korhonen *et al.*, 2002) i.e. it plays a vital role in maintaining the overall integrity of the tissue. Secondly, as the articular surface was in close proximity to the infected synovial fluid *in vivo*, it followed that the response of SZ chondrocytes to defined *S. aureus* toxins should be of particular interest. Given the zonal heterogeneity of articular cartilage, it was also considered important to investigate the response of *in situ* chondrocytes to *S. aureus* toxins throughout the depth of the tissue, an assessment that was not possible with axial imaging alone due to the limitations of stain penetration.

Success was achieved with coronal imaging, accepting that it did entail imaging through a scalpel-wounded cut-edge. The small, but detectable degree of chondrocyte death induced by the scalpel blade (**Figures 3.7 and 4.6**) was minimised by trimming each explant immediately prior to staining.

The technique of fluorescence-mode CLSM was central to this study and its use was advantageous for several reasons:

1. Prior to CLSM, each specimen could be illuminated with an excitation light source (mercury lamp fitted within each CLSM system) and visualised thereafter to ensure that the region selected for CLSM imaging was indeed representative of the generalised cellular response to experimental challenge throughout the specimen. In addition, it further enabled the identification and subsequent rejection of both microscopically degenerate explants, which were typically characterised by the presence of chondrocyte clusters, and iatrogenically injured explants.

2. In comparison to conventional histology, where physical sectioning of the specimen is required and thus artefacts can be created, axial CLSM imaging permitted the assessment of undisturbed SZ chondrocytes. Although the coronal imaging of chondrocytes within different cartilage zones necessitated the imaging through a cut-edge and hence disturbed cartilage, these 'clean' scalpel-induced edges, which were established well away from the 'ragged'

edges created at the time of explant harvesting, were only fashioned at the time of staining i.e. upon leaving the bacterial culture vessel and thus no toxins were present at this stage. Therefore, the experimental fate of the cells was already established i.e. PI-labelled cells arising as a result of Hla-induced death were still labelled with PI post trimming. It was accepted that the scalpel cut did induce a degree of dead-cell artefact, however this was consistently found to be minimal and did not significantly interfere with the analysis of coronal chondrocyte viability assays (**Figures 3.7 and 4.6**). A possible solution to overcome the dead cell artifact would be to trim the explants post-fixation. Unfortunately, this was not possible due to stain penetration limitations.

3. As low powered CLSM was utilised, relatively large areas of cartilage were imaged (approx. 1mm x 1mm) thereby permitting the response of a large number of cells to be assessed simultaneously. For axial images, the 50% field-of-view ROI typically contained approx. 3000 chondrocytes while there was in excess of 1000 cells within the combined ROIs for each coronal image. For CMFDA- and PI-labelled specimens, subsequent quantitative analyses of chondrocyte viability based on such large numbers of cells ensured a more accurate representation of the overall response of articular cartilage to *S. aureus* toxins.

4. As CLSM imaging was to a depth of approx. 100μm in both the axial and coronal planes, the imaged volume within CLSM reconstructions

considerably exceeded that of the fine sections used for conventional histology. CLSM reconstructions therefore enabled the visualisation of cartilage in more detail, especially in coronal section (**Figure 7.1**).

5. A unique feature of CLSM was that it had the capacity to image living tissue and thus *in situ* cells in fine morphological detail. Moreover, dynamic responses within chondrocytes could be visualised and quantified in real time. In Chapter 6, alterations in $[Ca^{2+}]_i$ within living chondrocytes following Hla exposure took the imaging strategy to a level of sophistication beyond the imaging of fixed specimens and the scope of conventional histology.

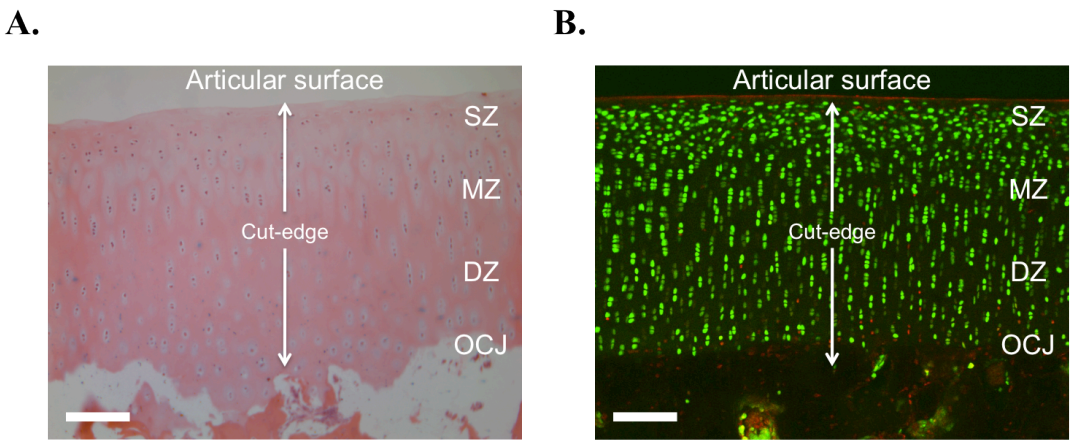

Figure 7.1: A comparison between the cellular detail of articular cartilage obtained with conventional histology and CLSM using a low power objective (x10)

(**A**) A 10μm thick coronal section of haematoxylin and eosin stained bovine articular cartilage. (**B**) An approx. 100μm thick coronal section of CMFDA- and PI-labelled bovine articular cartilage. Although both images demonstrated the full thickness of articular cartilage and thus provided an appreciation of the zonal heterogeneity, there was considerably more cellular detail in the image acquired through CLSM due to the greater imaged volume i.e. more cells are visualised (scale bar = 100μm). Image (**A**) kindly provided by Dr Asima Karim, Centre for Integrative Physiology, The University of Edinburgh.

As with any experimental technique, there were limitations associated with the use of fluorescence-mode CLSM. Firstly, CLSM could only capture images from fluorescently labelled tissue and there was therefore a depth limitation to image acquisition that arose as a result of the limited ability of the fluorescent stains to penetrate cartilage. Thus, with increasing depth the ability of the laser light to excite fluorescent stains decreased. Secondly, there was the potential for adverse effects on cell viability (phototoxicity) as a result of sequential focused high power laser excitation of the tissue (Frigault *et al.*, 2009). Indeed, a study by Knight *et al.* (2003)

demonstrated that serial high-powered laser excitation was toxic to isolated chondrocytes. Laser-induced toxicity was not a concern for the chondrocyte viability studies as the CMFDA- and PI-labelled explants were fixed in formaldehyde prior to imaging. Regardless of laser power and exposure time it was not possible for chondrocyte viability to alter in these specimens, although fluorescence levels could decline with time (author observation). Nevertheless, it was a potential issue for the live-cell intracellular Ca^{2+} imaging studies. No such problems were encountered during these studies, perhaps reflecting reduced exposure time coupled with recent advances in CLSM laser technology or, alternatively, a protective influence of the ECM, which wasn't present in the study by Knight *et al.* (2003) i.e. isolated chondrocytes were investigated.

7.3. Quantification of *in situ* chondrocyte viability

With the exception of the intracellular Ca^{2+} imaging studies detailed in Chapter 6 (see this chapter for a detailed discussion on the CLSM assessment of alterations in chondrocyte $[Ca^{2+}]_i$), the majority of experiments detailed within this thesis involved the assessment of percentage chondrocyte death following experimental challenge. This was assessed by conducting automated cell viability counts on CMFDA- and PI-labelled chondrocytes within defined axial and coronal ROIs using Volocity 4 software. This was achieved by using a previously validated and reproducible algorithm based on thresholding percentage voxel intensity (Jomha *et al.*, 2003; Lin *et al.*, 2005; Amin *et al.*, 2008), which minimised background noise whilst, at the same time, maximising the inclusion of cells despite signal attenuation. Such a technique, which has both a high sensitivity and specificity (Jadin, 2005), and has

additionally been specifically validated for use with fluorophores used to label viable and non-viable chondrocytes (Jomha *et al.*, 2003), enabled the rapid and accurate estimation of chondrocyte viability within large populations of cells.

The use of CMFDA and PI is an accepted method utilised by many studies to fluorescently label living and dead cells, respectively (Jones and Senft, 1985; Bush and Hall, 2003; Lewis *et al.*, 2003; Unal Cevik and Dalkara, 2003; Huntley *et al.*, 2005; Jones *et al.*, 2005; Amin *et al.*, 2008; Bubeck-Wardenburg and Schneewind, 2008). The question remained whether PI-labelled cells potentially represented membrane-damaged chondrocytes that, with time, could subsequently repair the membrane insult and, ultimately, survive. The results from the long-term post-infection chondrocyte viability study detailed in Chapter 3 demonstrated that PI-labelled chondrocytes at 40hrs were incapable of labelling green with CMFDA to indicate that they had recovered viability (**Figures 3.9 and 3.10**). This finding therefore provided confirmation that PI-labelled chondrocytes were indeed dead.

7.4 Conclusions

An *in vitro* bovine osteochondral explant model of *S. aureus*-induced septic arthritis was developed in this study. Utilising fluorescence-mode CLSM, the model, which avoided the complexities of a host immune response, permitted an assessment of the following: (1) the spatial and temporal quantification of *in situ* chondrocyte viability following exposure to both a laboratory 'wild-type' (*S. aureus* 8325-4) and clinical strains of *S. aureus*; (2) the influence of *S. aureus* Hla, Hlb and Hlg on *in situ* chondrocyte viability through the use of specific 'haemolysin-knockout' mutant

strains; (3) the influence of altered culture medium osmolarity and $[Ca^{2+}]_o$ on Hla-induced *in situ* chondrocyte death; and (4) dynamic changes in $[Ca^{2+}]_i$ within *in situ* chondrocytes following Hla exposure. The key conclusions from the experiments are summarised below:

1. *S. aureus* 8325-4 and *S. aureus* clinical strains rapidly reduced *in situ* chondrocyte viability (>45% chondrocyte death at 40hrs) (**Figures 3.3 and 3.6**). The increased acidity, observed during bacterial culture, had a minimal effect on chondrocyte viability (**Figure 3.4**). Chondrocyte death commenced within the SZ of cartilage and rapidly progressed to the DZ (**Figure 3.7**). Simultaneous exposure of SZ and DZ chondrocytes to *S. aureus* 8325-4 toxins, achieved with the use of subchondral bone-free explants, demonstrated that SZ chondrocytes were more susceptible to the toxins than DZ chondrocytes (**Figure 3.11**).

2. When explants were cultured in the presence of a selection of isogenic *S. aureus* mutants, with varying Hla, Hlb and Hlg production capabilities (all originating from *S. aureus* 8325-4), Hla-producing mutants induced significant *in situ* chondrocyte death compared to a toxin-deficient control ($Hla^-Hlb^-Hlg^-$) (**Figures 4.2 and 4.4**). In contrast, mutants producing Hlb and Hlg in the absence of Hla were unable to induce significant chondrocyte death (**Figure 4.3**). Hla alone was therefore identified as the key damaging toxin to *in situ* chondrocyte viability.

3. Raised culture medium osmolarity had no influence on Hla-induced *in situ* chondrocyte death (**Figure 5.1**). In the absence of Hla, a high $[Ca^{2+}]_o$ (20mM) had no influence on chondrocyte viability during the experimental period (**Figure 5.2**). Hla-induced chondrocyte death increased in the presence of raised $[Ca^{2+}]_o$ thereby confirming a role of Ca^{2+} in the chondrocyte death pathway (**Figures 5.3, 5.4 and 5.5**). There was no significant difference between *S. aureus* growth in high and low Ca^{2+} culture media (**Table 5.1**), although the influence of raised $[Ca^{2+}]_o$ on *S. aureus* Hla synthesis could not be excluded.

4. When live osteochondral explants stained with the Ca^{2+}-sensitive fluorophore Fluo-4 were cultured with an Hla-containing *S. aureus* supernatant (*S. aureus* 8325-4 ($Hla^+Hlb^+Hlg^+$)) there was a significant rise in $[Ca^{2+}]_i$ in comparison to those explants exposed to a non-Hla-containing supernatant (*S. aureus* DU5938 ($Hla^-Hlb^-Hlg^-$)) (**Figures 6.8 and 6.9**). The Hla-induced Ca^{2+} transients, which lasted approx. 20mins, were always followed by chondrocyte death. Thus, Hla-induced chondrocyte death was associated with a rise in $[Ca^{2+}]_i$.

Figure 7.2 illustrates a simplified proposed model of *S. aureus* Hla-induced chondrocyte death based on the findings presented within this study. The translational relevance of the above conclusions with regard to current clinical practice and future scientific research are now considered.

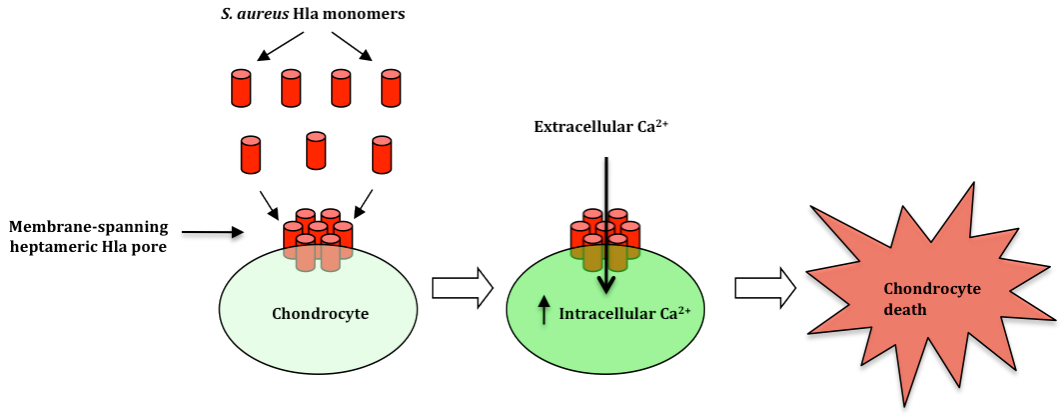

Figure 7.2: A proposed model of Hla-induced chondrocyte death

Hla forms membrane-spanning heptameric pores on the chondrocyte that permit the unregulated influx of Ca^{2+} into the cell. The resulting rise in intracellular Ca^{2+} culminates in chondrocyte death.

7.5 Joint lavage and antibiotic selection

The identification of rapid *S. aureus*-induced chondrocyte death firstly advocates the prompt and thorough removal of both bacteria and their associated toxins from infected joints; treatment with antibiotics alone should never be considered appropriate. Two common forms of joint lavage include serial bedside aspirations and surgical washout, with the most common irrigation solution being normal saline (Gredlein *et al.*, 2000; Klinger *et al.*, 2010). Whilst there is currently no evidence to suggest that one irrigation strategy is superior (Manadan and Block, 2004; Ravindran *et al.*, 2009), it has been posited that surgical washout provides a more comprehensive evacuation of bacteria and their toxins from the joint. In addition, given the observation that Ca^{2+} was associated with Hla-induced chondrocyte death then the use of Ca^{2+}-free irrigation solutions may be beneficial.

The finding that *S. aureus*-induced chondrocyte death was primarily mediated by Hla may challenge the appropriateness of current antibiotics. When patients present with

suspected septic arthritis, the joint in question is initially aspirated to enable microbiological assessment of the infected synovial fluid. An urgent gram stain may alert the clinician as to the likely causative organism but the full microbiological profile may take 24-48hrs. Patients are therefore empirically commenced on broad-spectrum intravenous antibiotics, commonly flucloxacillin and benzyl penicillin (Goldenberg, 1998; Shirtliff and Mader, 2002; Mathews *et al.*, 2008). In some circumstances several hours may pass between the commencement of antibiotics and formal joint lavage i.e. lack of operating theatre availability, thereby making initial antibiotic selection a potential key stage in the successful treatment of septic arthritis. At present, there is a lack of scientific evidence on which to base the choice of first-line antibiotic treatment (Mathews *et al.*, 2008).

Flucloxacillin and benzyl penicillin are classed as bactericidal antibiotics in that their ultimate mode of action is bacterial lysis (Bergeron *et al.*, 1976; Elliott *et al.*, 1979). Whilst this process kills the bacteria, there is the potential for the inadvertent release of intracellular contents, including bacterial toxins i.e. Hla, into the immediate surrounding environment (Pankey and Sabath, 2004). *In vivo*, it is possible and likely that Hla secreted into the synovial fluid prior to clinical presentation may have resulted in some degree of chondrocyte death. The bacterial rupture induced by bactericidal antibiotics may result in a 'pulse' of potent Hla that could cause additional chondrocyte death over and above that produced when the bacteria were alive. Minimising chondrocyte death during an episode of septic arthritis is likely to be pivotal to ensuring a satisfactory long-term outcome i.e. reducing the chance of

long-term problems such as early onset osteoarthritis. The choice of first-line antibiotics could therefore be crucial.

In contrast to bactericidal antibiotics, bacteriostatic antibiotics act by inhibiting bacterial growth (Kohanski *et al.*, 2010). The bacteria remain intact and are removed in a controlled manner by the host immune response (Varley *et al.*, 2009). In theory, there should be considerably lower levels of Hla released into the joint following their administration in comparison to bactericidal antibiotics. There has been exciting and encouraging experimental data that the bacteriostatic antibiotic Linezolid has the ability to suppress Hla synthesis by *S. aureus* intrinsically (Gemmell, 2002; Bernardo *et al.*, 2004), thereby making it a potential ideal first-line antibiotic for the treatment of septic arthritis. A proposed future study may therefore utilise the model of *S. aureus*-induced septic arthritis detailed within this thesis to assess *in situ* chondrocyte viability following treatment with a variety of commonly used bacteriostatic and bactericidal antibiotics.

7.6 Improved diagnosis of septic arthritis

Given the potential catastrophic consequences of a missed diagnosis of septic arthritis (outlined in Chapter 1), it is of critical importance that a diagnosis is quickly established in all cases. Sometimes the diagnosis can be challenging, as inflammatory markers may not be always be significantly elevated and the urgent gram stain is frequently inconclusive (Mathews *et al.*, 2010). In addition, current imaging studies, which include plain radiographs, CT, MRI and Ultrasonography, do

not have a high sensitivity or specificity for the diagnosis of septic arthritis (Shirtliff and Mader, 2002; Chander and Coakley, 2011).

Nuclear medicine could make an important future contribution to the diagnosis of ambiguous cases. Recent studies have investigated the role of radiolabelled antimicrobial peptides (AMPs) for infection detection. AMPs are a unique and varied group of primitive molecules that are considered to be part of the host innate immune response, the principal defence system for the majority of living organisms ranging from prokaryotes to humans (Boman, 1995; Zasloff, 2002; Giuliani *et al.*, 2007). They are small, positively charged, amphipathic molecules, possessing both hydrophobic and hydrophilic regions, that typically contain less than 100 amino acid residues (Peters *et al.*, 2010). They are mobilised shortly after infection and act rapidly to neutralise a broad range of microorganisms including bacteria, fungi, protozoa and viruses (Shai, 2002; Klotman and Chang, 2006; Peters *et al.*, 2010). To date, more than 800 AMPs have been isolated from a wide range of organisms (Peters *et al.*, 2010). In humans and other mammals, the two main AMP families, produced predominantly by the cells of the immune system, are cathelicidins and defensins (Bals and Wilson, 2003; Ganz, 2003; Zanetti, 2003; Lehrer, 2004).

The exact mechanism through which AMPs kill microorganisms is not yet fully understood although it is hypothesised that AMPs cause microbial membrane permeation with the subsequent disruption to transmembrane electrochemical gradients and, ultimately, cellular demise (Shai, 2002). AMPs utilise a fundamental difference between the design of microbial and multicellular organism membranes to

target invading microorganisms selectively (Zasloff, 2002). The organisation of the bacterial membrane is such that the outermost leaflet of the bilayer i.e. the surface exposed to the external environment, is heavily populated by lipids with negatively charged phospholipid head groups (Epand and Vogel, 1999; Matsuzaki, 1999; Shai, 1999). In contrast, the outer leaflet of the plasma membrane of mammalian cells is composed principally of lipids with no net charge; the majority of lipids with negatively charged head groups are contained within the inner leaf i.e. facing the cytoplasm (Zasloff, 2002). Thus, the positively charged AMPs are attracted to the negatively charged bacterial membrane only.

The preferential binding of AMPs to bacterial cell membranes has offered a potential target for the development of novel radiopharmaceuticals in order to expedite the diagnosis of septic arthritis in ambiguous cases. Ubiquicidin 29-41 (UBI 29-41), an AMP that was originally isolated from murine macrophages (Akhtar *et al.*, 2004), has been the subject of recent investigation. In an *in vivo* study by Welling *et al.* (2000), whereby mice were intramuscularly infected with a variety of bacteria, ^{99m}Tc-labelled UBI 29-41 was able to detect both gram-positive and gram-negative bacteria 5-30mins after injection. It was also found to be able to discriminate between bacterial infection and sterile inflammatory processes. Interestingly, a small clinical pilot study by Akhtar *et al.* (2005), investigating 18 individuals with suspected bone, soft tissue or prosthesis infection, has demonstrated encouraging results. The reported sensitivity, specificity and overall diagnostic accuracy of ^{99m}Tc-labelled UBI 29-41 for infection localisation were 100, 80 and 94.4%, respectively, with no adverse reactions observed during or after image acquisition.

Although subsequent small pilot studies have continued to show promising results (Beiki *et al.*, 2013; Saeed *et al.*, 2013), further large-scale studies are required to validate the routine use of ^{99m}Tc-labelled UBI 29-41 in clinical practice. In the meantime, for all ambiguous cases of septic arthritis, the '*if in doubt, washout*' approach is often most appropriate.

7.7 Strategies to inhibit the activity of Hla

The identification of Hla alone as the key damaging toxin to *in situ* chondrocyte viability (**Figures 4.4 and 4.5**), with its destructive action being associated with a rise in $[Ca^{2+}]_i$, stimulates the concept of a future potential therapeutic target to reduce the extent of cartilage destruction during and after an episode of septic arthritis.

The process of Hla pore-formation on eukaryotic cells is summarised as follows: (1) Hla is secreted as soluble monomers by *S. aureus*; (2) monomeric Hla molecules bind to a cell surface receptor, recently identified as ADAM10 (Inoshima *et al.*, 2011); (3) the Hla monomers undergo oligomerisation into a heptameric prepore on the cell surface and finally; (4) the heptameric prepore undergoes a conformational change leading to the formation of a 14-stranded transmembrane β-barrel (Gouaux, 1998). There are two key stages where activity of Hla could be inhibited: (1) pre- and (2) post-pore formation.

Inhibition at a pre-pore stage would necessitate the prevention of Hla cellular binding either through direct neutralisation or competitive inhibition. Interestingly, potent anti-Hla monoclonal antibodies have recently been identified and have been shown

to reduce lesion size significantly in a murine model of *S. aureus*-induced dermonecrosis (skin necrosis arising as a result of *S. aureus* infection) (Tkaczyk *et al.*, 2012). Tkaczyk *et al.* (2012) subsequently identified that these inhibitory monoclonal antibodies acted by blocking Hla hepatamer formation. Another potential strategy would be to attempt to develop high affinity antibodies for ADAM10 that would competitively inhibit the activity of Hla.

Once the membrane-spanning Hla pore has been established, it is unlikely that it will be amenable to antibody targeting and the focus therefore shifts to blocking the Hla pore. A recent exciting development in the field of Hla research is the ability of β-cyclodextrin derivatives to block Hla pores specifically (Karginov *et al.*, 2007; McCormick *et al.*, 2009; Ragle *et al.*, 2010; Inoshima *et al.*, 2011; Yannakopoulou *et al.*, 2011). Encouragingly, Ragle *et al.* (2010) demonstrated that administration of a β-cyclodextrin compound in a murine model of *S. aureus* pneumonia both prevented and treated disease while a study by McCormick *et al.* (2009) demonstrated that the administration of methyl-β-cyclodextrin-cholesterol in a murine model of *S. aureus* keratitis was effective in arresting corneal damage. It is possible that the administration of β-cyclodextrin compounds in a murine model of *S. aureus*-induced septic arthritis may be similarly advantageous.

7.8 Future studies

The experimental model of *S. aureus*-induced septic arthritis developed during this study will now be used for further investigations including: (1) the detailed study of intracellular Ca^{2+} pathways associated with Hla-induced chondrocyte death; (2) the

assessment of *in situ* chondrocyte viability during infection and following treatment with a variety of commonly used bacteriostatic and bactericidal antibiotics and; (3) the assessment of the chondroprotective potential of Hla-inhibiting agents such as Hla-specific monoclonal antibodies and β-cyclodextran compounds.

Studies will ultimately need to move to an animal model of septic arthritis in order to ascertain the chondrocyte-damaging role of the host immune response *in vivo*. The *S. aureus* 'haemolysin-knockout' mutant strains utilised in the current study may make such an experiment achievable. Any *in vivo* chondrocyte death observed following the establishment of septic arthritis with the $Hla^{-}Hlb^{-}Hlg^{-}$ mutant will likely be due to the host immune response. The extent of chondrocyte death present at the time of clinical presentation in humans is currently unknown. However, this could be estimated using an animal model to assess chondrocyte viability at the point of appearance of clinical manifestations of disease, and subsequent time points thereafter.

BIBLIOGRAPHY

Abid, N., Bhatti, M., Azharuddin, M. & Islam, M. (2006) Septic arthritis in a tertiary care hospital. *J Pak Med Assoc,* **56,** 95-98.

Adams, J. C. & Watt, F. M. (1993) Regulation of development and differentiation by the extracellular matrix. *Development,* **117,** 1183-1198.

Adams, M. A. (2006) The mechanical environment of chondrocytes in articular cartilage. *Biorheology,* **43,** 537-545.

Afoke, N. Y., Byers, P. D. & Hutton, W. C. (1987) Contact pressures in the human hip joint. *J Bone Joint Surg Br,* **69,** 536-541.

Akhtar, M. S., Iqbal, J., Khan, M. A., Irfanullah, J., Jehangir, M., Khan, B., Ul-Haq, I., Muhammad, G., Nadeem, M. A., Afzal, M. S. & Imran, M. B. (2004) 99mTc-labeled antimicrobial peptide ubiquicidin (29-41) accumulates less in Escherichia coli infection than in *Staphlococcus aureus* infection. *J Nucl Med,* **45,** 849-856.

Akhtar, M. S., Qaisar, A., Irfanullah, J., Iqbal, J., Khan, B., Jehangir, M., Nadeem, M. A., Khan, M. A., Afzal, M. S., Ul-Haq, I. & Imran, M. B. (2005) Antimicrobial peptide 99mTc-ubiquicidin 29-41 as human infection-imaging agent: clinical trial. *J Nucl Med,* **46,** 567-573.

Akinyoola, A. L., Obiajunwa, P. O. & Oginni, L. M. (2006) Septic arthritis in children. *West Afr J Med,* **25,** 119-123.

Amin, A. K., Huntley, J. S., Bush, P. G., Simpson, A. H. R. W. & Hall, A. C. (2008) Osmolarity influences chondrocyte death in wounded articular cartilage. *J Bone Joint Surg Am,* **90,** 1531-1542.

Amin, A. K., Huntley, J. S., Bush, P. G., Simpson, A. H. R. W. & Hall, A. C. (2009a) Chondrocyte death in mechanically injured articular cartilage- the influence of extracellular calcium. *J Orthop Res,* **27,** 778-784.

Amin, A. K., Huntley, J. S., Patton, J. T., Brenkel, I. J., Simpson, A. H. R. W. & Hall, A. C. (2011) Hyperosmolarity protects chondrocytes from mechanical injury in human articular cartilage: an experimental report. *J Bone Joint Surg Br,* **93,** 277-284.

Amin, A. K., Huntley, J. S., Simpson, A. H. R. W. & Hall, A. C. (2009b) Chondrocyte survival in articular cartilage: the influence of subchondral bone in a bovine model. *J Bone Joint Surg Br,* **91,** 691-699.

Amin, A. K., Huntley, J. S., Simpson, A. H. R. W. & Hall, A. C. (2010) Increasing the osmolarity of joint irrigation solutions may avoid injury to cartilage: a pilot study. *Clin Orthop Relat Res,* **468,** 875-884.

Appelbaum, P. C. (2007) Microbiology of antibiotic resistance in *Staphylococcus aureus*. *Clin Infect Dis,* **45 Suppl 3,** S165-70.

Archer, C. W. (1994) Skeletal development and osteoarthritis. *Ann Rheum Dis,* **53,** 624-630.

Ateschrang, A., Albrecht, D., Schröter, S., Hirt, B., Weise, K. & Dolderer, J. H. (2011) Septic arthritis of the knee: Presentation of a novel irrigation-suction system tested in a cadaver study. *BMC Musculoskelet Disord,* **12,** 180.

Ateshian, G. A., Lai, W. M., Zhu, W. B. & Mow, V. C. (1994) An asymptotic solution for the contact of two biphasic cartilage layers. *J Biomech,* **27,** 1347-1360.

Ateshian, G. A. & Wang, H. (1995) A theoretical solution for the frictionless rolling contact of cylindrical biphasic articular cartilage layers. *J Biomech,* **28,** 1341-1355.

Athanasiou, K. A., Rosenwasser, M. P., Buckwalter, J. A., Malinin, T. I. & Mow, V. C. (1991) Interspecies comparisons of *in situ* intrinsic mechanical properties of distal femoral cartilage. *J Orthop Res,* **9,** 330-340.

Bals, R. & Wilson, J. M. (2003) Cathelicidins - a family of multifunctional antimicrobial peptides. *Cell Mol Life Sci,* **60,** 711-720.

Bartlett, A. H., Foster, T. J., Hayashida, A. & Park, P. W. (2008) Alpha-toxin facilitates the generation of CXC chemokine gradients and stimulates neutrophil homing in *Staphylococcus aureus* pneumonia. *J Infect Dis,* **198,** 1529-1535.

Becker, W. & Meller, J. (2001) The role of nuclear medicine in infection and inflammation. *Lancet Infect Dis,* **1,** 326-333.

Beiki, D., Yousefi, G., Fallahi, B., Tahmasebi, M. N., Gholamrezanezhad, A., Fard-Esfahani, A., Erfani, M. & Eftekhari, M. (2013) 99mTc-Ubiquicidin [29-41],

a oromising radiopharmaceutical to differentiate orthopedic implant infections from sterile inflammation. *Iran J Pharm Res,* **12,** 347-353.

Benson, J. A. & Ferrieri, P. (2001) Rapid pulsed-field gel electrophoresis method for group B *streptococcus* isolates. *J Clin Microbiol,* **39,** 3006-3008.

Berberat, J. E., Nissi, M. J., Jurvelin, J. S. & Nieminen, M. T. (2009) Assessment of interstitial water content of articular cartilage with T1 relaxation. *Magn Reson Imaging,* **27,** 727-732.

Bergeron, M. G., Brusch, J. L., Barza, M. & Weinstein, L. (1976) Bactericidal activity and pharmacology of flucloxacillin. *The American journal of the medical sciences,* **271,** 13-20.

Bernardo, K., Pakulat, N., Fleer, S., Schnaith, A., Utermohlen, O., Krut, O., Muller, S. & Kronke, M. (2004) Subinhibitory concentrations of linezolid reduce *Staphylococcus aureus* virulence factor expression. *Antimicrob Agents Chemother,* **48,** 546-555.

Berridge, M. J. (1993) Inositol trisphosphate and calcium signalling. *Nature,* **361,** 315-325.

Berridge, M. J., Bootman, M. D. & Lipp, P. (1998) Calcium - a life and death signal. *Nature,* **395,** 645-648.

Berridge, M. J., Lipp, P. & Bootman, M. D. (2000) The versatility and universality of calcium signalling. *Nat Rev Mol Cell Biol,* **1,** 11-21.

Berube, B. J. & Bubeck-Wardenburg, J. (2013) Staphylococcus aureus α-toxin: nearly a century of intrigue. *Toxins,* **5,** 1140-1166.

Bhakdi, S., Muhly, M., Korom, S. & Hugo, F. (1989) Release of interleukin-1 beta associated with potent cytocidal action of *staphylococcal* alpha-toxin on human monocytes. *Infect Immun,* **57,** 3512-3519.

Bhakdi, S. & Tranum-Jensen, J. (1991) Alpha-toxin of *Staphylococcus aureus*. *Microbiol Rev,* **55,** 733-19.

Bhosale, A. M. & Richardson, J. B. (2008) Articular cartilage: structure, injuries and review of management. *Br Med Bull,* **87,** 77-95.

Bobechko, W. P. & Mandell, L. (1975) Immunology of cartilage in septic arthritis. *Clin Orthop Relat Res***,** 84-89.

Bodén, M. K. & Flock, J. I. (1994) Cloning and characterization of a gene for a 19 kDa fibrinogen-binding protein from *Staphylococcus aureus*. *Mol Microbiol,* **12,** 599-606.

Bollet, A. J. & Nance, J. L. (1966) Biochemical findings in normal and osteoarthritic articular cartilage. II. Chondroitin sulfate concentration and chain length, water, and ash content. *J Clin Invest,* **45,** 1170-1177.

Boman, H. G. (1995) Peptide antibiotics and their role in innate immunity. *Annu Rev Immunol,* **13,** 61-92.

Bowerman, S. G., Green, N. E. & Mencio, G. A. (1997) Decline of bone and joint infections attributable to *haemophilus influenzae* type b. *Clin Orthop Relat Res***,** 128-133.

Bramley, A. J., Patel, A. H., O'reilly, M., Foster, R. & Foster, T. J. (1989) Roles of alpha-toxin and beta-toxin in virulence of *Staphylococcus aureus* for the mouse mammary gland. *Infect Immun,* **57,** 2489-2494.

Bubeck-Wardenburg, J., Patel, R. J. & Schneewind, O. (2007) Surface Proteins and Exotoxins Are Required for the Pathogenesis of *Staphylococcus aureus* Pneumonia. *Infect Immun,* **75,** 1040-1044.

Bubeck-Wardenburg, J. & Schneewind, O. (2008) Vaccine protection against *Staphylococcus aureus* pneumonia. *J Exp Med,* **205,** 287-294.

Buchanan, W. W. (2003) Sir Benjamin Collins Brodie (1783-1862). *Rheumatology (Oxford),* **42,** 689-691.

Buckwalter, J. A. & Mankin, H. J. (1997a) Articular cartilage. Part I: tissue design and chondrocyte-matrix interactions. *J Bone Joint Surg Am,* **79,** 600-611.

Buckwalter, J. A. & Mankin, H. J. (1997b) Articular cartilage. Part II: degeneration and osteoarthritis, repair, regeneration, and transplantation. *J Bone Joint Surg Am,* **47,** 487-504.

Buckwalter, J. A., Mankin, H. J. & Grodzinsky, A. J. (2005) Articular cartilage and osteoarthritis. *Instr Course Lect,* **54,** 465-480.

Budd, S. L. & Nicholls, D. G. (1996) A reevaluation of the role of mitochondria in neuronal Ca2+ homeostasis. *J Neurochem,* **66,** 403-411.

Burnside, K., Lembo, A., De Los Reyes, M., Iliuk, A., Binhtran, N.-T., Connelly, J. E., Lin, W.-J., Schmidt, B. Z., Richardson, A. R., Fang, F. C., Tao, W. A. &

Rajagopal, L. (2010) Regulation of Hemolysin Expression and Virulence of *Staphylococcus aureus* by a Serine/Threonine Kinase and Phosphatase. *Plos One,* **5,** e11071.

Buschmann, M. D., Gluzband, Y. A., Grodzinsky, A. J., Kimura, J. H. & Hunziker, E. B. (1992) Chondrocytes in agarose culture synthesize a mechanically functional extracellular matrix. *J Orthop Res,* **10,** 745-758.

Buschmann, M. D., Hunziker, E. B., Kim, Y. J. & Grodzinsky, A. J. (1996) Altered aggrecan synthesis correlates with cell and nucleus structure in statically compressed cartilage. *J Cell Sci,* **109 (Pt 2),** 499-508.

Bush, P. G. & Hall, A. C. (2001a) The osmotic sensitivity of isolated and *in situ* bovine articular chondrocytes. *J Orthop Res,* **19,** 768-778.

Bush, P. G. & Hall, A. C. (2001b) Regulatory volume decrease (RVD) by isolated and *in situ* bovine articular chondrocytes. *J Cell Physiol,* **187,** 304-314.

Bush, P. G. & Hall, A. C. (2003) The volume and morphology of chondrocytes within non-degenerate and degenerate human articular cartilage. *Osteoarthritis Cartilage,* **11,** 242-251.

Bush, P. G., Hodkinson, P. D., Hamilton, G. L. & Hall, A. C. (2005) Viability and volume of *in situ* bovine articular chondrocytes-changes following a single impact and effects of medium osmolarity. *Osteoarthritis Cartilage,* **13,** 54-65.

Bush, P. G., Pritchard, M., Loqman, M. Y., Damron, T. A. & Hall, A. C. (2010) A key role for membrane transporter NKCC1 in mediating chondrocyte volume increase in the mammalian growth plate. *J Bone Miner Res,* **25,** 1594-1603.

Callegan, M. C., Engel, L. S., Hill, J. M. & O'callaghan, R. J. (1994) Corneal virulence of *Staphylococcus aureus*: roles of alpha-toxin and protein A in pathogenesis. *Infect Immun,* **62,** 2478-2482.

Campbell, J., Filardo, G., Bruce, B., Bajaj, S., Friel, N., Hakimiyan, A., Wood, S., Grumet, R., Shafikhani, S., Chubinskaya, S. & Cole, B. J. (2014) Salvage of contaminated osteochondral allografts: the effects of chlorhexidine on human articular chondrocyte viability. *Am J Sports Med,* **42,** 973-978.

Carafoli, E. (1991) Calcium pump of the plasma membrane. *Physiol Rev,* **71,** 129-153.

Casewell, M. W. & Hill, R. L. (1986) The carrier state: methicillin-resistant *Staphylococcus aureus*. *J Antimicrob Chemother,* **18 Suppl A,** 1-12.

Castano Oreja, M. T., Quintáns Rodriguez, M., Crespo Abelleira, A., Giráldez García, M. A., Saavedra García, M. A. & Jorge Barreiro, F. J. (1995) Variation in articular cartilage in rabbits between weeks six and eight. *Anat Rec,* **241,** 34-38.

Cernanec, J. M., Weinberg, J. B., Batinic-Haberle, I., Guilak, F. & Fermor, B. (2007) Influence of oxygen tension on interleukin 1-induced peroxynitrite formation and matrix turnover in articular cartilage. *J Rheumatol,* **34,** 401-407.

Chander, S. & Coakley, G. (2011) What's new in the management of bacterial septic arthritis? *Curr Infect Dis Rep,* **13,** 478-484.

Chang, J. & Poole, C. A. (1997) Confocal analysis of the molecular heterogeneity in the pericellular microenvironment produced by adult canine chondrocytes cultured in agarose gel. *Histochem J,* **29,** 515-528.

Chappuis, J., Sherman, I. A. & Neumann, A. W. (1983) Surface tension of animal cartilage as it relates to friction in joints. *Ann Biomed Eng,* **11,** 435-449.

Cheng, A. G., Kim, H. K., Burts, M. L., Krausz, T., Schneewind, O. & Missiakas, D. M. (2009) Genetic requirements for *Staphylococcus aureus* abscess formation and persistence in host tissues. *The FASEB Journal,* **23,** 3393-3404.

Chevalier, X. (1993) Fibronectin, cartilage, and osteoarthritis. *Semin Arthritis Rheum,* **22,** 307-318.

Chevalier, X., Groult, N., Larget-Piet, B., Zardi, L. & Hornebeck, W. (1994) Tenascin distribution in articular cartilage from normal subjects and from patients with osteoarthritis and rheumatoid arthritis. *Arthritis Rheum,* **37,** 1013-1022.

Chiquet-Ehrismann, R., Kalla, P., Pearson, C. A., Beck, K. & Chiquet, M. (1988) Tenascin interferes with fibronectin action. *Cell,* **53,** 383-390.

Clapham, D. E. (1995) Calcium signaling. *Cell,* **80,** 259-268.

Clark, C. C., Iannotti, J. P., Misra, S. & Richards, C. F. (1994) Effects of thapsigargin, an intracellular calcium-mobilizing agent, on synthesis and secretion of cartilage collagen and proteoglycan. *J Orthop Res,* **12,** 601-611.

Clark, J. M. (1990) The organisation of collagen fibrils in the superficial zones of articular cartilage. *J Anat,* **171,** 117-130.

Claxton, N. S., Fellers, T. J. & Davidson, M. W. 2006. *Laser scanning confocal microscopy* [Online]. Department of Optical Microscopy and Digital Imaging, National High Magnetic Field Laboratory, The Florida State University, Tallahassee, Florida, USA. Available: www.olympusconfocal.com/theory/LSCMIntro.pdf.

Clyne, M., De Azavedo, J., Carlson, E. & Arbuthnott, J. (1988) Production of gamma-hemolysin and lack of production of alpha-hemolysin by *Staphylococcus aureus* strains associated with toxic shock syndrome. *J Clin Microbiol,* **26,** 535-539.

Coakley, G., Mathews, C., Field, M., Jones, A., Kingsley, G., Walker, D., Phillips, M., Bradish, C., Mclachlan, A., Mohammed, R. & Weston, V. 2006. BSR & BHPR, BOA, RCGP and BSAC guidelines for management of the hot swollen joint in adults. *Rheumatology (Oxford).*

Cockburn, I. A., Amino, R., Kelemen, R. K., Kuo, S. C., Tse, S.-W., Radtke, A., Mac-Daniel, L., Ganusov, V. V., Zavala, F. & Ménard, R. (2013) *In vivo* imaging of CD8+ T cell-mediated elimination of malaria liver stages. *Proc Natl Acad Sci U S A,* **110,** 9090-9095.

Coleman, D. C., Arbuthnott, J. P., Pomeroy, H. M. & Birkbeck, T. H. (1986) Cloning and expression in *Escherichia coli* and *Staphylococcus aureus* of the beta-lysin determinant from *Staphylococcus aureus*: evidence that bacteriophage conversion of beta-lysin activity is caused by insertional inactivation of the beta-lysin determinant. *Microb Pathog,* **1,** 549-564.

Combs, C. A. (2010) Fluorescence microscopy: a concise guide to current imaging methods. *Curr Protoc Neurosci,* **2,** Unit2.1.

Coutlakis, P. J., Roberts, W. N. & Wise, C. M. (2002) Another look at synovial fluid leukocytosis and infection. *J Clin Rheumatol,* **8,** 67-71.

Cruz, L. F., Cobine, P. A. & De La Fuente, L. (2012) Calcium increases *Xylella fastidiosa* surface attachment, biofilm formation, and twitching motility. *Appl Environ Microbiol,* **78,** 1321-1331.

Cunningham, R., Cockayne, A. & Humphreys, H. (1996) Clinical and molecular aspects of the pathogenesis of *Staphylococcus aureus* bone and joint infections. *J Med Microbiol,* **44,** 157-164.

D'lima, D. D., Hashimoto, S., Chen, P. C., Lotz, M. K. & Colwell, C. W. (2001) *In vitro* and *in vivo* models of cartilage injury. *J Bone Joint Surg Am,* **83-A Suppl 2,** 22-24.

Dagan, R. (1993) Management of acute hematogenous osteomyelitis and septic arthritis in the pediatric patient. *Pediatr Infect Dis J,* **12,** 88-92.

Dailey, M., Marrs, G., Satz, J. & Waite, M. (1999) Concepts in imaging and microscopy. Exploring biological structure and function with confocal microscopy. *Biol Bull,* **197,** 115-122.

Dajcs, J. J., Thibodeaux, B. A., Girgis, D. O. & O'callaghan, R. J. (2002) Corneal virulence of *Staphylococcus aureus* in an experimental model of keratitis. *DNA Cell Biol,* **21,** 375-382.

De Boeck, H. (2005) Osteomyelitis and septic arthritis in children. *Acta Orthop Belg,* **71,** 505-515.

De Haas, C. J. C., Veldkamp, K. E., Peschel, A., Weerkamp, F., Van Wamel, W. J. B., Heezius, E. C. J. M., Poppelier, M. J. J. G., Van Kessel, K. P. M. & Van Strijp, J. a. G. (2004) Chemotaxis inhibitory protein of *Staphylococcus aureus*, a bacterial antiinflammatory agent. *J Exp Med,* **199,** 687-695.

Démarteau, O., Pillet, L., Inaebnit, A., Borens, O. & Quinn, T. M. (2006) Biomechanical characterization and *in vitro* mechanical injury of elderly human femoral head cartilage: comparison to adult bovine humeral head cartilage. *Osteoarthritis Cartilage,* **14,** 589-596.

Dicesare, P. E., Mörgelin, M., Mann, K. & Paulsson, M. (1994) Cartilage oligomeric matrix protein and thrombospondin 1. Purification from articular cartilage, electron microscopic structure, and chondrocyte binding. *Eur J Biochem,* **223,** 927-937.

Diep, B. A., Sensabaugh, G. F., Somboonna, N., Somboona, N. S., Carleton, H. A. & Perdreau-Remington, F. (2004) Widespread skin and soft-tissue infections due to two methicillin-resistant *Staphylococcus aureus* strains harboring the genes for Panton-Valentine leucocidin. *J Clin Microbiol,* **42,** 2080-2084.

Dinges, M. M., Orwin, P. M. & Schlievert, P. M. (2000) Exotoxins of *Staphylococcus aureus*. *Clin Microbiol Rev,* **13,** 16-34.

Dingle, J. T., Fell, H. B. & Glauert, A. M. (1969) Endocytosis of sugars in embryonic skeletal tissues in organ culture. IV. Lysosomal and other biochemical effects. General discussion. *J Cell Sci,* **4,** 139-153.

Donlan, R. M. & Costerton, J. W. (2002) Biofilms: Survival Mechanisms of Clinically Relevant Microorganisms. *Clin Microbiol Rev,* **15,** 167-193.

Dragneva, Y., Anuradha, C. D., Valeva, A., Hoffmann, A., Bhakdi, S. & Husmann, M. (2001) Subcytocidal attack by *staphylococcal* alpha-toxin activates NF-kappaB and induces interleukin-8 production. *Infect Immun,* **69,** 2630-2635.

Dubost, J. J., Fis, I., Denis, P., Lopitaux, R., Soubrier, M., Ristori, J. M., Bussiére, J. L., Sirot, J. & Sauvezie, B. (1993) Polyarticular septic arthritis. *Medicine (Baltimore),* **72,** 296-310.

Dubost, J. J., Soubrier, M., De Champs, C., Ristori, J. M., Bussiére, J. L. & Sauvezie, B. (2002) No changes in the distribution of organisms responsible for septic arthritis over a 20 year period. *Ann Rheum Dis,* **61,** 267-269.

Duchen, M. R. (1999) Contributions of mitochondria to animal physiology: from homeostatic sensor to calcium signalling and cell death. *J Physiol (Lond),* **516 (Pt 1),** 1-17.

Edwards, A. M., Potts, J. R., Josefsson, E. & Massey, R. C. (2010) *Staphylococcus aureus* host cell invasion and virulence in sepsis is facilitated by the multiple repeats within FnBPA. *PLoS Pathogens,* **6,** e1000964.

Ejrnaes, K., Sandvang, D., Lundgren, B., Ferry, S., Holm, S., Monsen, T., Lundholm, R. & Frimodt-Moller, N. (2006) Pulsed-field gel electrophoresis typing of *Escherichia coli* strains from samples collected before and after pivmecillinam or placebo treatment of uncomplicated community-acquired urinary tract infection in women. *J Clin Microbiol,* **44,** 1776-1781.

Elliott, T. S., Greenwood, D., Rodgers, F. G. & O&Apos;Grady, F. (1979) The response of *Staphylococcus aureus* to benzylpenicillin. *Br J Exp Pathol,* **60,** 14-23.

Epand, R. M. & Vogel, H. J. (1999) Diversity of antimicrobial peptides and their mechanisms of action. *Biochim Biophys Acta,* **1462,** 11-28.

Erdahl, W. L., Chapman, C. J., Taylor, R. W. & Pfeiffer, D. R. (1994) Ca2+ transport properties of ionophores A23187, ionomycin, and 4-BrA23187 in a well defined model system. *Biophys J,* **66,** 1678-1693.

Erickson, G. R., Northrup, D. L. & Guilak, F. (2003) Hypo-osmotic stress induces calcium-dependent actin reorganization in articular chondrocytes. *Osteoarthritis Cartilage,* **11,** 187-197.

Essmann, F., Bantel, H., Totzke, G., Engels, I. H., Sinha, B., Schulze-Osthoff, K. & Jänicke, R. U. (2003) *Staphylococcus aureus* alpha-toxin-induced cell death: predominant necrosis despite apoptotic caspase activation. *Cell Death Differ,* **10,** 1260-1272.

Fisher, L. W., Termine, J. D. & Young, M. F. (1989) Deduced protein sequence of bone small proteoglycan I (biglycan) shows homology with proteoglycan II (decorin) and several nonconnective tissue proteins in a variety of species. *J Biol Chem,* **264,** 4571-4576.

Foerster, C., Voelxen, N., Rakhmanov, M., Keller, B., Gutenberger, S., Goldacker, S., Thiel, J., Feske, S., Peter, H.-H. & Warnatz, K. (2010) B cell receptor-mediated calcium signaling is impaired in B lymphocytes of type Ia patients with common variable immunodeficiency. *J Immunol,* **184,** 7305-7313.

Foster, T. J. (2005) Immune evasion by *staphylococci*. *Nat Rev Microbiol,* **3,** 948-958.

Francis, R. J., Kotecha, S. & Hallett, M. B. (2013) Ca2+ activation of cytosolic calpain induces the transition from apoptosis to necrosis in neutrophils with externalized phosphatidylserine. *J Leukoc Biol,* **93,** 95-100.

Fried, J., Perez, A. G. & Clarkson, B. D. (1976) Flow cytofluorometric analysis of cell cycle distributions using propidium iodide. Properties of the method and mathematical analysis of the data. *J Cell Biol,* **71,** 172-181.

Frigault, M. M., Lacoste, J., Swift, J. L. & Brown, C. M. (2009) Live-cell microscopy - tips and tools. *J Cell Sci,* **122,** 753-767.

Fry, H. & Robertson, W. V. (1967) Interlocked stresses in cartilage. *Nature,* **215,** 53-54.

Fuchs, S., Pané-Farré, J., Kohler, C., Hecker, M. & Engelmann, S. (2007) Anaerobic gene expression in *Staphylococcus aureus*. *J Bacteriol,* **189,** 4275-4289.

Ganz, T. (2003) Defensins: antimicrobial peptides of innate immunity. *Nature Reviews Immunology,* **3,** 710-720.

Gao, Y., Liu, S., Huang, J., Guo, W., Chen, J., Zhang, L., Zhao, B., Peng, J., Wang, A., Wang, Y., Xu, W., Lu, S., Yuan, M. & Guo, Q. (2014) The ECM-cell interaction of cartilage extracellular matrix on chondrocytes. *Biomed Res Int,* **2014,** 648459.

García-Arias, M., Balsa, A. & Mola, E. M. (2011) Septic arthritis. *Best Pract Res Clin Rheumatol,* **25,** 407-421.

Gargiulo, B. J., Cragg, P., Richardson, J. B., Ashton, B. A. & Johnson, W. E. (2002) Phenotypic modulation of human articular chondrocytes by bistratene A. *Eur Cell Mater,* **3,** 9-18.

Gee, K. R., Brown, K. A., Chen, W. N., Bishop-Stewart, J., Gray, D. & Johnson, I. (2000) Chemical and physiological characterization of fluo-4 Ca2+-indicator dyes. *Cell Calcium,* **27,** 97-106.

Gemmell, C., Goutcher, S., Reid, R. & Sturrock, R. (1997) Role of certain virulence factors in a murine model of *Staphylococcus aureus* arthritis. *J Med Microbiol,* **46,** 208-213.

Gemmell, C. G. (2002) Virulence factor expression by Gram-positive cocci exposed to subinhibitory concentrations of linezolid. *J Antimicrob Chemother,* **50,** 665-672.

Ghasemi, A. & Zahediasl, S. (2012) Normality tests for statistical analysis: a guide for non-statisticians. *Int J Endocrinol Metab,* **10,** 486-489.

Gibson, T. & Davis, W. B. (1958) The distortion of autogenous cartilage grafts: its cause and prevention. *Br J Plast Surg,* **10,** 257-274.

Gillet, Y., Issartel, B., Vanhems, P., Fournet, J.-C., Lina, G., Bes, M., Vandenesch, F., Piémont, Y., Brousse, N., Floret, D. & Etienne, J. (2002) Association between *Staphylococcus aureus* strains carrying gene for Panton-Valentine leukocidin and highly lethal necrotising pneumonia in young immunocompetent patients. *Lancet,* **359,** 753-759.

Giuliani, A., Pirri, G. & Nicoletto, S. F. (2007) Antimicrobial peptides: an overview of a promising class of therapeutics. *Central European Journal of Biology,* **2,** 1-33.

Goldenberg, D. L. (1998) Septic arthritis. *Lancet,* **351,** 197-202.

Goldring, M. B. (2012) Chondrogenesis, chondrocyte differentiation, and articular cartilage metabolism in health and osteoarthritis. *Ther Adv Musculoskelet Dis,* **4,** 269-285.

Goldring, M. B. & Marcu, K. B. (2009) Cartilage homeostasis in health and rheumatic diseases. *Arthritis Res Ther,* **11,** 224.

Gordon, R. J. & Lowy, F. D. (2008) Pathogenesis of methicillin-resistant *Staphylococcus aureus* infection. *Clin Infect Dis,* **46 Suppl 5,** S350-9.

Gouaux, E. (1998) Alpha-hemolysin from *Staphylococcus aureus*: an archetype of beta-barrel, channel-forming toxins. *J Struct Biol,* **121,** 110-122.

Graif, M., Schweitzer, M. E., Deely, D. & Matteucci, T. (1999) The septic versus nonseptic inflamed joint: MRI characteristics. *Skeletal Radiol,* **28,** 616-620.

Gray, G. S. & Kehoe, M. (1984) Primary sequence of the alpha-toxin gene from *Staphylococcus aureus* wood 46. *Infect Immun,* **46,** 615-618.

Gredlein, C. M., Silverman, M. L. & Downey, M. S. (2000) Polymicrobial septic arthritis due to Clostridium species: case report and review. *Clin Infect Dis,* **30,** 590-594.

Guilak, F., Jones, W. R., Ting-Beall, H. P. & Lee, G. M. (1999) The deformation behavior and mechanical properties of chondrocytes in articular cartilage. *Osteoarthritis Cartilage,* **7,** 59-70.

Gupta, M. N., Sturrock, R. D. & Field, M. (2001) A prospective 2-year study of 75 patients with adult-onset septic arthritis. *Rheumatology (Oxford),* **40,** 24-30.

Gwag, B. J., Canzoniero, L. M., Sensi, S. L., Demaro, J. A., Koh, J. Y., Goldberg, M. P., Jacquin, M. & Choi, D. W. (1999) Calcium ionophores can induce either apoptosis or necrosis in cultured cortical neurons. *Neuroscience,* **90,** 1339-1348.

Hall, A. C., Horwitz, E. R. & Wilkins, R. J. (1996a) The cellular physiology of articular cartilage. *Exp Physiol,* **81,** 535-545.

Hall, A. C., Starks, I., Shoults, C. L. & Rashidbigi, S. (1996b) Pathways for K+ transport across the bovine articular chondrocyte membrane and their sensitivity to cell volume. *Am J Physiol,* **270,** C1300-10.

Han, S.-K., Wouters, W., Clark, A. & Herzog, W. (2012) Mechanically induced calcium signaling in chondrocytes in situ. *J Orthop Res,* **30,** 475-481.

Haque, R. U. & Baldwin, J. N. (1964) Types of hemolysins produced by *Staphylococcus aureus*, as determined by the replica plating technique. *J Bacteriol,* **88,** 1442-1447.

Harris, L. G., Foster, S. J. & Richards, R. G. (2002) An introduction to *Staphylococcus aureus*, and techniques for identifying and quantifying *S. aureus* adhesins in relation to adhesion to biomaterials: review. *Eur Cell Mater,* **4,** 39-60.

Hauselmann, H. J., Flechtenmacher, J., Michal, L., Thonar, E. J., Shinmei, M., Kuettner, K. E. & Aydelotte, M. B. (1996) The superficial layer of human articular cartilage is more susceptible to interleukin-1-induced damage than the deeper layers. *Arthritis Rheum,* **39,** 478-488.

Hayashida, A., Bartlett, A. H., Foster, T. J. & Park, P. W. (2009) *Staphylococcus aureus* beta-toxin induces lung injury through syndecan-1. *Am J Pathol,* **174,** 509-518.

Hedbom, E., Antonsson, P., Hjerpe, A., Aeschlimann, D., Paulsson, M., Rosa-Pimentel, E., Sommarin, Y., Wendel, M., Oldberg, A. & Heinegård, D. (1992) Cartilage matrix proteins. An acidic oligomeric protein (COMP) detected only in cartilage. *J Biol Chem,* **267,** 6132-6136.

Herbert, S., Ziebandt, A. K., Ohlsen, K., Schafer, T., Hecker, M., Albrecht, D., Novick, R. & Gotz, F. (2010) Repair of global regulators in *Staphylococcus aureus* 8325 and comparative analysis with other clinical isolates. *Infect Immun,* **78,** 2877-2889.

Himmel, H. M., Riehle, R., Stieler, K. & Siess, M. (1990) Effects of the divalent cation ionophore ionomycin on the performance of isolated guinea-pig atria. *Basic Res Cardiol,* **85,** 247-256.

Hodge, W. A., Fijan, R. S., Carlson, K. L., Burgess, R. G., Harris, W. H. & Mann, R. W. (1986) Contact pressures in the human hip joint measured in vivo. *Proc Natl Acad Sci U S A,* **83,** 2879-2883.

Hoffmann, E. K., Lambert, I. H. & Pedersen, S. F. (2009) Physiology of cell volume regulation in vertebrates. *Physiol Rev,* **89,** 193-277.

Hollander, A. P., Pidoux, I., Reiner, A., Rorabeck, C., Bourne, R. & Poole, A. R. (1995) Damage to type II collagen in aging and osteoarthritis starts at the articular surface, originates around chondrocytes, and extends into the cartilage with progressive degeneration. *J Clin Invest,* **96,** 2859-2869.

Howden, B. P., Mcevoy, C. R. E., Allen, D. L., Chua, K., Gao, W., Harrison, P. F., Bell, J., Coombs, G., Bennett-Wood, V., Porter, J. L., Robins-Browne, R., Davies, J. K., Seemann, T. & Stinear, T. P. (2011) Evolution of multidrug resistance during *Staphylococcus aureus* infection involves mutation of the essential two component regulator WalKR. *PLoS Pathogens,* **7,** e1002359.

Hruz, P., Zinkernagel, A. S., Jenikova, G., Botwin, G. J., Hugot, J.-P., Karin, M., Nizet, V. & Eckmann, L. (2009) NOD2 contributes to cutaneous defense against *Staphylococcus aureus* through alpha-toxin-dependent innate immune activation. *Proc Natl Acad Sci U S A,* **106,** 12873-12878.

Hudson, M. C., Ramp, W. K., Nicholson, N. C., Williams, A. S. & Nousiainen, M. T. (1995) Internalization of *Staphylococcus aureus* by cultured osteoblasts. *Microb Pathog,* **19,** 409-419.

Hume, E. B., Dajcs, J. J., Moreau, J. M. & O'callaghan, R. J. (2000) Immunization with alpha-toxin toxoid protects the cornea against tissue damage during experimental *Staphylococcus aureus* keratitis. *Infect Immun,* **68,** 6052-6055.

Hunter, W. (1743) Of the Structure and Diseases of Articulating Cartilages, by William Hunter, Surgeon. *Philos Trans R Soc Lond,* **42,** 514-521.

Huntley, J. S., Simpson, A. H. & Hall, A. C. (2005) Use of non-degenerate human osteochondral tissue and confocal laser scanning microscopy for the study of chondrocyte death at cartilage surgery. *Eur Cell Mater,* **9,** 13-22.

Hunziker, E. B. (2002) Articular cartilage repair: basic science and clinical progress. A review of the current status and prospects. *Osteoarthritis Cartilage,* **10,** 432-463.

Huseby, M., Shi, K., Brown, C. K., Digre, J., Mengistu, F., Seo, K. S., Bohach, G. A., Schlievert, P. M., Ohlendorf, D. H. & Earhart, C. A. (2007) Structure and biological activities of beta toxin from *Staphylococcus aureus*. *J Bacteriol,* **189,** 8719-8726.

Huser, C. a. M. & Davies, M. E. (2007) Calcium signaling leads to mitochondrial depolarization in impact-induced chondrocyte death in equine articular cartilage explants. *Arthritis Rheum,* **56,** 2322-2334.

Inoshima, I., Inoshima, N., Wilke, G. A., Powers, M. E., Frank, K. M., Wang, Y. & Bubeck-Wardenburg, J. (2011) A *Staphylococcus aureus* pore-forming toxin subverts the activity of ADAM10 to cause lethal infection in mice. *Nat Med,* **17,** 1310-1314.

Jackson, M. A., Burry, V. F. & Olson, L. C. (1992) Pyogenic arthritis associated with adjacent osteomyelitis: identification of the sequela-prone child. *Pediatr Infect Dis J,* **11,** 9-13.

Jackson, R. W. (1985) The septic knee--arthroscopic treatment. *Arthroscopy,* **1,** 194-197.

Jadin, K. D. (2005) Depth-varying density and organization of chondrocytes in immature and mature bovine articular cartilage assessed by 3D imaging and analysis. *J Histochem Cytochem,* **53,** 1109-1119.

Jalbert, I., Stapleton, F., Papas, E., Sweeney, D. F. & Coroneo, M. (2003) *In vivo* confocal microscopy of the human cornea. *Br J Ophthalmol,* **87,** 225-236.

Janzon, L. & Arvidson, S. (1990) The role of the delta-lysin gene (hld) in the regulation of virulence genes by the accessory gene regulator (agr) in *Staphylococcus aureus*. *EMBO J,* **9,** 1391-1399.

Jasin, H. E. (1983) Bacterial lipopolysaccharides induce in vitro degradation of cartilage matrix through chondrocyte activation. *J Clin Invest,* **72,** 2014-2019.

Jerosch, J., Hoffstetter, I., Schröder, M. & Castro, W. H. (1995) Septic arthritis: Arthroscopic management with local antibiotic treatment. *Acta Orthop Belg,* **61,** 126-134.

Jerry, G. J., Rand, J. A. & Ilstrup, D. (1988) Old sepsis prior to total knee arthroplasty. *Clin Orthop Relat Res***,** 135-140.

Johnson, J. A., Christie, M. J., Sandler, M. P., Parks, P. F., Homra, L. & Kaye, J. J. (1988) Detection of occult infection following total joint arthroplasty using sequential technetium-99m HDP bone scintigraphy and indium-111 WBC imaging. *J Nucl Med,* **29,** 1347-1353.

Jomha, N. M., Anoop, P. C., Elliott, J. a. W., Bagnall, K. & Mcgann, L. E. (2003) Validation and reproducibility of computerised cell-viability analysis of tissue slices. *BMC Musculoskelet Disord,* **4,** 5.

Jonas, D., Walev, I., Berger, T., Liebetrau, M., Palmer, M. & Bhakdi, S. (1994) Novel path to apoptosis: small transmembrane pores created by staphylococcal alpha-toxin in T lymphocytes evoke internucleosomal DNA degradation. *Infect Immun,* **62,** 1304-1312.

Jones, C., Smolinski, D., Keogh, A., Kirk, T. & Zheng, M. (2005) Confocal laser scanning microscopy in orthopaedic research. *Prog Histochem Cytochem,* **40,** 1-71.

Jones, K. H. & Senft, J. A. (1985) An improved method to determine cell viability by simultaneous staining with fluorescein diacetate-propidium iodide. *J Histochem Cytochem,* **33,** 77-79.

Jönsson, K., Signäs, C., Müller, H. P. & Lindberg, M. (1991) Two different genes encode fibronectin binding proteins in *Staphylococcus aureus*. The complete nucleotide sequence and characterization of the second gene. *Eur J Biochem,* **202,** 1041-1048.

Jouaville, L. S., Ichas, F., Holmuhamedov, E. L., Camacho, P. & Lechleiter, J. D. (1995) Synchronization of calcium waves by mitochondrial substrates in *Xenopus laevis* oocytes. *Nature,* **377,** 438-441.

Kaandorp, C. J., Dinant, H. J., Van De Laar, M. A., Moens, H. J., Prins, A. P. & Dijkmans, B. A. (1997a) Incidence and sources of native and prosthetic joint infection: a community based prospective survey. *Ann Rheum Dis,* **56,** 470-475.

Kaandorp, C. J., Krijnen, P., Moens, H. J., Habbema, J. D. & Van Schaardenburg, D. (1997b) The outcome of bacterial arthritis: a prospective community-based study. *Arthritis Rheum,* **40,** 884-892.

Kaatz, G. W., Mcaleese, F. & Seo, S. M. (2005) Multidrug resistance in *Staphylococcus aureus* due to overexpression of a novel multidrug and toxin extrusion (MATE) transport protein. *Antimicrob Agents Chemother,* **49,** 1857-1864.

Kaech, C., Elzi, L., Sendi, P., Frei, R., Laifer, G., Bassetti, S. & Fluckiger, U. (2006) Course and outcome of *Staphylococcus aureus* bacteraemia: a retrospective analysis of 308 episodes in a Swiss tertiary-care centre. *Clinical Microbiology and Infection,* **12,** 345-352.

Kahl, B., Herrmann, M., Everding, A. S., Koch, H. G., Becker, K., Harms, E., Proctor, R. A. & Peters, G. (1998) Persistent infection with small colony variant strains of *Staphylococcus aureus* in patients with cystic fibrosis. *J Infect Dis,* **177,** 1023-1029.

Kahl, B. C., Goulian, M., Van Wamel, W., Herrmann, M., Simon, S. M., Kaplan, G., Peters, G. & Cheung, A. L. (2000) *Staphylococcus aureus* RN6390 Replicates and Induces Apoptosis in a Pulmonary Epithelial Cell Line. *Infect Immun,* **68,** 5385-5392.

Kang, S.-W., Bada, L. P., Kang, C.-S., Lee, J.-S., Kim, C.-H., Park, J.-H. & Kim, B.-S. (2008) Articular cartilage regeneration with microfracture and hyaluronic acid. *Biotechnol. Lett.,* **30,** 435-439.

Karginov, V. A., Nestorovich, E. M., Schmidtmann, F., Robinson, T. M., Yohannes, A., Fahmi, N. E., Bezrukov, S. M. & Hecht, S. M. (2007) Inhibition of *S. aureus* alpha-hemolysin and *B. anthracis* lethal toxin by beta-cyclodextrin derivatives. *Bioorg Med Chem,* **15,** 5424-5431.

Katayama, Y., Baba, T., Sekine, M., Fukuda, M. & Hiramatsu, K. (2013) Beta-Hemolysin Promotes Skin Colonization by *Staphylococcus aureus*. *J Bacteriol,* **195,** 1194-1203.

Keinan-Adamsky, K., Shinar, H. & Navon, G. (2005) The effect of detachment of the articular cartilage from its calcified zone on the cartilage microstructure, assessed by 2H-spectroscopic double quantum filtered MRI. *J Orthop Res,* **23,** 109-117.

Kelly, I. P., Cunney, R. J., Smyth, E. G. & Colville, J. (1996) The management of human bite injuries of the hand. *Injury,* **27,** 481-484.

Kennedy, C. L., Smith, D. J., Lyras, D., Chakravorty, A. & Rood, J. I. (2009) Programmed cellular necrosis mediated by the pore-forming alpha-toxin from *Clostridium septicum*. *PLoS Pathogens,* **5,** e1000516.

Kielian, T., Cheung, A. & Hickey, W. F. (2001) Diminished virulence of an alpha-toxin mutant of *Staphylococcus aureus* in experimental brain abscesses. *Infect Immun,* **69,** 6902-6911.

Kim, C. S., Jeon, S. Y., Min, Y. G., Rhyoo, C., Kim, J. W., Yun, J. B., Park, S. W. & Kwon, T. Y. (2000) Effects of beta-toxin of *Staphylococcus aureus* on ciliary activity of nasal epithelial cells. *Laryngoscope,* **110,** 2085-2088.

Kiviranta, I., Jurvelin, J., Tammi, M., Säämänen, A. M. & Helminen, H. J. (1987) Weight bearing controls glycosaminoglycan concentration and articular cartilage thickness in the knee joints of young beagle dogs. *Arthritis Rheum,* **30,** 801-809.

Kiviranta, I., Tammi, M., Jurvelin, J., Säämänen, A. M. & Helminen, H. J. (1988) Moderate running exercise augments glycosaminoglycans and thickness of articular cartilage in the knee joint of young beagle dogs. *J Orthop Res,* **6,** 188-195.

Klaus, A. V., Kulasekera, V. L. & Schawaroch, V. (2003) Three-dimensional visualization of insect morphology using confocal laser scanning microscopy. *J Microsc,* **212,** 107-121.

Klinger, H.-M., Baums, M. H., Freche, S., Nusselt, T., Spahn, G. & Steckel, H. (2010) Septic arthritis of the shoulder joint: an analysis of management and outcome. *Acta Orthop Belg,* **76,** 598-603.

Klotman, M. E. & Chang, T. L. (2006) Defensins in innate antiviral immunity. *Nature Reviews Immunology,* **6,** 447-456.

Knapp, O., Maier, E., Mkaddem, S. B., Benz, R., Bens, M., Chenal, A., Geny, B., Vandewalle, A. & Popoff, M. R. (2010) *Clostridium septicum* alpha-toxin forms pores and induces rapid cell necrosis. *Toxicon,* **55,** 61-72.

Knight, M., Roberts, S., Lee, D. & Bader, D. (2003) Live cell imaging using confocal microscopy induces intracellular calcium transients and cell death. *Am J Physiol Cell Physiol,* **284,** C1083-C1089.

Kohanski, M. A., Dwyer, D. J. & Collins, J. J. (2010) How antibiotics kill bacteria: from targets to networks. *Nat Rev Microbiol,* **8,** 423-435.

Korhonen, R. K., Wong, M., Arokoski, J., Lindgren, R., Helminen, H. J., Hunziker, E. B. & Jurvelin, J. S. (2002) Importance of the superficial tissue layer for the indentation stiffness of articular cartilage. *Med Eng Phys,* **24,** 99-108.

Koschinski, A., Repp, H., Unver, B., Dreyer, F., Brockmeier, D., Valeva, A., Bhakdi, S. & Walev, I. (2006) Why Escherichia coli alpha-hemolysin induces calcium oscillations in mammalian cells- the pore is on its own. *FASEB J,* **20,** 973-975.

Kreger, A. S., Kim, K. S., Zaboretzky, F. & Bernheimer, A. W. (1971) Purification and properties of *staphylococcal* delta hemolysin. *Infect Immun,* **3,** 449-465.

Krieg, A. M. (1999) A possible cause of joint destruction in septic arthritis. *Arthritis Res Ther,* **1,** 3-4.

Krishan, A. (1975) Rapid flow cytofluorometric analysis of mammalian cell cycle by propidium iodide staining. *J Cell Biol,* **66,** 188-193.

Kristian, T. & Siesjo, B. K. (1998) Calcium in Ischemic Cell Death. *Stroke,* **29,** 705-718.

Kurebayashi, N., Harkins, A. B. & Baylor, S. M. (1993) Use of fura red as an intracellular calcium indicator in frog skeletal muscle fibers. *Biophys J,* **64,** 1934-1960.

Kwak, Y.-K., Vikström, E., Magnusson, K.-E., Vécsey-Semjén, B., Colque-Navarro, P. & Möllby, R. (2012) The *Staphylococcus aureus* alpha-toxin perturbs the barrier function in Caco-2 epithelial cell monolayers by altering junctional integrity. *Infect Immun,* **80,** 1670-1680.

Lammers, A., Nuijten, P. J. & Smith, H. E. (1999) The fibronectin binding proteins of *Staphylococcus aureus* are required for adhesion to and invasion of bovine mammary gland cells. *FEMS Microbiol Lett,* **180,** 103-109.

Lane, J. G., Falahee, M. H., Wojtys, E. M., Hankin, F. M. & Kaufer, H. (1990) Pyarthrosis of the knee. Treatment considerations. *Clin Orthop Relat Res***,** 198-204.

Lane, S. E. (2000) Intra-articular corticosteroids in septic arthritis: beneficial or barmy? *Ann Rheum Dis,* **59,** 240.

Lavy, C. B. D. (2007) Septic arthritis in Western and sub-Saharan African children - a review. *Int Orthop,* **31,** 137-144.

Lee, M. S., Ueng, S. W., Shih, C. H. & Chao, C. C. (2001) Primary cultures of human chondrocytes are susceptible to low inocula of *Staphylococcus aureus* infection and undergo apoptosis. *Scand J Infect Dis,* **33,** 47-50.

Lefevre, S., Ruimy, D., Jehl, F., Neuville, A., Robert, P., Sordet, C., Ehlinger, M., Dietemann, J.-L. & Bierry, G. (2011) Septic arthritis: monitoring with USPIO-enhanced macrophage MR imaging. *Radiology,* **258,** 722-728.

Lehrer, R. I. (2004) Primate defensins. *Nat Rev Microbiol,* **2,** 727-738.

Leroux, M. A., Arokoski, J., Vail, T. P., Guilak, F., Hyttinen, M. M., Kiviranta, I. & Setton, L. A. (2000) Simultaneous changes in the mechanical properties, quantitative collagen organization, and proteoglycan concentration of articular cartilage following canine meniscectomy. *J Orthop Res,* **18,** 383-392.

Levene, S. D. & Zimm, B. H. (1987) Separations of open-circular DNA using pulsed-field electrophoresis. *Proc Natl Acad Sci U S A,* **84,** 4054-4057.

Levine, M. & Siegel, L. B. (2003) A swollen joint: why all the fuss? *Am J Ther,* **10,** 219-224.

Lewis, J. L., Deloria, L. B., Oyen-Tiesma, M., Thompson, R. C., Ericson, M. & Oegema, T. R. (2003) Cell death after cartilage impact occurs around matrix cracks. *J Orthop Res,* **21,** 881-887.

Li, S. F. (2004) Laboratory Tests in Adults with Monoarticular Arthritis: Can They Rule Out a Septic Joint? *Acad Emerg Med,* **11,** 276-280.

Lin, G., Bjornsson, C. S., Smith, K. L., Abdul-Karim, M.-A., Turner, J. N., Shain, W. & Roysam, B. (2005) Automated image analysis methods for 3-D quantification of the neurovascular unit from multichannel confocal microscope images. *Cytometry,* **66A,** 9-23.

Lina, G., Piémont, Y., Godail-Gamot, F., Bes, M., Peter, M. O., Gauduchon, V., Vandenesch, F. & Etienne, J. (1999) Involvement of Panton-Valentine leukocidin-producing Staphylococcus aureus in primary skin infections and pneumonia. *Clin Infect Dis,* **29,** 1128-1132.

Linn, F. C. & Sokoloff, L. (1965) Movement and composition of interstitial fluid of cartilage. *Arthritis Rheum,* **8,** 481-494.

Lipinska, U., Hermans, K., Meulemans, L., Dumitrescu, O., Badiou, C., Duchateau, L., Haesebrouck, F., Etienne, J. & Lina, G. (2011) Panton-Valentine leukocidin does play a role in the early stage of *Staphylococcus aureus* skin infections: a rabbit model. *Plos One,* **6,** e22864.

Liu, C. & Hermann, T. E. (1978) Characterization of ionomycin as a calcium ionophore. *J Biol Chem,* **253,** 5892-5894.

Liu, P. Y., Shi, Z. Y., Lau, Y. J., Hu, B. S., Shyr, J. M., Tsai, W. S., Lin, Y. H. & Tseng, C. Y. (1996) Use of restriction endonuclease analysis of plasmids and pulsed-field gel electrophoresis to investigate outbreaks of methicillin-resistant *Staphylococcus aureus* infection. *Clin Infect Dis,* **22,** 86-90.

Loeser, R. F. (2000) Chondrocyte integrin expression and function. *Biorheology,* **37,** 109-116.

Loeser, R. F. (2002) Integrins and cell signaling in chondrocytes. *Biorheology,* **39,** 119-124.

Lohmander, L. S., Saxne, T. & Heinegård, D. K. (1994) Release of cartilage oligomeric matrix protein (COMP) into joint fluid after knee injury and in osteoarthritis. *Ann Rheum Dis,* **53,** 8-13.

Loret, B. & Simões, F. M. F. (2004) Articular cartilage with intra- and extrafibrillar waters: a chemo-mechanical model. *Mechanics of Materials,* **36,** 515-541.

Lotz, M. M., Burdsal, C. A., Erickson, H. P. & Mcclay, D. R. (1989) Cell adhesion to fibronectin and tenascin: quantitative measurements of initial binding and subsequent strengthening response. *J Cell Biol,* **109,** 1795-1805.

Lowy, F. D. (1998) *Staphylococcus aureus* infections. *N Engl J Med,* **339,** 520-532.

Lowy, F. D. (2003) Antimicrobial resistance: the example of *Staphylococcus aureus*. *J Clin Invest,* **111,** 1265-1273.

Luhmann, J. D. & Luhmann, S. J. (1999) Etiology of septic arthritis in children: an update for the 1990s. *Pediatr Emerg Care,* **15,** 40-42.

Luong, T. T. & Lee, C. Y. (2002) Overproduction of type 8 capsular polysaccharide augments *Staphylococcus aureus* virulence. *Infect Immun,* **70,** 3389-3395.

Lupetti, A., Welling, M. M., Pauwels, E. K. & Nibbering, P. H. (2003) Radiolabelled antimicrobial peptides for infection detection. *Lancet Infect Dis,* **3,** 223-229.

Madden, R. M. J., Han, S.-K. & Herzog, W. (2014) The effect of compressive loading magnitude on in situ chondrocyte calcium signaling. *Biomech Model Mechanobiol*.

Malgaroli, A., Milani, D., Meldolesi, J. & Pozzan, T. (1987) Fura-2 measurement of cytosolic free Ca2+ in monolayers and suspensions of various types of animal cells. *J Cell Biol,* **105,** 2145-2155.

Malinin, T. & Ouellette, E. A. (2000) Articular cartilage nutrition is mediated by subchondral bone: a long-term autograft study in baboons. *Osteoarthritis Cartilage,* **8,** 483-491.

Manadan, A. M. & Block, J. A. (2004) Daily needle aspiration versus surgical lavage for the treatment of bacterial septic arthritis in adults. *Am J Ther,* **11,** 412-415.

Mankin, H. J. (1982) The response of articular cartilage to mechanical injury. *J Bone Joint Surg Am,* **64,** 460-466.

Mansfield, J., Yu, J., Attenburrow, D., Moger, J., Tirlapur, U., Urban, J., Cui, Z. & Winlove, P. (2009) The elastin network: its relationship with collagen and cells in articular cartilage as visualized by multiphoton microscopy. *J Anat,* **215,** 682-691.

Maroudas, A., Bayliss, M. T., Uchitel-Kaushansky, N., Schneiderman, R. & Gilav, E. (1998) Aggrecan turnover in human articular cartilage: use of aspartic acid racemization as a marker of molecular age. *Arch Biochem Biophys,* **350,** 61-71.

Mascia, F., Denning, M., Kopan, R. & Yuspa, S. H. (2012) The black box illuminated: signals and signaling. *J Invest Dermatol,* **132,** 811-819.

Mateo Soria, L., Olivé Marqués, A., García Casares, E., García Melchor, E., Holgado Pérez, S. & Tena Marsà, X. (2009) Polyarticular septic arthritis: analysis of 19 cases. *Reumatol Clin,* **5,** 18-22.

Mathews, C. J., Kingsley, G., Field, M., Jones, A., Weston, V. C., Phillips, M., Walker, D. & Coakley, G. (2008) Management of septic arthritis: a systematic review. *Postgrad Med J,* **84,** 265-270.

Mathews, C. J., Weston, V. C., Jones, A., Field, M. & Coakley, G. (2010) Bacterial septic arthritis in adults. *Lancet,* **375,** 846-855.

Matsuzaki, K. (1999) Why and how are peptide-lipid interactions utilized for self-defense? Magainins and tachyplesins as archetypes. *Biochim Biophys Acta,* **1462,** 1-10.

Mcadam, P. R., Holmes, A., Templeton, K. E. & Fitzgerald, J. R. (2011) Adaptive evolution of *Staphylococcus aureus* during chronic endobronchial infection of a cystic fibrosis patient. *Plos One,* **6,** e24301.

Mccormick, C. C., Caballero, A. R., Balzli, C. L., Tang, A. & O'callaghan, R. J. (2009) Chemical inhibition of alpha-toxin, a key corneal virulence factor of *Staphylococcus aureus*. *Invest Ophthalmol Vis Sci,* **50,** 2848-2854.

Mcgann, L. E., Stevenson, M., Muldrew, K. & Schachar, N. (1988) Kinetics of osmotic water movement in chondrocytes isolated from articular cartilage and applications to cryopreservation. *J Orthop Res,* **6,** 109-115.

Mcgavin, M. H., Krajewska-Pietrasik, D., Ryden, C. & Höök, M. (1993) Identification of a *Staphylococcus aureus* extracellular matrix-binding protein with broad specificity. *Infect Immun,* **61,** 2479-2485.

Menestrina, G., Dalla Serra, M., Comai, M., Coraiola, M., Viero, G., Werner, S., Colin, D. A., Monteil, H. & Prévost, G. (2003) Ion channels and bacterial infection: the case of beta-barrel pore-forming protein toxins of *Staphylococcus aureus*. *FEBS Lett,* **552,** 54-60.

Menzies, B. E. & Kourteva, I. (1998) Internalization of *Staphylococcus aureus* by endothelial cells induces apoptosis. *Infect Immun,* **66,** 5994-5998.

Miller, L. G., Perdreau-Remington, F., Rieg, G., Mehdi, S., Perlroth, J., Bayer, A. S., Tang, A. W., Phung, T. O. & Spellberg, B. (2005) Necrotizing fasciitis caused by community-associated methicillin-resistant *Staphylococcus aureus* in Los Angeles. *N Engl J Med,* **352,** 1445-1453.

Millward-Sadler, S. J. & Salter, D. M. (2004) Integrin-dependent signal cascades in chondrocyte mechanotransduction. *Ann Biomed Eng,* **32,** 435-446.

Mollenhauer, J., Bee, J. A., Lizarbe, M. A. & Von Der Mark, K. (1984) Role of anchorin CII, a 31,000-mol-wt membrane protein, in the interaction of chondrocytes with type II collagen. *J Cell Biol,* **98,** 1572-1579.

Molyneux, E. & French, G. (1982) *Salmonella* joint infection in Malawian children. *J Infect,* **4,** 131-138.

Monecke, S., Müller, E., Buechler, J., Rejman, J., Stieber, B., Akpaka, P. E., Bandt, D., Burris, R., Coombs, G., Hidalgo-Arroyo, G. A., Hughes, P., Kearns, A., Abós, S. M., Pichon, B., Skakni, L., Söderquist, B. & Ehricht, R. (2013) Rapid detection of Panton-Valentine leukocidin in *Staphylococcus aureus* cultures by use of a lateral flow assay based on monoclonal antibodies. *J Clin Microbiol,* **51,** 487-495.

Moo, E. K., Abu Osman, N. A. & Pingguan-Murphy, B. (2011) The metabolic dynamics of cartilage explants over a long-term culture period. *Clinics,* **66,** 1431-1436.

Moreillon, P., Entenza, J. M., Francioli, P., Mcdevitt, D., Foster, T. J., François, P. & Vaudaux, P. (1995) Role of *Staphylococcus aureus* coagulase and clumping factor in pathogenesis of experimental endocarditis. *Infect Immun,* **63,** 4738-4743.

Morgan, A. J. & Jacob, R. (1994) Ionomycin enhances Ca2+ influx by stimulating store-regulated cation entry and not by a direct action at the plasma membrane. *Biochem J,* **300 (Pt 3),** 665-672.

Morgan, D. S., Fisher, D., Merianos, A. & Currie, B. J. (1996) An 18 year clinical review of septic arthritis from tropical Australia. *Epidemiol Infect,* **117,** 423-428.

Morotomi-Yano, K., Akiyama, H. & Yano, K.-I. (2014) Different involvement of extracellular calcium in two modes of cell death induced by nanosecond pulsed electric fields. *Arch Biochem Biophys,* **555-556,** 47-54.

Mortimer, R. K. & Schild, D. (1985) Genetic map of *Saccharomyces cerevisiae*, edition 9. *Microbiol Rev,* **49,** 181-213.

Mow, V. C. & Guo, X. E. (2002) Mechano-electrochemical properties of articular cartilage: their inhomogeneities and anisotropies. *Annu Rev Biomed Eng,* **4,** 175-209.

Mow, V. C., Holmes, M. H. & Lai, W. M. (1984) Fluid transport and mechanical properties of articular cartilage: a review. *J Biomech,* **17,** 377-394.

Muir, H. (1995) The chondrocyte, architect of cartilage. Biomechanics, structure, function and molecular biology of cartilage matrix macromolecules. *Bioessays,* **17,** 1039-1048.

Murchan, S., Kaufmann, M. E., Deplano, A., De Ryck, R., Struelens, M., Zinn, C. E., Fussing, V., Salmenlinna, S., Vuopio-Varkila, J., El Solh, N., Cuny, C., Witte, W., Tassios, P. T., Legakis, N., Van Leeuwen, W., Van Belkum, A., Vindel, A., Laconcha, I., Garaizar, J., Haeggman, S., Olsson-Liljequist, B., Ransjo, U., Coombes, G. & Cookson, B. (2003) Harmonization of pulsed-field gel electrophoresis protocols for epidemiological typing of strains of methicillin-resistant *Staphylococcus aureus*: a single approach developed by consensus in 10 European laboratories and its application for tracing the spread of related strains. *J Clin Microbiol,* **41,** 1574-1585.

Nade, S. (2003) Septic arthritis. *Best Pract Res Clin Rheumatol,* **17,** 183-200.

Nduati, R. W. & Wamola, I. A. (1991) Bacteriology of acute septic arthritis. *J Trop Pediatr,* **37,** 172-175.

Neher, E. & Augustine, G. J. (1992) Calcium gradients and buffers in bovine chromaffin cells. *J Physiol (Lond),* **450,** 273-301.

Nilsson, I.-M., Hartford, O., Foster, T. & Tarkowski, A. (1999) Alpha-toxin and gamma-toxin jointly promote *Staphylococcus aureus* virulence in murine septic arthritis. *Infect Immun,* **67,** 1045-1049.

Nilsson, I. M., Lee, J. C., Bremell, T., Ryden, C. & Tarkowski, A. (1997) The role of *staphylococcal* polysaccharide microcapsule expression in septicemia and septic arthritis. *Infect Immun,* **65,** 4216-4221.

Noble, W. C., Valkenburg, H. A. & Wolters, C. H. (1967) Carriage of *Staphylococcus aureus* in random samples of a normal population. *J Hyg (Lond),* **65,** 567-573.

North, A. J. (2006) Seeing is believing? A beginner's guide to practical pitfalls in image acquisition. *J Cell Biol,* **172,** 9-18.

Novick, R. (1967) Properties of a cryptic high-frequency transducing phage in *Staphylococcus aureus*. *Virology,* **33,** 155-166.

Nunn, T. R., Cheung, W. Y. & Rollinson, P. D. (2007) A prospective study of pyogenic sepsis of the hip in childhood. *J Bone Joint Surg Br,* **89,** 100-106.

Nwaneshiudu, A., Kuschal, C., Sakamoto, F. H., Anderson, R. R., Schwarzenberger, K. & Young, R. C. (2012) Introduction to confocal microscopy. *J Invest Dermatol,* **132,** e3.

O'callaghan, R. J., Callegan, M. C., Moreau, J. M., Green, L. C., Foster, T. J., Hartford, O. M., Engel, L. S. & Hill, J. M. (1997) Specific roles of alpha-toxin and beta-toxin during *Staphylococcus aureus* corneal infection. *Infect Immun,* **65,** 1571-1578.

O'reilly, M., De Azavedo, J. C., Kennedy, S. & Foster, T. J. (1986) Inactivation of the alpha-haemolysin gene of *Staphylococcus aureus* 8325-4 by site-directed mutagenesis and studies on the expression of its haemolysins. *Microb Pathog,* **1,** 125-138.

O'riordan, K. & Lee, J. C. (2004) *Staphylococcus aureus* capsular polysaccharides. *Clin Microbiol Rev,* **17,** 218-234.

Ochiai, T. (2001) Staphylococcus aureus requires increased level of Ca(2+) or Mn(2+) to grow normally in a high-NaCl/low-Mg(2+) medium. *Microbiol Immunol,* **45,** 769-776.

Oldberg, A., Antonsson, P., Lindblom, K. & Heinegård, D. (1989) A collagen-binding 59-kd protein (fibromodulin) is structurally related to the small interstitial proteoglycans PG-S1 and PG-S2 (decorin). *EMBO J,* **8,** 2601-2604.

Olney, B. W., Papasian, C. J. & Jacobs, R. R. (1987) Risk of iatrogenic septic arthritis in the presence of bacteremia: a rabbit study. *J Pediatr Orthop,* **7,** 524-526.

Onoda, T., Enokizono, J., Kaya, H., Oshima, A., Freestone, P. & Norris, V. (2000) Effects of calcium and calcium chelators on growth and morphology of *Escherichia coli* L-form NC-7. *J Bacteriol,* **182,** 1419-1422.

Onogawa, T. (2002) *Staphylococcal* alpha-toxin synergistically enhances inflammation caused by bacterial components. *FEMS Immunol Med Microbiol,* **33,** 15-21.

Osiri, M., Ruxrungtham, K., Nookhai, S., Ohmoto, Y. & Deesomchok, U. (1998) IL-1beta, IL-6 and TNF-alpha in synovial fluid of patients with non-*gonococcal* septic arthritis. *Asian Pac J Allergy Immunol,* **16,** 155-160.

Palmoski, M., Perricone, E. & Brandt, K. D. (1979) Development and reversal of a proteoglycan aggregation defect in normal canine knee cartilage after immobilization. *Arthritis Rheum,* **22,** 508-517.

Palmqvist, N., Josefsson, E. & Tarkowski, A. (2004) Clumping factor A-mediated virulence during *Staphylococcus aureus* infection is retained despite fibrinogen depletion. *Microbes Infect,* **6,** 196-201.

Pankey, G. A. & Sabath, L. D. (2004) Clinical relevance of bacteriostatic versus bactericidal mechanisms of action in the treatment of Gram-positive bacterial infections. *Clin Infect Dis,* **38,** 864-870.

Papadimitriou, J. C., Phelps, P. C., Shin, M. L., Smith, M. W. & Trump, B. F. (1994) Effects of Ca2+ deregulation on mitochondrial membrane potential and cell viability in nucleated cells following lytic complement attack. *Cell Calcium,* **15,** 217-227.

Paredes, R. M., Etzler, J. C., Watts, L. T., Zheng, W. & Lechleiter, J. D. (2008) Chemical calcium indicators. *Methods,* **46,** 143-151.

Park, S., Krishnan, R., Nicoll, S. B. & Ateshian, G. A. (2003) Cartilage interstitial fluid load support in unconfined compression. *J Biomech,* **36,** 1785-1796.

Patel, A. H., Nowlan, P., Weavers, E. D. & Foster, T. (1987) Virulence of protein A-deficient and alpha-toxin-deficient mutants of *Staphylococcus aureus* isolated by allele replacement. *Infect Immun,* **55,** 3103-3110.

Patrauchan, M. A. (2005) Calcium influences cellular and extracellular product formation during biofilm-associated growth of a marine *Pseudoalteromonas sp*. *Microbiology,* **151,** 2885-2897.

Patti, J. M., Jonsson, H., Guss, B., Switalski, L. M., Wiberg, K., Lindberg, M. & Höök, M. (1992) Molecular characterization and expression of a gene encoding a *Staphylococcus aureus* collagen adhesin. *J Biol Chem,* **267,** 4766-4772.

Pearle, A. D., Warren, R. F. & Rodeo, S. A. (2005) Basic science of articular cartilage and osteoarthritis. *Clin Sports Med,* **24,** 1-12.

Pecze, L., Blum, W. & Schwaller, B. (2013) Mechanism of capsaicin receptor TRPV1-mediated toxicity in pain-sensing neurons focusing on the effects of Na(+)/Ca(2+) fluxes and the Ca(2+)-binding protein calretinin. *Biochim Biophys Acta,* **1833,** 1680-1691.

Pedersen, D. R., Goetz, J. E., Kurriger, G. L. & Martin, J. A. (2013) Comparative digital cartilage histology for human and common osteoarthritis models. *Orthop Res Rev,* **2013,** 13-20.

Peltola, H., Kallio, M. J. & Unkila-Kallio, L. (1998) Reduced incidence of septic arthritis in children by *Haemophilus influenzae* type-b vaccination. Implications for treatment. *J Bone Joint Surg Br,* **80,** 471-473.

Pennington, H. (2010) *Escherichia coli* O157. *Lancet,* **376,** 1428-1435.

Pérez-Alvarez, A., Araque, A. & Martín, E. D. (2013) Confocal microscopy for astrocyte *in vivo* imaging: Recycle and reuse in microscopy. *Front Cell Neurosci,* **7,** 51.

Perron, A. D., Miller, M. D. & Brady, W. J. (2002) Orthopedic pitfalls in the ED: fight bite. *Am J Emerg Med,* **20,** 114-117.

Peters, B. M., Shirtliff, M. E. & Jabra-Rizk, M. A. (2010) Antimicrobial peptides: primeval molecules or future drugs? *PLoS Pathogens,* **6,** e1001067.

Petersen, C. C., Petersen, O. H. & Berridge, M. J. (1993) The role of endoplasmic reticulum calcium pumps during cytosolic calcium spiking in pancreatic acinar cells. *J Biol Chem,* **268,** 22262-22264.

Petersen, O. H., Petersen, C. C. & Kasai, H. (1994) Calcium and hormone action. *Annu Rev Physiol,* **56,** 297-319.

Poole, A. R., Rosenberg, L. C., Reiner, A., Ionescu, M., Bogoch, E. & Roughley, P. J. (1996) Contents and distributions of the proteoglycans decorin and biglycan in normal and osteoarthritic human articular cartilage. *J Orthop Res,* **14,** 681-689.

Poole, C. A. (1997) Articular cartilage chondrons: form, function and failure. *J Anat,* **191,** 1-13.

Poole, C. A., Ayad, S. & Gilbert, R. T. (1992) Chondrons from articular cartilage. V. Immunohistochemical evaluation of type VI collagen organisation in isolated chondrons by light, confocal and electron microscopy. *J Cell Sci,* **103 (Pt 4),** 1101-1110.

Poole, C. A., Flint, M. H. & Beaumont, B. W. (1984) Morphological and functional interrelationships of articular cartilage matrices. *J Anat,* **138,** 113-138.

Powers, M. E., Kim, H. K., Wang, Y. & Bubeck-Wardenburg, J. (2012) ADAM10 mediates vascular injury induced by *Staphylococcus aureus* α-hemolysin. *J Infect Dis,* **206,** 352-356.

Prévost, G., Couppie, P., Prevost, P., Gayet, S., Petiau, P., Cribier, B., Monteil, H. & Piémont, Y. (1995) Epidemiological data on *Staphylococcus aureus* strains producing synergohymenotropic toxins. *J Med Microbiol,* **42,** 237-245.

Proctor, R. A. & Peters, G. (1998) Small colony variants in *staphylococcal* infections: diagnostic and therapeutic implications. *Clin Infect Dis,* **27,** 419-422.

Proctor, R. A., Van Langevelde, P., Kristjansson, M., Maslow, J. N. & Arbeit, R. D. (1995) Persistent and relapsing infections associated with small-colony variants of Staphylococcus aureus. *Clin Infect Dis,* **20,** 95-102.

Projan, S. J., Kornblum, J., Kreiswirth, B., Moghazeh, S. L., Eisner, W. & Novick, R. P. (1989) Nucleotide sequence: the beta-hemolysin gene of *Staphylococcus aureus*. *Nucleic Acids Res,* **17,** 3305.

Prunier, A.-L., Malbruny, B., Laurans, M., Brouard, J., Duhamel, J.-F. & Leclercq, R. (2003) High rate of macrolide resistance in *Staphylococcus aureus* strains from patients with cystic fibrosis reveals high proportions of hypermutable strains. *J Infect Dis,* **187,** 1709-1716.

Puliti, M., Von Hunolstein, C., Bistoni, F., Mosci, P., Orefici, G. & Tissi, L. (2002) The beneficial effect of interleukin-12 on arthritis induced by group B *streptococci* is mediated by interferon-gamma and interleukin-10 production. *Arthritis Rheum,* **46,** 806-817.

Ragle, B. E. & Bubeck-Wardenburg, J. (2009) Anti-alpha-hemolysin monoclonal antibodies mediate protection against *Staphylococcus aureus* pneumonia. *Infect Immun,* **77,** 2712-2718.

Ragle, B. E., Karginov, V. A. & Bubeck-Wardenburg, J. (2010) Prevention and treatment of *Staphylococcus aureus* pneumonia with a beta-cyclodextrin derivative. *Antimicrob Agents Chemother,* **54,** 298-304.

Rajadhyaksha, M., Grossman, M., Esterowitz, D., Webb, R. H. & Anderson, R. R. (1995) *In vivo* confocal scanning laser microscopy of human skin: melanin provides strong contrast. *J Invest Dermatol,* **104,** 946-952.

Ravindran, V., Logan, I. & Bourke, B. E. (2009) Medical vs surgical treatment for the native joint in septic arthritis: a 6-year, single UK academic centre experience. *Rheumatology (Oxford),* **48,** 1320-1322.

Riegels-Nielsen, P., Frimodt-Möller, N., Sørensen, M. & Jensen, J. S. (1989) Antibiotic treatment insufficient for established septic arthritis. *Staphylococcus aureus* experiments in rabbits. *Acta Orthop Scand,* **60,** 113-115.

Riegels-Nielson, P., Frimodt-Möller, N. & Jensen, J. S. (1987) Rabbit model of septic arthritis. *Acta Orthop Scand,* **58,** 14-19.

Roberts, S., Weightman, B., Urban, J. & Chappell, D. (1986a) Mechanical and biochemical properties of human articular cartilage from the femoral head after subcapital fracture. *J Bone Joint Surg Br,* **68,** 418-422.

Roberts, S., Weightman, B., Urban, J. & Chappell, D. (1986b) Mechanical and biochemical properties of human articular cartilage in osteoarthritic femoral heads and in autopsy specimens. *J Bone Joint Surg Br,* **68,** 278-288.

Rogers, B. A., Murphy, C. L., Cannon, S. R. & Briggs, T. W. R. (2006) Topographical variation in glycosaminoglycan content in human articular cartilage. *J Bone Joint Surg Br,* **88,** 1670-1674.

Roghmann, M., Taylor, K. L., Gupte, A., Zhan, M., Johnson, J. A., Cross, A., Edelman, R. & Fattom, A. I. (2005) Epidemiology of capsular and surface polysaccharide in *Staphylococcus aureus* infections complicated by bacteraemia. *J Hosp Infect,* **59,** 27-32.

Rosenbloom, J. (1996) Molecular Cloning and Expression of the Gene for Elastin-binding Protein (ebpS) in *Staphylococcus aureus*. *J Biol Chem,* **271,** 15803-15809.

Roughley, P. J. (2001) Articular cartilage and changes in arthritis: noncollagenous proteins and proteoglycans in the extracellular matrix of cartilage. *Arthritis Res,* **3,** 342-347.

Roughley, P. J. (2006) The structure and function of cartilage proteoglycans. *Eur Cell Mater,* **12,** 92-101.

Roughley, P. J., Rodriguez, E. & Lee, E. R. (1995) The interactions of 'non-aggregating' proteoglycans. *Osteoarthritis Cartilage,* **3,** 239-248.

Ryan, M., Kavanagh, R., Wall, P. & Hazleman, B. (1997) Bacterial joint infections in England and Wales: Analysis of bacterial isolates over a four year period. *Br J Rheumatol,* **36,** 370-373.

Saeed, S., Zafar, J., Khan, B., Akhtar, A., Qurieshi, S., Fatima, S., Ahmad, N. & Irfanullah, J. (2013) Utility of 99mTc-labelled antimicrobial peptide ubiquicidin (29-41) in the diagnosis of diabetic foot infection. *European Journal of Nuclear Medicine and Molecular Imaging,* **40,** 737-743.

Salter, D. M., Godolphin, J. L. & Gourlay, M. S. (1995) Chondrocyte heterogeneity: immunohistologically defined variation of integrin expression at different sites in human fetal knees. *J Histochem Cytochem,* **43,** 447-457.

Salter, R. B., Bell, R. S. & Keeley, F. W. (1981) The protective effect of continuous passive motion in living articular cartilage in acute septic arthritis: an experimental investigation in the rabbit. *Clin Orthop Relat Res***,** 223-247.

Sánchez, J. C., Danks, T. A. & Wilkins, R. J. (2003) Mechanisms involved in the increase in intracellular calcium following hypotonic shock in bovine articular chondrocytes. *Gen Physiol Biophys,* **22,** 487-500.

Sánchez, J. C., Powell, T., Staines, H. M. & Wilkins, R. J. (2006) Electrophysiological demonstration of Na+/Ca2+ exchange in bovine articular chondrocytes. *Biorheology,* **43,** 83-94.

Sarkisova, S., Patrauchan, M. A., Berglund, D., Nivens, D. E. & Franklin, M. J. (2005) Calcium-induced virulence factors associated with the extracellular matrix of mucoid *Pseudomonas aeruginosa* biofilms. *J Bacteriol,* **187,** 4327-4337.

Sasaki, S., Nishikawa, S., Miura, T., Mizuki, M., Yamada, K., Madarame, H., Tagawa, Y. I., Iwakura, Y. & Nakane, A. (2000) Interleukin-4 and interleukin-10 are involved in host resistance to *Staphylococcus aureus* infection through regulation of gamma interferon. *Infect Immun,* **68,** 2424-2430.

Saxne, T. & Heinegård, D. (1992) Cartilage oligomeric matrix protein: a novel marker of cartilage turnover detectable in synovial fluid and blood. *Br J Rheumatol,* **31,** 583-591.

Schattner, A. & Vosti, K. L. (1998) Bacterial arthritis due to beta-hemolytic *streptococci* of serogroups A, B, C, F, and G. Analysis of 23 cases and a review of the literature. *Medicine (Baltimore),* **77,** 122-139.

Schinagl, R. M., Gurskis, D., Chen, A. C. & Sah, R. L. (1997) Depth-dependent confined compression modulus of full-thickness bovine articular cartilage. *J Orthop Res,* **15,** 499-506.

Schmitz, F. J., Veldkamp, K. E., Van Kessel, K. P., Verhoef, J. & Van Strijp, J. A. (1997) Delta-toxin from *Staphylococcus aureus* as a costimulator of human neutrophil oxidative burst. *J Infect Dis,* **176,** 1531-1537.

Schwartz, D. C. & Cantor, C. R. (1984) Separation of yeast chromosome-sized DNAs by pulsed field gradient gel electrophoresis. *Cell,* **37,** 67-75.

Seara, J. V., T, B., H, S. & J, E. (2002) Arthroscopic treatment of septic joints: prognostic factors. *Arch Orthop Trauma Surg,* **122,** 204-211.

Seeger, W., Bauer, M. & Bhakdi, S. (1984) *Staphylococcal* alpha-toxin elicits hypertension in isolated rabbit lungs. Evidence for thromboxane formation and the role of extracellular calcium. *J Clin Invest,* **74,** 849-858.

Semwogerere, D. & Weeks, E. R. 2008. Confocal microscopy. *In:* Wnek, G. E. & Bowlin, G. L. (eds.) *Encyclopedia of Biomaterials and Biomedical Engineering* 2nd ed. New York: Informa Healthcare, USA, Inc., 705-714.

Shai, Y. (1999) Mechanism of the binding, insertion and destabilization of phospholipid bilayer membranes by alpha-helical antimicrobial and cell non-selective membrane-lytic peptides. *Biochim Biophys Acta,* **1462,** 55-70.

Shai, Y. (2002) From innate immunity to de-novo designed antimicrobial peptides. *Curr Pharm Des,* **8,** 715-725.

Sharif, M., Saxne, T., Shepstone, L., Kirwan, J. R., Elson, C. J., Heinegård, D. & Dieppe, P. A. (1995) Relationship between serum cartilage oligomeric matrix protein levels and disease progression in osteoarthritis of the knee joint. *Br J Rheumatol,* **34,** 306-310.

Sharp, J. C., Ritchie, L. D., Curnow, J. & Reid, T. M. (1994) High incidence of haemorrhagic colitis due to *Escherichia coli* O157 in one Scottish town: clinical and epidemiological features. *J Infect,* **29,** 343-350.

Shetty, A. K. & Gedalia, A. (2004) Management of septic arthritis. *Indian J Pediatr,* **71,** 819-824.

Shirtliff, M. E. & Mader, J. T. (2002) Acute septic arthritis. *Clin Microbiol Rev,* **15,** 527-544.

Siczkowski, M. & Watt, F. M. (1990) Subpopulations of chondrocytes from different zones of pig articular cartilage. Isolation, growth and proteoglycan synthesis in culture. *J Cell Sci,* **97 (Pt 2),** 349-360.

Simon, W. H., Richardson, S., Herman, W., Parsons, J. R. & Lane, J. (1976) Long-term effects of chondrocyte death on rabbit articular cartilage *in vivo*. *J Bone Joint Surg Am,* **58,** 517-526.

Simpkin, V. L., Murray, D. H., Hall, A. P. & Hall, A. C. (2007) Bicarbonate-dependent pH(i) regulation by chondrocytes within the superficial zone of bovine articular cartilage. *J Cell Physiol,* **212,** 600-609.

Siqueira, J. A., Speeg-Schatz, C., Freitas, F. I., Sahel, J., Monteil, H. & Prévost, G. (1997) Channel-forming leucotoxins from *Staphylococcus aureus* cause severe inflammatory reactions in a rabbit eye model. *J Med Microbiol,* **46,** 486-494.

Slowman, S. D. & Brandt, K. D. (1986) Composition and glycosaminoglycan metabolism of articular cartilage from habitually loaded and habitually unloaded sites. *Arthritis Rheum,* **29,** 88-94.

Smith, M. W., Phelps, P. C. & Trump, B. F. (1991) Cytosolic Ca2+ deregulation and blebbing after HgCl2 injury to cultured rabbit proximal tubule cells as determined by digital imaging microscopy. *Proc Natl Acad Sci U S A,* **88,** 4926-4930.

Smith, M. W., Phelps, P. C. & Trump, B. F. (1992) Injury-induced changes in cytosolic Ca2+ in individual rabbit proximal tubule cells. *Am J Physiol,* **262,** F647-55.

Smith, R. L. & Schurman, D. J. (1983) Comparison of cartilage destruction between infectious and adjuvant arthritis. *J Orthop Res,* **1,** 136-143.

Smith, R. L., Schurman, D. J., Kajiyama, G., Mell, M. & Gilkerson, E. (1987) The effect of antibiotics on the destruction of cartilage in experimental infectious arthritis. *J Bone Joint Surg Am,* **69,** 1063-1068.

Smith, S. M. (1991) D-lactic acid production as a monitor of the effectiveness of antimicrobial agents. *Antimicrob Agents Chemother,* **35,** 237-241.

Smith, S. P., Thyoka, M., Lavy, C. B. D. & Pitani, A. (2002) Septic arthritis of the shoulder in children in Malawi. A randomised, prospective study of aspiration versus arthrotomy and washout. *J Bone Joint Surg Br,* **84,** 1167-1172.

Soltz, M. A. & Ateshian, G. A. (1998) Experimental verification and theoretical prediction of cartilage interstitial fluid pressurization at an impermeable contact interface in confined compression. *J Biomech,* **31,** 927-934.

Soltz, M. A. & Ateshian, G. A. (2000) Interstitial fluid pressurization during confined compression cyclical loading of articular cartilage. *Ann Biomed Eng,* **28,** 150-159.

Sophia Fox, A. J., Bedi, A. & Rodeo, S. A. (2009) The basic science of articular cartilage: structure, composition, and function. *Sports Health,* **1,** 461-468.

Sorensen, M., Funch, P., Hooge, M. & Tyler, S. (2003) Musculature of *Notholca acuminata* (Rotifera: Ploima: Brachionidae) revealed by confocal scanning laser microscopy. *Invertebr Biol,* **122,** 223-230.

Stahl, J. P. (2009) Maximizing positive outcomes for patients with *staphylococcal* infections. *Clinical Microbiology and Infection,* **15 Suppl 6,** 26-32.

Stengel, D., Bauwens, K., Sehouli, J., Ekkernkamp, A. & Porzsolt, F. (2001) Systematic review and meta-analysis of antibiotic therapy for bone and joint infections. *Lancet Infect Dis,* **1,** 175-188.

Stoddart, M. J., Furlong, P. I., Simpson, A., Davies, C. M. & Richards, R. G. (2006) A comparison of non-radioactive methods for assessing viability in *ex vivo* cultured cancellous bone: technical note. *Eur Cell Mater,* **12,** 16-25-discussion 16-25.

Stranden, A., Frei, R. & Widmer, A. F. (2003) Molecular typing of methicillin-resistant *Staphylococcus aureus*: can PCR replace pulsed-field gel electrophoresis? *J Clin Microbiol,* **41,** 3181-3186.

Struglics, A. & Hansson, M. (2012) MMP proteolysis of the human extracellular matrix protein aggrecan is mainly a process of normal turnover. *Biochem J,* **446,** 213-223.

Stutz, G., Kuster, M. S., Kleinstuck, F. & Gachter, A. (2000) Arthroscopic management of septic arthritis: stages of infection and results. *Knee Surg Sports Traumatol Arthrosc,* **8,** 270-274.

Suttorp, N., Fuhrmann, M., Tannert-Otto, S., Grimminger, F. & Bhadki, S. (1993) Pore-forming bacterial toxins potently induce release of nitric oxide in porcine endothelial cells. *J Exp Med,* **178,** 337-341.

Suttorp, N., Seeger, W., Dewein, E., Bhakdi, S. & Roka, L. (1985) *Staphylococcal* alpha-toxin-induced PGI2 production in endothelial cells: role of calcium. *Am J Physiol Cell Physiol,* **248,** C127-34.

Svoboda, K. K. (1998) Chondrocyte-matrix attachment complexes mediate survival and differentiation. *Microsc Res Tech,* **43,** 111-122.

Switalski, L. M., Patti, J. M., Butcher, W., Gristina, A. G., Speziale, P. & Höök, M. (1993) A collagen receptor on *Staphylococcus aureus* strains isolated from patients with septic arthritis mediates adhesion to cartilage. *Mol Microbiol,* **7,** 99-107.

Talan, D. A., Abrahamian, F. M., Moran, G. J., Citron, D. M., Tan, J. O. & Goldstein, E. J. C. (2003) Clinical presentation and bacteriologic analysis of infected human bites in patients presenting to emergency departments. *Clin Infect Dis,* **37,** 1481-1489.

Tenover, F. C., Arbeit, R. D., Goering, R. V., Mickelsen, P. A., Murray, B. E., Persing, D. H. & Swaminathan, B. (1995) Interpreting chromosomal DNA restriction patterns produced by pulsed-field gel electrophoresis: criteria for bacterial strain typing. *J Clin Microbiol,* **33,** 2233-2239.

Thakker, M., Park, J. S., Carey, V. & Lee, J. C. (1998) *Staphylococcus aureus* serotype 5 capsular polysaccharide is antiphagocytic and enhances bacterial virulence in a murine bacteremia model. *Infect Immun,* **66,** 5183-5189.

Thay, B., Wai, S. N. & Oscarsson, J. (2013) *Staphylococcus aureus* α-toxin-dependent induction of host cell death by membrane-derived vesicles. *Plos One,* **8,** e54661.

Thomas, D., Tovey, S. C., Collins, T. J., Bootman, M. D., Berridge, M. J. & Lipp, P. (2000) A comparison of fluorescent Ca2+ indicator properties and their use in measuring elementary and global Ca2+ signals. *Cell Calcium,* **28,** 213-223.

Tissi, L., Mcrae, B., Ghayur, T., Von Hunolstein, C., Orefici, G., Bistoni, F. & Puliti, M. (2004) Role of interleukin-18 in experimental group B *streptococcal* arthritis. *Arthritis Rheum,* **50,** 2005-2013.

Tkaczyk, C., Hua, L., Varkey, R., Shi, Y., Dettinger, L., Woods, R., Barnes, A., Macgill, R. S., Wilson, S., Chowdhury, P., Stover, C. K. & Sellman, B. R. (2012) Identification of anti-alpha toxin monoclonal antibodies that reduce the severity of *Staphylococcus aureus* dermonecrosis and exhibit a correlation between affinity and potency. *Clin Vaccine Immunol,* **19,** 377-385.

Tomita, T. & Kamio, Y. (1997) Molecular biology of the pore-forming cytolysins from *Staphylococcus aureus*, alpha- and gamma-hemolysins and leukocidin. *Biosci Biotechnol Biochem,* **61,** 565-572.

Traber, K. E., Lee, E., Benson, S., Corrigan, R., Cantera, M., Shopsin, B. & Novick, R. P. (2008) agr function in clinical *Staphylococcus aureus* isolates. *Microbiology,* **154,** 2265-2274.

Trong, H. N. G., Prunier, A.-L. & Leclercq, R. (2005) Hypermutable and fluoroquinolone-resistant clinical isolates of *Staphylococcus aureus*. *Antimicrob Agents Chemother,* **49,** 2098-2101.

Trump, B. F. & Berezesky, I. K. (1995) Calcium-mediated cell injury and cell death. *FASEB J,* **9,** 219-228.

Tsien, R. Y. & Waggoner, A. 2006. Fluorophores for confocal microscopy. *In:* Pawley, J. B. (ed.) *Handbook of Biological Confocal Microscopy.* 3rd ed. New York: Springer Science and Business Media, 267-279.

Uhlén, M., Guss, B., Nilsson, B., Gatenbeck, S., Philipson, L. & Lindberg, M. (1984) Complete sequence of the *staphylococcal* gene encoding protein A. A gene evolved through multiple duplications. *J Biol Chem,* **259,** 1695-1702.

Unal Cevik, I. & Dalkara, T. (2003) Intravenously administered propidium iodide labels necrotic cells in the intact mouse brain after injury. *Cell Death Differ,* **10,** 928-929.

Urban, J. P. (1994) The chondrocyte: a cell under pressure. *Br J Rheumatol,* **33,** 901-908.

Urban, J. P., Hall, A. C. & Gehl, K. A. (1993) Regulation of matrix synthesis rates by the ionic and osmotic environment of articular chondrocytes. *J Cell Physiol,* **154,** 262-270.

Vacaru, A. M., Unlu, G., Spitzner, M., Mione, M., Knapik, E. W. & Sadler, K. C. (2014) *In vivo* cell biology in zebrafish - providing insights into vertebrate development and disease. *J Cell Sci,* **127,** 485-495.

Valeva, A., Walev, I., Gerber, A., Klein, J., Palmer, M. & Bhakdi, S. (2000) *Staphylococcal* alpha-toxin: repair of a calcium-impermeable pore in the target cell membrane. *Mol Microbiol,* **36,** 467-476.

Valhmu, W. B. & Raia, F. J. (2002) myo-Inositol 1,4,5-trisphosphate and Ca(2+)/calmodulin-dependent factors mediate transduction of compression-induced signals in bovine articular chondrocytes. *Biochem J,* **361,** 689-696.

Van Griethuysen, A., Bes, M., Etienne, J., Zbinden, R. & Kluytmans, J. (2001) International multicenter evaluation of latex agglutination tests for identification of *Staphylococcus aureus*. *J Clin Microbiol,* **39,** 86-89.

Van Huyssteen, A. L. & Bracey, D. J. (1999) Chlorhexidine and chondrolysis in the knee. *J Bone Joint Surg Br,* **81,** 995-996.

Varley, A. J., Sule, J. & Absalom, A. R. (2009) Principles of antibiotic therapy. *Contin Educ Anaesth Crit Care Pain,* **9,** 184-188.

Venn, M. & Maroudas, A. (1977) Chemical composition and swelling of normal and osteoarthrotic femoral head cartilage. I. Chemical composition. *Ann Rheum Dis,* **36,** 121-129.

Verdon, J., Girardin, N., Lacombe, C., Berjeaud, J.-M. & Héchard, Y. (2009) δ-hemolysin, an update on a membrane-interacting peptide. *Peptides,* **30,** 817-823.

Verteramo, A. & Seedhom, B. B. (2004) Zonal and directional variations in tensile properties of bovine articular cartilage with special reference to strain rate variation. *Biorheology,* **41,** 203-213.

Verzijl, N., Degroot, J., Thorpe, S. R., Bank, R. A., Shaw, J. N., Lyons, T. J., Bijlsma, J. W., Lafeber, F. P., Baynes, J. W. & Tekoppele, J. M. (2000) Effect of collagen turnover on the accumulation of advanced glycation end products. *J Biol Chem,* **275,** 39027-39031.

Von Eiff, C., Becker, K., Machka, K., Stammer, H. & Peters, G. (2001) Nasal carriage as a source of *Staphylococcus aureus* bacteremia. . *N Engl J Med,* **344,** 11-16.

Walczysko, P., Wagner, E. & Albrechtová, J. T. (2000) Use of co-loaded Fluo-3 and Fura Red fluorescent indicators for studying the cytosolic Ca2+ concentrations distribution in living plant tissue. *Cell Calcium,* **28,** 23-32.

Walev, I., Martin, E., Jonas, D., Mohamadzadeh, M., Müller-Klieser, W., Kunz, L. & Bhakdi, S. (1993) *Staphylococcal* alpha-toxin kills human keratinocytes by permeabilizing the plasma membrane for monovalent ions. *Infect Immun,* **61,** 4972-4979.

Wan, L. Q., Jiang, J., Arnold, D. E., Guo, X. E., Lu, H. H. & Mow, V. C. (2008) Calcium concentration effects on the mechanical and biochemical properties of chondrocyte-alginate constructs. *Cell Mol Bioeng,* **1,** 93-102.

Wang, Y., Wei, L., Zeng, L., He, D. & Wei, X. (2013) Nutrition and degeneration of articular cartilage. *Knee Surg Sports Traumatol Arthrosc,* **21,** 1751-1762.

Waters, J. C. (2009) Accuracy and precision in quantitative fluorescence microscopy. *J Cell Biol,* **185,** 1135-1148.

Waters, J. R., Sharp, J. C. & Dev, V. J. (1994) Infection caused by *Escherichia coli* O157:H7 in Alberta, Canada, and in Scotland: a five-year review, 1987-1991. *Clin Infect Dis,* **19,** 834-843.

Welling, M. M., Paulusma-Annema, A., Balter, H. S., Pauwels, E. K. & Nibbering, P. H. (2000) Technetium-99m labelled antimicrobial peptides discriminate between bacterial infections and sterile inflammations. *Eur J Nucl Med,* **27,** 292-301.

Weston, V. C., Jones, A. C., Bradbury, N., Fawthrop, F. & Doherty, M. (1999) Clinical features and outcome of septic arthritis in a single UK Health District 1982-1991. *Ann Rheum Dis,* **58,** 214-219.

Wiberg, C., Hedbom, E., Khairullina, A., Lamandé, S. R., Oldberg, A., Timpl, R., Mörgelin, M. & Heinegård, D. (2001) Biglycan and decorin bind close to the n-terminal region of the collagen VI triple helix. *J Biol Chem,* **276,** 18947-18952.

Wiberg, C., Heinegård, D., Wenglén, C., Timpl, R. & Mörgelin, M. (2002) Biglycan organizes collagen VI into hexagonal-like networks resembling tissue structures. *J Biol Chem,* **277,** 49120-49126.

Widaa, A., Claro, T., Foster, T. J., O'brien, F. J. & Kerrigan, S. W. (2012) *Staphylococcus aureus* Protein A Plays a Critical Role in Mediating Bone Destruction and Bone Loss in Osteomyelitis. *Plos One,* **7,** e40586.

Wilke, G. A. & Bubeck-Wardenburg, J. (2010) Role of a disintegrin and metalloprotease 10 in *Staphylococcus aureus* alpha-hemolysin-mediated cellular injury. *Proc Natl Acad Sci U S A,* **107,** 13473-13478.

Wilkins, R. J., Browning, J. A. & Ellory, J. C. (2000) Surviving in a matrix: membrane transport in articular chondrocytes. *J Membr Biol,* **177,** 95-108.

Williams, P. R., Morgan, J. L., Kerschensteiner, D. & Wong, R. O. L. (2013) *In Vivo* Imaging of Zebrafish Retina. *Cold Spring Harbor Protocols,* **2013,** pdb.prot072652.

Williams, R., Smith, R. & Schurman, D. (1991) Purified *Staphylococcal* culture-medium stimulates neutral metalloprotease secretion from human articular-cartilage. *J Orthop Res,* **9,** 258-265.

Williams, R. E., Jevons, M. P., Shooter, R. A., Hunter, C. J., Girling, J. A., Griffiths, J. D. & Taylor, G. W. (1959) Nasal *staphylococci* and sepsis in hospital patients. *Br Med J,* **2,** 658-662.

Williams, R. J., Smith, R. L. & Schurman, D. J. (1990) Septic arthritis. *Staphylococcal* induction of chondrocyte proteolytic activity. *Arthritis Rheum,* **33,** 533-541.

Wilson, N. I. & Di Paola, M. (1986) Acute septic arthritis in infancy and childhood. 10 year's experience. *J Bone Joint Surg Br,* **68,** 584-587.

Wiseman, G. M. (1975) The hemolysins of *Staphylococcus aureus*. *Bacteriol Rev,* **39,** 317-344.

Wu, J. P., Kirk, T. B. & Zheng, M. H. (2008) Study of the collagen structure in the superficial zone and physiological state of articular cartilage using a 3D confocal imaging technique. *J Orthop Surg Res,* **3,** 29.

Wysenbeek, A. J., Volchek, J., Amit, M., Robinson, D., Boldur, I. & Nevo, Z. (1998) Treatment of *staphylococcal* septic arthritis in rabbits by systemic antibiotics and intra-articular corticosteroids. *Ann Rheum Dis,* **57,** 687-690.

Yagupsky, P., Dagan, R., Howard, C. W., Einhorn, M., Kassis, I. & Simu, A. (1992) High prevalence of *Kingella kingae* in joint fluid from children with septic arthritis revealed by the BACTEC blood culture system. *J Clin Microbiol,* **30,** 1278-1281.

Yamashita, K., Kawai, Y., Tanaka, Y., Hirano, N., Kaneko, J., Tomita, N., Ohta, M., Kamio, Y., Yao, M. & Tanaka, I. (2011) Crystal structure of the octameric pore of *staphylococcal* γ-hemolysin reveals the β-barrel pore formation mechanism by two components. *Proc Natl Acad Sci U S A,* **108,** 17314-17319.

Yannakopoulou, K., Jicsinszky, L., Aggelidou, C., Mourtzis, N., Robinson, T. M., Yohannes, A., Nestorovich, E. M., Bezrukov, S. M. & Karginov, V. A. (2011) Symmetry requirements for effective blocking of pore-forming toxins: comparative study with alpha-, beta-, and gamma-cyclodextrin derivatives. *Antimicrob Agents Chemother,* **55,** 3594-3597.

Yellowley, C. E., Jacobs, C. R., Li, Z., Zhou, Z. & Donahue, H. J. (1997) Effects of fluid flow on intracellular calcium in bovine articular chondrocytes. *Am J Physiol,* **273,** C30-6.

Zanetti, M. (2003) Cathelicidins, multifunctional peptides of the innate immunity. *J Leukoc Biol,* **75,** 39-48.

Zasloff, M. (2002) Antimicrobial peptides of multicellular organisms. *Nature,* **415,** 389-395.

Zhao, Y. X., Nilsson, I. M. & Tarkowski, A. (1998) The dual role of interferon-gamma in experimental *Staphylococcus aureus* septicaemia versus arthritis. *Immunology,* **93,** 80-85.

Zhivotovsky, B. & Orrenius, S. (2011) Calcium and cell death mechanisms: a perspective from the cell death community. *Cell Calcium,* **50,** 211-221.

Zhou, S., Cui, Z. & Urban, J. P. G. (2004) Factors influencing the oxygen concentration gradient from the synovial surface of articular cartilage to the cartilage-bone interface: a modeling study. *Arthritis Rheum,* **50,** 3915-3924.

Zhu, W., Mow, V. C., Koob, T. J. & Eyre, D. R. (1993) Viscoelastic shear properties of articular cartilage and the effects of glycosidase treatments. *J Orthop Res,* **11,** 771-781.

Zieger, M. M., Dörr, U. & Schulz, R. D. (1987) Ultrasonography of hip joint effusions. *Skeletal Radiol,* **16,** 607-611.

APPENDIX I

List of published papers, abstracts and presentations related to this work

Published Paper

1. Smith, I.D.M. Winstanley, J.P. Milto, K.M. Doherty, C.J. Czarniak, E. Amyes, S.G.B. Simpson, A.H.R.W. Hall, A.C. Rapid *in situ* chondrocyte death induced by *Staphylococcus aureus* toxins in a bovine cartilage explant model of septic arthritis. *Osteoarthritis and Cartilage*. 2013; 21(11):1755-65.
   (Based on Chapter 3 of this thesis)

Published abstracts

1. Smith, I.D.M. Cyrulik, K.M. Aymes, S.G.B. Simpson, A.H.R.W. Hall, A.C. A bovine cartilage explant model for the study of *Staphylococcus aureus*–induced septic arthritis. *J Bone Joint Surg(Br).* 2012; 94-B:Supp 36, 75.

2. Smith, I.D.M. Cyrulik, K.M. Aymes, S.G.B. Simpson, A.H.R.W. Hall, A.C. The effect of *Staphylococcus aureus* toxins on *in situ* bovine chondrocytes. *J Bone Joint Surg(Br).* 2012; 94-B:Supp 33, 11.

3. Smith, I.D.M. Milto, K.M. Doherty, C.J. Amyes, S.G.B. Simpson, A.H.R.W. Hall, A.C. Alpha toxin of *Staphylococcus aureus* causes *in situ* chondrocyte death. *Bone Joint J.* 2013; 95-B:Supp 10, 17.

4. Smith, I.D.M. Milto, K.M. Doherty, C.J. Amyes, S.G.B. Simpson, A.H.R.W. Hall, A.C. Alpha toxin of *Staphylococcus aureus* is the major cause of *in situ* chondrocyte death in a bovine cartilage explant model of septic arthritis. *Bone Joint J.* 2013; 95-B:Supp 13, 37.

5. Smith, I.D.M. Winstanley, J.P. Doherty, C.J. Amyes, S.G.B. Simpson, A.H.R.W. Hall, A.C. Increased sensitivity of superficial zone chondrocyte to *Staphylococcus aureus* toxins present in septic arthritis. *Bone Joint J.* 2013; 95-B:Supp 13, 28.

Oral presentations

1. Smith, I.D.M. Cyrulik, K.M. Amyes, S.G.B. Simpson, A.H.R.W. Hall, A.C. The effect of *Staphylococcus aureus* toxins on *in situ* bovine chondrocytes. Annual scientific meeting of the Scottish Orthopaedic Club (SCOT), Dunblane, 20th May 2011.

2. Smith, I.D.M. Cyrulik, K.M. Amyes, S.G.B. Simpson, A.H.R.W. Hall, A.C. The zonal pattern of chondrocyte death in a bovine cartilage explant model of

septic arthritis. Jospeh Lister Centenary Meeting, The Royal College of Surgeons of Edinburgh, 9th February 2012.

3. Smith, I.D.M. Milto, K.M. Doherty, C.J. Amyes, S.G.B. Simpson, A.H.R.W. Hall, A.C. Alpha toxin of *Staphylococcus aureus* causes *in situ* chondrocyte death. Annual scientific meeting of the Scottish Orthopaedic Club (SCOT), Dunblane, 8th June 2012.

4. Smith, I.D.M. Milto, K.M. Doherty, C.J. Amyes, S.G.B. Simpson, A.H.R.W. Hall, A.C. Alpha toxin of *Staphylococcus aureus* is the major cause of *in situ* chondrocyte death in a bovine cartilage explant model of septic arthritis. Annual British Orthopaedic Research Society Meeting, London, 24th-25th September 2012.

Poster presentations

1. Smith, I.D.M. Cyrulik, K.M. Amyes, S.G.B. Simpson, A.H.R.W. Hall, A.C. A bovine cartilage explant model for the study of *Staphylococcus aureus*-induced septic arthritis. Combined meeting of the British Orthopaedic Research Society and Bone Research Society, Cambridge, 27th-29th June 2011.

2. Smith, I.D.M. Winstanley, J.P. Doherty, C.J. Amyes, S.G.B. Simpson, A.H.R.W. Hall, A.C. Increased sensitivity of superficial zone chondrocyte to *Staphylococcus aureus* toxins present in septic arthritis. Annual British Orthopaedic Research Society Meeting, London, 24th-25th September 2012.

APPENDIX II

Reprint of a published paper based on the work presented in Chapter 3